

N 63 14683

N 63 14709

NATIONAL AERONAUTICS AND SPACE ADMINISTRATION

NASA CONFERENCE ON V/STOL AIRCRAFT

A COMPILATION OF THE PAPERS PRESENTED

Langley Research Center
Langley Field, Virginia

November 17-18, 1960



CASCOPEY
FILE

A

NASA CONFERENCE ON

V/STOL AIRCRAFT

A Compilation of the Papers Presented

Langley Research Center
Langley Field, Va.

November 17-18, 1960

TABLE OF CONTENTS

	Page
INTRODUCTION	vii
LIST OF CONFEREES	ix

TECHNICAL PAPERS PRESENTED

November 17, 1960

AERODYNAMICS

Session Chairman: John P. Campbell

1. Review of Basic Principles of V/STOL Aerodynamics . . . Richard E. Kuhn	1
2. Aerodynamic Characteristics of Propeller-Driven VTOL Aircraft . . . Robert H. Kirby	19
3. Large-Scale Wind-Tunnel Studies of Several VTOL Types . . . Mark W. Kelly	35
4. Aerodynamics of Tilting Ducted-Fan Configurations . . . Paul F. Yaggy and Kenneth W. Goodson	49
5. Aerodynamics of a Fan-in-Fuselage Model . . . Ralph L. Maki and David H. Hickey	65
6. Induced Interference Effects on Jet and Buried-Fan VTOL Configurations in Transition . . . Kenneth P. Spreemann . . .	79
7. Ground Interference Effects . . . Robert O. Schade	87
8. Considerations of Methods of Improving Helicopter Efficiency . . . Richard C. Dingeldein	101

HANDLING QUALITIES

Session Chairman: Charles W. Harper

9. Operational Technique for Transition of Several Types of V/STOL Aircraft . . . Fred J. Drinkwater III	119
10. Handling Qualities Experience With Several VTOL Research Aircraft . . . John P. Reeder	131
11. Aerodynamic Observations From Flight Tests of Two VTOL Aircraft . . . F. B. Gustafson, Robert J. Pegg, and Henry L. Kelly	149
12. Characteristics of a Deflected-Jet VTOL Aircraft . . . L. Stewart Rolls	171
13. The Effect of Blade Flapping on the Dynamic Stability of a Tilting-Rotor Convertiplane . . . Hervey C. Quigley and David C. Koenig	177

November 18, 1960

14. Highlights of Handling Qualities Criteria for V/STOL Aircraft . . . Seth B. Anderson	187
15. Criteria for Primary Handling Qualities Characteristics of VTOL Aircraft in Hovering and Low-Speed Flight . . . Robert J. Tapscott	195
16. Attitude Control Requirements for Hovering Determined Through the Use of a Piloted Simulator	207
17. The Use of Piloted Simulators in the Study of VTOL Flight . . . Donovan R. Heinle	223

OPERATING PROBLEMS

Session Chairman: Philip Donely

18. Operational Aspects of V/STOL Aircraft	235
. . . James B. Whitten	

19. Operating Problems of V/STOL Aircraft in STOL-Type Landing and Approach . . . Robert C. Innis and Curt A. Holzhauser	247
20. Considerations of the Effect of VTOL Downwash on the Ground Environment . . . Thomas C. O'Bryan	261
21. Noise Considerations in the Design and Operation of V/STOL Aircraft . . . Domenic J. Maglieri, David A. Hilton, and Harvey H. Hubbard	269

LOADS AND STRUCTURES

Session Chairman: Philip Donely

22. Some Recent Studies in Structural Dynamics of Rotor Aircraft . . . George W. Brooks and Milton A. Silveira	285
23. Structural-Loads Surveys on Two Tilt-Wing VTOL Configurations . . . John F. Ward	301
24. Summary of Rotor-Blade Vibratory-Load Studies . . . LeRoy H. Ludi	315
25. Factors in Evaluating Fatigue Life of Structural Parts . . . Walter Illg	325

SUMMARY

26. Summary of the V/STOL State of the Art . . . Charles H. Zimmerman	335
--	-----

INTRODUCTION

This document contains reproductions of technical papers presented by staff members of NASA Research Centers at the NASA Conference on V/STOL Aircraft held at the Langley Research Center on November 17-18, 1960. The primary purpose of the conference was to convey to the military services and the industry the results of recent NASA research pertinent to low to moderate subsonic speed aircraft having VTOL capability.

A list of conferees is included.

LIST OF CONFEREES

The following were registered at the NASA Conference on V/STOL Aircraft, Langley Research Center, Langley Field, Va., November 17-18, 1960:

ABBOTT, Ira H.	NASA Headquarters
ACHITOFF, Louis	The Port of New York Authority
ADAMS, Fred	The Bendix Corp.
ADAMSON, A. P.	General Electric Co.
AIKEN, William S., Jr.	Tactical Air Command
ALLEN, Edward M.	Curtiss-Wright Corp.
ALLEN, Walter	Republic Aviation Corp.
AMES, Milton B.	NASA Headquarters
ANDERSON, Lt. Col. E. A.	U.S. Marine Corps
ANDERSON, Seth B.	NASA - Ames Research Center
ARCIDIACONO, Thomas	Fairchild Engine and Airplane Corp.
ARMSTRONG, Comdr. A. W.	Canadian Joint Staff
ARMSTRONG, Comdr. J. G.	Dept. of the Navy
ATKINSON, A. S.	Bureau of Naval Weapons
BAILEY, Capt. Cecil D.	Air Research and Development Command
BARNES, William B.	Federal Aviation Agency
BARNETT, W. F.	David Taylor Model Basin
BASTEDO, Walter, Jr.	Gyrodyne Co. of America, Inc.
BEEBE, John	Dept. of the Army
BELSLEY, Stephen E.	NASA - Ames Research Center
BENSEN, Igor B.	Bensen Aircraft Corp.
BERG, R. A.	Douglas Aircraft Co., Inc.
BEST, Rube	North American Aviation, Inc.
BINNEY, Maj. Gen. A. F.	U.S. Marine Corps
BLAKE, C. L.	Convair
BLANTON, J. W.	General Electric Co.
BOHLING, R. F.	Bureau of Naval Weapons
BOREN, T. C.	Convair
BORGES, L. J., Jr.	Dept. of the Army
BORRER, Constance	Bureau of Naval Weapons
BORST, H. V.	Curtiss-Wright Corp.
BRABSON, Lt. Col. W. H.	Dept. of Defense
BREHAUS, W. O.	Cornell Aeronautical Lab., Inc.
BRESIN, Sheldon O.	Aeronutronic
BREWER, Jack D.	NASA Headquarters
BRIGHT, George	Hiller Aircraft Corp.
BROOKS, George W.	NASA - Langley Research Center
BROWN, Clinton E.	NASA - Langley Research Center
BROWN, Comdr. F. W., Jr., USCG	Dept. of the Navy

BROWN, Harvey H.
BRYANT, Glenn
BUNCHEER, John A.
BURGAN, E. T.
BURNSTEIN, S.
BUSEMANN, Dr. Adolf
BUSH, Lt. Col. Harry L.
BUTT, C. S.
BYWATERS, Maj. Richard E.

CALHOUN, J. T.
CAMPBELL, John P.
CAREY, Alex M.
CARNEY, Charles J.
CARPENTER, Paul
CARTER, Edward S., Jr.
CASSIDY, Col. R. F.
CHAMBERS, Capt. L. S.
CHURCHILL, Gary B.
COLLINS, T. E.
COLLINS, Thomas L.
COMERFORD, L. P.
CONSTANTINE, N. J.
COOK, William H., Jr.

CRAIG, S. J.
CRAWFORD, Charles C.
CRIM, A. D.
CRONE, R. M.
CRONVICH, L. L.
CROTSLEY, H. H.
CROWDER, J. R.
CROXALL, A. D.
CURTIS, Lt. Col. James

DANCIK, P.
DANIEL, J. Nelson
DAUSMAN, George E.
DAVIS, Charles
DEAN, F. H.
DeCALLES, Lt. Comdr. R. N.
DESMOND, G. L.
DETHLEFS, Capt. H. J.

DINGELDEIN, Richard C.
DOAK, E. R.
DONELY, Philip

NASA Headquarters
Mississippi State Univ.
Army Transportation Materiel Command
David Taylor Model Basin
Canadair, Ltd.
NASA - Langley Research Center
Dept. of the Army
Bureau of Naval Weapons
Dept. of the Army

Beech Aircraft Corp.
NASA - Langley Research Center
U.S. Coast Guard
Goodyear Aircraft Corp.
Army Transportation Research Command
Sikorsky Aircraft
Continental Army Command
Bureau of Naval Weapons
Goodyear Aircraft Corp.
Convair
The Port of New York Authority
Servomechanisms, Inc.
General Electric Co.
NASA Committee on Aircraft Operating
Problems
Chance Vought Aircraft, Inc.
Air Force Flight Test Center
Bureau of Naval Weapons
North American Aviation, Inc.
Applied Physics Laboratory - J.H.U.
North American Aviation, Inc.
Bureau of Naval Weapons
United Aircraft Corp.
Air Research and Development Command

Vertol
Army Transportation Research Command
Wright Air Development Div.
Bell Helicopter Co.
Curtiss-Wright Corp.
Office of Naval Research
NASA Committee on Aircraft Aerodynamics
Combats Development Office, Ft. Rucker,
Ala.
NASA - Langley Research Center
Doak Aircraft Co., Inc.
NASA - Langley Research Center

DOUGLAS, L. L.	Vertol
DREES, Jan M.	Bell Helicopter Co.
DRINKWATER, Fred J., III	NASA - Ames Research Center
DUDDY, R. R.	British Embassy
DUNNING, Robert W.	NASA Headquarters
DUTTON, Donnell H.	Georgia Institute of Technology
EDKINS, D. P.	General Electric Co.
EDWARDS, Col. J. C.	Air Materiel Command
EHLERS, H.	North American Aviation, Inc.
EVANS, Albert J.	NASA Headquarters
FARRELL, Andrew	The Bendix Corp.
FAYE, Alan E., Jr.	NASA - Ames Research Center
FEDZIUK, Henry A.	NASA - Langley Research Center
FEISTEL, Terrell	Mississippi State Univ.
FERSCH, K. E.	Curtiss-Wright Corp.
FISCHEL, Jack	NASA Flight Research Center
FLATT, Joseph	Tech. Development, Inc.
FORD, Capt. Earl P.	Army Transportation Materiel Command
FORMHALS, E. J.	Bureau of Naval Weapons
FORRESTER, Lt. J. E.	Bureau of Naval Weapons
FOSHAG, William F.	Aerophysics Co.
FOULDS, Bert A.	Douglas Aircraft Co., Inc.
FOWLER, Harlan D.	Consultant
FRICK, C. W.	Convair
FRIEND, Carl F.	Ryan Aeronautical Co.
FROST, J. C. M.	AVRO Aircraft Limited
FURLICK, W. J.	Curtiss-Wright Corp.
GALL, Lt. Col. John	Federal Aviation Agency
GARRARD, W. C.	Lockheed Aircraft Corp.
GARRICK, I. E.	NASA - Langley Research Center
GEBHARD, D.	Grumman Aircraft Engineering Corp.
GERSTENBERGER, Walter	Sikorsky Aircraft
GILCHRIST, A. W.	Defence Research Board of Canada
GILMORE, K. B.	Vertol
GLUHAREFF, Michael E.	Sikorsky Aircraft
GOODHAND, Col. O. Glenn	Air Research and Development Command
GOODSON, Kenneth W.	NASA - Langley Research Center
GOODWIN, Lt. Col. Frederick C.	Federal Aviation Agency
GOTTSCHALL, Richard C.	The Bendix Corporation
GOUGH, Melvin N.	NASA Committee on Aircraft Operating Problems
GOUGH, William V.	NASA - Lewis Research Center
GUSTAFSON, F. B.	NASA - Langley Research Center
GRAHAM, R. R.	Army Transportation Research Command

GREATOREX, Donald P.
GROGAN, George C.
GRUDBERG, Henry B.
GRUNSKA, William

Pratt & Whitney Aircraft
Norair
Systems Technology, Inc.
Pratt & Whitney Aircraft

HAAGENSON, Kenneth
HAAS, S. G. F.
HAMIL, Leonard
HAMILTON, William T.
HAMMOND, Comdr. R. E.
HARPER, Charles W.
HARPER, John A.
HARRIS, Thomas A.
HAUETER, Paul E.
HECHT, Herbert
HEINLE, Donovan R.
HELDENFELS, Richard R.
HEMSWORTH, M. C.
HEWIN, Larry M.
HIGGINS, H. C.
HILL, K. F.
HILTON, David A.
HISCOCKS, R. D.
HOFFMAN, Maj. Jack N.
HOHENEMSER, K. H.
HOLCOMBE, P. J.
HOLLENBERG, H. L.
HOLLOWELL, Lt. Col. G. L.
HOLZHAUSER, Curt A.
HOPKINS, J. W.
HORTON, Cyril F.
HOVEGARD, Paul
HOWELL, Col. Joseph W.
HUBBARD, Harvey H.
HURKAMP, C. H.
HURST, Maj. R. H.

Republic Aviation Corp.
Convair
Chrysler Corp.
NASA Committee on Aircraft Aerodynamics
U.S. Coast Guard
NASA - Ames Research Center
Lear, Inc.
NASA - Langley Research Center
Wright Air Development Div.
Sperry Phoenix Co.
NASA - Ames Research Center
NASA - Langley Research Center
General Electric Co.
Army Transportation Research Command
Boeing Airplane Co.
Rohr Aircraft Corp.
NASA - Langley Research Center
DeHavilland A/C of Canada
NASA Committee on Aircraft Aerodynamics
McDonnell Aircraft Corp.
IBM Corp.
Bureau of Naval Weapons
Bureau of Naval Weapons
NASA - Ames Research Center
Convair
Dept. of Defense
Boeing Airplane Co.
NASA Committee on Aircraft Aerodynamics
NASA - Langley Research Center
Fairchild Engine and Airplane Corp.
Continental Army Command

ILLG, Walter
INNIS, Robert C.

NASA - Langley Research Center
NASA - Ames Research Center

JACOBSON, Daniel H.
JAMES, Comdr. Jack M.
JOHNSON, H. S.
JOHNSON, Maj. R. L.

JOHNSTON, Gp. Capt. E. A.
JOHNSTON, J. F.
JOSEPHS, L. C.

Allison Div.
Dept. of the Navy
Army Transportation Research Command
Office of Asst. Secy. of the Air
Force (R & D)
British Embassy
Lockheed Aircraft Corp.
Chance Vought Aircraft, Inc.

KAPLAN, David H.	Fairchild Engine and Airplane Corp.
KAPLAN, Capt. R. L.	Army Transportation Research Command
KAZAN, Elliott	Republic Aviation Corp.
KEEFER, Karl H.	Allison Div.
KEISTER, Comdr. H. M.	Naval Research Lab.
KELLEY, Henry L.	NASA - Langley Research Center
KELLY, Mark W.	NASA - Ames Research Center
KELSEY, Gen. B. S. (Ret.)	Booz-Allen Applied Research
KERKER, R.	Douglas Aircraft Co., Inc.
KIRBY, Robert H.	NASA - Langley Research Center
KLEIN, Edward C.	Aeronca Manufacturing Corp.
KLINGENHAGEN, Lt. Col. John L.	Army Transportation Materiel Command
KORSAK, K.	Plasecki Aircraft Corp.
KOSCIUSKO, Capt. H. M.	Bureau of Naval Weapons
KOSIN, R. E.	Norair
KOVEN, W.	Bureau of Naval Weapons
KRAMER, E.	North American Aviation, Inc.
KRAUSE, P. C.	Kellett Aircraft Corp.
KRESS, R.	Grumman Aircraft Engineering Corp.
KUHN, Richard E.	NASA - Langley Research Center
KWIATKOWSKI, S. F.	North American Aviation, Inc.
LEE, John G.	NASA Committee on Aircraft Aerodynamics
LICHTEN, Robert L.	NASA Committee on Aircraft Aerodynamics
LIGHTFOOT, Ralph B.	Sikorsky Aircraft
LINDEN, J. E.	Bureau of Naval Weapons
LOEDDING, A. C.	Air Research and Development Command
LOENING, Grover	Consultant
LOFTIN, Laurence K., Jr.	NASA - Langley Research Center
LONSDALE, James	Pratt & Whitney Aircraft
LOUFEK, John E.	Aerojet-General Corp.
LOVELL, P. M.	NASA Headquarters
LOVINGTON, P. L.	Lycoming Div.
LOW, Col. A. J., Jr.	Dept. of the Air Force
LUDI, LeRoy H.	NASA - Langley Research Center
LUNDIN, Bruce T.	NASA - Lewis Research Center
LYNCH, James P.	Dept. of the Navy
LYNN, R. R.	Bell Helicopter Co.
MACKIN, T. W.	North American Aviation, Inc.
MAGLIERI, Domenic J.	NASA - Langley Research Center
MAKI, Ralph L.	NASA - Ames Research Center
MARINELLI, Col. J. L.	NASA Committee on Aircraft Operating Problems
MARTIN, Stanley	Bell Helicopter Co.
MATTHEWS, George B.	University of Virginia
MAUZY, Capt. E. L.	Wright Air Development Div.

MAY, Ralph B.	NASA Headquarters
MAZZA, Carmen	Naval Air Development Center
McCONNELLY, R. E.	Douglas Aircraft Co., Inc.
McDONALD, J. E.	Canadian Joint Staff
McGUIRE, R. C.	Eastern Airlines, Inc.
McHUGH, J. G.	Army Transportation Research Command
McKINNEY, Marion O.	NASA - Langley Research Center
McQUEEN, Kenneth T.	Naval Air Development Center
McROBERT, Maj. P. P.	U.S. Marine Corps
MEAD, Merrill H.	NASA - Ames Research Center
MEYER, Maj. Gen. R. D.	Dept. of the Army
MICHAELSEN, O. E.	Canadair, Ltd.
MICHEL, P. L.	Sikorsky Aircraft
MILLER, Rene H.	Massachusetts Inst. of Technology
MITCHELL, Meade H.	Dept. of the Army
MOSER, Lt. Herbert H.	Army Transportation Research Command
MURTAUGH, Clyde	Bendix Corp.
MUSE, Thomas C.	Dept. of Defense
MYERS, Charles E., Jr.	Society of Experimental Test Pilots
NELSON, N. E.	Doak Aircraft Co., Inc.
NEWBY, C. T.	Bureau of Naval Weapons
NEWTON, F. C.	Douglas Aircraft Co., Inc.
NEYLAND, C. E.	Convair
NICHOLS, Mark R.	NASA - Langley Research Center
NIKOLSKY, A. A.	Princeton University
O'BRIEN, Jack	Republic Aviation Corp.
O'BRYAN, Thomas C.	NASA - Langley Research Center
O'DONNELL, Dr. William J.	NASA Committee on Aircraft Aerodynamics
OLEKSAK, William	Federal Aviation Agency
O'MALLEY, J. A., Jr.	Bell Aerospace Corp.
ORDWAY, Dr. D. E.	Therm, Inc.
PARKER, Col. D. B.	Dept. of the Army
PEARSON, Ernest O.	NASA Headquarters
PECK, W.	Vertol
PEGG, Robert J.	NASA - Langley Research Center
PELEHACK, M.	Grumman Aircraft Engineering Corp.
PERISHO, C. H.	McDonnell Aircraft Corp.
PERKINS, Dr. C. D.	Asst. Secretary of the Air Force (R & D)
PETTINGALL, Charles E.	Douglas Aircraft Co., Inc.
PHILLIP, Robert L.	Boeing Airplane Co.
PIASECKI, F. N.	Piasecki Aircraft Corp.
PICKERD, John A.	Rohr Aircraft Corp.
PROPPER, E. M.	Convair
PYNE, F. C.	Aluminum Co. of America

QUIGLEY, Hervey C.	NASA - Ames Research Center
RAY, George	Boeing Aircraft Co.
RAZAK, Kenneth	University of Wichita
RAZAK, V. L.	Beech Aircraft Corp.
REEDER, John P.	NASA - Langley Research Center
REEDER, W. D.	Convair
REICHERT, J. B.	Doak Aircraft Co., Inc.
REID, Dr. H. J. E.	NASA - Langley Research Center
REIGHARD, F. T.	Air Materiel Command
RETHORST, Dr. Scott	Vehicle Research Corp.
RICHARDSON, L. B., Jr.	Chance Vought Aircraft, Inc.
RINGHAM, R. F.	Chance Vought Aircraft, Inc.
ROBERTSON, Charyl	Skycraft, Inc.
ROBERTSON, James L.	Skycraft, Inc.
ROBINSON, D. W., Jr.	The Kaman Aircraft Corp.
ROCHEN, Herbert	NASA Headquarters
ROCHTE, Col. Lucian S.	Federal Aviation Agency
ROLLS, L. Stewart	NASA - Ames Research Center
ROSEN, G.	United Aircraft Corp.
RYAN, Comdr. D. H.	Canadian Joint Staff
SAXE, J.	Grumman Aircraft Engineering Corp.
SCHADE, Robert O.	NASA - Langley Research Center
SCHEIMAN, James	Army Transportation Research Command
SCHMIDT, Harry P., Jr.	R. Dixon Speas Associates
SCHNEIDER, Maj. A. G.	Tactical Air Command
SCHNEIDER, John J.	Vanguard Aircraft Air and Marine Corp.
SCHUCK, George I.	Army Transportation Research Command
SEAGER, D. B.	Lockheed Aircraft Corp.
SECKEL, E.	Princeton University
SEGNER, Maj. Donald R., USMC	U.S. Naval Air Test Center
SEIBEL, Charles M.	Cessna Aircraft Co.
SELLMAN, E. W.	Bureau of Naval Weapons
SHERIDAN, H. G.	Bureau of Naval Weapons
SHERIDAN, P.	Vertol
SHORTAL, Joseph A.	NASA - Langley Research Center
SIEVERS, A. G.	Curtiss-Wright Corp.
SILVEIRA, Milton A.	NASA - Langley Research Center
SING, Edward Y.	Bell Aerosystems Co.
SISSINGH, Dr. G. J.	Hiller Aircraft Corp.
SMITH, C. Branson	United Aircraft Corp.
SMITH, Giles K.	The Rand Corp.
SMITH, Lt. Comdr. R. P.	Naval Air Test Center
SOHN, R.	McDonnell Aircraft Corp.
SOLARSKI, A. H.	Cook Electric Co.
SOULE, Hartley A.	NASA - Langley Research Center

SPANGENBERG, G. A.	Bureau of Naval Weapons
SPOONER, S.	Army Transportation Research Command
SPREEMANN, Kenneth P.	NASA - Langley Research Center
STACK, John	NASA - Langley Research Center
STANGE, R. A.	Naval Air Test Center
STEELE, P. E.	North American Aviation, Inc.
STEEN, Lt. Col. C. H.	Dept. of the Air Force
STEPHENSON, J.	Lycoming Div.
STEPNIEWSKI, W. Z.	Vertol
STICKLE, George W.	Tactical Air Command
STOLARICK, John	Dept. of the Army
STONE, A.	Bureau of Naval Weapons
STROK, Col. M. J.	Army Transportation Research Command
STUART, Joseph, III	Hiller Aircraft Corp.
STUART, W. G.	Norair
SUGGS, R. L.	Petroleum Helicopters, Inc.
SULLIVAN, Comdr. P. L.	Naval Air Test Center
SUTTON, J. F.	Lockheed Aircraft Corp.
SWOPE, William A.	Army Aviation Test Activity
TAPSCOTT, Robert J.	NASA - Langley Research Center
TAYLOR, C. E.	Federal Aviation Agency
TAYLOR, Frank W.	Naval Air Test Center
TAYLOR, Harlan D.	United Aircraft Corp.
TERRANA, D.	Grumman Aircraft Engineering Corp.
THERIAULT, P. W.	Lockheed Aircraft Corp.
THOMPSON, Floyd L.	NASA - Langley Research Center
THORNTON, C. P.	National Aeronautical Establishment, Ottawa, Canada
TILLINGHAST, N. W., Jr.	Chance Vought Aircraft, Inc.
TOLL, Thomas A.	NASA Flight Research Center
TUCKER, A. W.	Cleveland Pneumatic Industries, Inc.
UBERTI, Bruno	Piasecki Aircraft Corp.
VANDERLIP, Edward G.	Vanguard Aircraft Air and Marine Corp.
VIDAL, Robert J.	Cornell Aeronautical Lab., Inc.
WACHS, M. A.	Sikorsky Aircraft
WAGNER, R. A.	Hughes Tool Co.
WARD, John F.	NASA - Langley Research Center
WATTSON, R. K., Jr.	Boeing Airplane Co.
WEBB, Charles, Jr.	Chrysler Corp.
WEIDHUNER, D. D.	Dept. of the Army
WEINBERG, Warren E.	AC Spark Plug Div.
WEISSMAN, Clem C.	NASA Committee on Aircraft Aerodynamics
WEITZEN, William	Dept. of the Air Force
WHEELER, Will L.	Ryan Aeronautical Co.

WHITAKER, H. Philip	Massachusetts Inst. of Technology
WHITE, J. W.	Army Transportation Research Command
WHITE, Richard P., Jr.	Cornell Aeronautical Lab., Inc.
WHITTEN, James B.	NASA - Langley Research Center
WIENER, L. S.	Curtiss-Wright Corp.
WIESNER, Wayne	Boeing Aircraft Co.
WILLIAMS, Col. R. R.	Dept. of the Army
WILSON, F. M., Jr.	Lockheed Aircraft Corp.
WILSON, Herbert A., Jr.	NASA - Langley Research Center
WILSON, Thomas	Office of Naval Research
WIMPRESS, John K.	Boeing Airplane Co.
WITHINGTON, H. W.	Boeing Airplane Co.
WOODCOCK, R. J.	Wright Air Development Div.
WRIGHT, Clifford B.	Allison Div.
YAGGY, Paul F.	NASA - Ames Research Center
YEATES, John	Army Transportation Research Command
YOUNG, Willis H., Jr.	Bureau of Naval Weapons
ZABINSKY, J.	Bell Aerosystems Co.
ZAISER, E.	United Aircraft Corp.
ZIMMERMAN, Charles H.	NASA - Langley Research Center

REVIEW OF BASIC PRINCIPLES OF V/STOL AERODYNAMICS

By Richard E. Kuhn

Langley Research Center

SUMMARY

L
1
4
1
0

This paper reviews the principal factors that determine the performance of V/STOL aircraft. These can be summarized as follows. In hovering, the power required, the fuel consumption, and the downwash dynamic pressure are all determined by and increase with increasing slipstream area loading. In transition the wing span, the distribution of load on that span, and the power required in hovering determine the shape of the power-required curve and through this the engine-out safety and STOL performance. In cruise some compromises are required but, generally, the same rules for designing good cruise performance into conventional airplanes still apply to V/STOL configurations, namely, attention to aerodynamic cleanliness to reduce the parasite power and a wing of appreciable span to reduce the induced power.

INTRODUCTION

During the past few years a great variety of V/STOL type aircraft have been proposed and investigated. The choice among these of a particular V/STOL configuration to fill a given mission will depend largely upon the specifications of the mission and a matching of the mission requirements with the airplane performance. This paper reviews the principal factors that govern the performance of V/STOL aircraft in the hovering, cruise, and transition speed ranges.

One of the primary performance considerations in any airplane is the power required. Most points concerning the performance of V/STOL aircraft can be made on the basis of the typical power-required curve for V/STOL aircraft such as shown in figure 1. The expressions that determine the power requirements in the three areas to be discussed are also shown.

SYMBOLS

A disk area of propeller or rotor, sq ft
A_e exit area of duct, sq ft

A_s	cross-sectional area of slipstream, sq ft
b	wing span, ft
$C_{D,o}$	parasite drag coefficient
$c_{l,i}$	design section lift coefficient
D	slipstream diameter, ft; also exit diameter of duct, ft
e	span efficiency factor
$(L/D)_{MAX}$	maximum lift-drag ratio
P	shaft power, hp
q	average downwash dynamic pressure, lb/sq ft
r	inlet radius, ft
S	wing area, sq ft
SFC	specific fuel consumption, lb/hp/hr
T	thrust, lb
t	time, hr
V	velocity, ft/sec unless otherwise noted
W	airplane weight, lb
W_f	fuel weight, lb
η	propulsive efficiency
η_{st}	static thrust efficiency (ratio of slipstream kinetic energy to shaft power), $\frac{T^{3/2}}{1100P\sqrt{\rho A_s}}$
ρ	mass density of air, slugs/cu ft

HOVERING PERFORMANCE

Power Required

As is well known, all hovering aircraft support themselves by accelerating air downward. A helicopter imparts a low downward velocity to a large diameter stream of air, whereas a jet V/STOL gives a very small diameter stream of air a very high downward velocity to produce the same vertical thrust. In both cases the thrust is given by $T = mV$ where m is the downward mass flow of air per unit time ($m = \rho A_S V$).

The power required to produce this thrust, however, is a function of the thrust multiplied by downward velocity imparted $\left(P = \frac{TV}{1100\eta_{st}} \right)$. Thus the power increases rapidly as the diameter of the actuator used decreases as shown in figure 2.

The major difference between the shrouded and unshrouded configurations is shown by the sketch at the top of the figure. The presence of the shroud prevents the contraction of the slipstream which occurs with the unshrouded configuration. Thus the diameter of a shrouded configuration can be about 70 percent of that of an unshrouded configuration. Note that it is the exit area of a shrouded configuration that governs the power required of this configuration.

Experimental data have shown that, for the unshrouded configurations, static thrust efficiencies between 0.7 and 0.8 (depending on the degree of compromise required with the high-speed characteristics) can be achieved.

For the shrouded configurations the reduction in tip losses due to the presence of the shroud should give some improvement in efficiency. However, careful attention must be paid to the internal drag of the shroud, struts, and counter vanes to prevent these losses from nullifying the gains due to tip-loss reductions. Very little full-scale data are available for the shrouded configurations but in general it is expected that static thrust efficiencies of 0.75 to 0.85 should be obtainable with careful design.

Fuel Consumption

Two other quantities are of concern in hovering: the fuel consumption, which is directly proportional to the power required, and the downwash dynamic pressure, which is one-half the slipstream area loading. These are plotted in figure 3.

The leaders from the configuration sketches in figure 3 do not indicate a specific point but rather the general area in which current practice usually places these configurations. All V/STOL configurations except jet pump schemes, which are not considered here, fall in one general band.

Turbojet and turboprop configurations, which were omitted from figure 2 because these engines are not usually thought of in terms of horsepower, are included in figure 3. If these configurations were presented in terms of power they would fall at or above the top edge of figure 2. These configurations have very high fuel consumption; one hour of hovering would burn a weight of fuel almost equal to the weight of the aircraft. Therefore, with these configurations, hovering time must be restricted to the $1\frac{1}{2}$ to 2 minutes required for take-off and landing. Obviously if long hovering time is required, a rotor configuration is dictated. A more complete discussion of power required and fuel consumption in hovering is presented in reference 1.

Downwash

A point of concern with V/STOL aircraft is the effect of the downwash from these aircraft on the ground under the aircraft. The average downwash from unshrouded configurations is equal to the disk loading and that from shrouded configurations is equal to one-half the exit-area loading. Experience has shown that loose sand and dirt will be blown up by helicopters with disk loadings, and therefore downwash dynamic pressures, as low as 2 to 3 pounds per square foot. On the other hand, good sod can withstand downwash dynamic pressures as high as 1,000 to 2,000 pounds per square foot. The downwash problem is discussed more fully in reference 2.

CRUISE PERFORMANCE

General Considerations

In figure 4 the power required for 40,000-pound cargo-type aircraft operating at sea level is plotted as a function of speed. V/STOL aircraft can be classified in three categories: those that use rotors for both lift and propulsion in cruise (the pure helicopters), those that operate as conventional aircraft using wing lift and separate propulsion in cruise, and combination configurations (the compound or unloaded helicopter). Requiring the helicopter rotor to provide both lift and propulsion in cruising flight results in problems of retreating blade stall and advancing blade compressibility effects which increase

the rotor profile power requirements of the helicopter and limit its cruising speed.

In the compound configuration the propulsion job is taken over by separate propellers or ducted fans and part of the lift is transferred to a wing; thus the rotor is unloaded and the speed capability is increased. The parasite drag of the rotor and pylon remains, however, with the result that the power required remains above that of more conventional aircraft.

The other V/STOL aircraft cruise on wing lift, and for these the same rules for obtaining good cruise performance that have always applied to conventional aircraft still apply, namely, aerodynamic cleanliness to reduce parasite drag and power and a wing designed for the desired cruising altitude and speed to minimize the induced power.

Good aerodynamic design is important not only at the highest speeds but throughout the speed range because most aircraft cruise in the speed range near the maximum lift-drag ratio where the span is important. A large wing span is needed to minimize induced drag and therefore power, as can be deduced from the expression of figure 1. A clean aerodynamic design is needed to minimize power throughout the speed range. A good case in point is the helicopter where the high parasite drag of current configurations is largely responsible for the difference in power between the helicopter and the airplane as shown in figure 4 near the speed for helicopter minimum power. This point is discussed more completely in reference 3.

The power required for the V/STOL aircraft in cruise is a little greater than that for the conventional airplane because of the reduction in propulsive efficiency which results from the fact that the propulsion units must also be designed to provide the lift in hovering for most V/STOL configurations; thus, a compromise in the design must be made.

Propulsive Efficiency Compromise

Each V/STOL type has a different propulsion-hovering design compromise. An example of one such design compromise for the propeller-driven V/STOL aircraft is shown in figure 5. For best static thrust a relatively large amount of camber, as indicated by the design section lift coefficient, is required. With a lot of camber, however, the cruise efficiency is relatively poor. Best cruise efficiency occurs with relatively little camber.

The design compromise for maximum range is shown by the solid symbol. If less camber is used, the weight of fuel that can be lifted in vertical take-off is reduced and this causes a reduction in range. Increases in

camber above this point give a small increase in fuel weight lifted but the cruise efficiency decreases so rapidly that again the range is decreased.

Another compromise for the propeller aircraft occurs in connection with the operating rotational speed. If the relatively wide-blade large-diameter propellers required for good static thrust are operated at hovering rotational speed while in cruise, the tip sections of the blade are operating well below their most efficient angle of attack. A reduction in rotational speed (to 80 percent in the case of fig. 5) is required to achieve good cruise efficiencies. This problem is even more severe for tilt-rotor configurations.

A different type of compromise is involved for the ducted-fan configuration as shown in figure 6. With a generous inlet radius a good level of static thrust is obtained. However, experimental investigations have shown that if a small inlet radius such as is desired for the cruise condition is used, the lip will stall internally and the thrust drops appreciably. Thus, either a thick shroud or a variable-geometry inlet must be used.

Also a compromise must be made at the duct exit. As mentioned in the section "Hovering Performance" the power required depends on the exit diameter. Thus a diffuser, as indicated, is desired to increase the exit diameter and thus reduce the power required. In cruising flight, however, the exit diameter is too large and the flow may separate from the diffuser. For the optimum duct performance it may in some cases be necessary to vary both the inlet and the exit geometry.

Cruising Speed

The cruising speed attained will depend on both the aerodynamic cleanliness and the power installed as shown in figure 7 where the compound helicopter, the flapped tilt wing, and the tilt-duct configuration are compared. The power installed must be somewhat greater than the bare power required to hover in order to allow for temperature and altitude effects and to provide a margin for climb.

At maximum cruise power the example compound helicopter used in figure 7 for illustration would have a speed of about 200 knots. The tilt-wing and tilt-duct configurations would have higher speeds, both because they can be cleaner aerodynamically and because of the higher installed power required for hovering. The tilt-duct configuration is shown above the tilt-wing configuration because design studies of these usually utilize a higher slipstream area loading in hovering.

Range

At maximum cruising speed at sea level the engine specific fuel consumption is low ($SFC = 0.50$, see fig. 8); this indicates that the engine is operating near peak efficiency. The range would be severely limited, however, because the airplane is operating far beyond the point of maximum aerodynamic efficiency or $(L/D)_{MAX}$. However, when current turbine engines are throttled to 20-percent power (as in this case), the fuel consumption is more than doubled so that again the range is far from optimum. Actually maximum range would occur between 175 and 200 knots for the example shown.

Conventional turbine-powered airplanes also face this same problem, and therefore current turbine transports operate at high altitude. As shown in figure 8 an altitude can be found, in this case 40,000 feet, at which both the engine and the airframe can be operated at or near maximum efficiency. In the present example, the range obtained by operating at 40,000 feet would be about three times that obtained by operating at the same speed at sea level.

It is recognized that in military operations it is sometimes desirable or necessary to fly "on the deck." The example airplane used could fly at about 180 knots on only one of four engines at a specific fuel consumption of about 0.50 and could thus almost match best aerodynamic efficiency and best engine efficiency at sea level. The resulting range would be only slightly less than that at altitude. Although it is recognized that shutting down and restarting engines in flight is not generally considered good practice, with current engines it will be necessary for operating personnel to make a choice between shutting down engines, flying at altitude, or accept the penalty in fuel consumption and range for high-speed on-the-deck flight.

As shown in figure 1, the parasite drag is the primary contribution to the power requirements at high speeds. For those missions in which very high-speed flight at sea level is of paramount importance, some decrease in power required and therefore increase in range at very high speeds can be achieved by reducing the wing size as shown in figure 9.

The altitude capability and maximum firing range would be seriously reduced, however, because of the increase in power at the speed for $(L/D)_{MAX}$, as shown in figure 9. This increase in power is, of course, due to the increase in induced power which, as shown in figure 1, is proportional to $(W/b)^2$.

The relative speed ranges of application for turbojet and turbo-prop propulsion systems are indicated in figure 10. At the higher speeds the approach of the transonic drag rise and the reduction in

propeller efficiency caused by the blade tips reaching transonic speeds causes a rapid increase in power required and therefore fuel consumption for the turboprop configuration as shown in figure 8.

Because of the high exhaust velocity of the turbojet the propulsive efficiency is low at low speeds but increases with speed and above 450 to 500 knots is better than that of the turboprop; thus, less fuel is consumed. This is the obvious speed range of operation for turbojet propulsion systems. However, the penalty for operating turbojet configurations at lower speeds is readily apparent.

TRANSONIC PERFORMANCE

General Considerations

Obviously, the most important requirement in transition is that the power required should not exceed the power required in hovering. However, two other considerations are also important. The first is the problem of the minimum speed at which flight can be continued in the event of partial power failure. The second is the problem of STOL performance with overload or in operation at altitudes and temperatures above those at which the airplane can hover. Both of these problems depend upon the rate of decrease in power with speed as the aircraft departs from hovering; a rapid decrease is desired from both considerations. The steepness of the back side of the power curve is definitely desirable from the viewpoint of performance; however, whether this steepness is a basic problem in handling qualities is yet to be decided.

The shape of the power-required curve in transition depends upon the following items: the disk loading, which determines the power required in hovering (the low-speed end point of the transition), and the wing span and the distribution of load on the span, which determine the power required at the high-speed part of the transition.

Effect of Span

Figure 11 shows the effect of span on the power required as a function of speed for a 40,000-pound airplane. Because of the low speeds involved the parasite power is small or negligible throughout most of the transition. The power required is all induced power which is determined, as shown in figure 1, by the span loading - that is, the weight divided by the wing span. The calculated power required shown in figure 11 is based on conventional low-speed aerodynamics (calculations performed with expressions from fig. 1) and indicates that throughout most of the transition the airplane is operating on wing lift. Below

about 30 knots there is a transition from wing lift to propeller lift in hovering.

A 25-percent reduction in wing span results in about a 50-percent increase in induced power because as shown in figure 1 the induced power is proportional to $(W/b)^2$. Thus, a decrease in span results in an increase in engine-out speed, and for the overloaded take-off condition, an increase in take-off distance because the short-span airplane would have to accelerate to a higher speed for take-off.

These curves are for the case without wing stall. If the wing stalls in transition, the power curve is even flatter. Design compromises necessary to avoid wing stall on flapped tilt-wing configurations are discussed in reference 4.

Effect of Load Distribution

The considerations shown in figure 11 are for the condition of a fairly uniform distribution of load. The effects of a poor load distribution are shown in figure 12. In cruising flight and at the high-speed end of the transition the load distribution would be fairly uniform, but as the airplane slows down in the transition the part of the wing that is not in the slipstream cannot continue to carry its share of the load. A load distribution of the type shown develops with the result that the power required corresponds to a wing of appreciably less span. These effects are shown for tilt-wing and tilt-duct configurations but apply also to buried-fan and even to a greater extent to jet V/STOL configurations.

COMPARISON OF CONFIGURATIONS

In figure 13 the hovering and cruise considerations have been used to present a plot of hovering time against the cruising speed range of application for several V/STOL aircraft. This comparison assumes burning a weight of fuel equal to three percent of the gross weight of the aircraft. The choice of configuration will depend on the mission to be filled. If long hovering time is of paramount importance a rotor configuration would be dictated. Obviously jet types will be restricted to missions where the only hovering time required is the $1\frac{1}{2}$ or 2 minutes required in take-off and landing.

Between these two extremes are several types that could find application as transport types but here no clear choice is indicated. For these configurations, as is frequently the case, off-design considerations

may dictate the choice. One such off-design consideration is the STOL performance as shown in figure 14.

The comparison is for overloaded conditions of 120 percent of the VTOL weight. The rotor types have relatively high take-off distances because the low power requirement in hovering results in a relatively flat variation of power with speed in the transition. The flapped tilt wing makes efficient use of wing lift in the transition and the other types suffer to varying degrees from a short span or a relatively poor load distribution in transition.

CONCLUDING REMARKS

In hovering the power required, the fuel consumption, and the downwash dynamic pressure are all determined by and increase with increasing slipstream area loading. In transition the wing span, the distribution of load on that span, and the power required in hovering determine the shape of the power-required curve and through this the engine-out safety and STOL performance. In cruise some compromises are required but, generally, the same rules for designing good cruise performance into conventional airplanes still apply to V/STOL configurations, namely attention to aerodynamic cleanliness to reduce the parasite power and a wing of appreciable span to reduce the induced power.

REFERENCES

1. Zimmerman, Charles H.: Some General Considerations Concerning VTOL Aircraft. SAE Trans., vol. 65, 1957, pp. 159-171.
2. McKinney, M. O.: Capabilities and Costs of Various Types of VTOL Aircraft. Presented to the V/STOL Symposium of AGARD (Paris, France), June 28-30, 1960.
3. Dingeldein, Richard C.: Consideration of Methods of Improving Helicopter Efficiency. (Prospective NASA paper.)
4. Kirby, Robert H.: Aerodynamic Characteristics of Propeller-Driven VTOL Aircraft. (Prospective NASA paper.)

POWER REQUIRED IN STEADY LEVEL FLIGHT

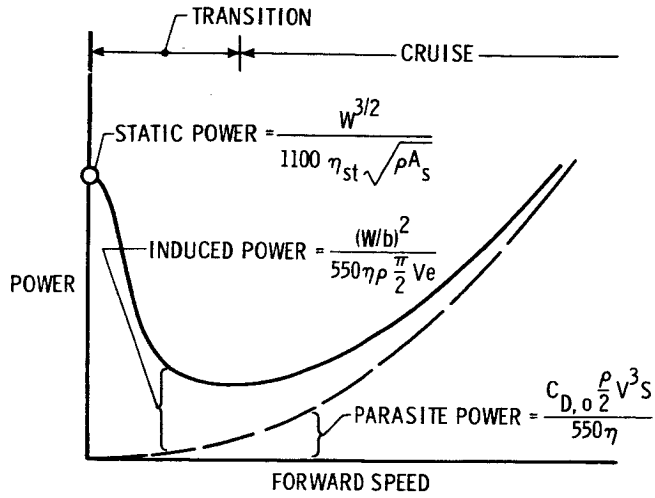


Figure 1

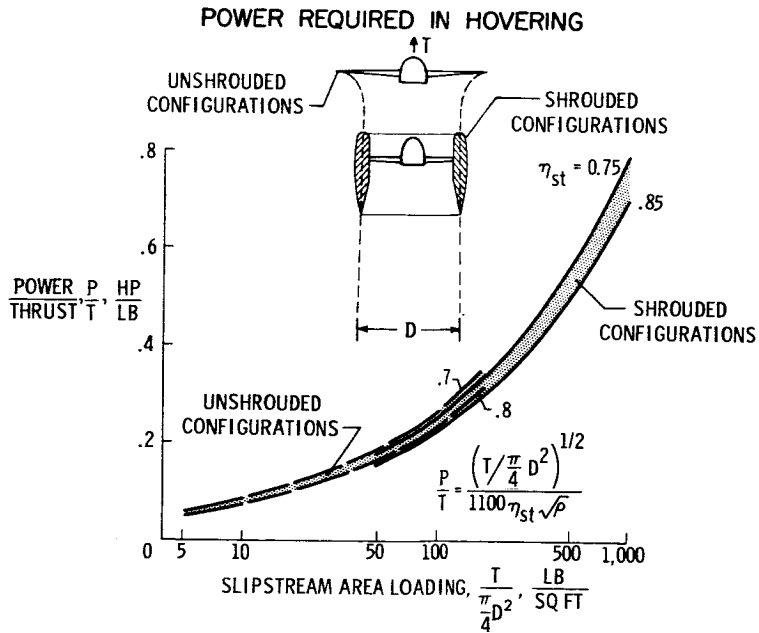


Figure 2

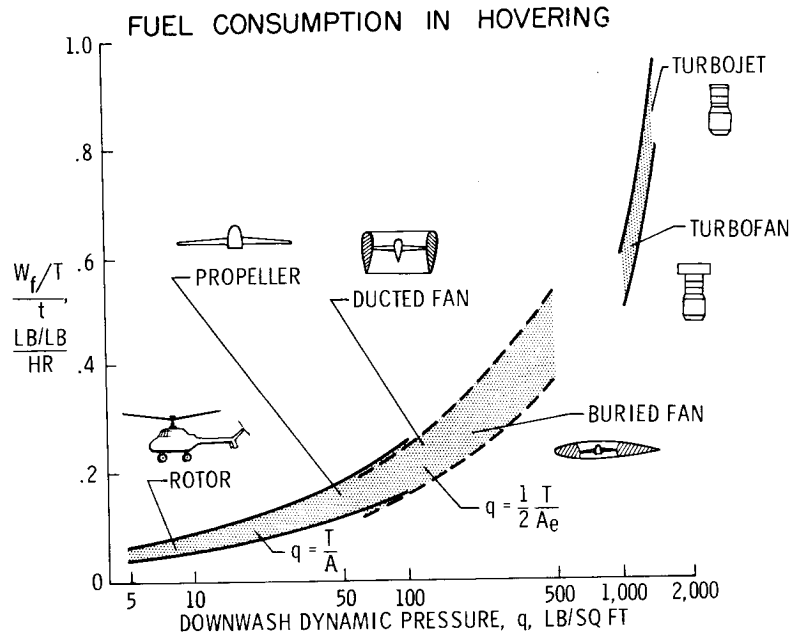


Figure 3

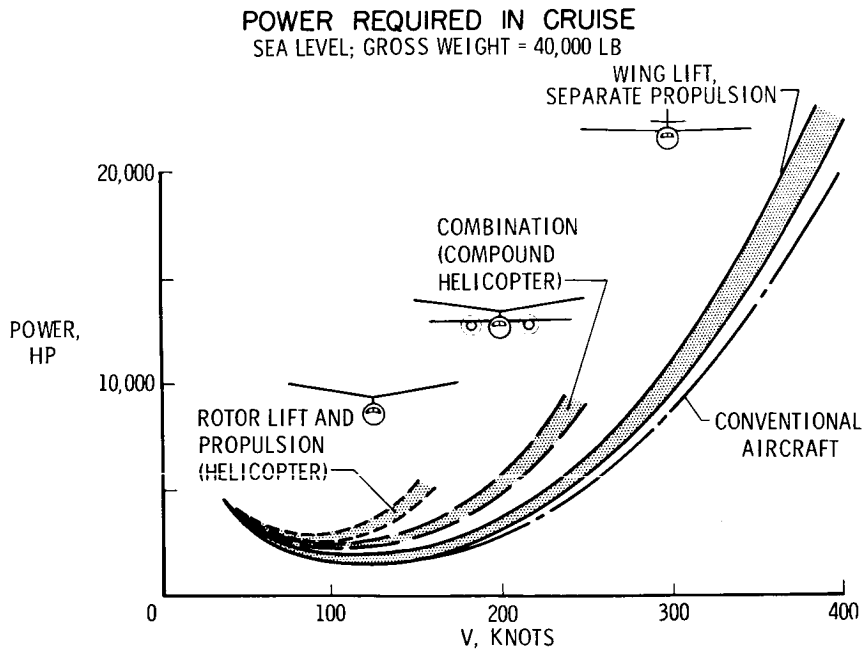


Figure 4

PROPELLER DESIGN COMPROMISE

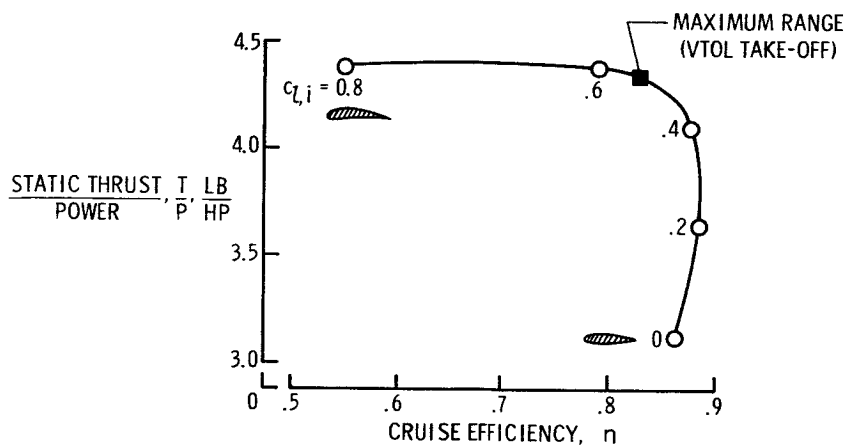


Figure 5

DUCTED-FAN DESIGN COMPROMISE

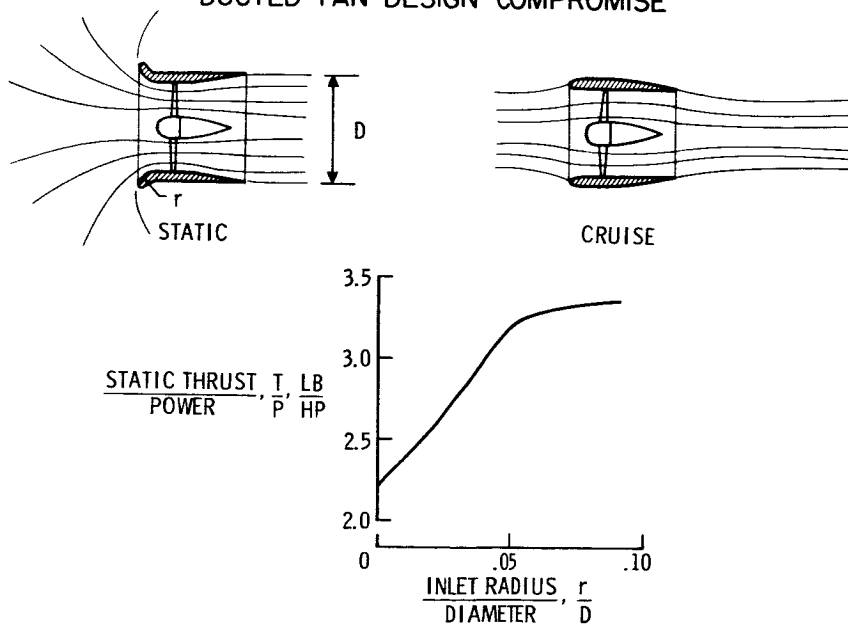


Figure 6

CRUISING SPEED AT SEA LEVEL
GROSS WEIGHT = 40,000 LB

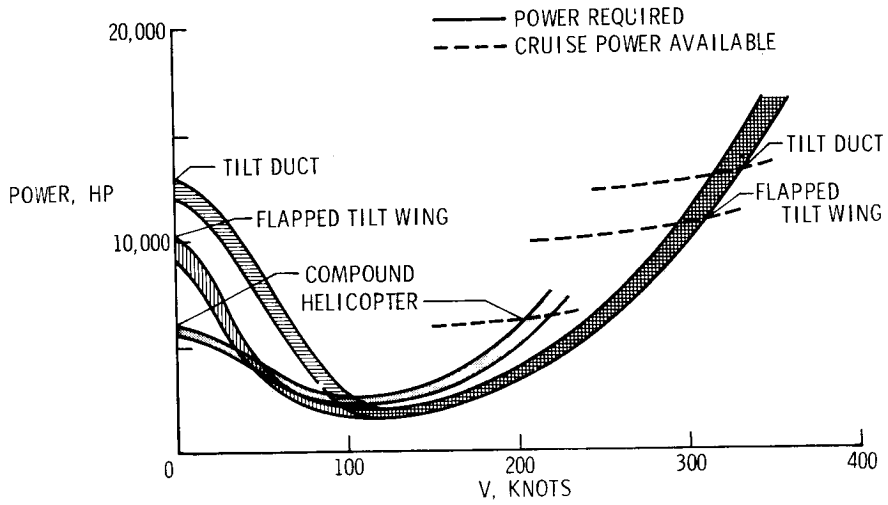


Figure 7

EFFECT OF ALTITUDE

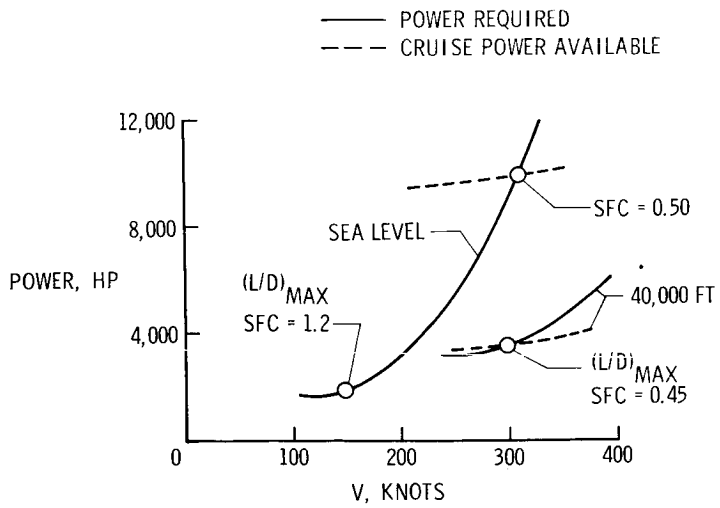


Figure 8

EFFECT OF WING SPAN AND AREA
 SEA LEVEL; GROSS WEIGHT = 40,000 LB; ASPECT RATIO = 7.6

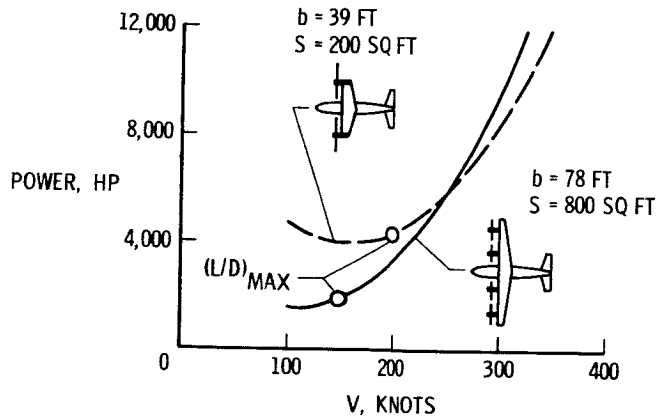


Figure 9

FUEL CONSUMPTION IN CRUISE
 40,000 FT ALTITUDE; GROSS WEIGHT = 40,000 LB

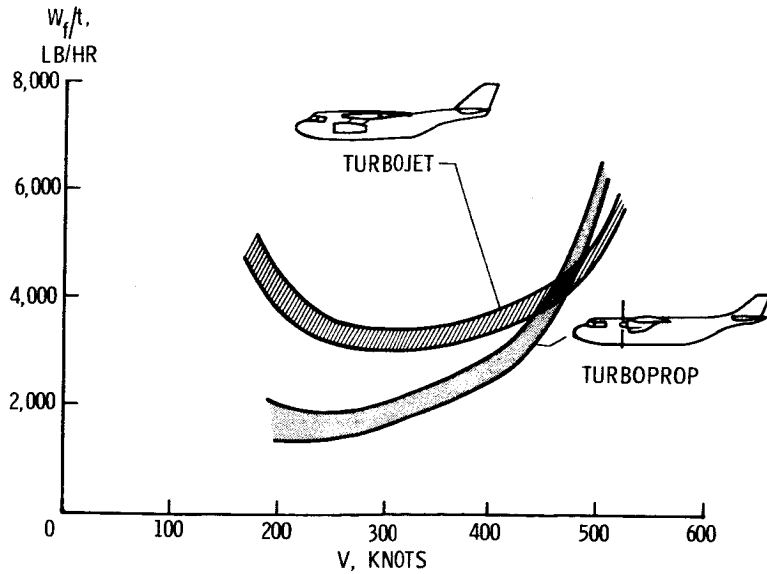


Figure 10

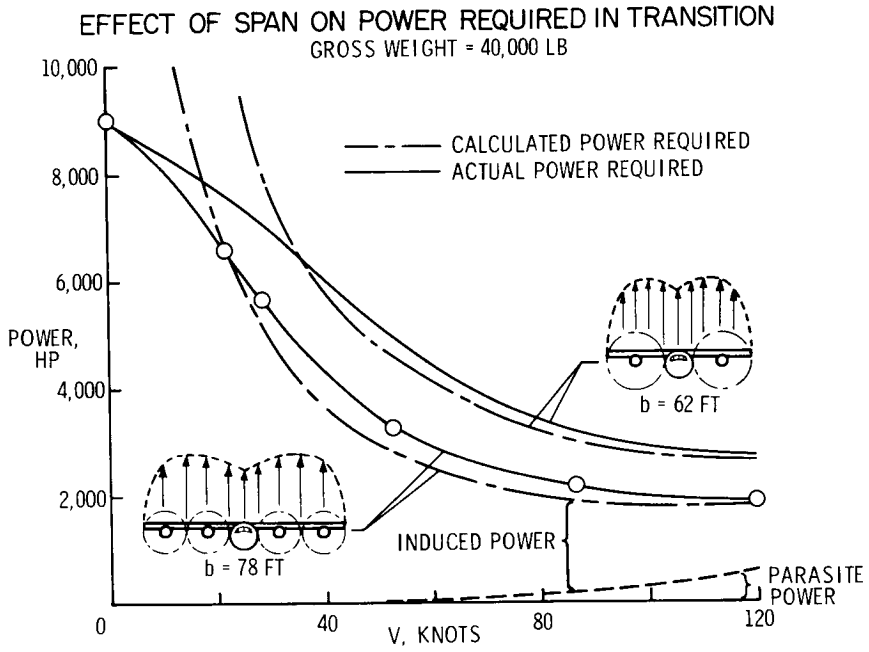


Figure 11

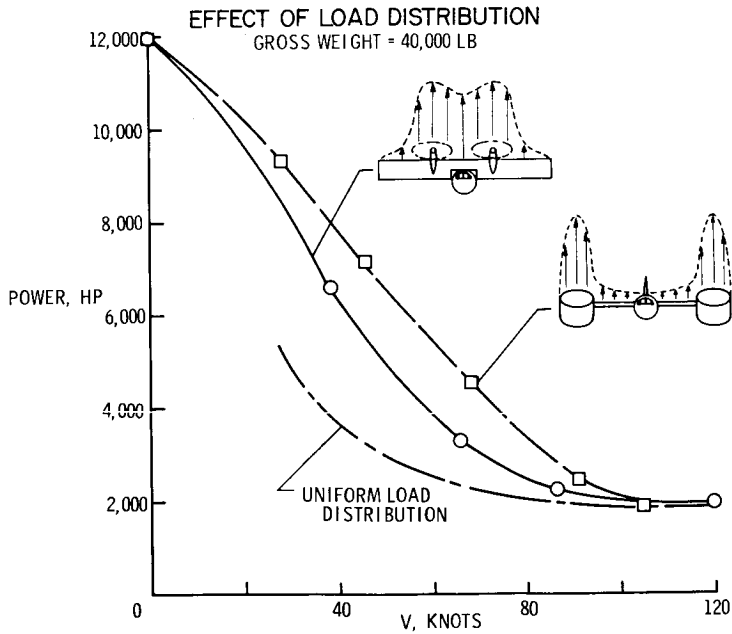


Figure 12

HOVERING AND CRUISE PERFORMANCE

$W_f = 0.03$ GROSS WEIGHT

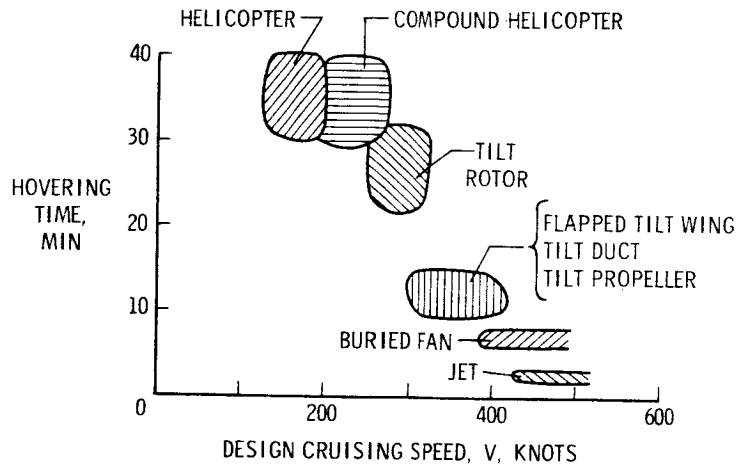


Figure 13

STOL PERFORMANCE

TAKE-OFF DISTANCE OVER 50-FOOT OBSTACLE;

$$\frac{W}{W_{VTOL}} = 1.2$$

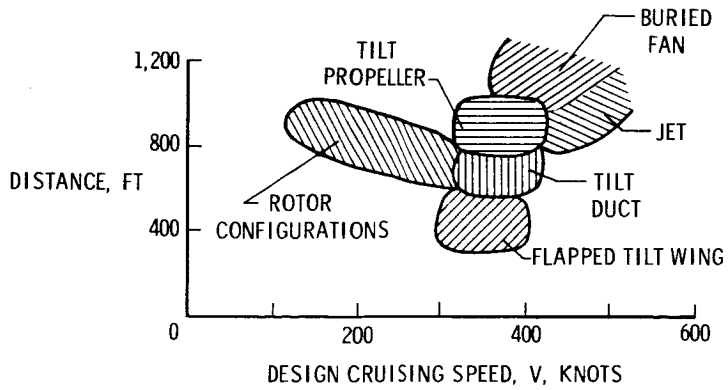


Figure 14

AERODYNAMIC CHARACTERISTICS OF PROPELLER-DRIVEN

VTOL AIRCRAFT

By Robert H. Kirby

Langley Research Center

SUMMARY

This paper discusses the two major configurations that are usually considered for achieving VTOL while keeping the fuselage essentially horizontal - that is, the tilt-wing and the deflected-slipstream configurations.

Because of the high turning losses incurred by deflected-slipstream configurations in hovering and because of the wing-stalling problem of the pure tilt-wing configurations during the transition, it appears that a combination of the two principles should be used. This tilt-wing and flap configuration should make use of a programed extensible-chord slotted flap together with a leading-edge high-lift device in order to avoid the performance and handling qualities problems associated with wing stalling during the transition while keeping the wing area as low as possible for efficiency in cruising flight.

INTRODUCTION

The purpose of this paper is to show some of the basic performance and aerodynamic characteristics of propeller-driven VTOL aircraft, to discuss the major problems involved, and to indicate solutions wherever possible. Under discussion are the two major propeller configurations that are usually considered for achieving VTOL while keeping the fuselage essentially horizontal - that is, the tilt-wing and the deflected-slipstream configurations. Only the hovering and transition ranges of flight are treated herein because in cruising flight these aircraft are essentially conventional propeller-driven airplanes with normal aerodynamic characteristics.

SYMBOLS

C_L	lift coefficient, $Lift/qS$
c	wing chord, ft
D	propeller diameter, ft
M_α	pitching moment due to change in angle of attack, ft-lb/deg
q	dynamic pressure, $\frac{1}{2}\rho V^2$, lb/cu ft
q_t	dynamic pressure at the tail, lb/cu ft
S	wing area, sq ft
V	airspeed, ft/sec
α	angle of attack, deg
ϵ	downwash angle, deg
ρ	air density, slugs/cu ft

DISCUSSION

Hovering

One of the major aerodynamic problems in hovering is illustrated in figure 1. In this figure the hovering effectiveness of deflected-slipstream configurations is shown in terms of the ratio of lift available for hovering to the propeller thrust plotted against the angle of slipstream deflection. For the deflected-slipstream configurations where large flaps are utilized to turn the slipstream through appreciable angles, there is a considerable loss in lift. The two curves in figure 1 are typical of the results obtained from tests on deflected-slipstream configurations. (See ref. 1.) The dashed curve, for a configuration employing two propellers, shows that only moderate angles of slipstream deflection can be achieved without incurring large losses. The solid curve, for a configuration with four propellers, shows that the turning losses are somewhat smaller. The effect resulting from the use of either two or four propellers is somewhat like an aspect-ratio effect - that is, the tip losses are greater for the two-propeller arrangement. These data

are for conditions out of ground effect; the effect of the ground on these and other VTOL configurations is discussed in reference 2. A tilt-wing configuration exhibits essentially no loss in lift because the propellers are tilted instead of the slipstream being deflected. These are the only points to be made in connection with the performance in the hovering flight range and the rest of the paper considers the characteristics in the transition range of flight.

Aerodynamic Factors Affecting Performance in Transition

In figure 2 is indicated the power required during transition for the tilt-wing and the deflected-slipstream configurations. These data and all other power-required data presented herein have been calculated for an assumed aircraft gross weight of 3,600 pounds. The dashed curve labeled "Ideal" shows the calculated induced power required with an assumed, uniform span loading without wing stalling, as discussed in reference 3. For hovering flight the deflected-slipstream configuration required considerably more power than that indicated by the ideal curve because of the losses incurred in turning; however, the power required for this configuration rapidly approaches that of the ideal curve as the speed increases. On the other hand, the tilt-wing configuration requires no more power than the ideal in hovering but rapidly diverges with forward speed and requires considerably more power during the transition than either the deflected-slipstream configuration or that indicated by the ideal curve. The excess power required during transition is caused by wing stalling. This wing stalling is a problem not only because of its effect on power required which is reflected in poor overload STOL performance (ref. 4) but also because of its large effect on handling qualities as is brought out in reference 5.

In order to understand this wing stalling, figure 3 is presented and shows in schematic form the wing angle of attack during transition flight for the level-flight, climb, and descent conditions. For the level-flight condition, a horizontal vector represents the forward-flight velocity and another vector represents the incremental velocity added by the propeller. These two vectors give the resultant velocity that is experienced by the wing. The angle of this resultant vector to the wing is then the angle of attack that the wing experiences. Of course, changes in disk loading change the incremental velocity added by the propellers. A higher disk loading gives a higher slipstream velocity and therefore reduces the wing angle of attack. Also, the portions of the wing that are not in the propeller slipstream experience a very high angle of attack under these conditions. This effect and the effect of changes in disk loading are discussed in the next paper by Mark W. Kelly. Also, in figure 3 are shown the effects of climb and descent on the wing angle of attack. The conditions shown are for maintaining constant

forward velocity and wing attitude with respect to the ground. For the descent condition, the power is reduced which, in turn, reduces the slipstream velocity increment added by the propeller, and the direction of the free-stream velocity is also changed. As a result of these two changes, there is a considerable increase in the angle of attack of the wing in descent. For the climb condition, the velocity changes are in the opposite direction and, therefore, the angle of attack is reduced.

Figure 4 shows a typical variation of angle of attack of the wing with forward speed for the descent, level-flight, and climb conditions. The dashed line shows the approximate stall angle of attack of a representative airfoil. Figure 4 shows that, if a wing was about at the stall angle in level flight, it would stall in descent over a wider range of speeds but would be unstalled in climbing flight. It also appears from this figure that stalling might not occur in level flight, except over a small range of speeds. However, the stall picture is not as clear cut as indicated by this figure. This representation is that which would be obtained with counterrotating propellers where there is no rotation in the slipstream. For the single-rotation propeller, the slipstream rotation complicates the problem, as indicated in figure 5.

Figure 5 shows the variation of wing section angle of attack with speed. The curve for level flight with no rotation is reproduced from figure 4. Actually, as shown by the sketch at the bottom of figure 5, the slipstream rotation causes an increase in angle of attack on one side of the propeller disk and a decrease on the other side. The magnitude of the change in angle of attack for the case indicated by the sketch is shown by the other two curves. The top curve shows that the wing sections experiencing upward flow from the slipstream are stalled for practically the entire transition range, whereas the bottom curve indicates an unstalled condition, at least for level flight, for the wing sections experiencing downward flow from the slipstream.

Figures 2 to 5 have presented the problem of wing stalling on tilt-wing configurations during the transition range of flight. Ways to reduce this problem are now considered. The approaches to use are indicated in a qualitative way in figure 6. This figure shows lift curves for a wing with high-lift devices. If the wing is near stall, one means of avoiding it is to increase the stall angle of the wing by the use of a slat or some other leading-edge device. Another means of avoiding stalling is to use a flap which, for the same lift, reduces the wing angle of attack to get away from the stall region. Of course, both the flap and slat can be used to get double benefit. Another way, which is not shown directly in figure 6, is to use more chord and therefore more wing area. With more wing area the required lift can be produced with a lower lift coefficient which again moves the wing farther from the stall region.

Figures 7 to 9 show some experimental data demonstrating the use of these cures. Figures 7 and 8 are based on the data contained in reference 6 and figure 9 is based on the data in reference 7.

Figure 7 shows the effect of wing chord on power required as a function of speed for wings having chord-diameter ratios of 0.33, 0.50, and 0.75. This might also be considered the effect of wing area - that is, the area immersed in the propeller slipstream. Figure 7 shows very readily that as the wing chord is increased, the power required is markedly reduced.

Figure 8 shows the effect of a slat on power required for the three wings of different chord-diameter ratios used in figure 7. For each wing curves are shown for no slat, slat on, and the ideal case. Again, it is evident that the slat made a significant improvement in the power required and presumably in the wing stalling.

The effect of flaps on the power required is shown in figure 9 for the pure tilt-wing configuration and for the same wing with a 40-percent extensible-chord slotted flap deflected 50° throughout the range of flight. The use of this flap gives a power-required curve that very closely approaches the ideal curve. With the flap deflected 50° , however, a considerable increase in power is required for hovering. In actual practice, then, it would seem more logical to program the movement of the flap so that the flap would be at 0° for hovering and cruise but would be deflected for intermediate angles of tilt through the speed range.

From figures 7 to 9 it can be seen that the use of either adequate wing chord, slats, or flaps tends to reduce the effect of wing stalling during the transition range of flight. The question, then, is which approach and how much of each to use. For example, for the case illustrated in figure 9, the use of a large wing chord and a flap ($c/D = 0.84$ with flap extended) results in performance that probably cannot be improved by the addition of a slat. In actual practice, however, the wing of a propeller-driven airplane tends to be overly large for maximum performance in cruising flight and therefore it is of interest to keep the wing area or wing chord as small as possible for cruising flight. For this reason, it appears that flaps and slats should be used to their fullest extent during transition and the chord should be made just large enough to avoid serious stalling. Also, it seems logical that a flap that extends the chord of the wing when deflected should be used in order to keep the area of the basic wing to a minimum for cruising flight.

Aerodynamic Factors Affecting Stability and Trim

In figure 10 the pitching moment for the steady-flight condition throughout the transition range is shown for the tilt-wing and deflected-slipstream configurations. The pitching moment is presented as the amount

of trim force required at the tail in percent of gross weight. Basically the tilt-wing configuration tends to give a nose-up pitching moment during transition because of a large nose-up moment produced by the propeller itself. The deflected-slipstream configuration has nose-down pitching moments because of the diving moments of the flaps about a center of gravity located at the quarter-chord station that was used in this figure. The magnitude of these pitching moments for both configurations is such that large trim forces would be required at the tail at airspeeds that are so low that the horizontal tail could not be expected to have an appreciable effect. These moments would therefore impose a severe additional requirement on the hovering controls which, from other considerations, would be required to produce a force at the tail of about ± 5 percent of the gross weight.

The two curves in figure 10 indicate that for a combination tilt-wing and deflected-slipstream configuration, the flaps could be programed to give effectively zero pitching moment throughout the whole transition range. This point has been checked out in wind-tunnel tests and it was found that the pitching moments can be trimmed out with a relatively modest amount of flap or by simply a single slotted or extensible-chord slotted flap. These tests also showed that for this combination tilt-wing and flap configuration the program of flap deflection required to eliminate the pitching moment was also very effective in minimizing wing stalling and in achieving a desirable low power-required curve.

Figure 11 indicates the characteristics of the air flow at the tail for an arrangement shown by the sketch. The data, however, are reasonably representative of the flow for either the tilt-wing, deflected-slipstream, or combination tilt-wing and flap configuration. The top curve shows that there is a considerable range of speeds where the dynamic pressure at the tail q_t is so low that the horizontal tail would not have any effectiveness and the pilot would have to rely entirely on the hovering controls. The middle curve shows that there is a large variation of downwash angle over the speed range and, therefore, a variable-incidence horizontal tail would probably have to be installed to keep the tail from producing undesirably large nose-up pitching moments during the latter part of the transition. The bottom curve shows the variation of the downwash factor $(1 - \frac{d\epsilon}{d\alpha})$, a stability factor which influences the effectiveness of the tail for producing static longitudinal stability. Small values indicate that the tail will be ineffective, whereas large values indicate that the tail will be very effective.

From the bottom and top curves of figure 11, it is evident that at low speed, not only is the force produced small because of low q_t but the force produced is not very effective for static stability because of the unfavorable downwash characteristics.

In figure 12 the variation of static longitudinal stability - that is, stability of attitude - in the transition range is presented for seven different configurations that have been tested: two deflected-slipstream, three tilt-wing, and two combination tilt-wing and flap configurations. The data show that all these configurations tend to be unstable at low speed and become stable at higher forward speeds, as expected from the results of the data in figure 11.

The degree of static longitudinal stability is indicated in figure 12 in dimensional terms (ft-lb/deg) since ordinary nondimensional coefficients based on forward speed lose their significance as the speed approaches zero. The data from these different configurations, both full scale and model, were scaled to represent an aircraft weighing about 3,600 pounds in order to show them in the same plot. The actual numbers are not important. The significant point is that the trend is about the same for all the widely different configurations and all become stable at about the same speed. The instability in the low speed range has not seemed to bother the pilots flying the test beds, probably because of the low speeds involved. Also, it should be remembered that the static stability parameter M_{α} is only one of the factors affecting longitudinal flight characteristics.

Control

The amount of control required for propeller-driven VTOL aircraft is discussed in reference 8 but the point to be discussed in this paper is the means of obtaining this control in hovering and low-speed flight with propeller-driven configurations. Roll control and yaw control are fairly straightforward. It is evident that the variable pitch propeller controls that will already be on the airplane can be used for roll control. It also seems likely that the flaps or ailerons, which would be in the propeller slipstream, can be used for yaw control, although this idea has been only partially checked out by research. Pitch control, however, is not so straightforward and depends to a great extent on the wing position, as is indicated in figure 13.

Shown in figure 13 are three possible wing arrangements: a low wing with the pivot forward on the wing chord and two high wings - one with a forward pivot, such as that used on the tilt-wing test beds, and one with a rear pivot. Concerning the low wing arrangement, it can be seen that the trailing-edge flaps have an appreciable moment arm from the aircraft center of gravity which gives the possibility of obtaining pitch control from these flaps in hovering and low-speed flight. However, with the high wing arrangements, the flap load is so close to the center of gravity that the flaps are ineffective for pitch control and some other means of control must be used. One method is the installation of cyclic pitch

control and flapping blades. Another and perhaps a simpler method would be the use of an auxiliary control such as a tail rotor, as indicated in the sketches of figure 13. Of course, aerodynamics is not the only consideration in selecting a wing arrangement. For example, two other considerations that are obvious from the sketches are that the low wing gives a high fuselage which results in loading problems (particularly for military applications) and that the high wing with forward pivot gives very little structural carry-through in the center of the wing since most of the wing chord has to pivot beside the fuselage.

CONCLUDING REMARKS

Because of the high turning losses incurred by deflected-slipstream configurations in hovering and because of the wing-stalling problem of the pure tilt-wing configuration during the transition, it appears that for a propeller-driven VTOL aircraft, a combination of the two principles should be used. This tilt-wing and flap configuration should make use of a large extensible-chord slotted flap together with a leading-edge high-lift device in order to avoid the performance and handling qualities problems associated with wing stalling during the transition while keeping the wing area as low as possible for efficiency in cruising flight.

The flap should be programmed so that it is at zero deflection with 90° wing incidence for high hovering efficiency and is deflected only in the transition range of flight. The actual flap programming can be chosen to give both minimum pitch trim through the transition range and near optimum results from the power-required and wing-stalling considerations. Since this arrangement results in a low power-required curve, it would also have good STOL performance.

REFERENCES

1. Kuhn, Richard E.: Semiempirical Procedure for Estimating Lift and Drag Characteristics of Propeller-Wing-Flap Configurations for Vertical- and Short-Take-Off-and-Landing Airplanes. NASA MEMO 1-16-59L, 1959.
2. Schade, Robert O.: Ground Interference Effects. (Prospective NASA paper.)
3. Kuhn, Richard E.: Review of Basic Principles of V/STOL Aerodynamics. (Prospective NASA paper.)
4. Kuhn, Richard E.: Take-Off and Landing Distance and Power Requirements of Propeller-Driven STOL Airplanes. Preprint No. 690, S.M.F. Pub. Fund Preprint, Inst. Aero. Sci., Inc., Jan. 1957.
5. Reeder, John P.: Handling Qualities Experience With Several VTOL Research Aircraft. (Prospective NASA paper.)
6. Taylor, Robert T.: Wind-Tunnel Investigation of Effect of Ratio of Wing Chord to Propeller Diameter With Addition of Slats on the Aerodynamic Characteristics of Tilt-Wing VTOL Configurations in the Transition Speed Range. NASA TN D-17, 1959.
7. Kuhn, Richard E., and Hayes, William C., Jr.: Wind-Tunnel Investigation of Longitudinal Aerodynamic Characteristics of Three Propeller-Driven VTOL Configurations in the Transition Speed Range, Including Effects of Ground Proximity. NASA TN D-55, 1960.
8. Anderson, Seth B.: An Examination of Handling Qualities Criteria for V/STOL Aircraft. NASA TN D-331, 1960.

HOVERING EFFECTIVENESS OF DEFLECTED-SLIPSTREAM CONFIGURATIONS

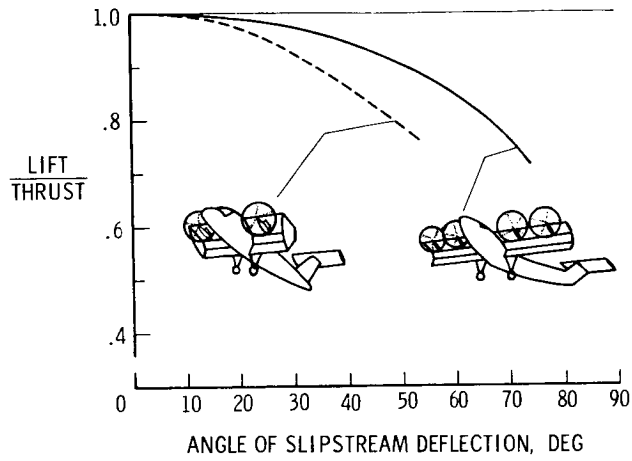


Figure 1

POWER REQUIRED DURING TRANSITION

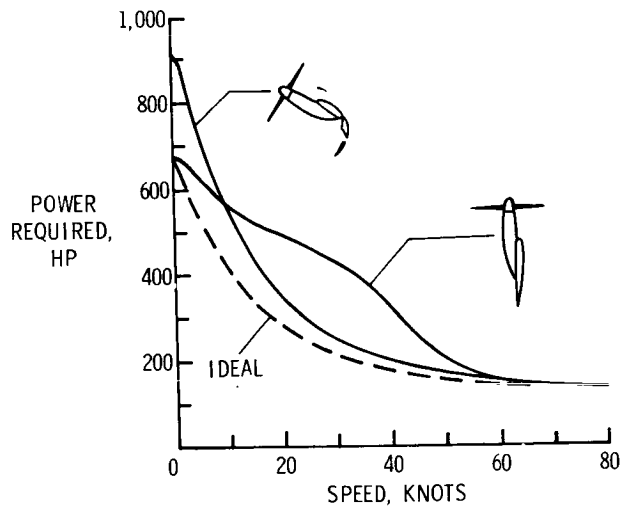


Figure 2

WING ANGLE OF ATTACK DURING TRANSITION FLIGHT

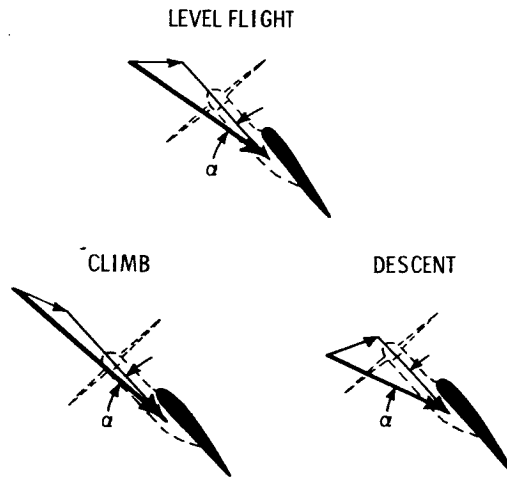


Figure 3

TYPICAL VARIATION OF ANGLE OF ATTACK WITH SPEED

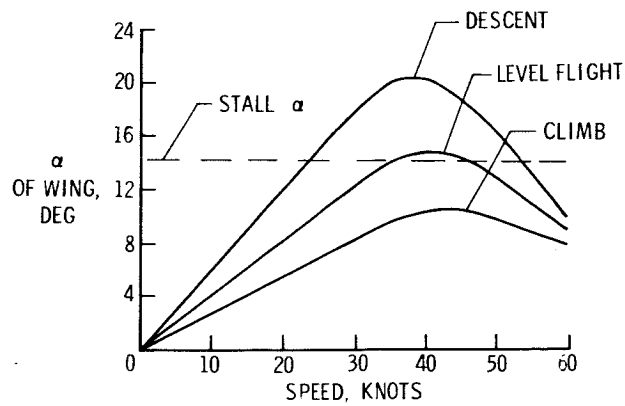


Figure 4

EFFECT OF SLIPSTREAM ROTATION ON ANGLE OF ATTACK

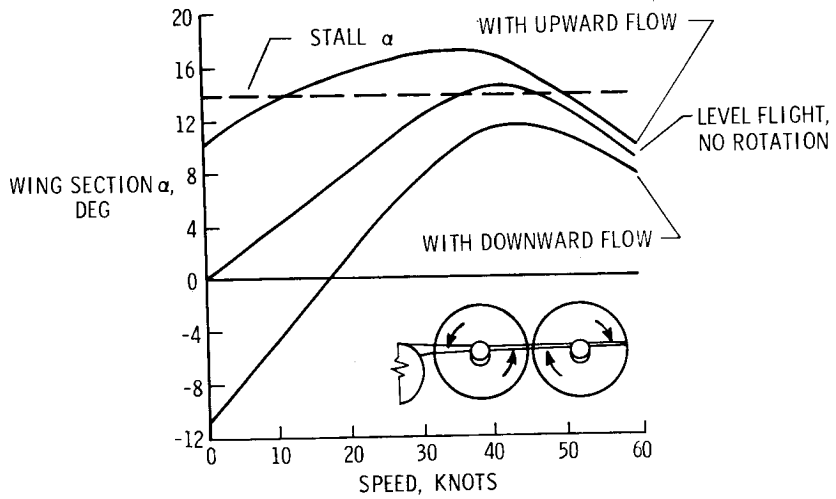


Figure 5

CHANGES IN LIFT CURVES CAUSED BY HIGH-LIFT DEVICES

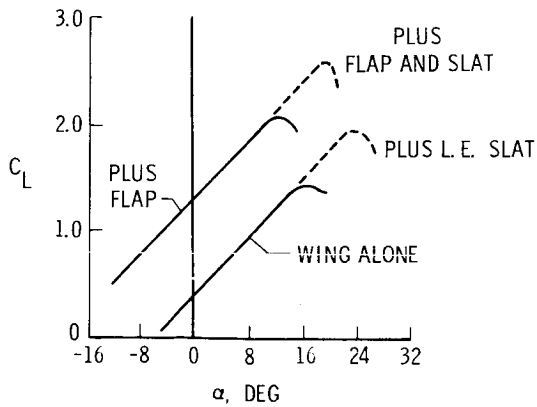


Figure 6

EFFECT OF WING CHORD

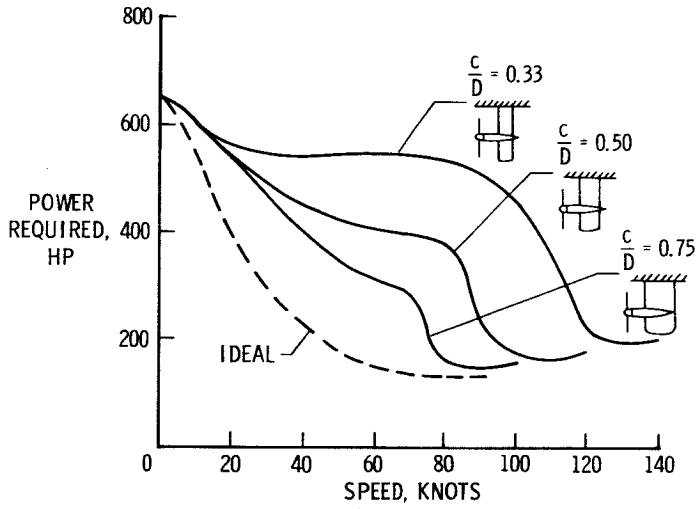


Figure 7

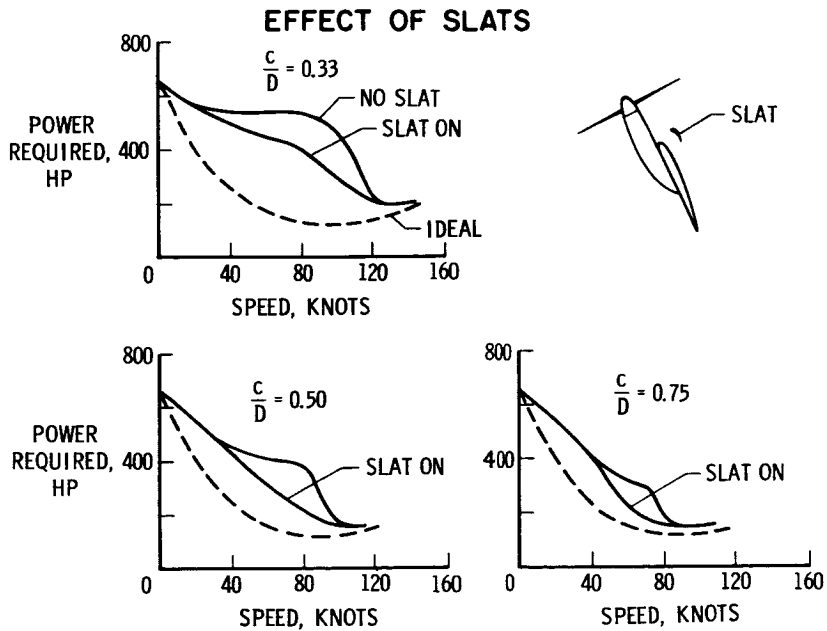


Figure 8

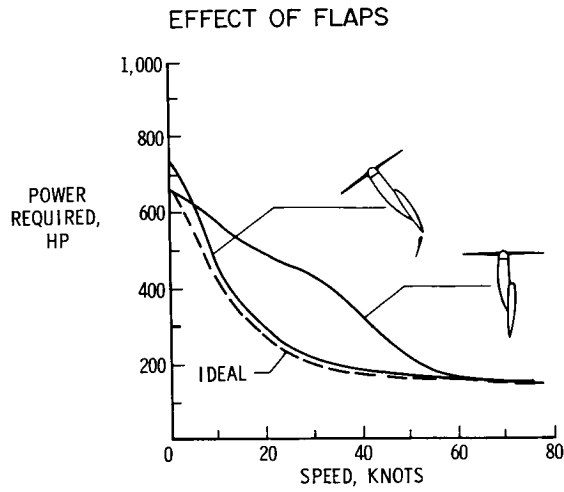


Figure 9

VARIATION OF PITCHING MOMENT WITH SPEED CENTER OF GRAVITY AT 0.25c̄ IN CRUISE

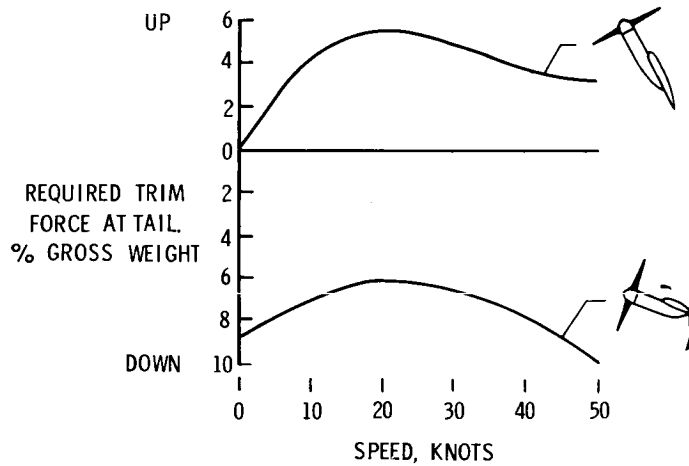


Figure 10

CHARACTERISTICS OF THE AIRFLOW AT TAIL

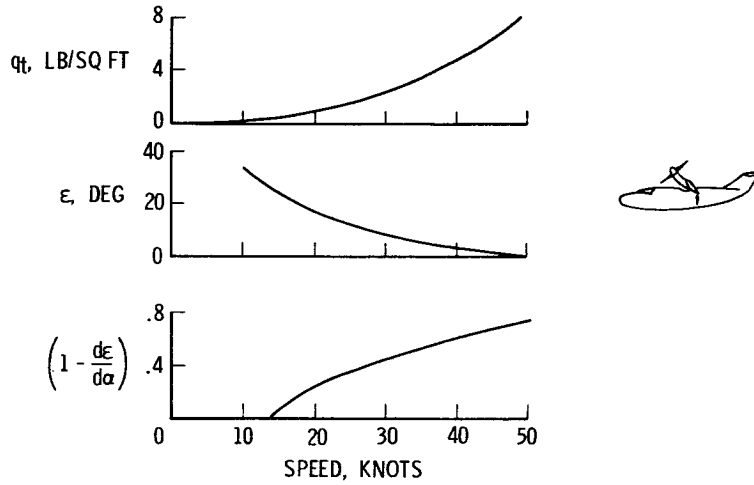


Figure 11

STATIC LONGITUDINAL STABILITY

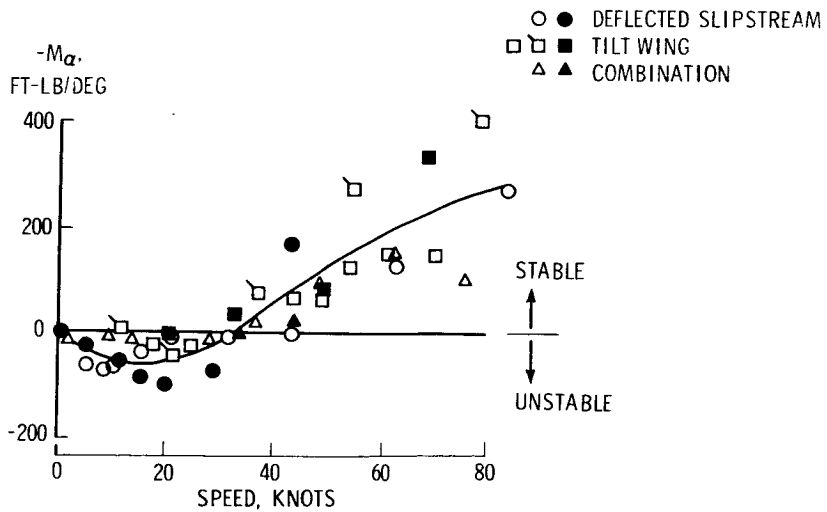
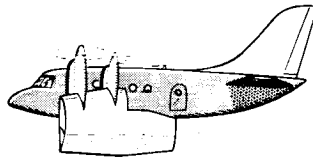
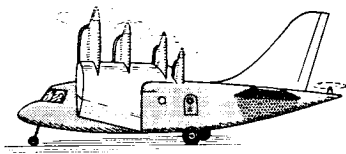


Figure 12

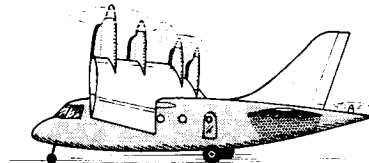
LOW AND HIGH WING ARRANGEMENTS



LOW WING, FORWARD PIVOT



HIGH WING, FORWARD PIVOT



HIGH WING, REAR PIVOT

Figure 13

LARGE-SCALE WIND-TUNNEL STUDIES OF SEVERAL VTOL TYPES

By Mark W. Kelly

Ames Research Center

INTRODUCTION

In recent years several full-scale wind-tunnel investigations of various VTOL airplane configurations have been made by the National Aeronautics and Space Administration. These investigations have ranged from concepts using helicopter-type rotor systems, intended generally for cruising speeds up to the order of 200 to 300 knots, to those using high-disk-loading fans or engines, intended for cruising at high subsonic or, ultimately, supersonic speeds.

Typical schematic arrangements of the three categories of VTOL aircraft to be discussed in this paper are shown in figure 1. They include: (1) those using lightly loaded helicopter-type rotors, (2) those using moderately loaded airplane-type propellers, and (3) those using highly loaded ducted fans or lifting engines. The aircraft are described in detail in references 1 to 3 and in a subsequent paper by Ralph L. Maki and David H. Hickey. The purpose of this paper is to summarize the main results and conclusions applicable to these three VTOL aircraft concepts and, in particular, to define those problem areas in which further research and development is required.

SYMBOLS

ΔL	lift due to fan
F_{F_0}	fan static thrust
ΔD_F	drag due to fan
ΔM_F	moment due to fan
R	fan radius
V_∞	free-stream velocity
A	rotor disk area

D_m	momentum drag
m_j	fan mass flow
F_j	fan gross thrust
v_j	jet velocity
θ	jet deflection angle
T	propeller thrust
q	dynamic pressure
$C_{L_{MAX}}$	maximum lift coefficient
α_w	local angle of attack of wing
V_s	slipstream velocity
C_D	drag coefficient
C_L	lift coefficient
δ_F	flap deflection
δ_w	wing tilt angle
γ	flight-path angle
S_B	blade area
q_∞	free-stream dynamic pressure
W	weight
L/D	lift-drag ratio
\bar{C}_L	blade section mean lift coefficient
ρ	density

V_T	tip speed
V/nD	advance ratio
η	propulsive efficiency
$\phi = \text{arc tan } \frac{V}{\pi nD}$	

DISCUSSION

VTOL Concepts Employing Helicopter-Type Rotor Systems

Two concepts of VTOL aircraft using lightly loaded helicopter-type rotors have been investigated: (1) the unloaded-rotor convertiplane, typified by the McDonnell XV-1 and (2) the tilting-rotor convertiplane, typified by the Bell XV-3. Both of these machines use rotors having hovering disk loadings of the order of 5 to 7 pounds per square foot, which result in relatively low slipstream velocities in hover, of the order of 20 to 30 knots.

The power-weight ratio as a function of flight velocity for the XV-1 unloaded-rotor convertiplane is shown in figure 2 for both autogyro flight at high rotor speed and unloaded-rotor flight at low rotor speed. For comparison, power-weight ratio for the airplane with the rotor removed is also shown. These data indicate what is believed to be a fundamental limitation to the performance of this type of machine, namely, the high profile drag associated with the unloaded rotor. For this particular airplane the drag of the rotor blades and hub accounted for 45 percent of the total drag of the machine in airplane flight. The drag of the rotor could be decreased by further reducing rotor speed; however, this reduction in rotor speed will tend to increase rotor-blade flapping problems. On future designs this rotor drag could perhaps be reduced, but it is believed that it will always represent a significant percentage of the total airplane drag.

A similar plot of power-weight ratio as a function of flight speed for the XV-3 tilting-rotor convertiplane in both helicopter configuration and airplane configuration, with high and low rotor speed, is shown in figure 3. It should be noted that the power shown here is shaft power and includes the rotor efficiency. If the rotor speed in airplane flight is the same as that used for helicopter flight, the increment in flight speed obtained by conversion from helicopter to airplane configuration is only about 10 knots and is largely due to a reduction in

propulsive efficiency of the rotor due to the low thrust required in airplane flight compared with that in helicopter flight. In order to avoid this loss in propulsive efficiency the XV-3 employs a gear shift to reduce rotor speed for cruise. This lower rotor speed enables the rotor blade elements to operate at high pitch closer to maximum L/D and results in propulsive efficiencies of the order of 80 percent. Even so, the maximum speed of the airplane is limited to approximately 125 knots. This limitation is due both to low installed power and to high profile drag. This high profile drag is not, of course, fundamentally involved in the tilting-rotor concept and could be reduced substantially on future designs. The effect of such a drag reduction on the XV-3 is shown in figure 4, which presents propulsive power available and propulsive power required for the existing XV-3 and for the airplane with the profile drag reduced by 50 percent. At the higher speeds there is a reduction in the power available due to a reduction in propulsive efficiency with increasing advance ratio for constant power coefficient. This reduction in propulsive efficiency could be alleviated by a further decrease in rotor speed. However, in the case of the teetering rotor used on the XV-3, such a reduction in rotor speed results in an increase in rotor blade flapping. As discussed in a subsequent paper by Hervey C. Quigley and David C. Koenig, this rotor flapping can lead to undesirable effects on airplane dynamic stability. This flapping problem can possibly be alleviated by mechanical means, such as pitch-flap coupling (δ_3), and it is believed that further research on this subject is definitely worthwhile.

It should be noted at this point that this necessity to operate the rotor at high advance ratios and high power coefficients to obtain high values of propulsive efficiency is not peculiar to low-disk-loading rotors such as that on the XV-3. The reason for this is that, regardless of disk loading, propellers having sufficient blade area to provide static thrust equal to aircraft weight in hovering flight will have too much blade area for efficient operation at the reduced thrust levels required during cruise, unless they are operated at high advance ratios. It is emphasized that this is true regardless of disk loading. The preceding statements are illustrated in figure 5, which shows the variation of propeller blade-loading coefficient with advance ratio required for optimum propulsive efficiency. Propeller blade-loading coefficient is defined here as propeller thrust per square foot of blade area divided by the free-stream dynamic pressure. For typical propellers, operation in or near the shaded area will result in propulsive efficiencies of the order of 80 percent or more over the range of advance ratios shown. A representative data point for the XV-3 rotor propeller at high rotor speed indicates the order of efficiency obtained when the propeller is operated far from the shaded area, in this case 60 percent. Also shown is a data point for the XV-3 rotor propeller at low rotor speed, which verifies that operation near the shaded area results in efficiencies of about 80 percent. From the equation shown in the upper right-hand

corner of figure 5, it is seen that, for all VTOL propellers, the blade-loading coefficient during cruise is equal to the blade loading in hover W/S_B divided by the product of airplane lift-drag ratio and free-stream dynamic pressure. This equation is obtained from the conditions that thrust equals drag and lift equals weight for level unaccelerated flight. From this equation it is seen that VTOL configurations having high lift-drag ratios and high cruise speeds will tend to low values of blade-loading coefficient and thus to high advance ratios for optimum propulsive efficiency. By noting that the blade-loading coefficient during cruise is the hovering blade loading W/S_B divided by the product of airplane lift-drag ratio and cruising dynamic pressure, it is seen that two methods of raising the blade-loading coefficient to a higher level exist: (1) the dynamic pressure for a given cruise velocity can be reduced by cruising at altitude, and (2) the hover blade loading can be increased. However, as shown in the lower equation in figure 5, the hover blade loading is determined by the blade-section mean lift coefficient and tip speed used in hovering flight. Thus, there is a limit to the value of blade loading that can be obtained if blade stall and compressibility losses are to be avoided. The use of variable-camber propellers to obtain high values of mean lift coefficient appears to be one promising way of obtaining the desired increase in hover blade loading.

This discussion has shown that propellers having sufficient blade area to provide thrust equal to weight in hover will have too much blade area for efficient operation at the low thrust levels required in cruise, unless they are operated at high advance ratios, regardless of disk loading. One favorable aspect of high-advance-ratio operation is that the blade twist required diminishes as the advance ratio is increased, which is in the direction to more nearly match the relatively low twist required for optimum hovering efficiency. For rotor propellers having blades free to flap, the magnitude of blade flapping will generally increase with increasing advance ratio, unless special measures are taken to avoid this effect.

VTOL Concepts Using Moderately Loaded

Airplane-Type Propellers

Two types of VTOL aircraft using moderately loaded airplane-type propellers are considered; namely, the deflected slipstream and the tilt-wing-deflected-slipstream configurations. One important requirement for these aircraft is that the slipstream velocity must be high enough to keep the local wing angle of attack below that for wing stall. The ratio of propeller disk loading to free-stream dynamic pressure required to keep the local wing angle of attack below 15° is shown in figure 6 as a

function of free-stream angle of attack. As noted in this figure, the ratio of disk loading to free-stream dynamic pressure is a function of the ratio of slipstream velocity to free-stream velocity. The boundary curve shown was computed from rotor momentum theory with the condition that the local wing angle of attack indicated in the velocity triangle should not exceed 15° . The ratio of disk loading to dynamic pressure can be increased basically in three ways: (1) by increasing propeller disk loading, (2) by decreasing wing loading, and (3) by increasing wing lift coefficient by the use of high-lift devices. Inasmuch as propeller disk loading directly affects hovering performance, whereas wing loading affects cruise performance, a careful study of these conflicting requirements must be made to obtain the best compromise.

The problem of wing stall is accentuated in descending or decelerating flight. Therefore, it is important that the selection of disk loading, wing loading, and high-lift devices be made to ensure that the desired angles of descent can be attained without encountering wing stall. The importance of wing stall is indicated in figure 7. On the left of this figure is shown lift coefficient as a function of net drag coefficient for the Ryan VZ-3RY deflected-slipstream airplane. The vertical axis ($C_D = 0$) represents a condition of steady level flight, whereas the sloping lines represent the conditions for angles of descent of 10° and 20° . For the ratio of disk loading to dynamic pressure shown, it is seen that steady level flight can be maintained with some margin on wing stall, whereas an angle of descent of 10° requires flight very near wing stall, and an angle of descent of 20° requires flight beyond wing stall.

On the right-hand side of figure 7 are presented similar data obtained from full-scale wind-tunnel tests of a deflected-slipstream-tilt-wing airplane. As shown in the sketch in the lower right-hand corner of the figure, this configuration utilized both leading- and trailing-edge flaps. The trailing-edge flaps were equipped with boundary-layer control to increase their effectiveness. With these high-lift devices and with the relatively high ratio of disk loading to wing loading of this configuration, higher descent angles were expected than were experimentally obtained. The reason for this result apparently was that a large area of flow separation was encountered on the center section of the wing which spanned the fuselage and was not in the propeller slipstream. This flow separation not only limited maximum lift but also resulted in severe buffet. With regard to this buffeting it should be noted that these data were obtained at free-stream velocities which corresponded to wing loadings of about 20 pounds per square foot. On larger aircraft with higher wing loadings and flying at correspondingly higher speeds, it is anticipated that this buffeting would be very objectionable. These results indicate the importance of minimizing flow separation on portions

of the wing outside of the propeller slipstream. Two possible approaches to alleviating this problem are (1) eliminate the flow separation by using more powerful stall control devices or lower wing tilt angles, and (2) minimize the area of the wing outside of the propeller slipstream.

Ducted Fans

Two general types of VTOL aircraft using ducted fans have been investigated, namely, those with fixed ducts such as the fan-in-wing or fan-in-fuselage designs, and those having tilting ducts. The flow mechanics involved in all ducted-fan units are illustrated in figure 8, which is a schematic sketch of the flow through a fan-in-fuselage configuration. The momentum of the free-stream air captured by the fan produces a drag force which is termed momentum drag. The line of action of this free-stream momentum is generally above the moment center of the vehicle; thus, a nose-up moment is also produced. If thrust is obtained by vectoring the fan exhaust rearward, as indicated by the example shown here, and if the line of action of this thrust force is below the center of gravity, an additional nose-up moment will be produced. These effects are illustrated in figure 9 which shows lift and drag due to the fan divided by fan static thrust, and moment due to the fan divided by the product of fan static thrust and fan radius, all plotted against free-stream velocity in knots. These data were obtained from full-scale wind-tunnel tests of the Vanguard fan-in-wing airplane and from a fan-in-fuselage configuration which utilized the General Electric lift-fan engine. These vehicles are shown in figure 10. The static disk loading for the fan-in-wing data was 12 pounds per square foot, whereas that for the fan-in-fuselage data was 215 pounds per square foot. The general characteristics anticipated from figure 8 are evident, namely, a buildup in drag and nose-up moment with speed. The indicated increase in lift with speed is due both to an increase in mass flow through the fan due to ramming of the inlet and to lift induced on the wing by the fan. It should be noted that the change of lift, drag, and moment with speed is more pronounced for the low-disk-loading configuration than it is for the high-disk-loading configuration, since a larger mass flow is required for a given thrust level.

The right-hand side of figure 9 presents the same lift, drag, and moment parameters as a function of nondimensionalized forward speed. For identical configurations this type of presentation should remove the effects of disk loading so that the differences shown here are primarily due to configuration differences. Also shown on the lift and drag plots is an estimated variation of lift and drag with speed by using simple momentum theory and assuming 100-percent inlet efficiency. As a matter of interest, the inlet loss on the fan-in-fuselage configuration was less than 5 percent of the dynamic pressure in the inlet for values of nondimensionalized speed up to 0.55. For this configuration the difference

between the estimated and experimentally obtained lift was found to be due to wing lift induced by the fan. For the fan-in-wing configuration, large inlet losses were encountered at the higher nondimensionalized forward speeds, and it is believed that this fact partly accounts for the lower lift and drag obtained. The results obtained from these two investigations are remarkably similar when the effects of disk loading are eliminated by nondimensionalizing the forward speed, in spite of the large differences between the two configurations. These results indicate that the drag is largely due to momentum drag, and it is likewise believed that the pitching moment is mainly due to the change in angular momentum of the air captured by the inlet. Since these momentum effects are a function of the product of fan mass flow and flight velocity, they can be reduced by reducing the mass flow as the flight velocity is increased. One method of doing this is to transfer as much of the load as possible to the wing during transition so that the fan thrust and mass flow may be progressively reduced as the speed is increased. Also, it should be noted that the power required to overcome the momentum drag may be either large or small, depending on how much of the energy of the captured air is dissipated in losses in the system.

These momentum changes are also important for the tilting-duct designs and result in large duct normal forces and pitching moments in the transition from hovering to forward flight. These duct moments can be reduced and, in principle, could be eliminated by the use of exit vanes in the duct exhaust so that the required momentum changes are accomplished aft as well as forward of the moment center.

Also, for the tilting-duct configuration, it should be noted that good propulsive efficiencies in cruise flight must be obtained with a unit which basically is sized to meet the hovering requirement. This situation is directly analogous to that discussed previously for VTOL propellers and will require the ability to vary fan blade angle and/or duct geometry.

CONCLUSIONS

In conclusion, full-scale wind-tunnel research on various VTOL aircraft concepts conducted thus far indicate that:

1. Rotor propellers and ducted fans having sufficient blade area to support the vehicle in hovering flight will have more blade area than that required for maximum efficiency in cruise flight, regardless of disk loading. This loss in propulsive efficiency may be minimized by operating the propeller at high advance ratios. The implications of high-advance-ratio operation on efficiency, loads, and blade motions are

believed to be worthy of further study, particularly for rotor-propellers having blades free to flap, where large flapping angles have been encountered.

2. The ability of vectored-slipstream and tilt-wing aircraft to make steep descents or to decelerate is limited by the occurrence of wing stall. Continued research to eliminate or alleviate the effects of wing flow separation is believed to be desirable, particularly at large scale.

3. For ducted-fan configurations the drag and pitching moment due to the momentum changes of the air captured by the fan will possibly result in serious power and control problems in transition flight. In general, it appears desirable from both a momentum-drag and pitching-moment standpoint to carry as much lift as possible on the wing in the transition; as a result, the fan thrust output can be reduced as the flight speed is increased and thereby the associated momentum drag and moment are reduced.

Finally, as stated in the introduction, the purpose of this paper was to present the basic problem areas encountered in the various VTOL concepts tested to date. Therefore, favorable aspects of the various configurations were presumed to be outside the scope of the present discussion. Although the various problem areas discussed are believed to be of a basic nature, it is not meant to be implied that they are insurmountable but rather that further work along the lines indicated is required.

REFERENCES

1. Hickey, David H.: Full-Scale Wind-Tunnel Tests of the Longitudinal Stability and Control Characteristics of the XV-1 Convertiplane in the Autorotating Flight Range. NACA RM A55K21a, 1956.
2. Koenig, David G., Greif, Richard K., and Kelly, Mark W.: Full-Scale Wind-Tunnel Investigation of the Longitudinal Characteristics of a Tilting-Rotor Convertiplane. NASA TN D-35, 1959.
3. James, Harry A., Wingrove, Rodney C., Holzhauser, Curt A., and Drinkwater, Fred J., III: Wind-tunnel and Piloted Flight Simulator Investigation of a Deflected-Slipstream VTOL Airplane, the Ryan VZ-3RY. NASA TN D-89, 1959.

THREE VTOL TYPES

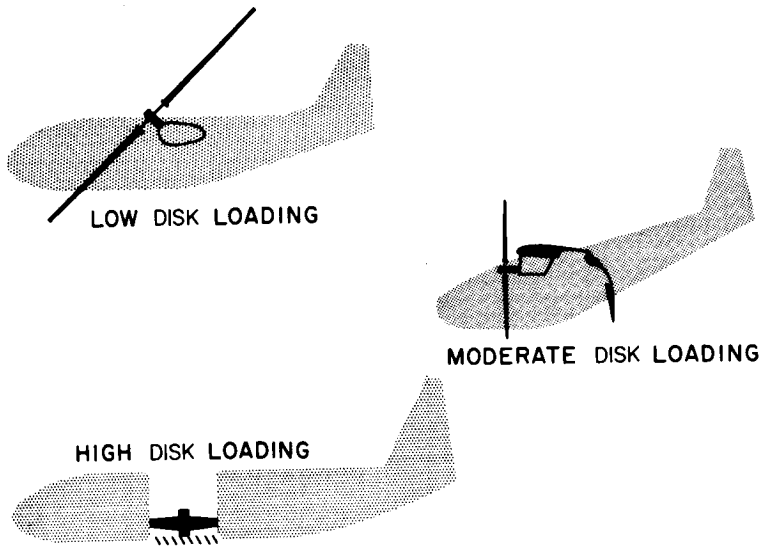


Figure 1

PROPULSIVE POWER REQUIRED VS AIRSPEED
FOR XV-1 UNLOADED ROTOR CONVERTIPLANE

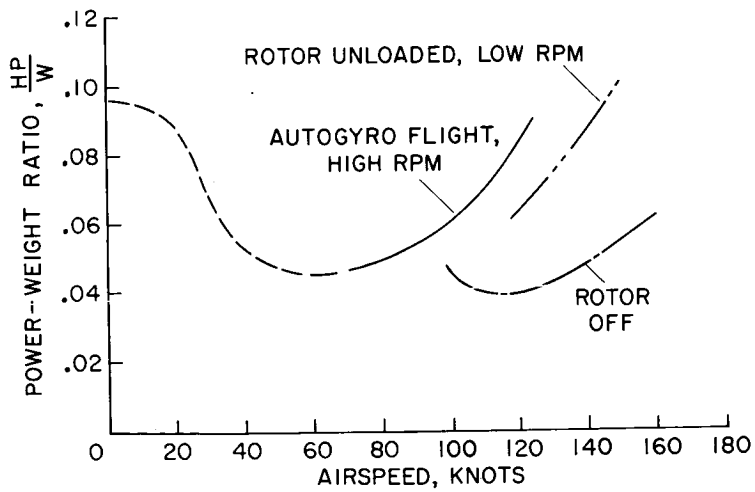


Figure 2

SHAFT POWER REQUIRED VS AIRSPEED
FOR XV-3 CONVERTIPLANE

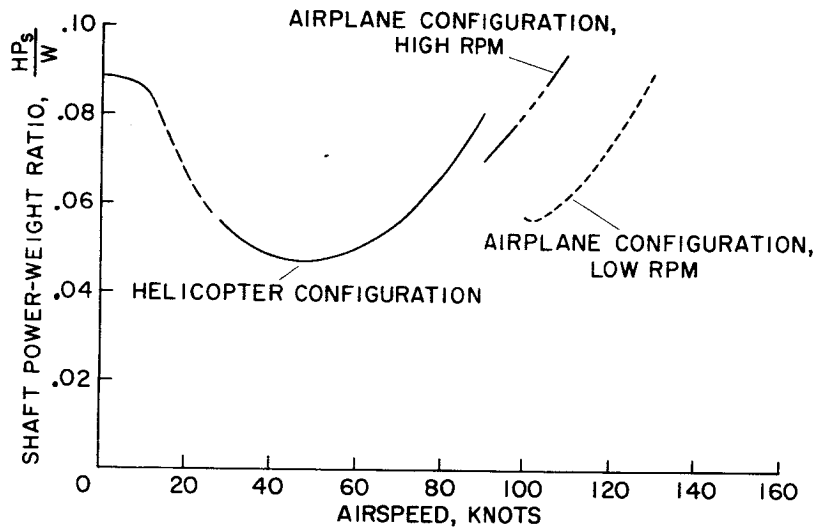


Figure 3

POWER REQUIRED AND POWER AVAILABLE
FOR XV-3 CONVERTIPLANE IN AIRPLANE FLIGHT

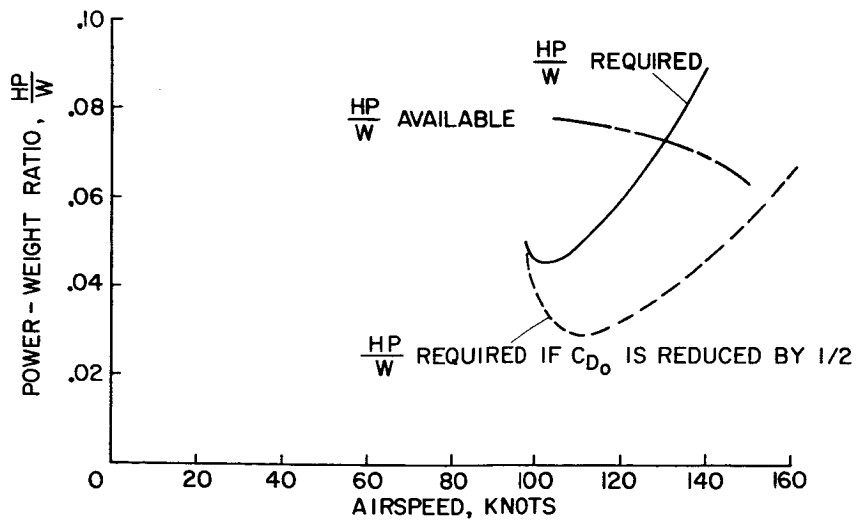


Figure 4

VARIATION OF BLADE LOADING COEFFICIENT, FOR OPTIMUM EFFICIENCY WITH ADVANCE RATIO

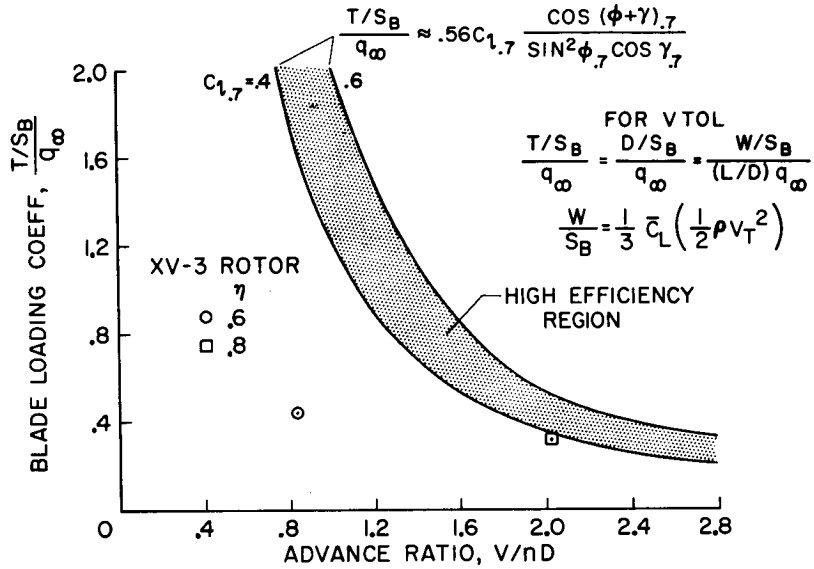


Figure 5

RATIO OF DISK LOADING TO DYNAMIC PRESSURE FOR WING STALL

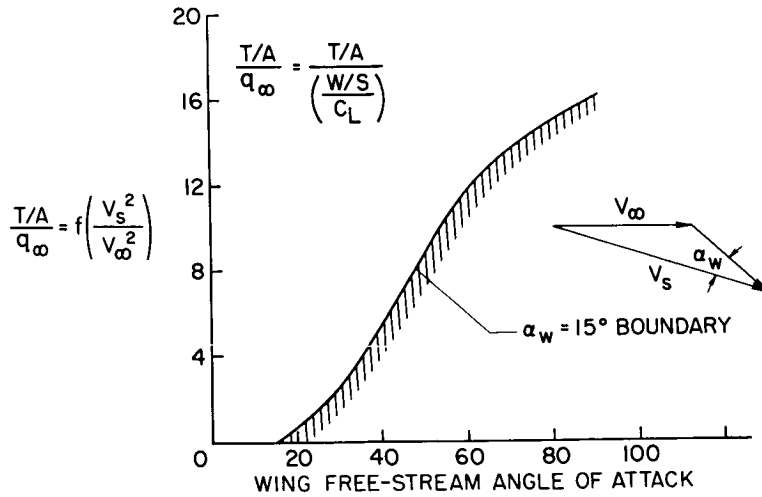


Figure 6

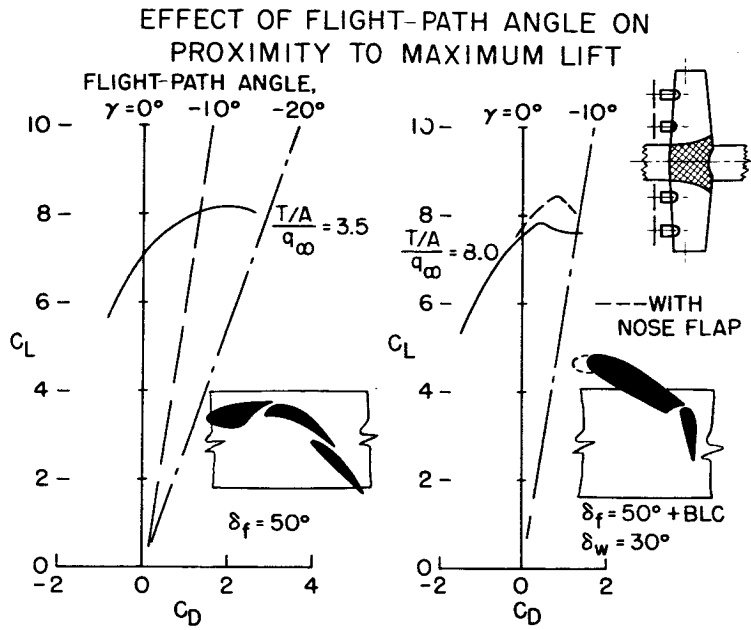


Figure 7

SOURCE OF MOMENTUM DRAG AND MOMENT ON DUCTED FANS

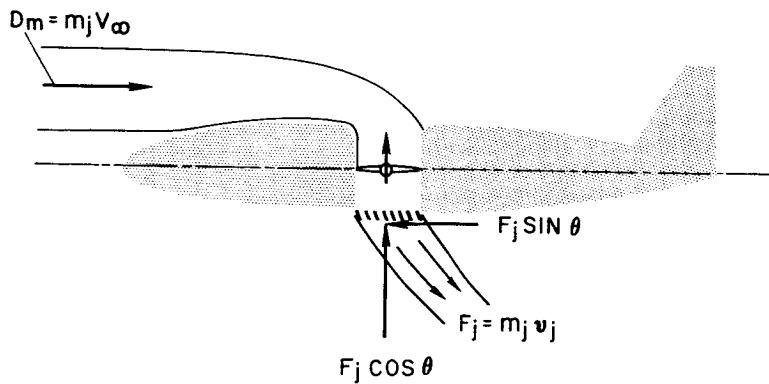


Figure 8

VARIATION OF LIFT, DRAG, AND MOMENT INCREMENTS WITH FORWARD SPEED

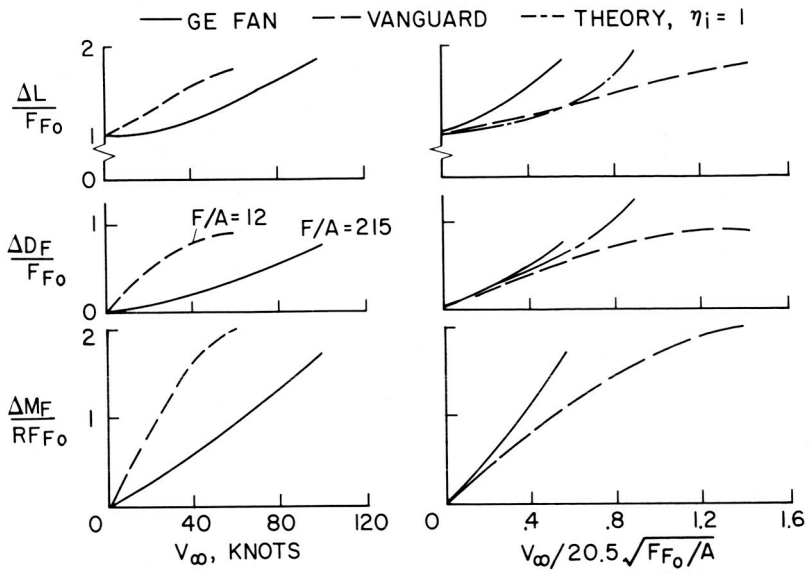
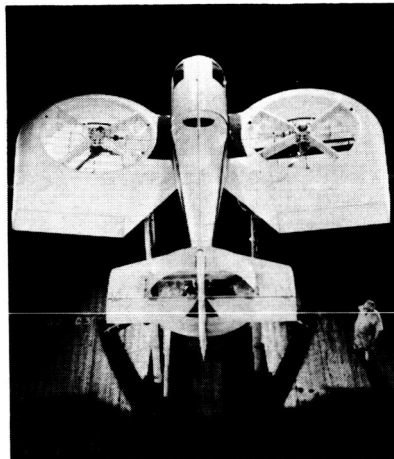


Figure 9

LIFT-FAN CONFIGURATIONS



G. E. FAN



VANGUARD

Figure 10

AERODYNAMICS OF TILTING DUCTED-FAN CONFIGURATIONS

By Paul F. Yaggy
Ames Research Center

and Kenneth W. Goodson
Langley Research Center

SUMMARY

Tests of a full-scale ducted fan have been made at the Ames Research Center. The results of these studies have indicated that the concept of wing-tip-mounted ducted fans has longitudinal problems similar to other V/STOL concepts; however, solution of these problems appears to be possible. An advantage of this concept is the ability to vary the thrust vector independent of the wing angle of attack. Thus, it is possible to keep the wing unstalled, even in descending flight.

INTRODUCTION

The concept of wing-tip-mounted ducted fans for V/STOL aircraft is one which has received less consideration in research programs than other types. As a consequence, only limited information concerning the aerodynamics of such units is available and most of this information was obtained with small-scale models. In order to provide additional information, tests of a full-scale ducted fan have been made at the Ames Research Center.

SYMBOLS

i_t	angle of incidence of horizontal tail, deg
l	moment arm, measured from airplane center of gravity, ft
M	pitching moment, ft-lb
M/I_y	control power, ft-lb/slug-ft ²
N	normal force, lb
α_w	angle of attack of wing, deg
δ_v	angle of deflection of inlet guide vane, deg

DESCRIPTION OF MODEL

The ducted fan used for these tests was one constructed for use on the Doak VZ-4DA airplane. The fan diameter was 48 inches and the shroud was 33 inches long with a thickness ratio of about 16 percent. Figure 1 is a photograph of the model in the wind tunnel ready for testing. It may be seen that the duct was mounted on a semispan wing. This wing approximated the Doak wing in span and section characteristics.

TESTS

Primarily, the tests were directed toward determining the variations of the duct angle, the power required, and the pitching moment that would be encountered in steady level flight over a range of airspeeds from hovering to airplane flight. Since the ducted fan and wing used in this investigation were designed for the Doak VZ-4DA airplane, the gross weight of 3,100 pounds and the drag characteristics of that airplane were assumed to apply to the model. Unless otherwise stated, all of the data presented in this paper are for the steady level flight condition.

A brief study of lateral control in hovering and low-speed flight was included in the investigation. These tests included a comparison of two methods of obtaining lateral control; namely, by deflecting radial guide vanes in the duct inlet to control the effective pitch angle of the fan blade and by varying the geometric fan-blade angle.

RESULTS AND DISCUSSION

The variation of duct angle relative to the wing and the variation of shaft horsepower for a transition from hovering to airplane flight are shown in figure 2. The wing angle was held constant at a value of 2° . Also shown on these graphs are points representing the results from flight tests of the Doak airplane during transition at the same wing angle of attack. The agreement indicates that the data obtained by the test procedure were representative of the flight case.

The variation of the distribution of lift between the duct and the wing for this transition is shown in figure 3. The contribution to the lift of each component was determined from tests of each component independent of the other. Of interest is the interaction between the wing and duct; that is, the wing and duct operating together produce a

lift larger than the sum of the lifts of each component operating independently and this effect increases in magnitude with airspeed.

Longitudinal Characteristics

The variation of the pitching moment during the transition described previously is also shown in figure 3. It is seen that the primary source of the pitching moment is the ducted fan operating at angle of attack to the airstream when the ducted fan is changing the direction of a large mass flow of air. It will be noted that the moment is zero at zero airspeed. The reason for this is that the thrust axis was assumed to be in the plane of the airplane center of gravity at the hovering condition as was the case on the Doak airplane. For this condition, it will be noted that the maximum pitching moment occurs at an airspeed of about 50 knots. At this speed, the horizontal tail is yet relatively ineffective because of the low dynamic pressure of the airstream; hence the moment available for trim is small. However, the problem is further complicated by the effect of the duct on the downwash at the horizontal tail plane.

The variations of downwash angle with airspeed for several values of wing angle of attack are shown in figure 4. These angles were measured at a location corresponding to the horizontal-tail location on the Doak airplane for steady level flight conditions at the values of constant wing angle of attack which are shown. At each wing angle of attack the variation in downwash is due entirely to the change in duct angle; hence, shifting weight to the wing by increasing wing angle of attack and reducing duct angle results in a lower value of downwash angle at a given airspeed. Figure 4 shows that a fixed tail incidence will produce increasing nose-up moments as speed is reduced, adding to those from the duct shown previously. Any attempt to eliminate the nose-up moments in the critical 50-knot speed range by fixed stabilizer setting will produce large nose-down moments in cruise flight. The desirability of a variable-incidence stabilizer with a large incidence range is evident; in the case of the Doak airplane the variable incidence was required to complete transition.

Although variable incidence reduced the trim problem during transition with the Doak airplane, longitudinal control remained weak, in part because a portion of the reaction control was being used for trim. Rather than add more control, means were sought for a reduction of the pitching moment generated by the ducted fan.

The flow from the duct exit was a continual source of high-energy air regardless of the airspeed and was located behind the duct axis of rotation. Therefore, a deflected vane in this flow would produce a moment counteracting the moment of the duct alone. The vane configuration installed for a study of this effect is shown in figure 5. The

vane was two-piece and had a 25-percent-chord flap. A representative setting of the vane and flap is shown in the sketch. As may be seen in figure 6, the exit vane was effective in reducing the maximum duct pitching moment in steady level flight, and thereby the required trimming moment. No attempt was made to determine the optimum setting from this study but simply to demonstrate the effectiveness of this modification; the most effective setting tested was with the vane at 10° and the flap at 20° . At this setting, the maximum pitching moment was reduced by nearly one-half. The effect of the vane on the power required was to increase the power by less than 3 percent.

Figure 6 shows that a fixed vane angle would produce nose-down moments at hover and high speed; programing the vane angle to vary with duct angle would eliminate this problem. The moment variation resulting from a programing based on the data obtained with the vane is compared with that for the duct with no vane in figure 7. It will be noted that with this particular programing, a speed range in which there is no change in trim requirement is realized. Further, since the vane would be undeflected at hover, there would be no increase in the hovering power requirement. The program of vane angle used here is not considered to be optimum because of the limited extent of the vane study. The results of a more optimum study of the exit vanes could show a larger reduction in the moment.

It is of interest to examine these balance-moment requirements of the wing-duct combination in terms of the handling-qualities requirements. For this purpose a hypothetical airplane which possesses only the balance-moment requirements and the tail length of the Doak airplane will be considered. The balance-moment-required curves from figure 7 are repeated in figure 8, but are plotted in terms of control power. Unlike the Doak airplane, it is assumed that the hypothetical airplane has a reaction control power equal to that specified for control in hover in the VTOL handling-qualities criteria (ref. 1). This power is less than one-half of that which was available in the Doak airplane. It is also assumed that this reaction control has constant power, as represented by the dashed line in figure 8. The net moment available to balance the airplane at any given airspeed will be that available from the reaction control plus that available from the variable-incidence tail. (The elevator is considered to be reserved for maneuvering as specified in ref. 1.) For example, the net moments available for tail incidences of 0° and 12° are shown in figure 8. (The tail volume was assumed to be 0.7.) It is seen that the tail at 0° incidence not only does not contribute to the moment available but requires first a portion, and eventually all, of the reaction control to neutralize its adverse effect. This situation does not exist with a tail incidence of 12° . At this setting, there is no adverse effect of the tail, but it does not supply the full trim requirement until speeds of 35 knots with exit

vanes and 50 knots without exit vanes have been reached (points 1 and 2 on fig. 8). Computations have shown that the elevator cannot supply the hover control requirement until a speed of 35 knots is reached. Therefore, a control deficiency exists up to this speed which is equal to that portion of the reaction control power absorbed in trimming the airplane less the power available from the elevator.

These deficiencies are illustrated in figure 9. It is seen that the trim deficiency at 0° tail incidence and without duct exit vanes is over three times the hover control requirement. The advantages of exit vanes and variable tail incidence are immediately apparent. The trim deficiency is reduced by nearly one-third in magnitude at 0° tail incidence when the exit vanes are added. However, a greater gain is made by increasing the tail incidence to 12° . Without the exit vanes, the trim deficiency is reduced to less than 25 percent of the initial value. By the addition of the exit vanes, the deficiency is reduced to less than 10 percent of the initial value.

A control deficiency is seen to exist at very low speeds. This does not mean that it could not be alleviated. As mentioned previously, the study of the vanes was limited in scope. Proper programming of the vanes in this region could do much to relieve this deficiency and a more optimum tail incidence might well relieve the remaining trim deficiency shown on the lower right-hand graph of figure 9.

In the absence of such optimum programming, a considerable increase in reaction control would be required to meet these deficiencies. For example, to obtain adequate control power for the Doak airplane in transition the reaction control was more than twice the value prescribed by the specifications for control in hover given in reference 1.

Although requirements for variable trimming devices are apparent from these observations, they are not peculiar to this concept but are more or less characteristic of V/STOL machines. From the pilot's viewpoint, it would be a distinct advantage to have the stabilizer and exit-vane angles programmed to the duct angle since the trimming of the aircraft would then require the pilot's attention to only one control. The shape of the curve for the programmed moment (fig. 7) indicates that, over a sizable range of airspeeds, there could be little or no change in the longitudinal trim requirement of the airplane.

This study of the longitudinal handling-qualities characteristics has been made for a single location of airplane center of gravity corresponding to that of the Doak airplane. The range of movement of airplane center of gravity for an operational airplane would alter the shape and position of the moment-required curves and, hence, the deficient regions. A compromise of center-of-gravity location might be attempted to lower the peak value of the moment-required curve. This

compromise would ultimately result in increasing the reaction control required at hover. While some benefit can be realized by adjustment of the duct position relative to the airplane center of gravity, it would appear that a means of reducing the duct pitching moment about its own axis is desirable.

A further consideration of the duct moment is its increase with gross weight as shown in figure 10. It is seen that, when the disk loading is held constant, the pitching moment does not vary linearly with weight but rather as the $3/2$ power. These results assume that the chord-to-diameter ratio of the duct is maintained constant, which is a likely requirement. Since the remainder of the airplane probably would increase in size by the square-cube law, with the wing loading increasing as the cube root of the weight, problems could arise in designing and housing the duct turning mechanism in the adjacent wing structure. The space available would be less in proportion, the force required to turn the duct would increase, and the wing stresses, already increased by the higher wing loading, would be further increased by the higher duct moment, the stresses rising as the $3/2$ power of the scaling factor. The moment can, of course, be reduced by increasing the disk loading as shown in figure 10. However, this would be at a cost in thrust-to-horsepower ratio. From these considerations, as well, it is desirable to reduce the duct moment about its own axis.

Since the reduction of the pitching moment is of such consequence to satisfactory operation of this type of machine, it would be desirable to know more of its origin. A limited approach to this subject may be had by examining the breakdown of the duct and fan moments as shown in figure 11. These results were obtained from tests of a $5/16$ -scale model in the Langley 7- by 10-foot tunnel. It may be seen that the moment is caused primarily by the duct; the contribution from the fan being primarily that due to the fan normal force times its moment arm from the duct rotation axis, assumed to be the location of the airplane center of gravity. The duct moment arises from the duct normal force times its arm from this same axis and from the differential thrust on the duct lips. The location of the duct normal-force vector relative to the airplane center of gravity thus is seen to be an important factor in limiting the magnitude of these moments. Thus far, little has been known of the location of the center of pressure on the duct. It is hoped that recent measurements of pressure distributions on the duct will provide information concerning this problem.

A concern for the ducted-fan concept has been that, at high rates of descent and low power conditions, the duct inlet lip may stall, thus creating a large, and perhaps uncontrollable, change in trim. Even at powers corresponding to one-half those required and for duct angles somewhat larger than those indicated for steady level flight, no lip stall was encountered on the full-scale test model. In subsequent

tests, the duct has been forced to stall under extreme operating conditions and stall is not beyond the realm of reasonable expectancy on other configurations with sharper inlets. However, for this duct configuration at normal operating conditions, the problem would not appear to be as great as was expected.

The effects of lip stall can be graphically illustrated by results of tests of the 5/16-scale model which are shown in figure 12. In these tests, because of the lower Reynolds number, stall occurred even at the steady level flight condition and it was necessary to double the upstream inlet-lip radius to prevent its occurrence. The large reduction in pitching moment verifies the expected change in trim. However, perhaps of even greater significance is the large increase in power required to a value which exceeded the value at hover by about 30 percent for the small-scale tests. From these results, it is apparent that operation in the region of lip stall should be avoided.

An additional stalling phenomenon encountered during the full-scale tests, which was attributed to an interference between the wing and the duct at conditions of high power and high wing lift, caused a fan blade stalling to occur. This interference also caused some separation to occur on the wing near the wing-duct juncture. The onset of this phenomenon was delayed by several degrees of wing angle of attack in the full-scale tests as a result of the addition of a leading-edge droop to the outboard third of the wing.

Lateral Characteristics

A comparison of the results of tests of two methods for obtaining lateral control by differentially varying duct thrust is shown in figure 13. It will be noted that the inlet vanes were effective only to a deflection of 16° after which they stalled. This value of incremental thrust corresponds to a fan-blade-angle change of 2° .

The significance of these results in terms of roll-control handling qualities will be examined in the next paragraph. However, first a comment about inlet guide vanes for thrust control at higher forward speeds is in order. As was noted, the largest effective-blade-angle change which could be obtained with inlet vanes was about 2° . While the increase in forward speed would change these relations slightly, it would not alter the vane effectiveness significantly and the large blade-angle changes which are required to maintain efficient fan operation at higher forward speeds could not be obtained. Thus, it would appear that, in the absence of variable duct geometry, a variable-pitch fan would be preferable to a configuration using inlet vanes for an operational airplane.

The ability of the inlet-guide-vane configuration to meet the roll-control handling-qualities requirements as set forth in reference 2 is shown in figure 14. These results are based on a moment of inertia representative of aircraft more sophisticated in design than the test-bed aircraft. It is apparent that, although the inlet vanes have limited capabilities for thrust control in forward flight, they would be sufficient to provide acceptable lateral control power at hover and low-speed forward flight. There is a loss in control power shown with increasing forward speed because of the reduction in thrust required. However, no account of the aileron contribution has been taken in this study. The value of control power would be nearly constant when the aileron is considered. For the larger moment of inertia of the Doak airplane, the control power and damping would be about one-half the values shown in figure 14.

CONCLUDING REMARKS

The ducted-fan concept of V/STOL aircraft has longitudinal-control problems similar to those of some other concepts; however, it appears that solution of these problems is possible. One distinct advantage of this concept is the ability to avoid operation at high wing lift conditions, especially in descent, where stalling of primary lifting surfaces may occur. This flexibility results from the ability to vary the thrust vector independent of the wing angle of attack and is characteristic of any concept which has this feature.

REFERENCES

1. Anderson, Seth B.: An Examination of Handling Qualities Criteria for V/STOL Aircraft. NASA TN D-331, 1960.
2. Tapscott, Robert J.: Criteria for Control and Response Characteristics of Helicopters and VTOL Aircraft in Hovering and Low-Speed Flight. Paper No. 60-51, Inst. Aero. Sci., Jan. 1960.

DOAK DUCTED FAN AND SEMISPAN WING
IN AMES 40'x 80' WIND TUNNEL



Figure 1

DUCT ANGLE AND SHAFT HORSEPOWER FOR
STEADY LEVEL FLIGHT

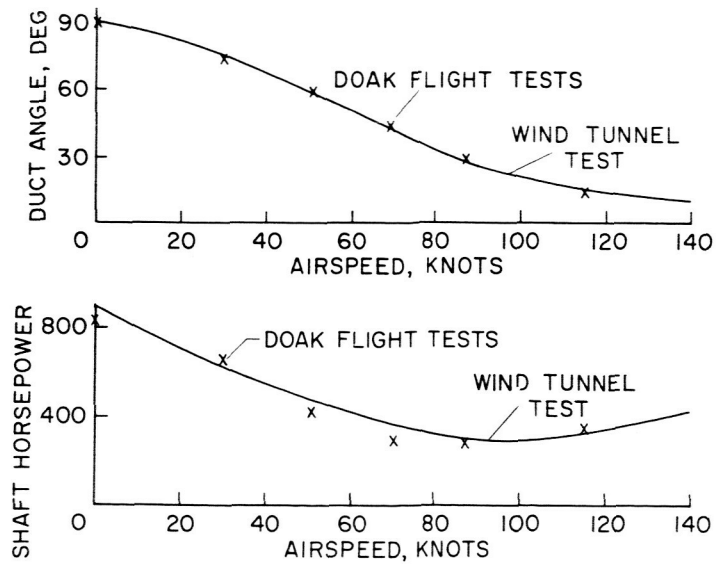


Figure 2

LIFT AND PITCHING MOMENT FOR STEADY LEVEL FLIGHT

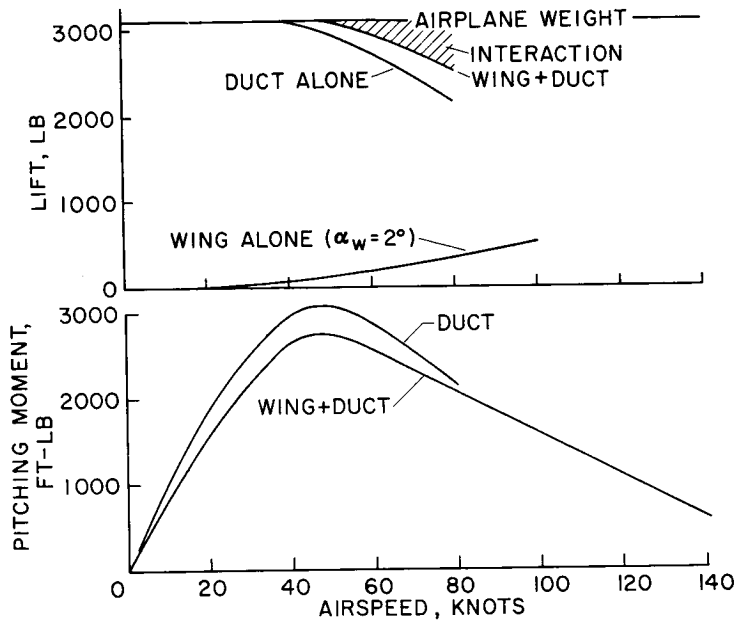


Figure 3

DOWNWASH ANGLE AT THE HORIZONTAL TAIL LOCATION - DOAK VZ-4DA

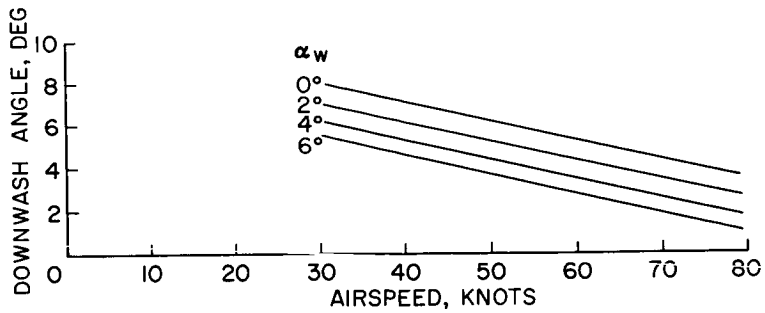


Figure 4

MODEL WITH DUCT EXIT VANE

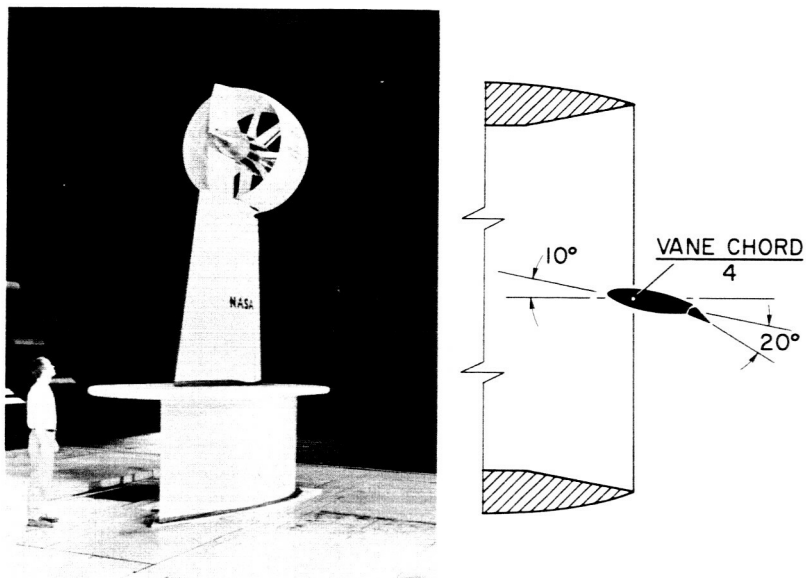


Figure 5

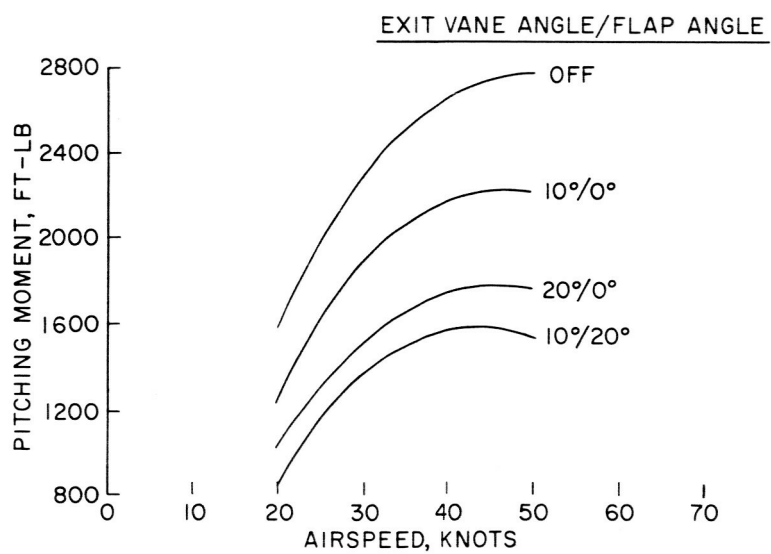
REDUCTION IN PITCHING MOMENT DUE TO
DUCT EXIT VANE DEFLECTION

Figure 6

BALANCE MOMENT WITH AND WITHOUT PROGRAMMED EXIT VANES

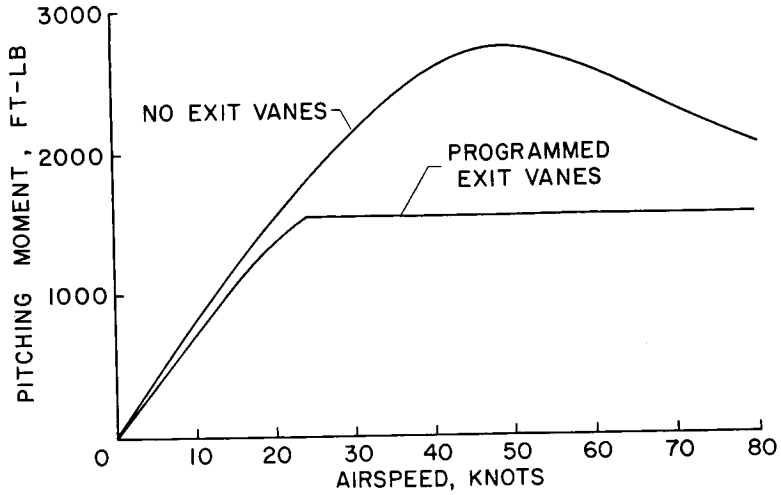


Figure 7

REQUIRED AND AVAILABLE BALANCE AND CONTROL MOMENTS

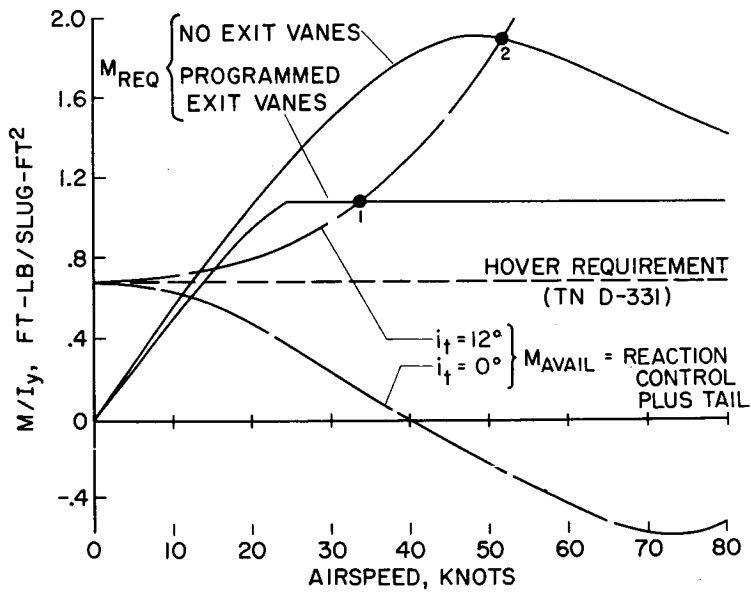


Figure 8

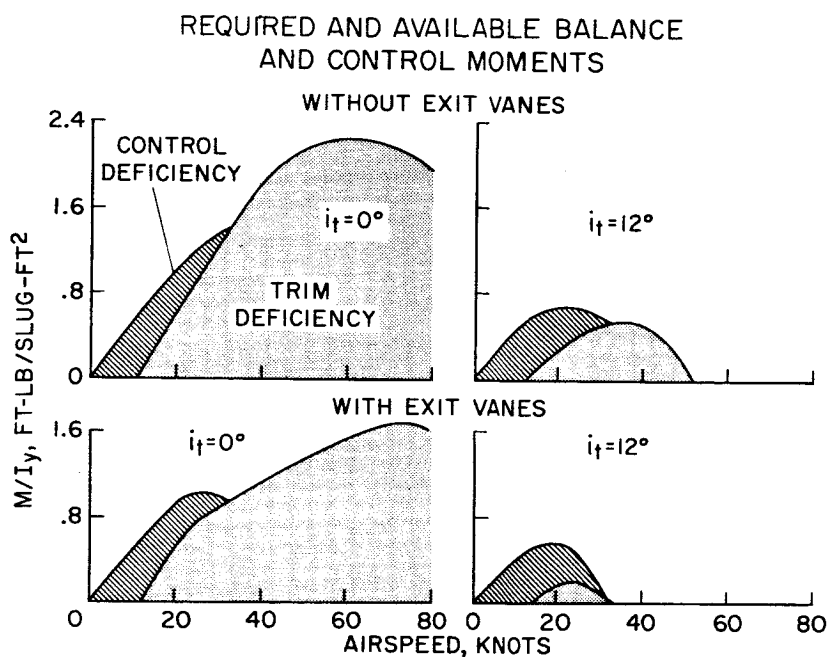


Figure 9

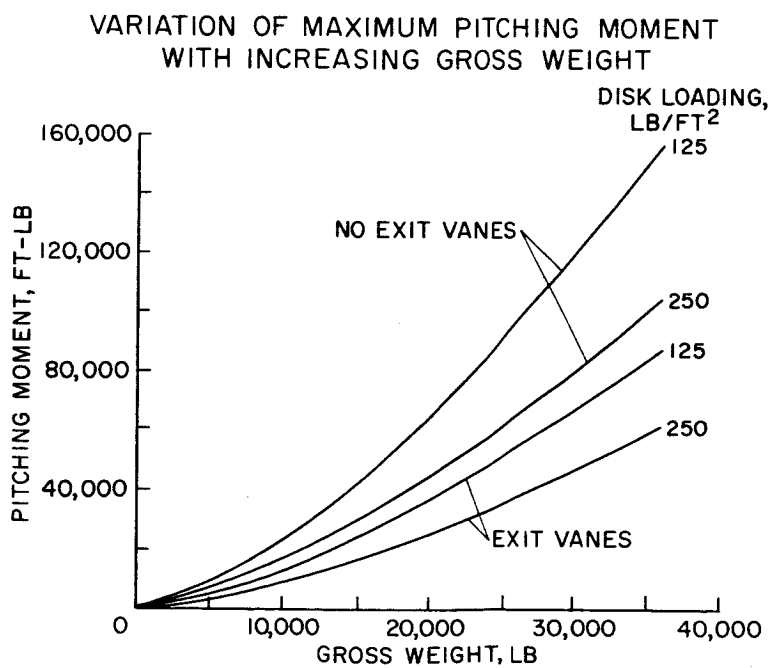


Figure 10

DUCT-FAN MOMENT BREAKDOWN

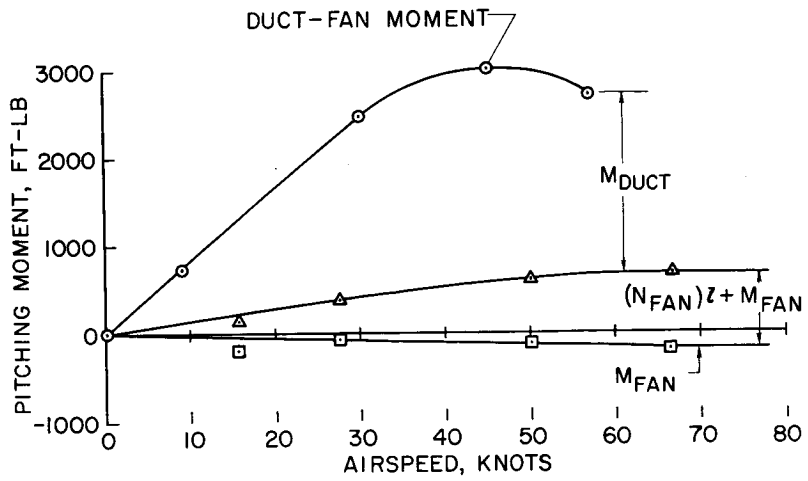


Figure 11

EFFECT OF LIP STALL ON PITCHING MOMENT AND HORSEPOWER

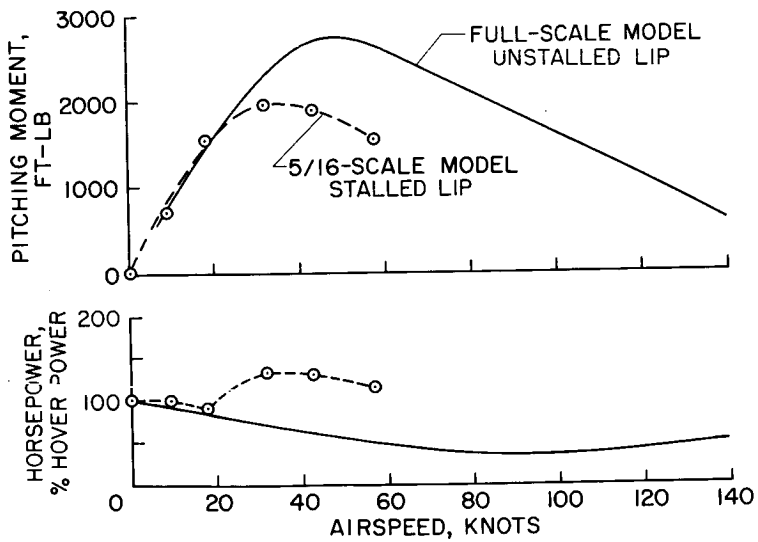


Figure 12

TWO METHODS OF THRUST CONTROL

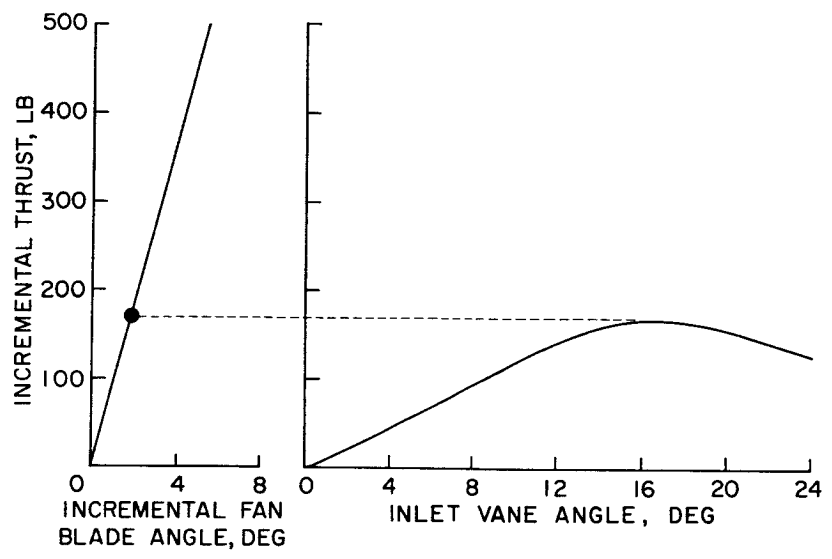


Figure 13

LATERAL CONTROL AVAILABLE WITH INLET VANES

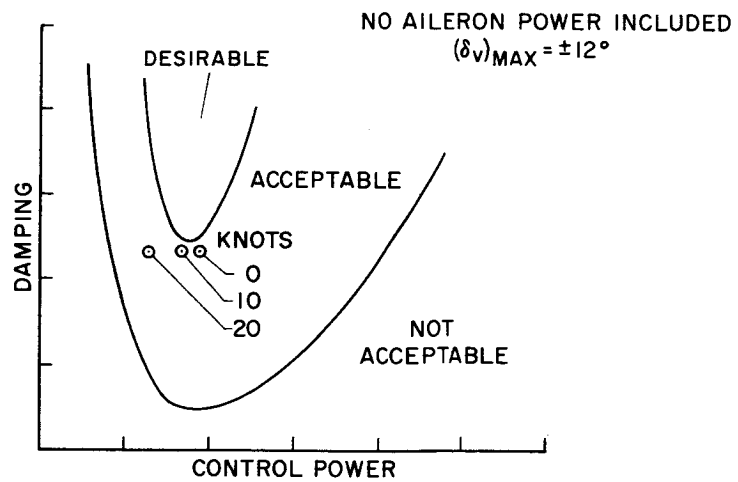


Figure 14

AERODYNAMICS OF A FAN-IN-FUSELAGE MODEL

By Ralph L. Maki and David H. Hickey

Ames Research Center

INTRODUCTION

Recent full-scale wind-tunnel tests of various VTOL designs at Ames Research Center include studies of the submerged-fan concept. One of these studies utilized a general research model with a high-disk-loading fan mounted in a deep duct in the model fuselage. These are the first large-scale complete-model results known to be available on either wing- or fuselage-mounted fan configurations. As indicated in a previous paper by Mark W. Kelly, the problems associated with submerged-fan vehicles will be similar for both wing and fuselage installations. Analysis of these data for the subject fan-in-fuselage model will, therefore, have some general applicability to the submerged-fan concept.

MODEL AND TESTS

Figure 1 is a photograph giving an overall view of the model installed in the Ames 40- by 80-foot wind tunnel. An unswept wing having an aspect ratio of 5, a taper ratio of 0.5, and 10-percent-thick sections was used. Wing incidence was 0° . Full-span plain trailing-edge flaps were installed. The high horizontal tail used had a volume coefficient of 0.6. The wing was sized to provide a fan-to-wing area ratio of 8 percent.

The lift fan is driven by a tip turbine which is powered by the exhaust gases from a General Electric prototype J85 engine. The fan is comprised of 36 blades with fixed pitch and a design disk loading of about 350 lb/sq ft. A single fixed vane in the duct inlet, visible in figure 1, aided in turning the inflow air at forward speed.

Details of the propulsion system can be seen in figure 2. The engine jet exhaust was ducted to the fan tip turbine by a flexible elbow to a scroll encircling half the tip-turbine arc. The lift-vectoring exit vanes at the base of the duct were remotely controlled and tested from 0° to approximately 40° rearward of the full-open position.

Some of the tests were made with the model balanced in lift, drag, and pitching moment for selected wing loadings up to 20 lb/sq ft. A vertical jet-reaction nozzle at the rear end of the fuselage was used to balance the model at trim conditions. A separate source of high-pressure air was used which was capable of producing more than adequate pitch control for the test purposes.

Combinations of low fan speed and relatively high forward speed were avoided when serious distortion of the fan inlet flow occurred.

RESULTS

The wind-tunnel study was directed at obtaining information pertinent to performance, stability, and control during transition from hovering in fan-supported flight to wing-supported flight.

The propulsion system developed a maximum static fan lift (or thrust) of about 7,000 pounds at a weight rate of engine airflow of about 515 lb/sec and 3,900 gas horsepower. This fan lift includes the induced effects on the shroud. The variation of fan thrust and overall model lift with forward speed is illustrated in figure 3. These data are for a constant fan speed with the model at 0° angle of attack; the exit vanes are fully open, and the horizontal tail is off. There are large increases in both fan thrust and overall lift with increasing forward speed. The data show no evidence of a "suck down" effect at low forward speeds. (In this connection, it is to be noted that the model was essentially out of ground effect with the duct exit about 3 fan diameters above the tunnel floor. Furthermore, there was no measurable evidence of tunnel-wall influence or recirculation effects in the closed test section.) Overall lift exceeds thrust indicating induced lift due to fan operation. At 100 knots forward speed total lift has increased to 90 percent more than its static value, and induced lift accounts for 35 percent of this total. With the wing at 0° incidence and 0° angle of attack, this lift gain is directly attributable to wing loading due to fan operation. Small-scale tests of a similar model with lower-disk-loading fans (about 60 lb/sq ft) had not shown the existence of this lift. The power required to maintain constant fan speed did not vary materially through the speed range.

Lift, drag, and pitching-moment coefficients are plotted as functions of tip-speed ratio in figure 4. Tip-speed ratio is defined as the ratio of forward speed to fan-blade tip speed. Increases in tip-speed ratio thus correspond to increases in forward speed or decreases in fan speed. These data were obtained with the model at 0° angle of attack; the exit vanes were fully open, and the horizontal tail was off.

The component contributions to lift and drag account for 80 to approximately 100 percent of the measured values. Wing lift accounts for an increasing percent of total lift with increasing tip-speed ratio - almost 30 percent of the total lift at a tip-speed ratio of 0.3.

The power-off drag is a measured value. Ram drag is that force necessary to arrest a mass of free-stream air equal to the mass of air flowing through the duct. The gas-generator ram drag is also included but is small in magnitude.

Pitching moments were measured about a point on the fan thrust axis longitudinally and near the fuselage center line vertically. Of the total measured pitching moments only a small portion is attributable to the wing lift and drag on the engine package. The major portion of the measured moments is due to the effects of turning the inflow air into the duct. Calculations showed that almost half of this moment increment arises as a consequence of the vertical displacement of the chosen moment center below the duct inlet. A shallow duct configuration, such as would be used in fan-in-wing vehicles, might avoid this part of the duct moments.

The effects of deflecting the duct exit vanes on the lift, drag, and moment characteristics are shown in figure 5. Tip-speed ratio is again used as the independent parameter. Vane deflection is measured rearward from the full-open position as indicated in the inset sketch. The loss in lift with vane deflection at finite forward speed is expected; however, part of the loss is due to a reduction of the induced wing lift. Sizable thrust forces are available through the speed range. Adequate thrust for trimmed flight to a forward speed of about 100 knots was attained with vanes deflected approximately 40° . Exit-vane deflection caused large moment increases at low forward speeds, as would be expected with the vanes positioned well below the center of gravity. These moments could be alleviated by duct redesign or duct inclination, as will be shown subsequently.

Longitudinal characteristics of the model at several power settings (or tip-speed ratios) and with the horizontal tail on are presented in figure 6. The effect of power on the lift-curve slope is negligible. Operation of the fan induced more negative pressures on the wing leading edge, with small effects still evident at the wing tips. Fan operation did not materially affect longitudinal stability. Data with the horizontal tail off showed sizable downwash at the tail throughout the speed range tested.

DISCUSSION

The data presented are a brief digest of the test program. These test results have been used to study the longitudinal control characteristics in steady-flight transitions at 1 g from hovering to flight on the wing at forward speed. These studies serve to illustrate the various problems that can be encountered with fan-in-wing and fan-in-fuselage VTOL airplanes.

A variety of transition programs are possible and many were, in fact, studied. The purpose here is not to seek an optimum method of accomplishing transition but rather to illustrate the general problem areas. Three transition programs were selected for this purpose and are depicted in figure 7. The selected airplane weight, 5,000 pounds, corresponds to a wing loading of 20 lb/sq ft on the model. The transition programs are shown in terms of the variation of angle of attack with speed.

A type of transition which has been proposed is to utilize a low-drag configuration at a low constant angle of attack to provide high acceleration to a speed at which flight on the wing is possible. The first transition plan of figure 7 illustrates this method with the model at 0° angle of attack. (The model is limited to about 100 knots in this configuration due to thrust-vectoring limitations of the duct exit vanes.) Note that the angle-of-attack program is discontinuous at the end of the transition. A large abrupt increase in angle of attack is required to support 1 g flight on the wing. Not only is this angular rotation undesirable but, as is shown in figure 8, serious pitching-moment problems make this type of transition unacceptable. Shown in figure 8 is the variation of untrimmed pitching moment with speed. The low-drag method of transition (plan ①) develops high moments and has a large trim discontinuity at the end of transition.

As was pointed out in the discussion of figure 4, the duct moments with the model at 0° angle of attack are quite large. Rotating the model to negative angle of attack should relieve the duct moments.

Transition plan ② (fig. 7) was programed at -7.5° angle of attack to study this effect. Wing flaps were deflected 30° to retain positive lift at this attitude; flap deflection also aids in reducing the positive moments. It is seen in figure 8 that the moments are reduced considerably, but large trim and angle-of-attack discontinuities still occur at the end of transition. (The speed selected for transfer of lift from fan to wing is 30 percent above stall speed, the same as for transition plan ①.) It is therefore necessary to vary angle of attack

gradually through transition, as in transition plan ③ of figure 7, to eliminate both the discontinuous angle-of-attack change and the trim discontinuity (fig. 8).

The necessity of varying angle of attack in this manner to reduce the untrimmed moments and to allow a smooth continuous transition introduces a new problem which is shown in figure 9. For the low-drag method of transition, fan power is abruptly stopped at the end of transition, and direct engine thrust applied for normal airplane flight. This is desirable since it requires only a two-position jet-exhaust diverter valve. For the variable angle-of-attack plan, on the other hand, the power required by the lift fan reduces gradually to zero. (These transition results were extrapolated through the region where fan speed is low.) Therefore, some direct jet thrust must also be provided to supplement the limited thrust available from duct exit vane vectoring of the fan lift in this intermediate speed range. In order to obtain this division of the gas-generator exhaust, the jet engine must be operable with the flow diverter valve in positions intermediate to either full fan drive or full jet thrust.

One additional point should be noted in connection with figure 9. As the fan speed must decrease gradually to zero in the variable angle-of-attack transition, fan-inlet-flow distortion will occur. Since the fan rotating stresses will be low, it had been expected that the oscillating stresses would cause no difficulty. (More recent tests of the model have been conducted under such conditions with no serious effects.)

In figure 10 the untrimmed pitching-moment variations with speed are repeated (from fig. 8) for transition plans ① and ③. The purpose here is to compare the trim requirements with the stabilizer capability. It can be seen that stabilizer power is insufficient for trim throughout transition for the constant 0° angle-of-attack case and insufficient up to 55 knots for the variable angle-of-attack case. Addition of elevator control would provide some additional trimming power but would also be relatively ineffective at the lower speeds. A pitch control device effective at hover and low forward speeds is necessary to handle these trim deficiencies. Vertical jet-reaction control in the region of the horizontal tail was used for the wind-tunnel tests and is used in this analysis. The elevator is reserved for control rather than trim, as demanded by handling-qualities criteria.

The moments required from the reaction control to handle the trim deficiencies for the low-drag and the variable-angle-of-attack transition programs are plotted against speed in figure 11. The requirements are plotted in terms of the control parameter M/I_y . The incremental

control power required for maneuvering and damping as specified by VTOL handling-qualities criteria is shown by a shaded area above each of the trim-deficiency curves. (Where the shaded areas reduce and/or disappear, estimated elevator control is being phased in as it becomes effective at the higher dynamic pressures.) For the constant-angle-of-attack transition (plan ①), the maximum control moment required represents a reaction force of 9 percent of the airplane gross weight. When angle of attack was varied through transition (plan ③), the maximum requirement is only one-third as large, and no reaction control is needed above 60 knots forward speed. It is to be noted that in either case the magnitude of the reaction control force is specified by the requirements in transition, not those in hovering; this force could be as much as 6 times the hover requirement for the constant-angle-of-attack transition.

These control requirements are, of course, applicable to the specific fan-in-fuselage model tested and could be altered materially by changes in design such as those suggested in figure 12. The sketch at the left side of the figure is a simplified diagram of the duct geometry as tested. It has been calculated that with a design as shown on the right side of the figure, in which there is about 15° of tilt in the duct and less duct depth, the pitch control problems would be alleviated. Moment diagrams applicable to each design are shown below the sketches. It is estimated that this revised design would almost eliminate any added control-power requirement over that for maneuvering and damping at hover with the center of gravity positioned as shown. The moments arising from operation of submerged fans are, however, quite sensitive to center-of-gravity changes so that even with careful duct design normal center-of-gravity travel will introduce moment problems of the nature discussed in this paper.

CONCLUDING REMARKS

From consideration of 1 g steady-flight conditions derived from wind-tunnel data, it has been shown that a variety of transition flight plans are possible with the fan-in-fuselage model tested. In order to satisfy the longitudinal handling-qualities criteria, angle of attack must be varied to provide smooth transition from fan-supported flight to wing-supported flight. Inherent in both fan-in-wing and fan-in-fuselage designs is a large untrimmed pitching-moment variation with forward speed. The transition flight plan must be selected with care; otherwise, excessive trim and control power will be required. It was shown that lift-force vectoring must be supplemented by some direct thrust during transition flight to eliminate discontinuous attitude and trim changes. Such a provision for diversion of the gas-generator flow

between fan drive and direct thrust implies the development of engines operable with the exhaust diverter valve in intermediate positions. Such a valve would allow more flexible programming of duct exit vanes to obtain further reductions in trim pitching moment. The need for variation of several controls to provide trim through transition suggests a programmed linkage of all trim controls to a single pilot cockpit control. Detailed design considerations can do much to reduce the control-power demands for successful transition flight.

FAN-IN-FUSELAGE MODEL



Figure 1

PROPULSION SYSTEM DETAILS

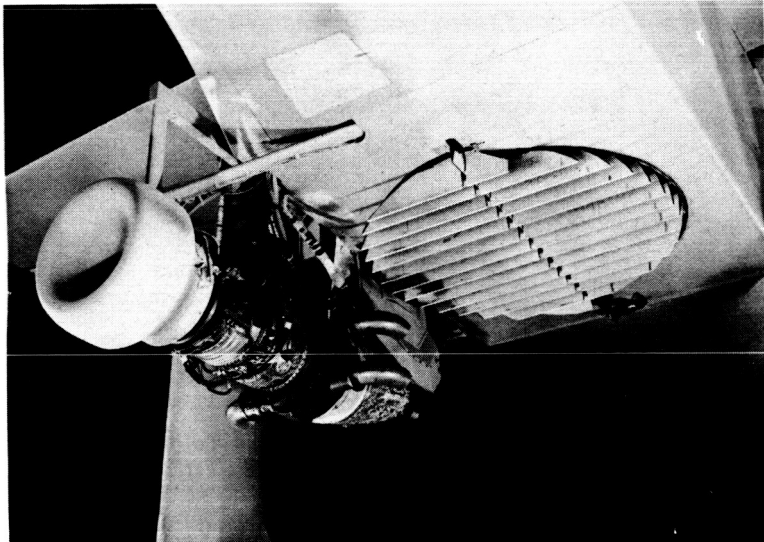


Figure 2

EFFECT OF AIRSPEED ON LIFT, THRUST AND POWER

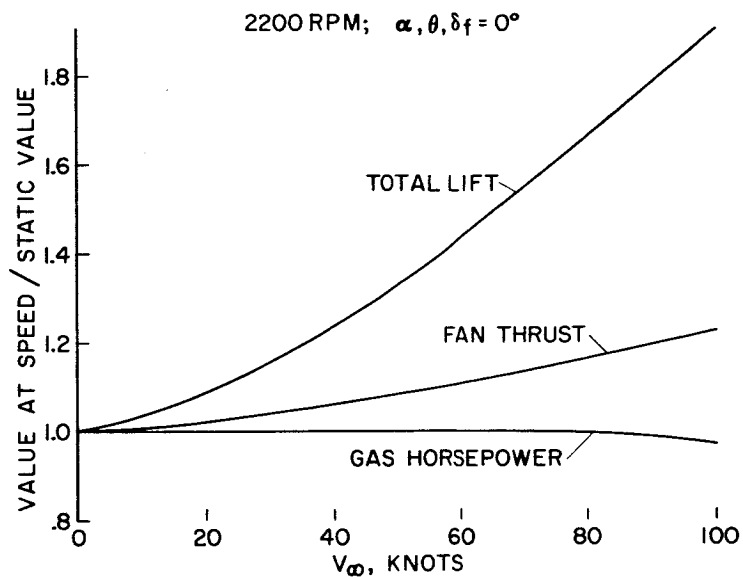


Figure 3

LONGITUDINAL CHARACTERISTICS OF THE MODEL

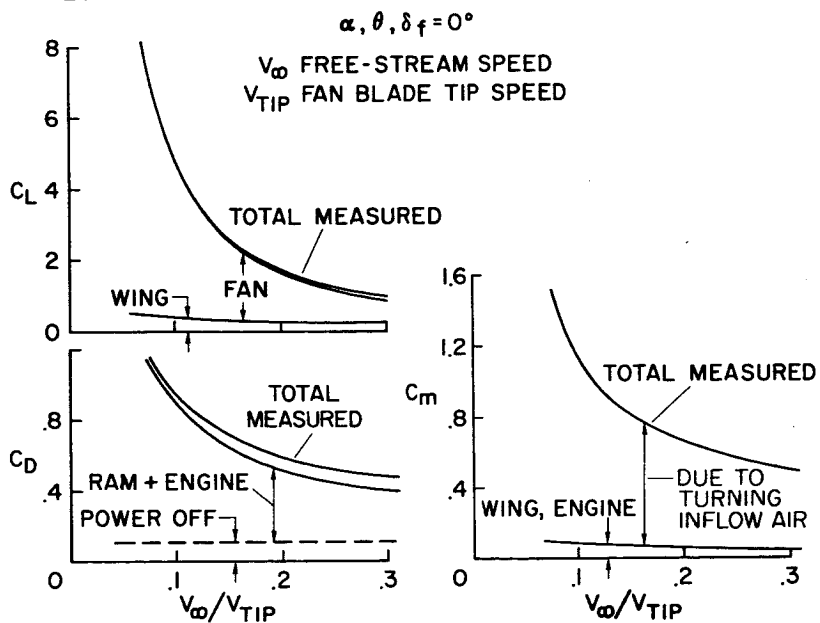


Figure 4

EFFECTS OF EXIT-VANE DEFLECTION

$\alpha, \delta_f = 0^\circ$

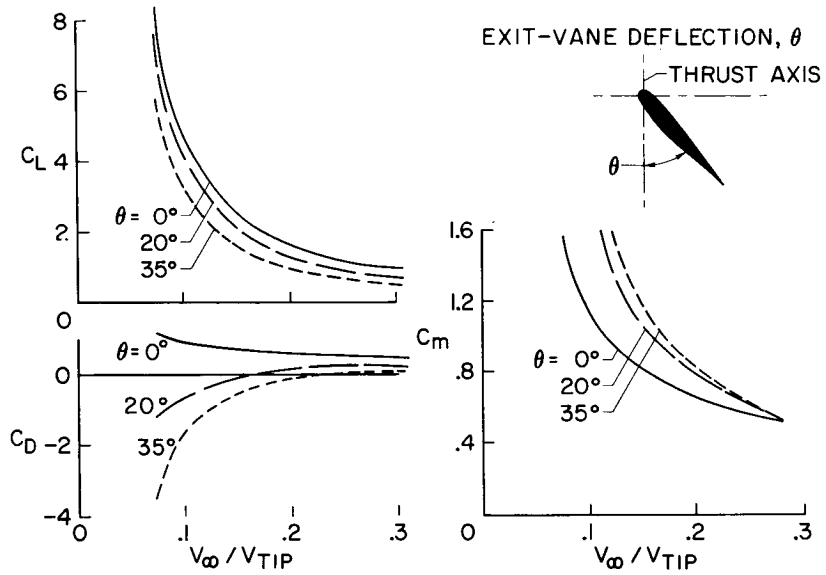


Figure 5

LONGITUDINAL CHARACTERISTICS OF THE MODEL

HORIZONTAL TAIL ON, $i_T = 0^\circ$

$\theta, \delta_f = 0^\circ$

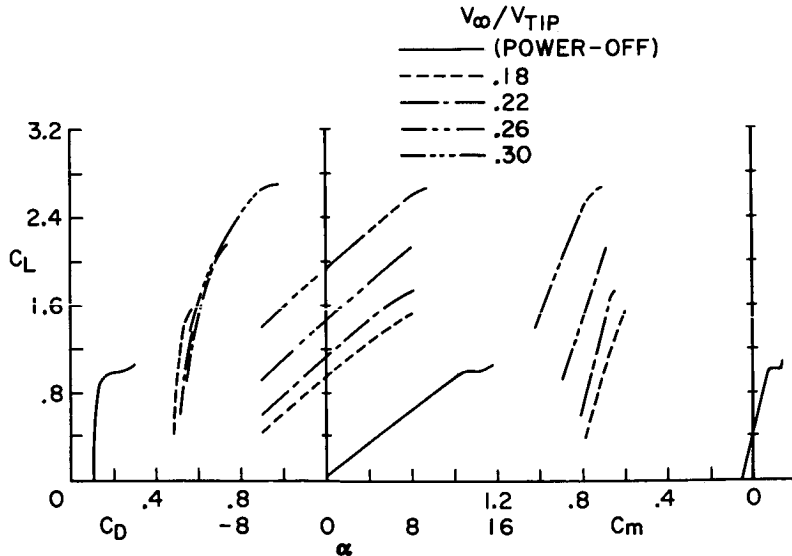


Figure 6

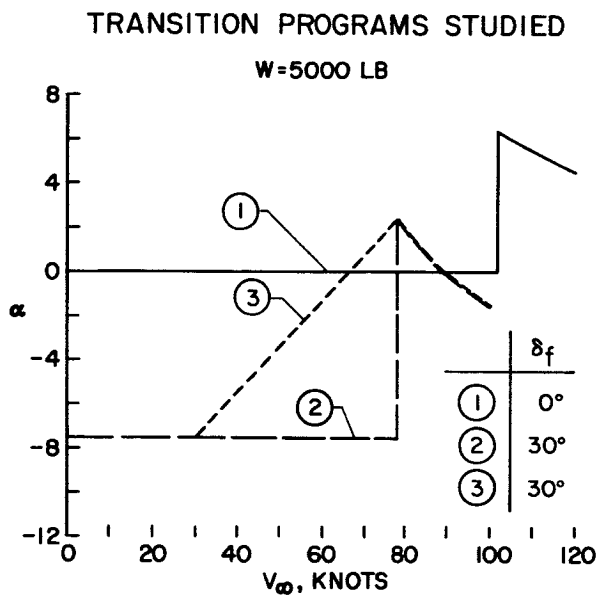


Figure 7

PITCHING MOMENTS IN TRANSITION

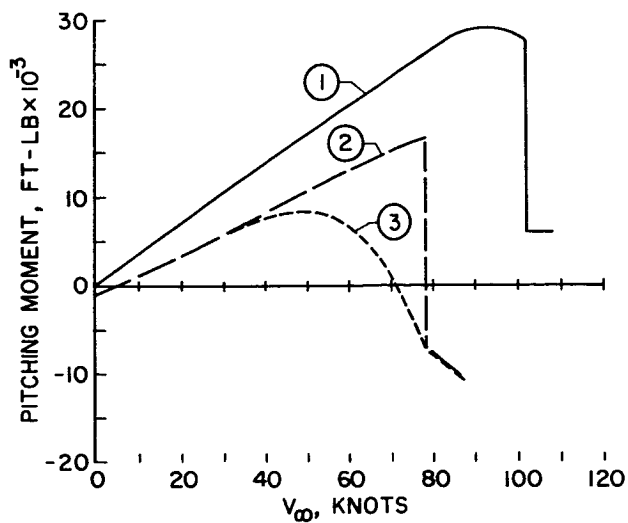


Figure 8

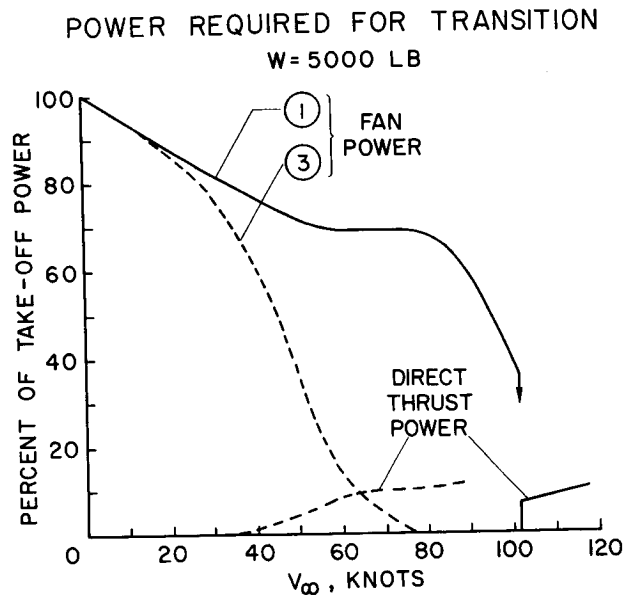


Figure 9

STABILIZER CONTROL AVAILABLE IN TRANSITION

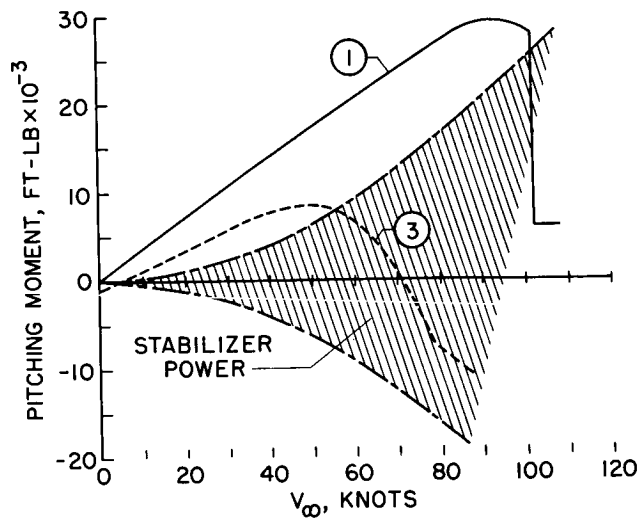


Figure 10

REACTION CONTROL REQUIRED FOR TRANSITION
 $W=5000 \text{ LB}$, $I_y = 6000 \text{ SLUG-FT}^2$

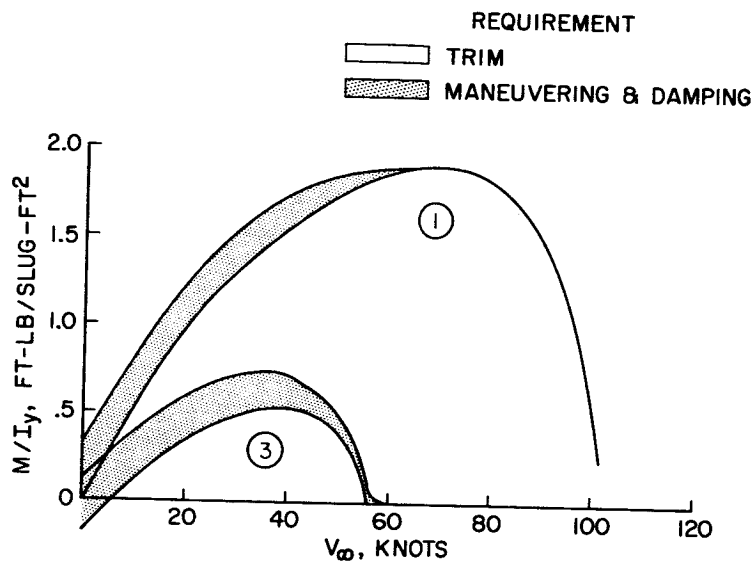


Figure 11

DUCT DESIGN FOR REDUCED PITCHING MOMENT

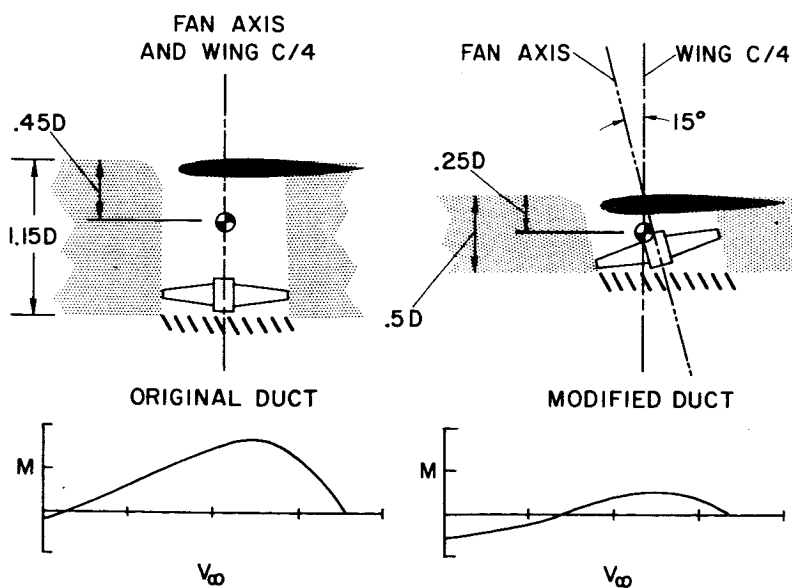


Figure 12

INDUCED INTERFERENCE EFFECTS ON JET AND BURIED-FAN
VTOL CONFIGURATIONS IN TRANSITION

By Kenneth P. Spreemann

Langley Research Center

SUMMARY

Recent investigations of some jet and buried-fan configurations have indicated that in the transition speed range configurations with considerable area surrounding the jet or buried fan can encounter large losses in lift and nose-up pitching moments due to the pressures induced on the lower surfaces by the interaction of the jet and free-stream flow. The obvious way of minimizing these effects is to reduce the surface area surrounding the jets or buried fans, that is, to consider these effects in the preliminary stages of the airplane design.

INTRODUCTION

Previously reported investigations have indicated how the performance of buried-fan VTOL configurations can be affected by the characteristics of the fan inlet flow. The exit flow of buried-fan and turbojet VTOL aircraft can also have important effects on the aerodynamics of these aircraft. This paper will deal primarily with the interaction of the existing jet and the free-stream flow which can induce pressures on the bottom of the wing or fuselage and cause losses in lift and nose-up pitching moments.

SYMBOLS

α	angle of attack, deg
A	area, sq ft
D	diameter, ft
L	lift, lb
M	pitching moment, ft-lb

T	thrust, lb
V	velocity
W	weight, lb

Subscripts:

∞	free stream
j	jet
w	wing

RESULTS AND DISCUSSION

Results of some recent investigations have indicated that serious interference effects can be encountered with some jet and buried-fan configurations in transition such as shown in figure 1. These effects can be shown to be principally the results of the interaction of the exiting jet and the free-stream flow, which induces pressures on the bottom of the wing or fuselage. These interference pressures can be illustrated with some pressure-distribution data that have recently been obtained on a flat plate with a jet issuing vertically beneath it.

Figure 2 shows the pressures schematically imposed on the plate lower surface. Positive pressures are generated in front of the jet and negative pressures behind the jet. Negative pressures as high as 3 to 4 times the free-stream dynamic pressure were measured. The pressures diminish with distance from the jet but extend 10 to 15 jet diameters downstream and 5 to 10 diameters to each side of the jet. The negative pressures outweigh the positive pressures and thus cause a loss in lift. The combination of positive pressures ahead of the jet and negative pressures behind gives a nose-up pitching moment.

There are two factors which affect the magnitude of the lift and nose-up moments: (1) the jet velocity which determines the amplitude of the pressures induced on the lower surface and (2) the extent of the surface area around the jet. For example, with a small plate high pressures on a relatively small area give a loss in lift and nose-up moments; however, with a large plate not only is there this loss in lift, but in addition pressures extend over a much larger area and therefore cause greater losses in lift and larger nose-up moments.

Some force and moment data are available on a number of models to show these effects. Sketches of some of the configurations on which

data are available are shown in figure 3. At the top are two buried-fan configurations and at the bottom two jet configurations. A fairly wide range of ratios of jet area to wing area is covered. Data for the semispan buried-fan configuration are given in reference 1 and for the configuration with the smallest ratio of jet area to wing area in reference 2. Data for the remaining two configurations are from unpublished investigations. It should be noted that the lowest ratio of jet area to wing area is probably impractical ($A_j/A_w = 0.009$). A more realistic area ratio for a jet aircraft would be somewhere between the largest jet and smallest fan-in-fuselage configurations.

Figure 4 shows some data that have been obtained for these models through the transition speed range at zero angle of attack. As can be seen from the figure, in general the lift losses increase with reductions in the ratio of jet area to wing area. Also the nose-up moments are increased with decreases in jet area to wing area.

The two buried-fan configurations include inlet flow over the top of the model which contributes to the nose-up moments. However, for the jet configuration there is no inlet flow and the moments are primarily due to the induced pressures on the lower surface.

These data are for zero angle of attack with the jet efflux perpendicular to the bottom of the wing or fuselage. For some configurations the loss in lift can be compensated for with wing lift by going to higher angles of attack.

Figure 5 shows some typical examples of transition at angles of attack of 0° , 10° , and 20° for the delta-wing jet model. At zero angle of attack the same adverse effects existed as were shown in figure 4. At 20° angle of attack the wing lift more than compensated for the loss in lift due to the jet interference throughout the transition; however, the pitching-moment problem remained.

Some efforts have been made to alleviate these losses in lift and nose-up moments with fixes such as flow diverters and various types of spoilers and ramps. These fixes have not been particularly helpful, possibly because the fixes were placed too close to the jet. However, in one full-scale flight investigation deflecting a trailing-edge flap reduced the losses in lift and nose-up pitching moments. The beneficial effects of the flaps on this configuration can be attributed to positive pressures being built up in front of the flap on the lower surface.

In addition to the trim problem there can be a problem of stability in transition on conventional aft-tailed configurations. This point is illustrated in figure 6, which shows the attitude stability parameter, pitching moment in foot-pounds per degree of angle of attack, plotted

against velocity in knots, for a 4-jet 9,000-pound airplane with a conventional aft tail. The data points on the curve correspond to the jet deflection angles required to maintain steady level flight. In the transition speed range the airplane is unstable up to about 170 knots.

A similar instability was pointed out in reference 3 for the propeller-driven VTOL configurations; however, the instability extended up to only 30 or 40 knots and consequently was not particularly troublesome to the pilots because of the low dynamic pressures involved. However, the higher dynamic pressures involved in the present case would be expected to cause some difficulty as has been verified by free-flight tests of a dynamically scaled model of this configuration which indicated some piloting problems in this speed range.

CONCLUDING REMARKS

All the data in this paper are based on model results at low Reynolds numbers. While full-scale results may differ somewhat in the magnitude of specific values, the general trends indicated would not be changed. Thus it appears that configurations with considerable lifting area surrounding the jet or buried fan can encounter large losses in lift and large nose-up moments at low forward speeds as a result of the pressures induced on the lower surfaces by the jets. The obvious way of minimizing these effects is to reduce the surface area surrounding the jets or buried fans, that is, to consider these effects in the preliminary stages of the airplane design.

In one full-scale flight investigation a trailing-edge flap reduced the losses in lift and nose-up moments in the transition speed range. Another problem is the reduction of the stabilizing contribution of an aft-mounted horizontal tail which may make flight in the transition speed range difficult.

REFERENCES

1. Hickey, David H., and Ellis, David R.: Wind-Tunnel Tests of a Semi-span Wing With a Fan Rotating in the Plane of the Wing. NASA TN D-88, 1959.
2. Williams, John: Some British Research on the Basic Aerodynamics of Powered Lift Systems. Jour. R.A.S., vol. 64, no. 595, July 1960, pp. 413-437.
3. Kirby, Robert H.: Aerodynamic Characteristics of Propeller-Driven VTOL Aircraft. (Prospective NASA Paper.)

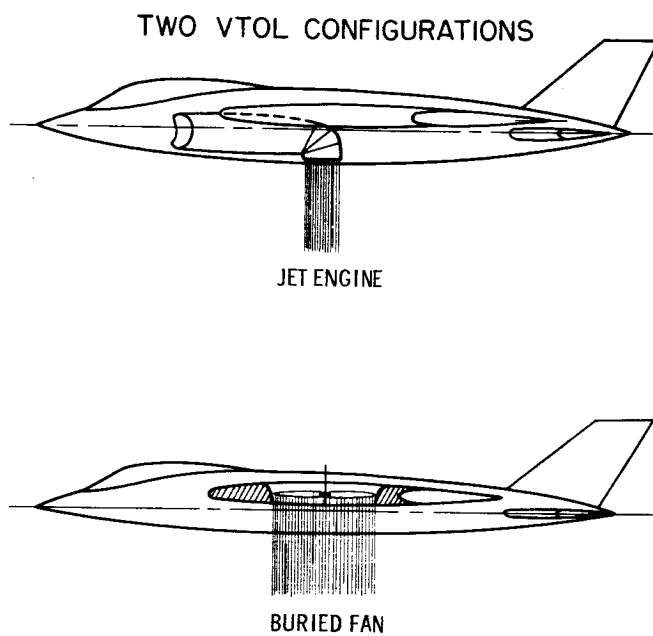


Figure 1

SCHEMATIC DIAGRAM OF PRESSURES ON PLATE

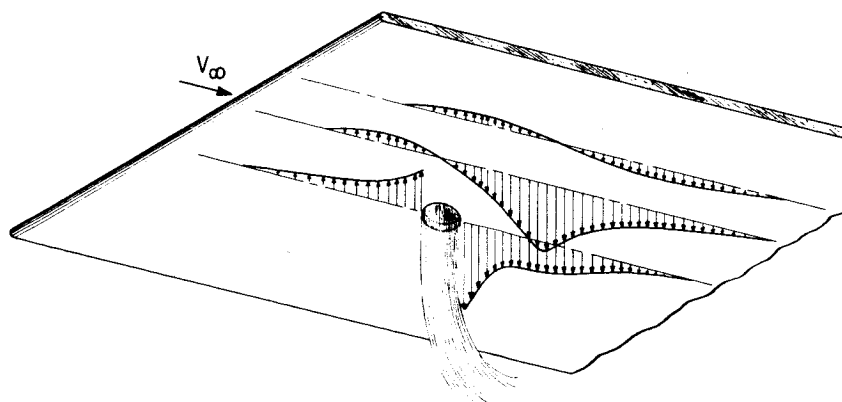


Figure 2

PLANFORMS STUDIED

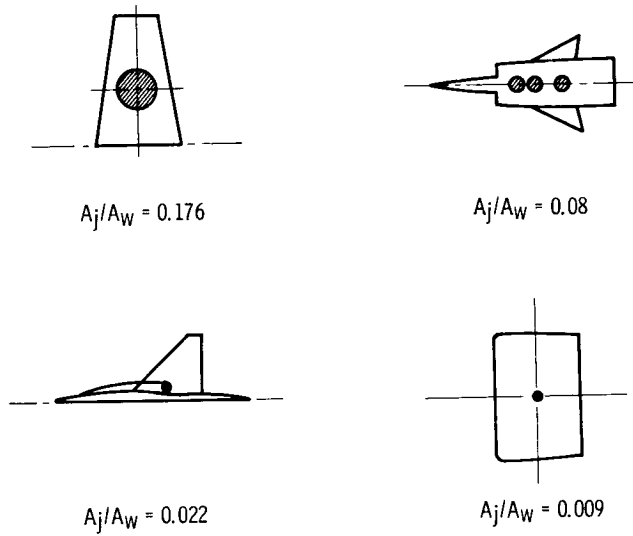


Figure 3

EFFECT OF SPEED ON LIFT AND PITCHING MOMENT

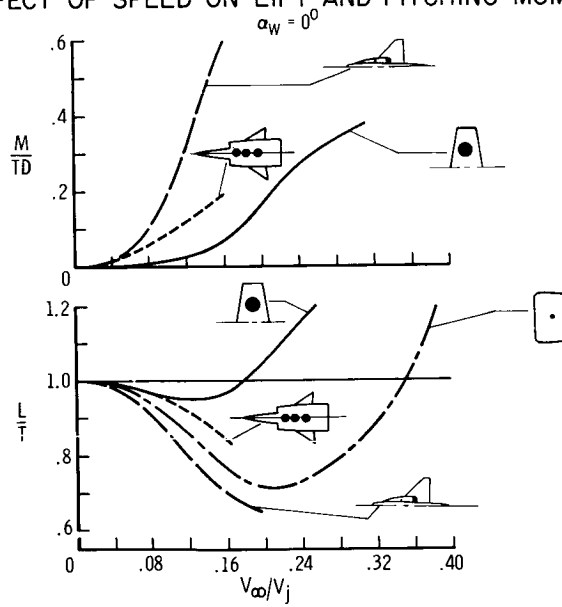


Figure 4

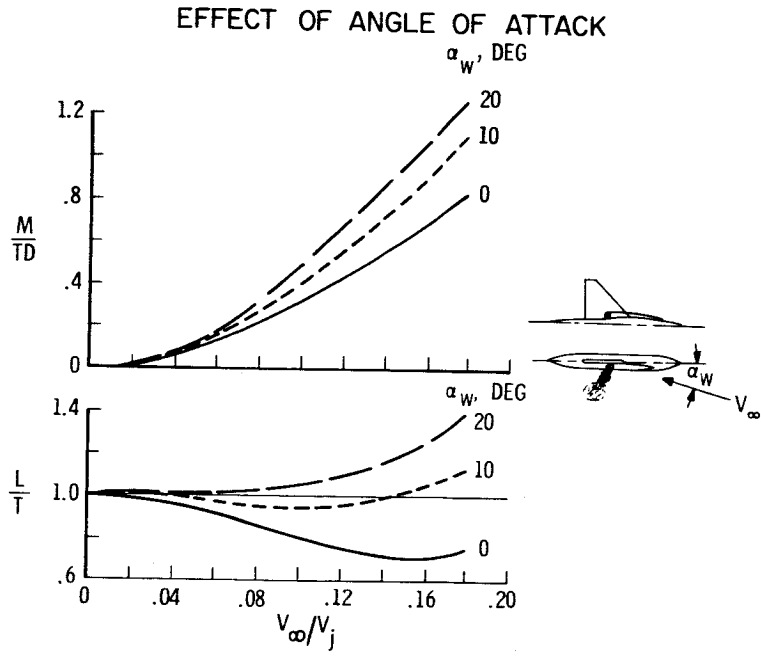


Figure 5

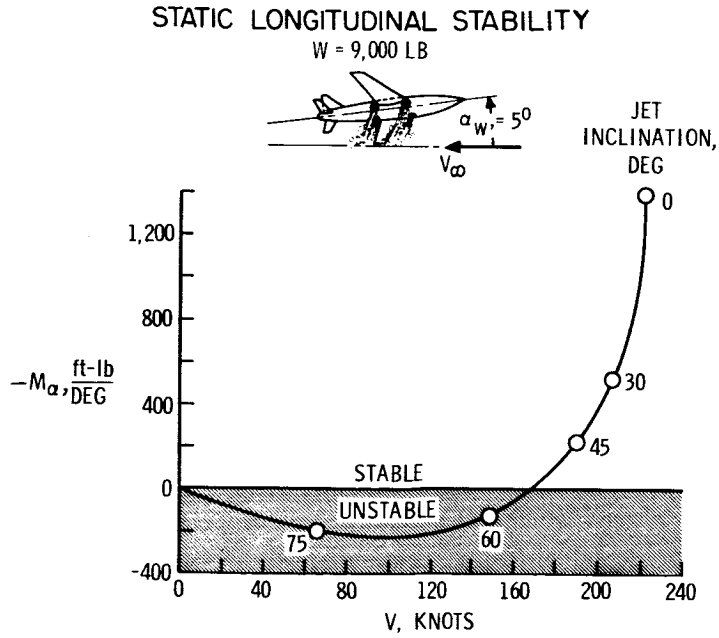


Figure 6

GROUND INTERFERENCE EFFECTS

By Robert O. Schade

Langley Research Center

SUMMARY

A study has been made to determine the basic phenomena associated with the ground interference effects for VTOL aircraft in an attempt to arrive at some generalized conclusions regarding the effect of the ground on the various types of VTOL aircraft.

The results showed that helicopter and other rotor aircraft generally experience favorable ground effect. In the case of propeller VTOL aircraft the tilt-wing configurations will usually experience a small favorable ground effect. For the deflected-slipstream configurations a large detrimental ground effect is experienced at low angles of attack of the thrust axis but little or no ground effect at angles of attack of 25° or 30°. For buried-fan and jet configurations the ground effect can be favorable or unfavorable depending upon the geometry of the fans or jets and the airframe. For single-jet configurations the ground effects are detrimental and cannot be eliminated by fixes on the airplane. For these cases, a perforated landing platform appears to offer promise as a means of minimizing the adverse ground effect. Ground effects experienced in hovering flight tend to decrease with increasing forward speed and are rather small at airspeeds that might be of interest for STOL operation of the various VTOL configurations. The qualitative predictions of the ground effect for various VTOL aircraft configurations can be made with a fair degree of confidence, but it appears at the present time that the magnitude of the effect for specific configurations will usually have to be obtained from test data.

INTRODUCTION

Ground interference effects have not proved to be very significant for conventional airplanes but they have assumed major importance for VTOL aircraft because the slipstream or jet exhaust is directed straight down for vertical take-off and landing. These ground interference effects can be either favorable or unfavorable depending upon the configuration.

It is the purpose of this paper to cover ground interference effects for all types of VTOL aircraft, with descriptions of the phenomena

L
1
4
1
6



involved and indications of possible means of minimizing the unfavorable interference effects where they exist.

It should be pointed out that the term "ground interference effects" used in this paper refers to the effect of the ground on the aerodynamics of the aircraft. Other effects of the slipstream impingement, such as ground erosion, recirculation of dust and debris, and effects on objects surrounding the landing area are covered in the paper by Thomas C. O'Bryan.

The ground interference effects discussed in this paper can be broken down into two parts: the effect on the thrust of the propulsion source itself and the effect on the airframe. Basic phenomena associated with these two kinds of interference are indicated and experimental data for various VTOL configurations are presented. Some indication of the particular interference effect involved in each case is given.

SYMBOLS

D	diameter
h	height
L	lift
L_{∞}	lift at infinite distance above ground
M_{α}	variation of pitching moment with angle of attack
β	propeller blade angle
θ_T	angle of thrust line

GROUND EFFECT ON PROPULSION SOURCE

Figure 1 shows the lift augmentation of propellers and rotors. The sketch in the figure indicates that as the rotor approaches the ground the slipstream fans out; the result is an increase in pressure and a decrease in velocity in the slipstream. This change causes the well-known increase in lift on the rotor as it approaches the ground. A typical variation of lift augmentation for a propeller or rotor is shown by the curve in figure 1. The term L/L_{∞} is the ratio of the amount of lift in ground effect to that out of ground effect. (Values

above 1.0 indicate favorable ground effect.) The ratio h/D is the height above the ground divided by the diameter.

For jet engines there is a similar flow which also spreads out as the ground is approached, but in this case an increase in lift is not obtained. In fact, a decrease in lift or thrust might be experienced because the increased pressure in the jet exhaust results in back pressure on the engine. However, this effect for a jet is not a significant one because the tail pipes of jets are usually not very close to the ground in terms of tail-pipe diameter.

Figure 2 shows the effect of the ground on a ducted fan with two different blade angles. When the blade angle is set for optimum efficiency in hovering out of ground effect, there is a loss in lift as the ground is approached. This detrimental ground effect is attributed to the fact that the higher disk loadings associated with ducted fans require higher blade angles, and there is a tendency for the blades to stall as the ground is approached. This stalling tendency can be reduced by using lower blade angles, and if the blade angle is reduced to a very low value, a favorable ground effect can be obtained as indicated by the top curve. Of course, it must be realized that this change from an unfavorable to a favorable ground effect is accomplished at the expense of some hovering efficiency out of ground effect.

EFFECT OF SLIPSTREAM ON AIRFRAME

Two-Dimensional Patterns

The upper sketches of figure 3 illustrate the two basic flow patterns resulting from different arrangements of slipstreams with respect to airframe surfaces. The two lower sketches show a vertical cross section through the slipstream. The induced pressures resulting from the two flow patterns are shown by the symbols + and - indicating positive and negative changes in pressure, respectively. At the left-hand side of the figure the case of a single slipstream emerging from the bottom of a surface is shown. There is an induced flow around the edges and under the surface as indicated by the broken lines; this flow results in a decreased pressure and therefore an unfavorable ground effect. At the right-hand side the case of two slipstreams at the edge of a surface is shown. In this case the flow pattern is upward in the middle resulting in increased pressure on the surface between the slipstreams and thus in a favorable ground effect.

With actual airplane configurations, of course, there are variations and combinations of these two basic flow patterns. For example, if two jets are exhausting from some intermediate positions there will

be both positive and negative induced pressures, and the ground effect can be either favorable or adverse depending on how much of the total surface area is between the jets.

Three-Dimensional Pattern

Figure 4 shows a three-dimensional slipstream pattern for a two-propeller tilt-wing configuration with the two columns, which represent the slipstreams from the two propellers, coming down and striking the ground. The lines with arrows indicate slipstream filaments as they flow radially outward. Because there is an equal and opposite flow along the ground at the plane of symmetry, the plane of symmetry effectively serves as a solid wall through which no flow can pass. Since the slipstream filaments cannot flow through the plane of symmetry, the slipstream must flow upward. This flow is straight upward directly between the propellers but goes upward at progressively smaller angles at greater distances ahead of and behind the propellers. This causes ground effect not only on surfaces between the propellers but also on surfaces all along the plane of symmetry. It should be emphasized that this discussion concerns only the idealized case where the flow is perfectly symmetrical and steady. Of course, in the practical case the recirculation is likely to be both unsymmetrical and unsteady particularly when flying in gusty air and over uneven terrain. Also, if the aircraft is banked, the upward flow instead of being in the plane of symmetry as shown here moves out along the span in the direction of the upgoing wing. The flow in these cases leads to random disturbances of the aircraft which can result in poor handling qualities when the aircraft is flying near the ground. This effect on handling qualities is discussed in the papers by John P. Reeder and by F. B. Gustafson, Robert J. Pegg, and Henry L. Kelley.

HELICOPTER AND ROTOR VTOL AIRCRAFT

For the helicopter and other rotor VTOL aircraft, the ground effect is for all practical purposes the ground effect on the rotor itself since the airframe is small relative to the rotor disk area. This effect of the ground on the rotor has already been discussed.

TILT-WING PROPELLER CONFIGURATIONS

The effect of the ground on two tilt-wing propeller configurations is shown in figure 5. Both of these configurations show an increase in lift as the ground is approached. The data for the four-propeller model

L
1
4
1
6

indicate that part of the favorable ground effect is provided by the propellers themselves and part by the buildup of pressure on the bottom of the fuselage. The favorable ground effect is greater for the Hiller X-18 model because this model has a fuselage with a wide flat bottom. These are small-scale data, but the large favorable ground effect has been verified in the case of the Hiller X-18 by full-scale tests which showed favorable ground effect of about the same magnitude as that shown in this figure. Figure 6 shows some information on the effect of the ground on the stability and control of the Hiller X-18 model. The lower plot shows the effect of the ground on the static longitudinal stability or stability of attitude. For hovering flight out of ground effect, of course, all VTOL aircraft have neutral attitude stability. It can be seen that as the aircraft approaches the ground it becomes stable. This stabilizing effect is a direct result of the favorable ground effect on the fuselage. A nose-down attitude puts the nose closer to the ground resulting in an increased lift augmentation on the forward portion of the fuselage which tends to restore the fuselage to its original attitude. The upper plot shows the variation of yaw control with height. Shown here is the ratio of the control effectiveness in ground effect to that out of ground effect. In considering the variation of yaw control with height, it is pointed out that the ailerons on the trailing edge of the wing within the slipstream are used for yaw control on this configuration. The decrease in yaw control to approximately 50 percent of its original value as the ground is approached, as shown by the upper plot, is the result of the decrease in slipstream velocity over the ailerons.

DEFLECTED-SLIPSTREAM PROPELLER CONFIGURATIONS

Figure 7 shows the effect of angle of the thrust line on the variation of lift augmentation with height for various deflected-slipstream propeller configurations. The research-model data were obtained at various angles of the thrust line from 0° to 24° , whereas the data on the Fairchild and Ryan research aircraft were obtained at angles of 25° and 30° , respectively. For an angle of 0° , large detrimental ground effects were obtained, but as the angle of the thrust line was increased, the detrimental effect became smaller until at angles around 25° or 30° the ground effect was negligible, as shown by the data on the Ryan and Fairchild machines. This effect can be explained as follows: As the wing-flap configuration approaches the ground, an adverse pressure gradient builds up over the upper surface of the wing tending to cause separation and loss of lift. This effect is apparently more pronounced for the 0° angle case where the wing-flap combination must turn the slipstream 90° ; the slipstream is therefore likely to be partially separated even out of ground effect. For an angle of 30° , of course, the slipstream need only be deflected 60° rather than 90° so there is better flow over the wing and less tendency to separate.

FAN-IN-WING ARRANGEMENT

The effect of the ground on the fan-in-wing arrangement is shown in figure 8. For the case of the wing and fans alone there is a detrimental ground effect shown by the lower curve. This effect apparently results from a negative pressure buildup under the outboard portion of the wing that is greater than the positive pressure buildup between the fans. The magnitude of this effect will, of course, vary with wing and fan geometries. The upper curve shows that a beneficial effect can be obtained by adding a fuselage below the wing. In this case the effect is rather large at the low values of h/D because the fuselage is flat and is almost touching the ground. It may be noted that the reversal in the slope of the upper curve indicates an unstable variation of power with height which would make it difficult for a pilot to maintain constant altitude when flying at this height. Of course, this same situation exists for all heights when the ground effect is adverse.

MULTIPLE-JET CONFIGURATIONS

Shown in figure 9 is the effect of the ground on multiple-jet configurations. For the two-jet arrangement there is a detrimental ground effect, shown by the long-dashed line. When four vertical fences are placed along the fuselage between the jets to form an open-bottom box to trap the recirculated jet exhaust, a beneficial ground effect is obtained but there is still some adverse ground effect at the intermediate heights.

With the four-jet configuration there is only a small negative ground effect. In this case, more of the jet exhaust is trapped between the jets resulting in a greater buildup of pressure in this region which almost balances out the losses caused by negative pressure under the remainder of the airframe. If this approach is followed to the extreme and if jets are placed all around the perimeter of the airframe, it is possible to end up with a very beneficial ground effect as has been shown in work with ground-effect machines. Incidentally, an attempt is being made to take advantage of this principle in the GETOL, ground-effect take-off and landing, machines currently being studied.

SINGLE-JET CONFIGURATIONS

In figure 10 the effect of the ground on single-jet configurations is shown. For the research model as shown by the dashed curve there is

negative ground effect because of the negative pressure produced under the airframe by the single jet. A similar effect was obtained on the Bell X-14 as shown by the solid line. Attempts to minimize this negative effect by fixes on the aircraft itself have not been too successful. For the Bell X-14, some improvement was obtained by lengthening the landing gear and effectively moving up along the curve. Another method proposed for minimizing the adverse ground effect of jet configurations is the use of a perforated landing platform a short distance above the ground. The principal effect of the perforated plate is to provide a barrier between the high-energy jet exhaust which flows along the ground and the air above that it tries to entrain. This method reduces the induced negative lift. With the use of this perforated plate on the research model the losses are reduced to almost zero for normal landing-gear heights.

EFFECT OF FORWARD SPEED ON GROUND EFFECT

So far, only ground effect in hovering flight has been considered. The effect of forward speed on the ground effect for three different VTOL configurations is shown in figure 11. In this figure lift augmentation is plotted against forward speed. The curves are for a helicopter with its favorable ground effect, for a deflected-jet configuration with its unfavorable ground effect, and for a deflected-slipstream configuration in the condition in which it experiences the most unfavorable ground effect - that is, at an angle of the thrust line of 0° . As discussed previously, this large unfavorable ground effect with the deflected-slipstream configuration in hovering can be eliminated by increasing the angle of the thrust line. This case is used only to illustrate the effect of forward speed on a very large detrimental ground effect. The data were obtained under conditions corresponding to a running take-off - that is, with the wheels on the ground. This information is therefore applicable to short take-off and landing, or STOL, operation. The main point to be obtained from this figure is that the ground effects, both favorable and unfavorable, generally tend to disappear as forward speed is increased and are rather small for airspeeds that might be of interest for STOL operation with the various configurations.

CONCLUDING REMARKS

From a study of ground interference effects on VTOL configurations the following conclusions were made:

Helicopter and other rotor aircraft generally experience favorable ground effect.

For propeller VTOL aircraft the tilt-wing configurations usually experience a small favorable ground effect. For the deflected-slipstream configurations a large detrimental ground effect is experienced at low angles of the thrust line but little or no ground effect is experienced at angles of 25° or 30° .

For buried-fan and jet configurations the ground effect can be favorable or unfavorable depending upon the geometry of the fans or jets and of the airframe.

For single-jet configurations the ground effects are detrimental and cannot be eliminated by fixes on the airplane. For this case, a perforated landing platform appears to offer promise as a means of minimizing the adverse ground effect.

Ground effects experienced in hovering flight tend to decrease with increasing forward speed and are rather small at airspeeds that might be of interest for STOL operation of the various VTOL configurations.

And, finally, although the qualitative predictions of the ground effect for various VTOL aircraft configurations can be made with a fair degree of confidence, the magnitude of the effect for a specific configuration will generally have to be obtained from test data.

LIFT AUGMENTATION OF PROPELLERS AND ROTORS

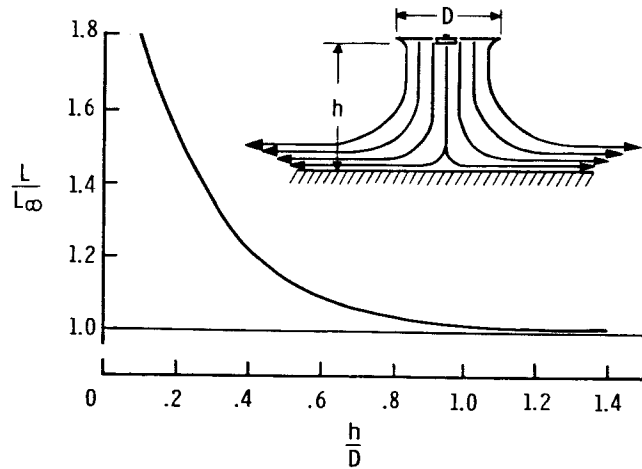


Figure 1

DUCTED FAN IN REGION OF GROUND EFFECT

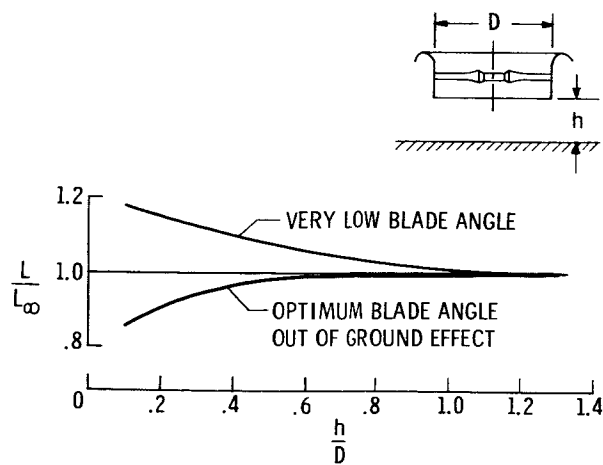


Figure 2

SLIPSTREAM PATTERNS

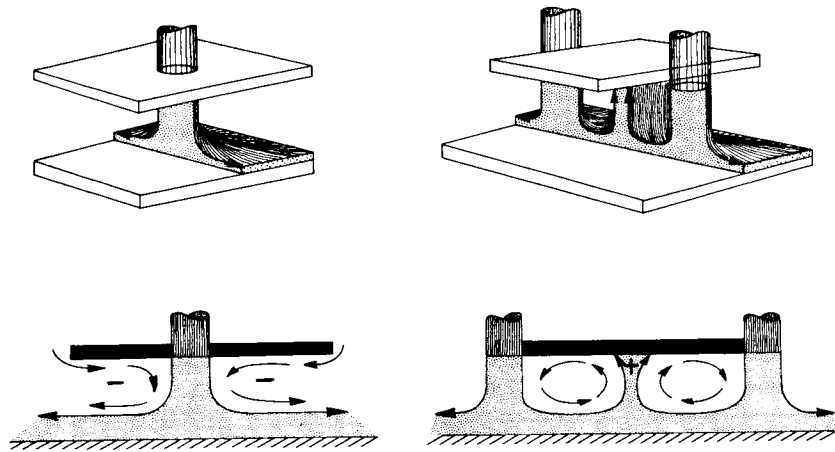


Figure 3

THREE-DIMENSIONAL SLIPSTREAM PATTERN

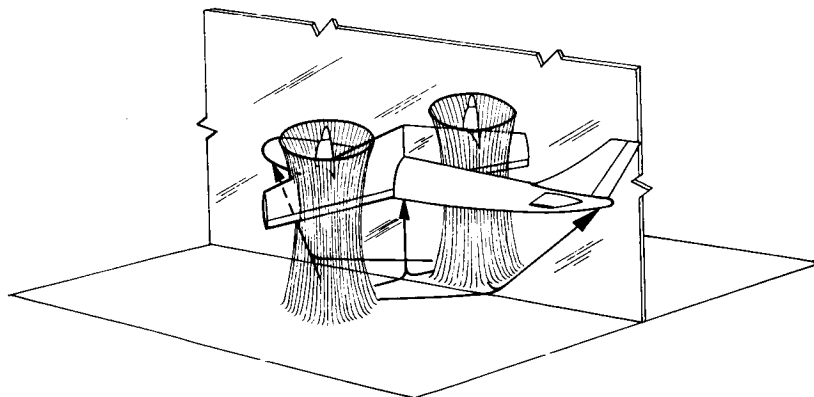


Figure 4

EFFECT OF THE GROUND ON TWO TILT-WING CONFIGURATIONS

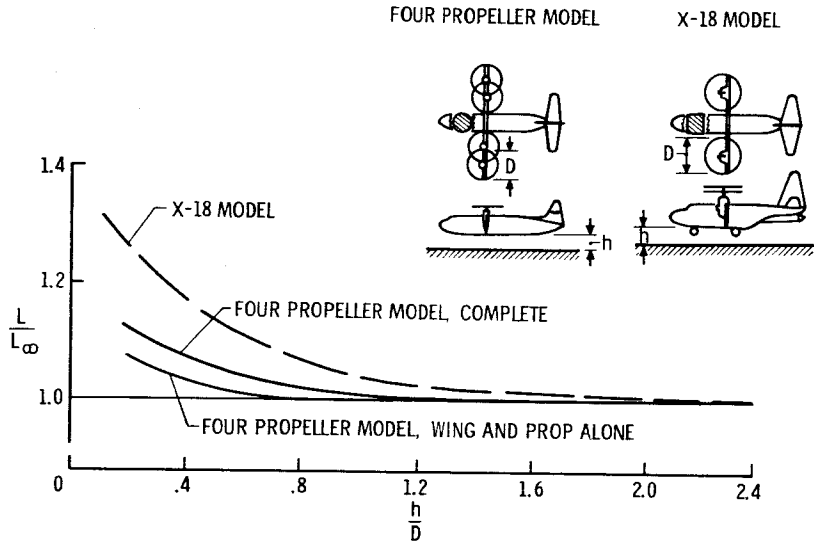


Figure 5

STABILITY AND CONTROL OF X-18 MODEL IN REGION OF GROUND EFFECT

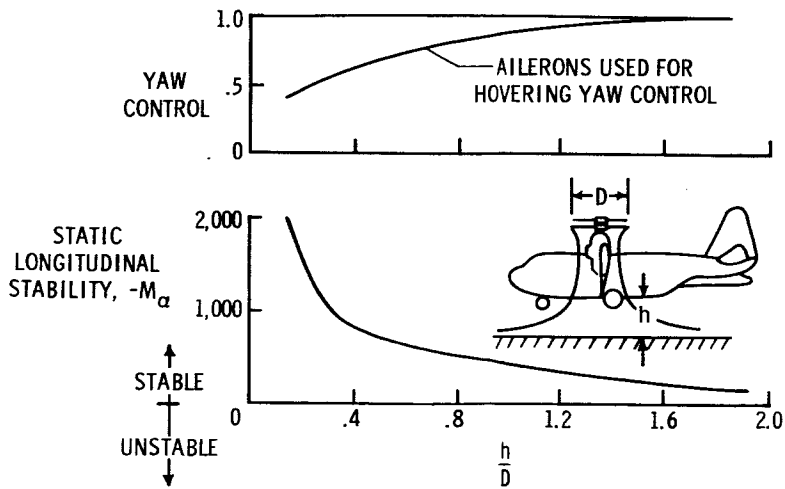


Figure 6

EFFECT OF THE GROUND ON DEFLECTED-SLIPSTREAM CONFIGURATIONS

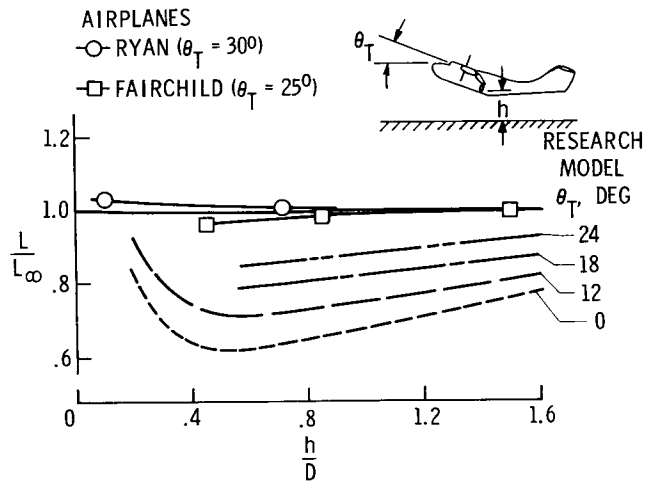


Figure 7

EFFECT OF THE GROUND ON FAN-IN-WING ARRANGEMENT

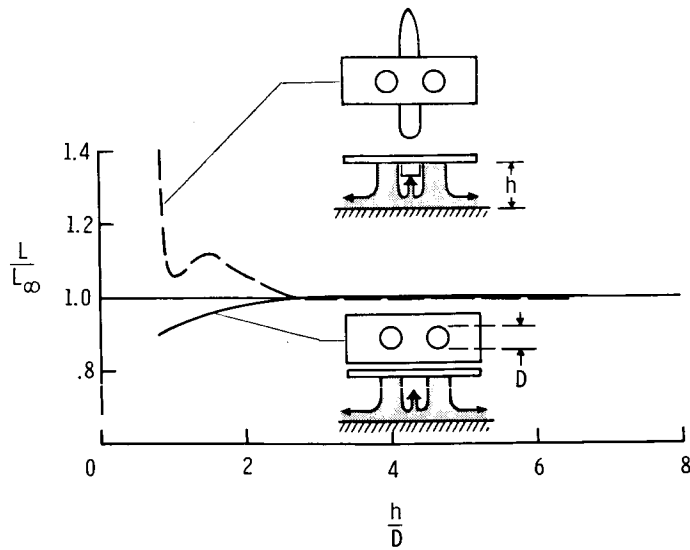


Figure 8

EFFECT OF THE GROUND
ON MULTIPLE - JET CONFIGURATIONS

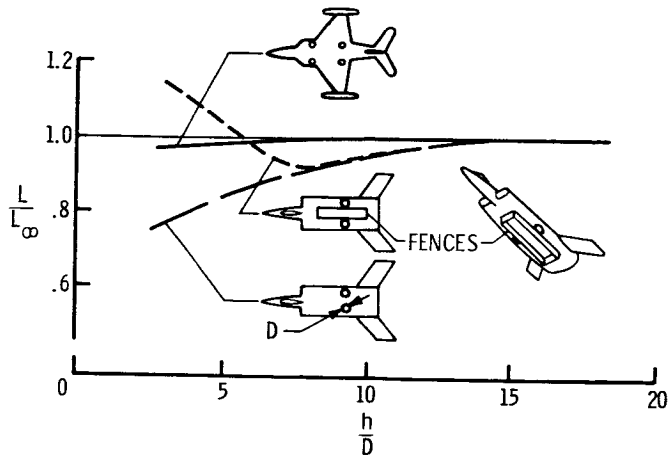


Figure 9

EFFECT OF THE GROUND ON SINGLE-JET CONFIGURATIONS

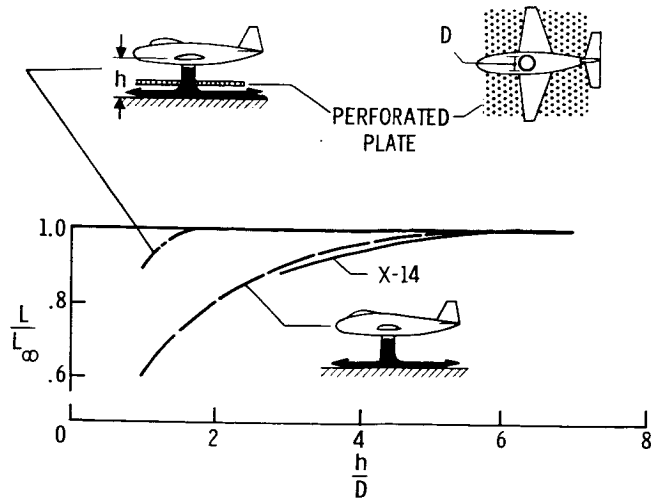


Figure 10

EFFECT OF FORWARD SPEED ON GROUND EFFECT

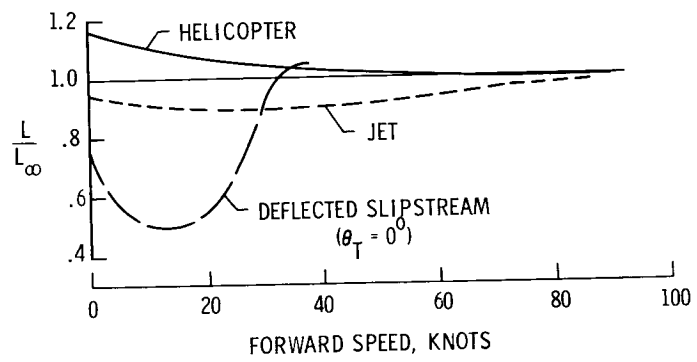


Figure 11

CONSIDERATIONS OF METHODS OF IMPROVING
HELICOPTER EFFICIENCY

By Richard C. Dingeldein

Langley Research Center

SUMMARY

Recent NASA helicopter research indicates that significant improvements in hovering efficiency, up to 7 percent, are available from the use of the NACA 63A015(230) airfoil section. This airfoil should be considered for flying-crane-type helicopters. Application of standard leading-edge roughness causes a large drop in efficiency; however, the cambered rotor is shown to retain its superiority over a rotor having a symmetrical airfoil when both rotors have leading-edge roughness.

A simple analysis of available rotor static-thrust data indicates a greatly reduced effect of compressibility effects on the rotor profile-drag power than predicted from calculations.

Preliminary results of an experimental study of helicopter parasite drag indicate the practicability of achieving an equivalent flat-plate parasite-drag area of less than 4 square feet for a rotor-head--pylon--fuselage configuration (landing gear retracted) in the 2,000-pound minimum-flying-weight class. The large drag penalty of a conventional skid-type landing (3.6 square feet) can be reduced by two-thirds by careful design. Clean, fair, and smooth fuselages that tend to have narrow, deep cross sections are shown to have advantages from the standpoint of drag and download. A ferry range of the order of 1,500 miles is indicated to be practicable for the small helicopter considered.

INTRODUCTION

This paper summarizes the results of recent research relating to improving the efficiency of a helicopter in hovering and in forward flight. The reader having competence in the field of helicopter aerodynamics will recognize no new or startling concepts. The data presented, however, are believed to assure the practicability of large helicopter performance improvements.

Large gains in rotor hovering efficiency are shown for a special airfoil formed by combining an NACA 6A-series thickness distribution and an NACA forward-camber mean line. The reduction in efficiency accompanying two different conditions of rotor-blade leading-edge roughness is given. Available static-thrust data obtained on a large number of helicopter rotors operated at high tip speeds are summarized to show the general effect of compressibility on the rotor profile-drag power coefficient and are compared with calculated predictions. In addition, preliminary results obtained from an experimental study of helicopter parasite drag are presented to show the relative drag of the different helicopter components. This information forms the basis of calculations used to demonstrate significant improvements in helicopter cruising efficiency.

SYMBOLS

b	number of rotor blades
c	blade chord at station x
c_e	equivalent blade chord, $\frac{\int_0^1 cx^2 dr}{\int_0^1 x^2 dr}$
D	parasite drag, lb
L	lift, lb
T	rotor thrust, lb
M	Mach number
P	rotor power, $\frac{\text{ft-lb}}{\text{sec}}$
R	rotor radius, ft
C_T	rotor thrust coefficient, $\frac{T}{\rho(\Omega R)^2 \pi R^2}$
C_P	rotor power coefficient, $\frac{P}{\rho(\Omega R)^3 \pi R^2}$

\bar{C}_L	rotor mean lift coefficient, $\frac{6C_T}{\sigma}$
r	radius to blade element, ft
$x = r/R$	
SFC	specific fuel consumption, lb/hp-hr
α	angle of attack
ρ	density of air, slugs/cu ft
Ω	rotor angular velocity, radians/sec
σ	rotor solidity, $\frac{bc_e}{\pi R}$
θ_1	rotor-blade geometric twist (negative sign denotes washout), deg

Subscripts:

O	profile drag
t	blade tip
div	denotes drag divergence of two-dimensional airfoil
f	fuselage

RESULTS AND DISCUSSION

Hovering Efficiency

Effect of camber.- The advantages of cambered rotor blades in respect to producing improved hovering and forward-flight efficiency are well known. (See refs. 1 to 3.) In an effort to define a rotor-blade airfoil section that would essentially realize the largest practicable gains in hovering efficiency that are available through airfoil selection, an NACA 63A015 thickness distribution was mated to an NACA 230 mean line. This thickness distribution was chosen because helicopter tower tests of a rotor having an NACA 63₂-015 airfoil section (ref. 4) indicated the highest overall combination of high maximum mean rotor lift coefficients and resistance to compressibility drag rise of a number

of full-scale rotors previously tested. The NACA 63A015 thickness distribution should have essentially the same aerodynamic characteristics as the NACA 632-015 thickness distribution (refs. 5 and 6) and its larger trailing-edge angle avoids construction problems associated with the cusped trailing edge. The expectation, then, was to realize the benefits of camber without introducing large quarter-chord pitching moments or early drag divergence. Rotor blades having the new airfoil (denoted as the NACA 63A015(230)) were tested on the Langley helicopter tower (ref. 7). A sample of the results is shown in figure 1, in which the rotor hovering efficiency (defined as the rotor figure of merit) is plotted against the rotor-blade tip Mach number for values of the rotor mean lift coefficient \bar{C}_L of 0.5, 0.7, and 0.9. This parameter is proportional to the rotor-blade loading. A utility helicopter would probably operate at the lower value shown, a flying-crane type at the higher values. Also shown are the data for the rotor having an NACA 632-015 airfoil section. These rotors were similar in respect to solidity, twist, and surface condition. Substantial gains due to camber, up to 6 or 7 percentage points, are indicated. At typical rotor disk loadings, a 5-percent gain in figure of merit is equivalent to an extra one-half to two-thirds of a pound of rotor thrust per horsepower delivered to the rotor. This value is equivalent to a 5- to 8-percent increase in the gross rotor thrust, or a 10- to 15-percent or more increase in the helicopter payload. The gains due to camber disappear as the rotor-tip Mach number increases past 0.6; however, this is not a range generally associated with a flying-crane helicopter.

It should be noted that the gains indicated in figure 1 did not require extreme care with the airfoil contour and surface condition. For example, the high efficiencies shown in figure 1 do not depend on a section drag polar having the familiar bucket shape. The contour was good and the blades were smooth and fair, but no elaborate quality-control procedures were taken.

It should also be stated that the data shown for the NACA 632-015 rotor average some 2- to 4-percent higher hovering efficiencies than were obtained on the helicopter tower from tests of a rotor having the widely used NACA 0012 airfoil.

Effect of leading-edge roughness.- Since rotor blades may not be operated in the smooth condition due to the abrading effects of field operation, two different amounts of leading-edge roughness were investigated. First, shellac of rather thick consistency was applied over an area extending 8 percent of the chord (measured along the surface) back from the leading edge on both the upper and lower surfaces. The resulting spanwise brush marks produced surface waves 0.002 to 0.004 inch in height. Next, the aforementioned condition was removed and NACA standard

leading-edge roughness was added. This roughness consisted in applying fresh shellac over the same area previously described and sprinkling with 0.005-inch grains of carborundum distributed to cover about 5 percent of the area. Measurements of the typical roughness heights showed variations from about 0.006 inch to 0.009 inch. The resulting hovering efficiencies are compared with the smooth rotor in figure 2. The shellac alone had very little effect, but the standard roughness caused up to a 12- or 13-percent drop in the hovering efficiency. This decrease in hovering efficiency, of course, corresponds to a similar increase in the power required to produce a given rotor thrust. The high hovering efficiency capabilities of the NACA 63A015(230) airfoil, therefore, cannot be expected unless the rotor blades are built and kept fairly smooth. The condition of NACA standard leading-edge roughness is believed comparable to the severe erosion that has already been noted in certain helicopter operations and with present blade leading-edge materials.

In figure 3 is shown a comparison between the rotors having NACA 63A015(230) and NACA 63₂-015 airfoil sections for the condition of NACA standard roughness applied to both rotors. It is seen that the cambered airfoil retains its considerable superiority in hovering efficiency over the range of test conditions presented.

Effect of reduced thickness and camber.- In an attempt to improve rotor hovering efficiency at rotor tip Mach numbers above 0.6 while retaining some of the advantages indicated for camber at the lower rotor tip Mach numbers, the NACA 63A012 thickness distribution was mated to an NACA 130 mean line. The results of testing a rotor having the resulting NACA 63A012(130) airfoil are shown in figure 4. The combined effects of reduced thickness and camber are seen to give reduced hovering efficiency compared with the NACA 63A015(230) rotor at $\bar{C}_L = 0.9$ and 0.7, and gains at $\bar{C}_L = 0.5$ only at the higher blade tip Mach numbers. For the range of conditions illustrated in figure 4, the NACA 63A012(130) rotor nevertheless indicates somewhat higher efficiencies than the NACA 63₂-015 rotor. It is believed that the NACA 63A015(230) airfoil represents as good a compromise for a load-lifter type helicopter as can be obtained from the standpoint of airfoil choice.

Effect of compressibility on rotor power requirements.- The preceding discussion of figures 1 and 3 has touched on the reduced hovering efficiency associated with the higher rotor-blade tip Mach numbers. From the standpoint of achieving higher forward speeds, the use of higher rotor tip speeds continues to be of interest. A number of large-scale helicopter rotors have been tested in static thrust at relatively high blade-tip Mach numbers, mostly on the Langley helicopter tower facility. (See, for example, refs. 4 and 8 to 11.) A summary of the test results, representing rotor-blade airfoil sections from 6 to 18 percent thick

and rotational blade-tip Mach numbers as high as 1, is shown in figure 5. The purpose of this figure is not to compare airfoils but to provide a quick, broad look at the overall effect of compressibility on the rotor hovering-power requirements. In an attempt to generalize the results, increments in the rotor profile-drag power coefficient measured over the available ranges of rotor tip Mach number and blade pitch angle afforded by the test data were divided by the rotor solidity and plotted against the amount by which the rotor-blade tip Mach number exceeded the drag-divergence Mach number determined from two-dimensional airfoil tests. Also shown is a shaded area representing the results of a number of strip calculations for two different NACA 0012 rotors using compressible airfoil section data and covering a range of blade pitch and tip Mach number. The experimental data are seen to group in a band that lies well below the calculated predictions. A substantial tip relief is also indicated. It therefore appears that greatly reduced effects of compressibility on the power required in forward flight were experienced compared with calculated estimates. The most serious effects of compressibility are probably associated with blade and rotor stability problems; however, these results can be considered as somewhat encouraging. This general research area requires more study.

Cruising Efficiency

Improvements in the forward-flight efficiency of helicopters, primarily with respect to cruising speed and range, are being sought by helicopter operators, particularly the military. Obtaining these improvements is mainly dependent upon the reduction of parasite drag. (See, for example, refs. 12 and 13; the powerplant installation is treated in ref. 14.) In the remainder of the paper the problem will be examined and the preliminary results of recent research will be discussed and used to illustrate the practicability of achieving significant improvements in helicopter forward-flight efficiency, particularly the ferry range.

Parasite drag.- There is considerable airplane-drag--cleanup experience to profit from. (See refs. 15 to 20.) However, the rotor-head--pylon--fuselage combination and the presence of potentially large fuselage downloads in hovering and in forward flight constitute problems peculiar to rotating-wing aircraft and hence warrant special study. An experimental model and full-scale test program has been initiated to study means of achieving low helicopter drag and to assess the drag penalties of various helicopter components. The model tests, conducted at 1/5 scale in the Langley 300-MPH 7- by 10-foot tunnel at a dynamic pressure of about 210 pounds per square foot, are primarily aimed at studying the effect of fuselage and pylon shape and to establish the primary problem areas. The full-scale tunnel test provides data essentially free of scale effects and permits the evaluation of actual hardware, such as antennas.

Sketches of the four model fuselage shapes tested are given in figure 6. Shapes A and B had narrow, deep cross sections in an attempt to reduce downloads in hovering and forward flight, as well as the drag variation with fuselage attitude. The other two shapes had only slightly oval cross sections forward. Shape D had a fairly constant-width forebody terminating in a rather abrupt narrowing of the planform aft of the cabin. The model fuselages were approximately 5 feet long. The projected frontal areas of shapes A, B, C, and D were, respectively, 0.75 square foot, 0.71 square foot, 0.75 square foot, and 0.75 square foot.

Sample equivalent flat-plate parasite-drag areas obtained for fuselage shape C and for a pylon, rotating rotor head, and two different skid-type landing gears are shown in figure 7 for a fuselage angle of attack of 0° . No support-interference corrections have been applied. The model data have been scaled up to the full-scale values, which, in this case, can be taken as representative of a helicopter having a minimum flying weight of the order of 2,000 pounds. The drag of the basic smooth, clean, and fair fuselage is 1 square foot. Adding a clean, streamlined pylon brings the total to 3 square feet. Adding an estimated allowance for the tail rotor brings the total to 3.5 square feet. Installing a conventional skid landing gear of tubular construction doubles the parasite drag to a value of 7.1 square feet. A skid gear which is designed for low drag by using streamlined support struts that track at the cruise attitude and intersect the fuselage normal to the surface rather than at an acute angle is seen to add only about one-third the drag of the conventional gear for a total helicopter parasite-drag area of 4.7 square feet. The literature (refs. 18 to 20) indicates a similar increment from a clean wheel-type gear. The penalty for a dirty-wheel arrangement can be several times this increment. The data provide good arguments for cleaning up or completely retracting the landing gear of a high-performance helicopter.

The Reynolds number of the tubular gear, based on the cylinder diameter, was below the critical value for the model tests. A consideration of the full-scale landing gear that it was patterned after indicates that it, too, would be below the critical Reynolds number for cruising speeds below 110 knots.

The fuselage and pylon parasite-drag values shown are not at all representative of current helicopters, which customarily penalize an already poor aerodynamic shape with additional drag from leakage and nonflush doors, windows, hatches, and other protuberances which not only contribute their own drag but also cause flow separation on the basic fuselage.

Additional preliminary lift and drag data obtained from the 1/5-scale model tests are given in figures 8 and 9. From figure 8 it is seen

that minimum equivalent flat-plate parasite-drag areas of fuselage shapes A and C of the order of 1 square foot were measured. Shapes B and D indicate progressively higher minimum drag, which is probably the result of flow separation in the vicinity of the tail-boom juncture and the abrupt planform closure, respectively. The advantages of a fuselage shape that tends to be narrow and deep rather than broad in cross section is clearly shown in figure 8. Greatly reduced downloads are indicated for fuselages A and B at typical forward-flight attitudes compared with fuselages C and D. Reduced downloads in hovering would also be expected for shapes A and B. Somewhat more favorable variation in the fuselage drag with angle of attack is also apparent. The fact that two of the four fuselages showed relatively low drag, somewhat higher drag being indicated for the two shapes (B and D) that were more subject to flow separation, indicates the importance of designing a smooth and fair shape that avoids sudden changes in contour if low parasite drag is to be achieved. Improved aircraft-construction practice similar to that used on high-performance conventional aircraft will be necessary.

The increase in parasite drag with angle of attack noted in figure 9 (about 1/2 square foot in going from $\alpha_f = 0^\circ$ to $\alpha_f = -5^\circ$) constitutes a performance penalty. Improved cruising efficiency can be obtained by installing the rotor shaft at an angle in order to keep the fuselage level in cruise.

A consideration of area and volume relationships indicates that it should be considerably less difficult to achieve a proportionately low parasite drag for heavier helicopters.

Ferry-range capability.- In order to determine a practicable ferry range for a clean turbine-powered helicopter of the type for which the previously presented drag data were obtained, limited performance estimates were made with available calculation procedures. (See refs. 21 to 23.) An equivalent parasite-drag area of 4 square feet, which assumes a retractable landing gear, was used. Also selected were a rotor solidity of 0.07, a blade twist of -8° , and a design rotor tip speed of 600 feet per second. These parameters were selected to provide good overweight performance. Calculations of the cruise performance were made over a range of gross weights. The maximum effective helicopter lift-drag ratios calculated, which occur at airspeeds of the order of 110 knots, are plotted in figure 10 over a range of ratios of gross weight to normal gross weight. The overload for the ferry mission would be primarily fuel. An L/D of about 7 is indicated at weight ratios above 1.4, which, incidentally, would require a running take-off. Reduced efficiency is indicated at normal gross weight, although the clean helicopter is seen to show to advantage over current practice. A flight procedure of gradually reducing the speed of the power turbine to 85-percent rated speed at the

normal gross weight has the effect of producing an almost constant value of L/D of 7 over the broad range of weight ratios shown.

By using a conservative average L/D of 6, a specific fuel consumption of 0.75 lb/hp-hr, and a minimum flying weight of 1,950 pounds (includes pilot and 1 crew), the ferry-range potential shown in figure 11 is calculated. The Breguet range equation was used; the results were multiplied by a 70-percent factor to allow for take-off, climb, headwinds, and fuel reserves. For a running take-off with 2,000 pounds of fuel on-board, a ferry range of 1,500 miles is indicated. The assumptions of this analysis are believed to be realistic, if not conservative.

CONCLUDING REMARKS

Considerations of the results of recent NASA helicopter research programs have indicated the practicability of large improvements in rotor hovering efficiency by the use of a smooth NACA 63A015(230) rotor airfoil section. Increases in the rotor figure of merit as high as 6 or 7 percent have been demonstrated over an improved rotor having symmetrical airfoil sections. Leading-edge roughness of the type that has been experienced in some helicopter operations is shown to reduce the hovering efficiency drastically. The gains associated with camber, however, are retained over the symmetrical airfoil with standard leading-edge roughness applied. The advantages of camber in this particular case tended to disappear above rotor-blade tip Mach numbers of 0.6.

A simple presentation of available helicopter rotor hovering data obtained over a broad range of airfoil sections, blade-tip Mach numbers, and pitch angles indicates greatly reduced rotor profile-drag power losses due to compressibility effects than predicted by calculations.

Preliminary results of a model study of helicopter parasite drag indicate the importance of using clean, fair, and smooth fuselage shapes if low drag is to be achieved. The use of fuselage cross sections that tend to be narrow and deep is shown to give a lower drag variation with angle of attack and greatly reduced downloads. The importance of cleaning up or completely retracting the landing gear is demonstrated. Equivalent total flat-plate parasite-drag areas of 7.1 square feet, 4.7 square feet, and 3.5 square feet are indicated for a full-scale helicopter (minimum flying weight of the order of 2,000 pounds) equipped with conventional skid gear, a low-drag skid gear, and a retractable gear, respectively. A ferry-range capability of 1,500 miles is estimated.

REFERENCES

1. Gustafson, F. B.: Effect on Helicopter Performance of Modifications in Profile-Drag Characteristics of Rotor-Blade Airfoil Sections. NACA WR L-26, 1944. (Formerly NACA ACR L4H05.)
2. Schaefer, Raymond F., and Smith, Hamilton A.: Aerodynamic Characteristics of the NACA 8-H-12 Airfoil Section at Six Reynolds Numbers from 1.8×10^6 to 11.0×10^6 . NACA TN 1998, 1949.
3. McCloud, John L., III, and McCullough, George B.: Wind-Tunnel Tests of a Full-Scale Helicopter Rotor With Symmetrical and With Cambered Blade Sections at Advance Ratios From 0.3 to 0.4. NACA TN 4367, 1958.
4. Shivers, James P., and Carpenter, Paul J.: Experimental Investigation on the Langley Helicopter Test Tower of Compressibility Effects on a Rotor Having NACA 632-015 Airfoil Sections. NACA TN 3850, 1956.
5. Loftin, Laurence K., Jr.: Theoretical and Experimental Data for a Number of NACA 6A-Series Airfoil Sections. NACA Rep. 903, 1948. (Supersedes NACA TN 1368.)
6. Lindsey, W. F., and Humphreys, Milton D.: Tests of the NACA 641-012 and 641A012 Airfoils at High Subsonic Mach Numbers. NACA RM L8D23, 1948.
7. Shivers, James P.: Hovering Tests of a Rotor Having an Airfoil Section Especially Suited for Flying-Crane Type Helicopters. (Prospective NASA paper.)
8. Jewel, Joseph W., Jr., and Harrington, Robert D.: Effect of Compressibility on the Hovering Performance of Two 10-Foot Diameter Helicopter Rotors Tested in the Langley Full-Scale Tunnel. NACA RM L58B19, 1958.
9. Carpenter, Paul J.: Lift and Profile-Drag Characteristics of an NACA 0012 Airfoil Section as Derived From Measured Helicopter-Rotor Hovering Performance. NACA TN 4357, 1958.
10. Shivers, James P., and Carpenter, Paul J.: Effects of Compressibility on Rotor Hovering Performance and Synthesized Blade-Section Characteristics Derived From Measured Rotor Performance of Blades Having NACA 0015 Airfoil Tip Sections. NACA TN 4356, 1958.

11. Shivers, James P.: High-Tip-Speed Static-Thrust Tests of a Rotor Having NACA 63(215)A018 Airfoil Sections With and Without Vortex Generators Installed. NASA TN D-376, 1960.
12. Harrington, Robert D.: Reduction of Helicopter Parasite Drag. NACA TN 3234, 1954.
13. Churchill, Gary B., and Harrington, Robert D.: Parasite-Drag Measurements of Five Helicopter Rotor Hubs. NASA MEMO 1-31-59L, 1959.
14. Henry, John R.: Aspects of Internal-Flow-System Design for Helicopter Propulsive Units. NACA RM L54F29, 1954.
15. Dearborn, C. H., and Silverstein, Abe: Drag Analysis of Single-Engine Military Airplane Tested in the NACA Full-Scale Wind Tunnel. NACA WR L-489, 1940. (Formerly NACA ACR, Oct. 1940.)
16. Lange, Roy H.: A Summary of Drag Results From Recent Langley Full-Scale-Tunnel Tests of Army and Navy Airplanes. NACA WR L-108, 1945. (Formerly NACA ACR L5A30.)
17. Bierman, David, and Herrnstein, William H., Jr.: The Interference Between Struts in Various Combinations. NACA Rep. 468, 1933.
18. Herrnstein, William H., Jr., and Bierman, David: The Drag of Airplane Wheels, Wheel Fairings, and Landing Gears - I. NACA Rep. 485, 1934.
19. Bierman, David, and Herrnstein, William H., Jr.: The Drag of Airplane Wheels, Wheel Fairings, and Landing Gears. II - Nonretractable and Partly Retractable Landing Gears. NACA Rep. 518, 1935.
20. Herrnstein, William H., Jr., and Bierman, David: The Drag of Airplane Wheels, Wheel Fairings, and Landing Gears - III. NACA Rep. 522, 1935.
21. Gessow, Alfred, and Tapscott, Robert J.: Charts for Estimating Performance of High-Performance Helicopters. NACA Rep. 1266, 1956. (Supersedes NACA TN 3323 by Gessow and Tapscott and TN 3482 by Tapscott and Gessow.)
22. Gustafson, F. B., and Gessow, Alfred: Effect of Blade Stalling on the Efficiency of a Helicopter Rotor As Measured in Flight. NACA TN 1250, 1947.
23. Gessow, Alfred, and Crim, Almer D.: A Theoretical Estimate of the Effects of Compressibility on the Performance of a Helicopter Rotor in Various Flight Conditions. NACA TN 3798, 1956.

EFFECT OF CAMBER ON HOVERING EFFICIENCY

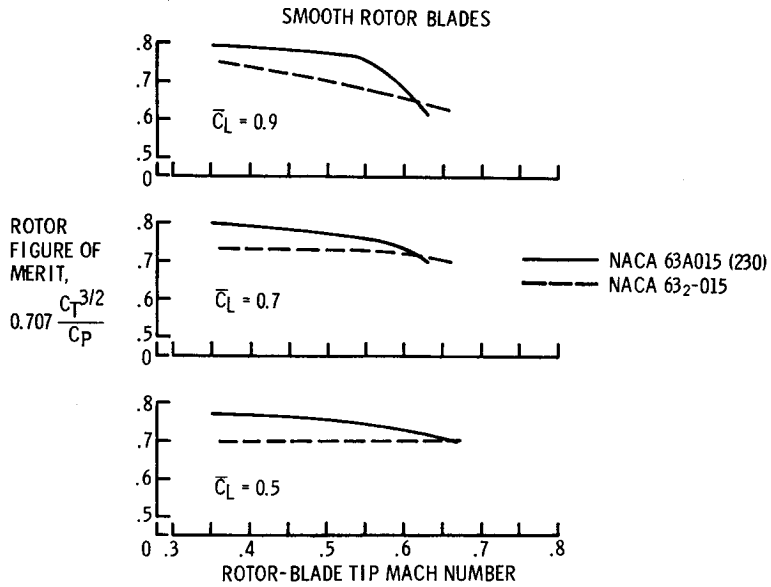


Figure 1

EFFECT OF ROUGHNESS ON HOVERING EFFICIENCY

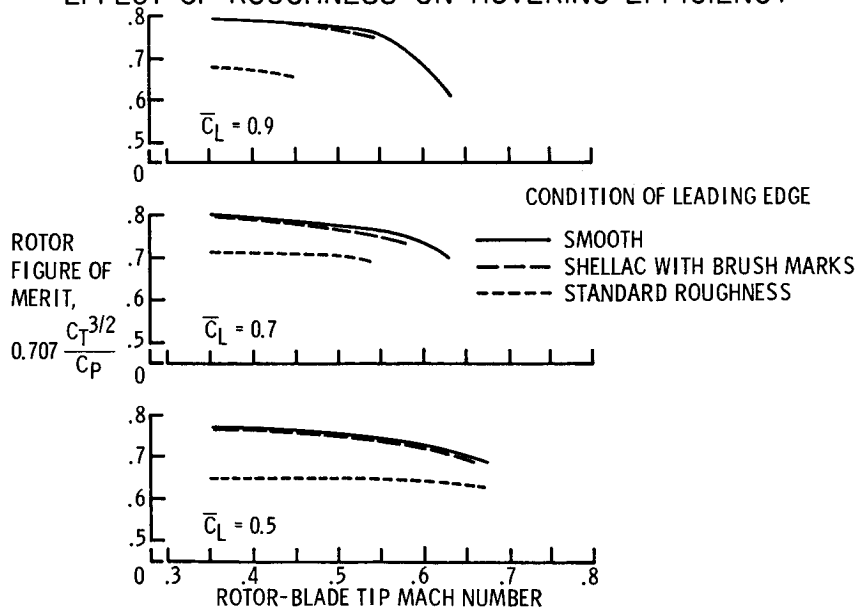


Figure 2

EFFECT OF CAMBER ON HOVERING EFFICIENCY
(NACA STANDARD L.E. ROUGHNESS)

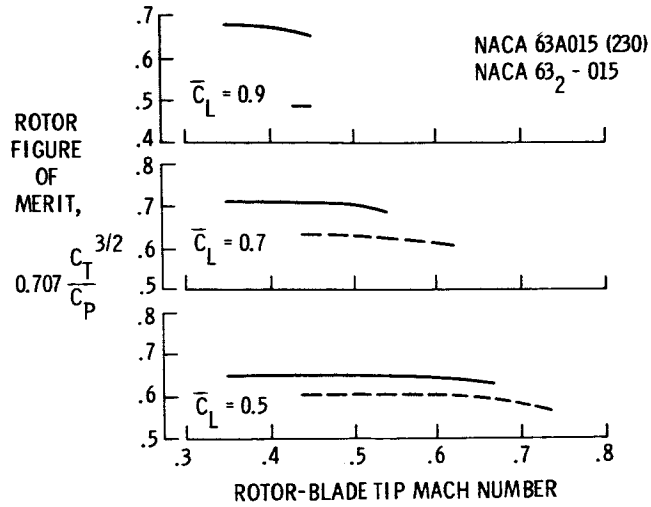


Figure 3

EFFECT OF AIRFOIL SECTION ON HOVERING EFFICIENCY

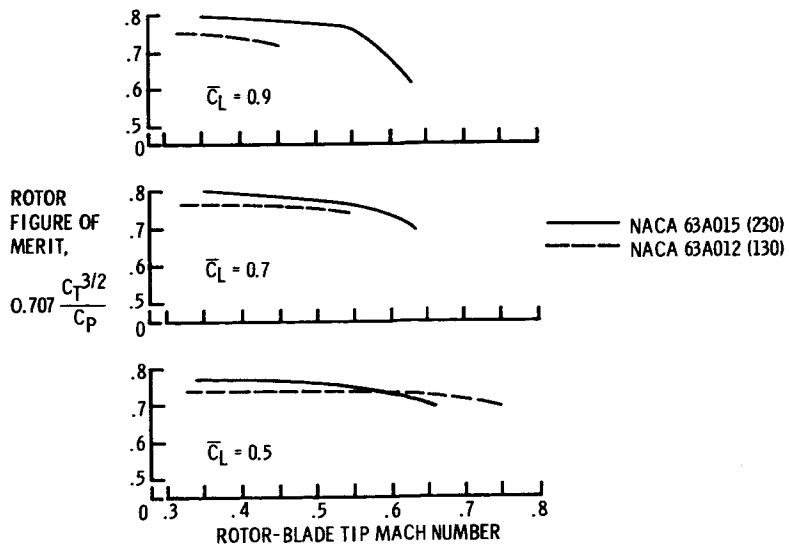


Figure 4

COMPRESSIBILITY EFFECTS ON HOVERING
HELICOPTER ROTORS

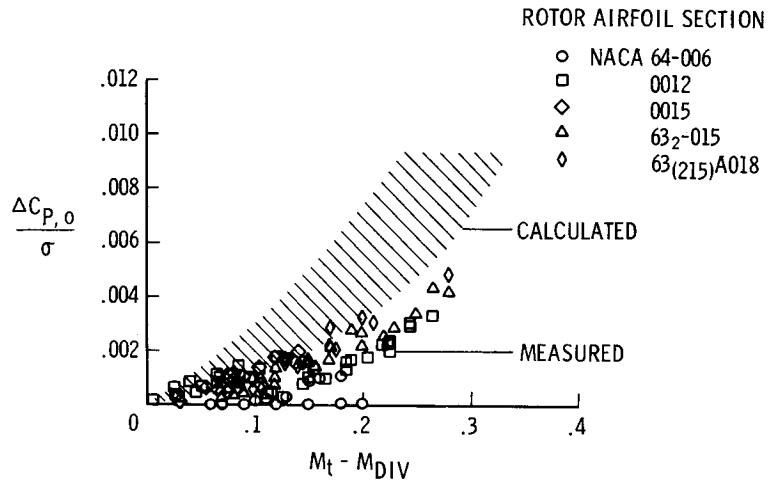


Figure 5

FUSELAGE SHAPES USED IN MODEL TESTS

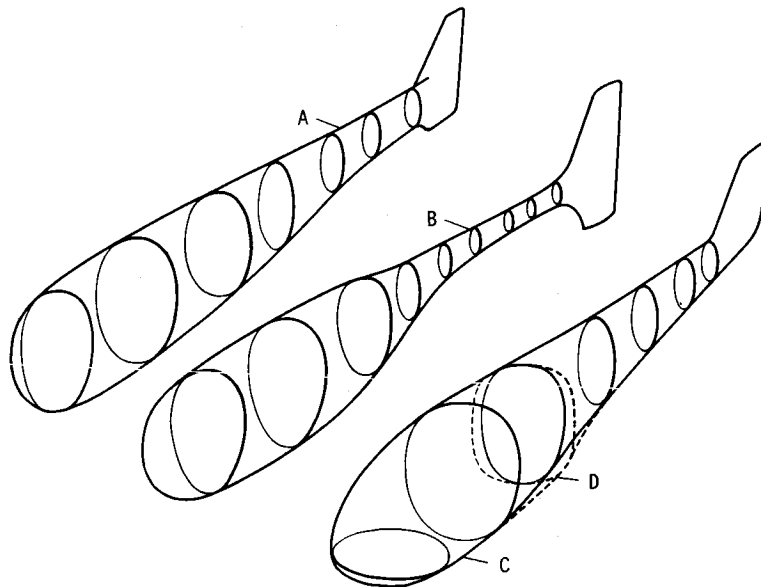


Figure 6

EQUIVALENT PARASITE DRAG AREAS OF VARIOUS HELICOPTER COMPONENTS

$\alpha_f = 0^\circ$

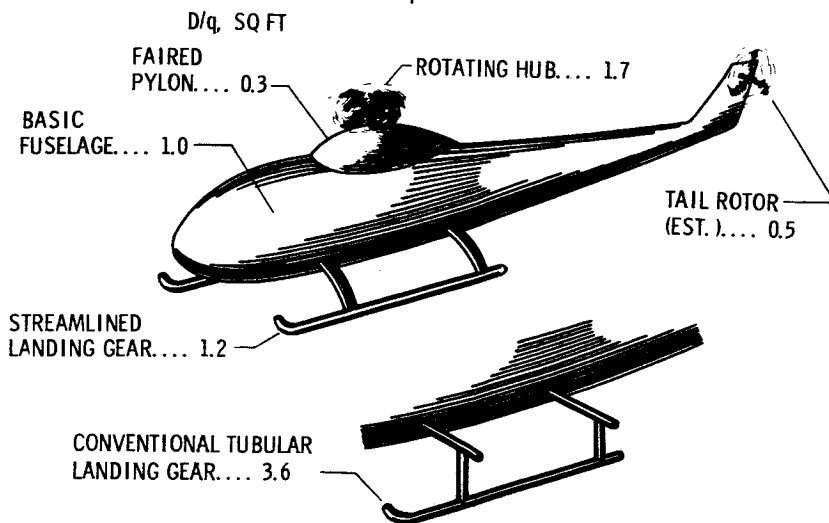


Figure 7

LIFT AND DRAG CHARACTERISTICS OF BASIC FUSELAGE SHAPES

(MODEL DATA PRESENTED FOR FULL-SCALE HELICOPTER)

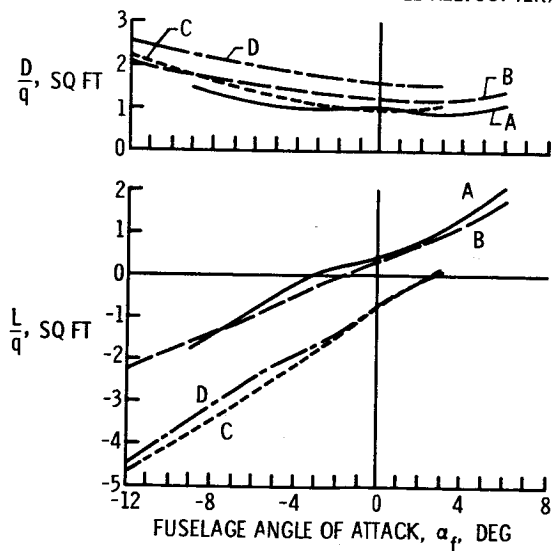


Figure 8

SAMPLE MODEL FUSELAGE DRAG DATA
RESULTS PRESENTED FOR FULL-SCALE HELICOPTER

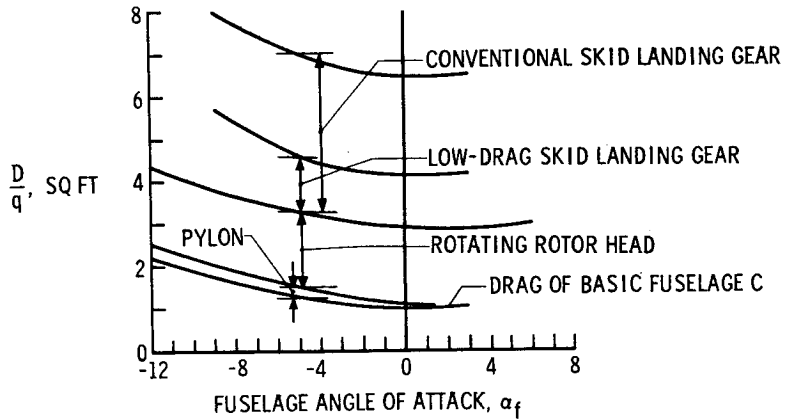


Figure 9

LIFT-DRAG RATIOS CALCULATED FOR SAMPLE HELICOPTER

$$\sigma = 0.07; \frac{D}{q} = 4 \text{ SQ FT}; \theta_1 = -8^\circ$$

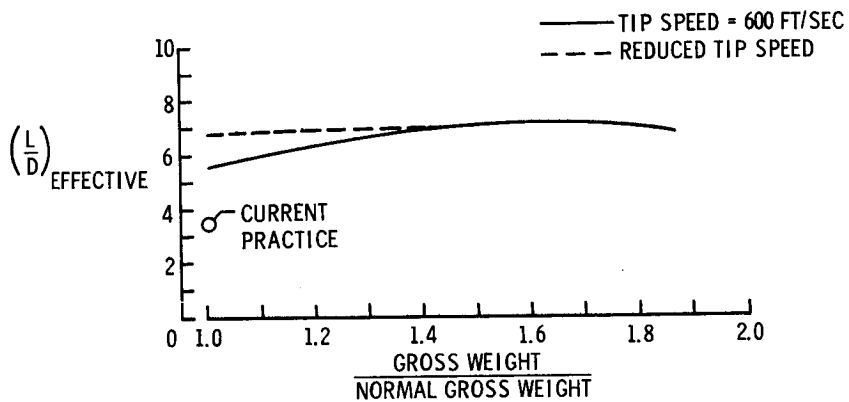


Figure 10

FERRY RANGE POTENTIAL

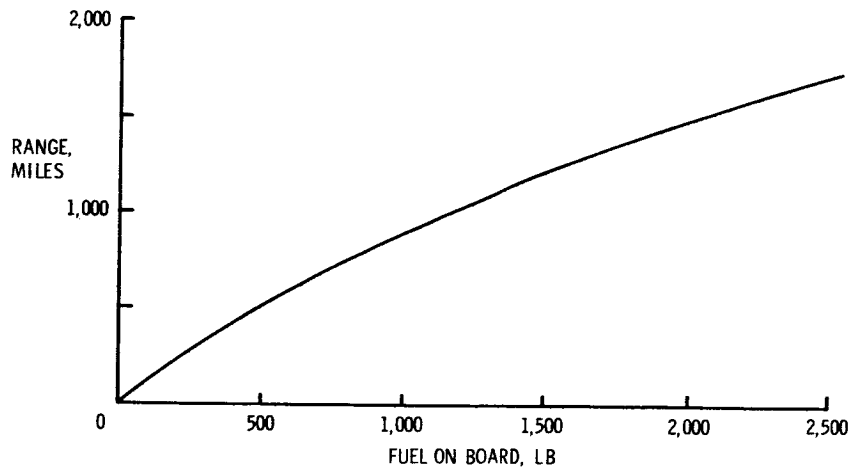
 $\frac{L}{D} = 6$; SFC = 0.75 LB/HP-HR; MINIMUM FLYING WEIGHT = 1,950 LB

Figure 11

OPERATIONAL TECHNIQUE FOR TRANSITION OF SEVERAL
TYPES OF V/STOL AIRCRAFT

By Fred J. Drinkwater III

Ames Research Center

INTRODUCTION

Five representative types of V/STOL aircraft have been made available to the NASA for flight research after they had successfully demonstrated their transition capabilities. Even though the flight test life of these aircraft has been limited, pilots have been able to evaluate several different types in order to better compare and understand the various V/STOL concepts. This paper considers primarily the results of one pilot's flight experience in the transition region of each of the test-bed aircraft and points out some airplane characteristics which have a significant effect on transition performance.

DISCUSSION

The significant feature of all aircraft tested was their ability to change the direction of engine-produced thrust from horizontal in order to provide thrust for forward or wing-lift flight to vertical in order to augment wing lift at low speeds and to permit hovering. Once either a vertical or a short take-off has been made, the transition to wing-lift or translational-lift flight is started. In most cases a major change in the aircraft configuration must be made in order to allow transition. These changes are shown in figure 1. The wing-rotor system rotates on the Vertol VZ-2; the large flaps are retracted on the Ryan VZ-3; the ducts rotate on the Doak VZ-4; the rotor system is tilted 90° on the Bell XV-3; and the thrust diverter angle is changed on the Bell X-14.

The transition from V/STOL operation to conventional airplane flight is considered to be complete when sufficient lift due to air-speed is obtained so that gliding flight is possible at a sinking rate which can be arrested without adding power. In general, therefore, STOL operation is dependent on engine power to augment aerodynamic lift and to change the effective lift-drag ratio. VTOL operation implies the ability to hover out of ground effect over a given ground position in no wind. The term "conversion" is used herein to denote the mechanical configuration changes made to the aircraft to permit transition from V/STOL operation to translational-lift flight.

In the transition speed range, therefore, if complete power failure occurs, the aircraft must be either very close to the ground or at sufficient height to allow translational lift to be obtained by diving and converting to the best glide configuration. The heights and airspeeds described in this manner roughly define "dead man's curves." The general combinations of height and airspeed or dead man's curves of a typical single-engine helicopter as compared with that of an airplane are shown in figure 2. Although the helicopter can lift off vertically, it stays close to the ground until sufficient translational lift develops. Since this occurs at a very low forward speed, the climbout and descent can be started very shortly after lift-off. The airplane, in contrast, must remain on the ground until translational lift or flying speed is attained. The transition region for V/STOL aircraft is between these two extremes - that is, translational lift must be augmented by engine-produced lift in order for the aircraft to be airborne. However, unless the dead man's curve is ignored, the aircraft should still stay very low until translational lift can support it. The alternative is to provide multiple interconnected engines for those V/STOL aircraft which do not have autorotational capability, so that the dead man's curve based on the loss of the most critical engine still allows steep take-offs and landings.

The effects of conversion on airspeed for the XV-3 is shown in figure 3. The results indicate that the XV-3 can cover a wide range of airspeeds without conversion. The solid line indicates the usual conversion-airspeed variation during transition, with the dashed lines indicating the reasonable limits to the procedure. Forward speed is gained from hovering by lowering the nose slightly by means of forward cyclic-pitch control. At about 50 knots the transition to translational lift was complete; that is, if the engine failed, an autorotative landing could be made; therefore, the climb could be started. Tilting the rotors about 15° to 30° improved the climb performance, or if a level transition was to be made, conversion to this angle permitted more rapid acceleration to a speed in excess of the wing stall speed, which was 80 knots in this case. At this time the rotors, operated as a helicopter, could be unloaded and rotated 90° and the blade pitch could be adjusted for the best cruise efficiency. As can be seen in figure 3, however, the conversion procedure was quite flexible and was only dictated by the combinations which gave best performance. The reasons for the limiting conditions are indicated to be deterioration in stability and control to wing stall along the low-speed boundary and the usual helicopter buffeting changing to a power-available or structural limitation along the high-speed boundary.

Results for the tilt-wing, the deflected-slipstream, and the tilting-ducted-fan aircraft are combined in figure 4 since these configurations are quite similar in the aspects presented. The solid line indicates

the usual conversion airspeed relation with the dashed lines indicating the reasonable limits. It is seen that these aircraft can gain very little forward speed without starting the conversion process. This limitation has certain advantages. One is that if the pilot kept the fuselage reasonably level the airspeed was dictated by the conversion angle during most of the transition and required little pilot attention. Consequently, fore-and-aft stick motions were more or less restricted to holding attitude, adjusting airspeed by the conversion control, and controlling vertical speed by power changes. Of course, as more translational lift was produced, angle-of-attack changes began to have a greater effect on flight-path angle as conventional airplane flight was approached.

There is a disadvantage in having a narrow band of airspeeds available at the start of conversion while hovering and attempting to control very low forward speeds with respect to the ground. Under these conditions small changes in conversion angle were more effective for speed control than attitude changes, but the on-off type of switching used for conversion-angle adjustments was not smooth and continuous as is required. Therefore, when speed control near hovering can be best obtained by changes in conversion angle rather than in pitch attitude, as it is in various degrees on the three types shown in figure 4, the conversion angle might be best controlled over a small range by fore-and-aft stick motion. In any case, better control of speed at very low speeds is needed for these types of VTOL aircraft.

The method of performing the transition was also similar for these three types. For example, the wing, duct, or flap angle was changed in increments at the start of the transition where airspeed was most dependent on the conversion angle. From about 40 knots the rate could be increased so that transition was completed in about 10 to 15 seconds. Large deviations from this program as indicated by the dashed lines caused some important changes in aircraft characteristics. The lowest speeds normally used at each conversion angle were limited primarily by fuselage attitude; however, a decrease in the lateral-directional damping was experienced on the Vertol VZ-2 and general controllability fell off rapidly. The deflected-slipstream Ryan VZ-3 airplane became longitudinally unstable and tended to pitch up. This characteristic brings up the point that although the aircraft handling qualities specifications define satisfactory stall characteristics and the helicopter specifications require satisfactory handling even in rearward flight, there are as yet no specifications which describe adequately the lower speed boundary which occurs at partial conversion angles. The lower speed boundary can be compared to the conventional airplane stall. However, whereas the airplane stall speed is a relatively fixed value varying with load factor, which the pilot can readily detect, and varying only little with power changes, the lower speed boundary at partial

conversion angles varies directly with engine power. The boundaries shown in figure 4 are at power for level flight. At other power settings either the angle-of-attack or the rate-of-descent indicators must be used to determine the onset of a critical condition.

The high-speed boundaries indicated are reached by pushing the nose over to steep attitudes. The boundary on the deflected-slipstream airplane was determined by the flap strength, on the tilting-duct airplane by the increasing nose-up pitching moment requiring full forward stick, and on the tilt-wing airplane by a less easily defined change in the lateral-directional behavior, particularly at the higher transition speeds where the wing was carrying more of the load. Under these conditions the fuselage is diving but the wing is flying straight and level, and the motions which result from a rudder kick are hard to describe; however, the important point is that there appeared to be a tendency for a divergence to occur. The measured static directional stability of this aircraft is discussed in a subsequent paper presented by John P. Reeder, which may indicate why the directional oscillation was unusual.

The transition boundaries as they apply to the deflected-jet X-14 airplane are shown in figure 5. The take-off transition is programmed almost in the same manner as the Vertol, Ryan, and Doak aircraft previously discussed in figure 4. That is, the thrust diverter must be rotated in small increments until about 40 knots are attained and then it can be converted continuously as the airplane accelerates very rapidly even at small conversion angles. In fact the stall speed is usually exceeded; that is, transition is completed before more than about 20 percent of conversion has been made, as is shown in figure 5. The reverse transition is made quite differently, however, since no large drag or moment changes were found to occur with change in thrust-diverter angle. The throttle was retarded and the diverter rotated directly to 90° (the hovering angle) while still at high speed. Power was added to keep the angle of attack below stall as the 1g stall speed was approached, and the aircraft then decelerated rapidly to about 20 knots, below which the speed was controlled by pitch attitude, more or less like a helicopter. The angle-of-attack indicator was used to determine the power setting needed to avoid stalling during the transition at airspeeds greater than about 20 knots. Below this speed the stall moments or forces were of little consequence.

Continuous flight in the transition region (that is, flight at partial conversion) is primarily useful in order to allow steep take-offs and landing approaches at speeds lower than would be allowed by wing lift alone. Even though these aircraft had VTOL capabilities, the pilot would not normally complete transition to hovering flight at 100 feet or so above a landing spot and then descend vertically as is popularly supposed any more than he would operate a helicopter in this

manner, and helicopters are the most efficient hovering devices yet conceived. One of the reasons for this restriction is the generally poor visibility straight down, but even if visibility were good, pilots find it difficult to observe the horizon when looking straight down and without this reference, attitude control becomes marginal. Also, the instruments cannot be readily observed when the pilot looks downward, and when the pilot tilts his head up and down he disturbs his sense of balance. In addition these vertical ascents and descents require nearly full engine power, so that fuel is used at a very high rate, and in most cases an engine failure under these conditions would mean loss of the aircraft.

For these reasons take-offs and landings were made at moderate angles on the test-bed aircraft with translational lift being augmented by engine power whenever possible. The translational lift, of course, is a function of the angle of attack, and in the transition region the angle of attack varies with engine power at a constant airspeed. If power is reduced in order to descend more steeply, the wing may stall, so that translational lift drops off rapidly. This loss of lift further increases the sinking rate and also the angle of attack. A large power increase is required to unstall the wing and when this happens, the added power plus the return of wing lift causes the airplane to climb. For the tilt-wing and deflected-slipstream aircraft the pilot determined his steep approach limits by reference to the rate of descent indication commensurate with his conversion angle. If he did not know the limiting conditions, the steep descent could turn out to be a series of stall recoveries. Since the wing was not in the slipstream on the tilt-duct or deflected-jet airplane, the steep descent conditions could be monitored on the angle-of-attack indicator. When wing stall was encountered at very high conversion angles and speeds less than about 25 knots, the change in lift did not create much of a problem on any of the test beds except for the deflected-slipstream airplane which still had a pitch-up problem until full conversion was reached.

The allowable vertical velocity variation with airspeed while descending in the transition region for the deflected-jet X-14 is shown in figure 6. The dashed line is the combination of rate of descent and airspeed which is limited by the wing angle of attack with the fuselage level and results in a descent angle of 10° in this case. A reduction in power to increase the rate of descent would cause the wing to stall. Figure 6 shows that below about 25 knots, however, the stall angle can be exceeded to some extent in practice since the aircraft is being supported mostly by engine thrust. The maximum flight-path angle indicated in the figure could be increased by having the wing stall at a higher angle of attack. In addition, if the jet could be deflected further than 90° relative to the fuselage, then these sinking speeds could be maintained with the fuselage in a slight nose-down attitude which would also allow steeper flight-path angles.

The rate-of-descent limitations for the tilting-rotor XV-3 are shown as a function of airspeed in figure 7. The line for a rotor-mast angle of 0° indicates the allowable sinking rates in the helicopter mode. For the most part, this is the autorotation or power-off curve except for very low speeds. At low speeds, the wing rotor interference made control difficult and limited the sinking rates to low values. At intermediate conversion angles shown on the remaining curves, the wing-stall speed is limiting again and it can be seen that there is nothing to gain in steep descents by using intermediate conversion angles. The best steep approach with the XV-3 was therefore made in the helicopter configuration.

Sinking rates of about 500 feet per minute were used during most of the landing approaches but, of course, even sinking rates of 500 feet per minute must be reduced to near zero before touchdown. The way that this is accomplished depends on how far into the transition the approach is being made. The lift-distribution variation during an approach in the transition region of a typical V/STOL aircraft is shown in figure 8. The force-weight ratio F/W is plotted against airspeed at airspeeds less than the $1g$ wing-stall speed. The curved line indicates the force produced by the wing when it is at the maximum angle of attack. The maximum wing-produced force-weight ratio is of course zero at zero airspeed and 1 at the $1g$ stall speed. As the transition proceeds into the lower airspeed region, more reliance is placed on engine-produced lift. When the wing is still doing most of the work as at the higher speeds, a conventional flare may produce enough increase in lift to arrest the approach sinking rate. As the wing is unloaded, however, and the engines are supporting more of the load, the flare for wing lift must be used with caution, since the angle of attack can increase rapidly with very little increase in lift and a stall is likely to occur at an inappropriate time. Previous flight tests indicate that when the flare is made by using wing lift alone, at least $1.2g$ of flare acceleration is required, since a minimum ratio of approach speed to stall speed under ideal conditions was found to be 1.1. This ratio will provide a flare acceleration of $1.2g$. The helicopter is at the other end of the spectrum and even though it may require full power to hover, a vertical acceleration of about $1.2g$ is available for a few seconds by increasing collective pitch and using the stored energy in the rotating blades. Neither of these methods of obtaining a transient increase in lift is available on most V/STOL designs during transition, so that this lift increment must come from an increase in power. Flight tests indicate that the excess power plus wing lift available should also permit a $1.2g$ flare for positive control of the touchdown for the V/STOL aircraft in any usable approach condition.

Since the final flare is a critical phase of the steep approach, the location of the flare controls is very important. Approaches were

made with all of these V/STOL aircraft where power had to be increased in order to arrest the sinking rate at touchdown. Three of them had conventional throttles moving fore and aft and the other two had collective pitch-type power control. The collective pitch-type throttle actuation is considered by the author to be the most natural and convenient when power is required to assist the flare. Additional considerations regarding the location and number of controls are discussed in the next paper by John P. Reeder.

CONCLUSIONS

1. Since pitch-attitude changes alone are not sufficient to control movement over the ground when at or near a hovering condition with some VTOL types, precise and continuous control of the conversion angle through a small range may be required.
2. A V/STOL aircraft test program should consider the effects of large deviations from the fuselage level trim speeds at partial conversion angles.
3. The wing should be capable of supporting the aircraft at as low a speed as possible in order to shorten the transition and to reduce the time spent in the critical region of high engine power.
4. The large variety of airspeed—power—conversion-angle combinations which will result in a stall requires that the pilot be given some positive indication that he is approaching a critical condition.
5. If a constant-power flare cannot be made, the power control should be actuated in a manner similar to a helicopter collective-pitch control.
6. If the V/STOL aircraft has no autorotational capability, then it should have multiple interconnected engines so that the advantages of steep ascents and descents can be realized.
7. The V/STOL aircraft must be capable of developing 1.2g for flare with the most critical engine out at its minimum acceptable approach speed.

FIVE VTOL CONCEPTS

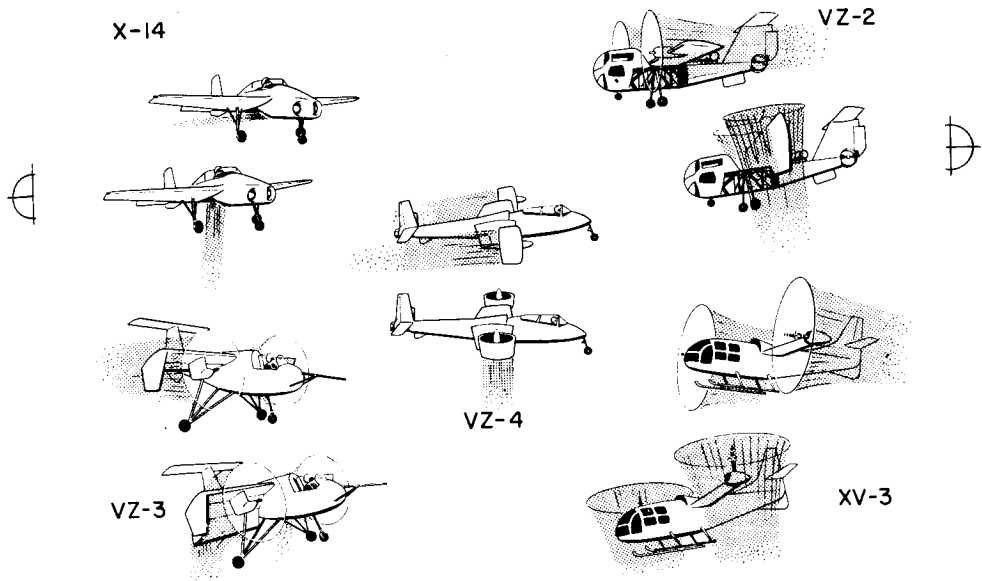


Figure 1

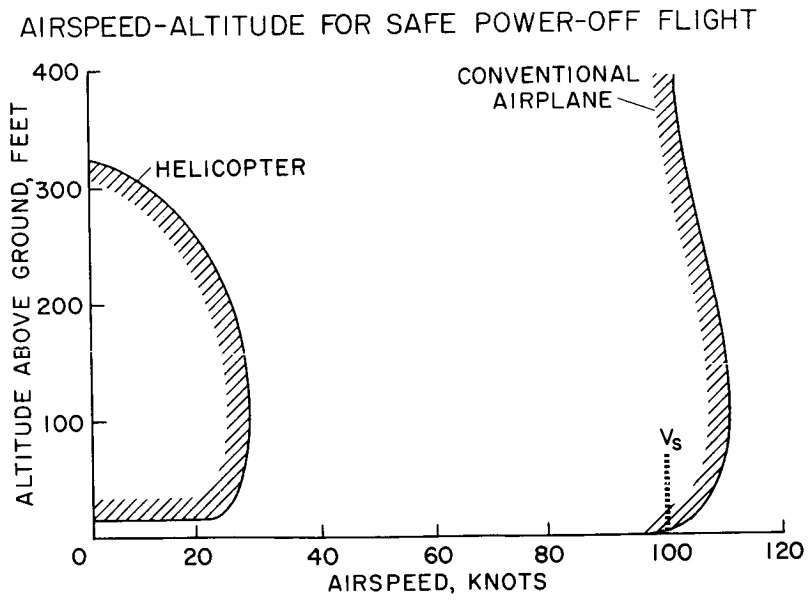


Figure 2

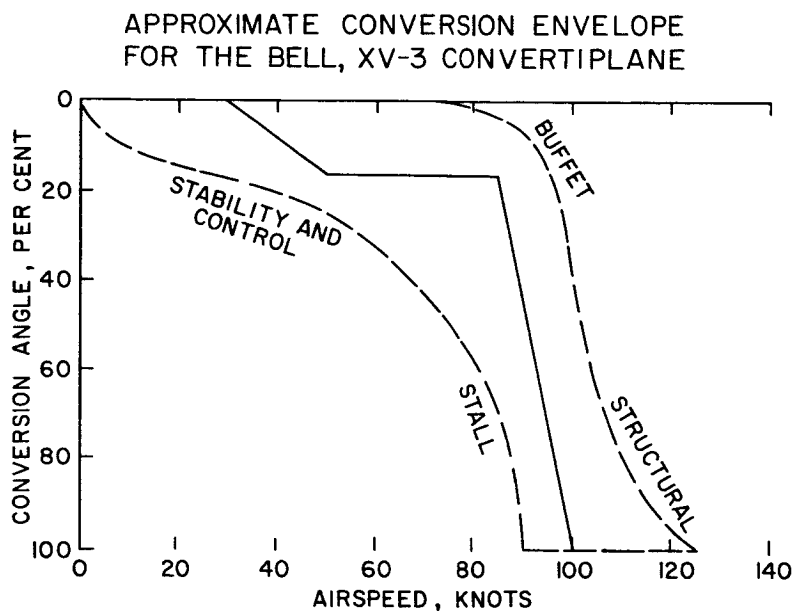


Figure 3

GENERALIZED CONVERSION ENVELOPE FOR
THE VERTOL VZ-2, RYAN VZ-3, AND DOAK VZ-4

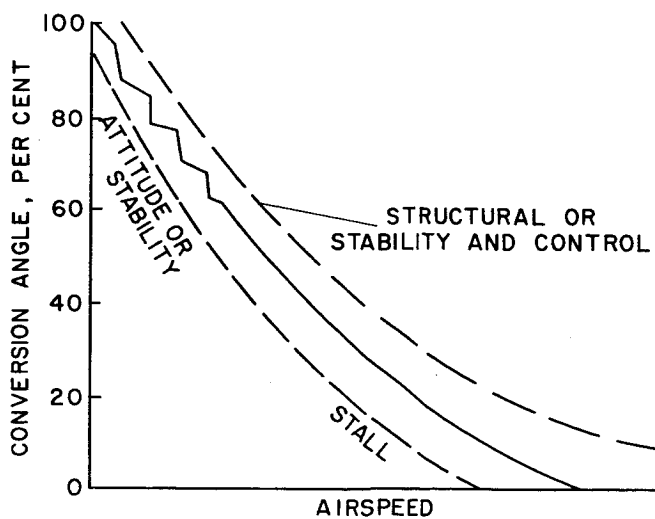


Figure 4

APPROXIMATE CONVERSION ENVELOPE
FOR THE BELL X-14 AIRPLANE

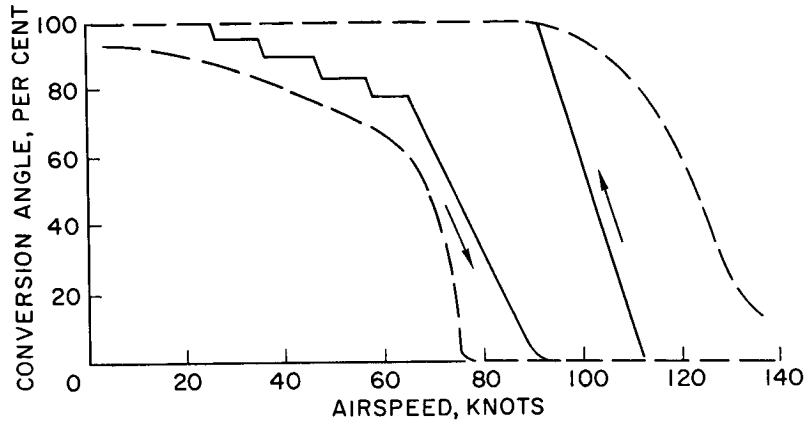


Figure 5

RATE OF DESCENT VARIATION WITH AIRSPEED
FOR BELL X-14 AIRPLANE
1g FLIGHT

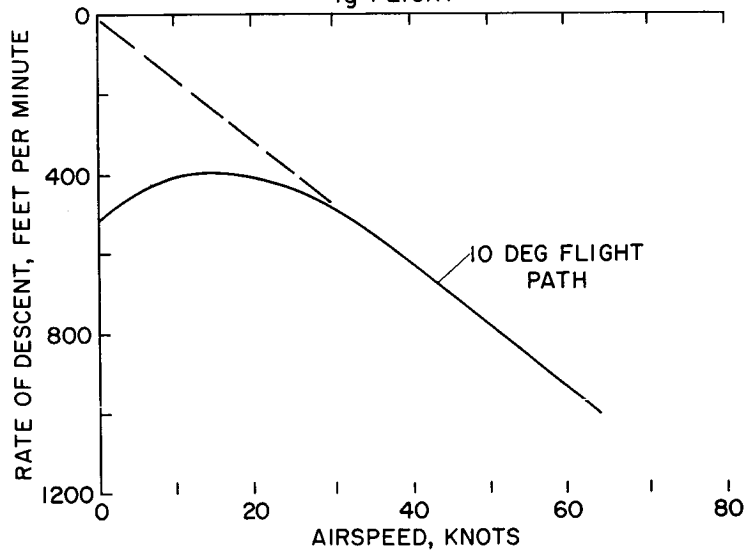


Figure 6

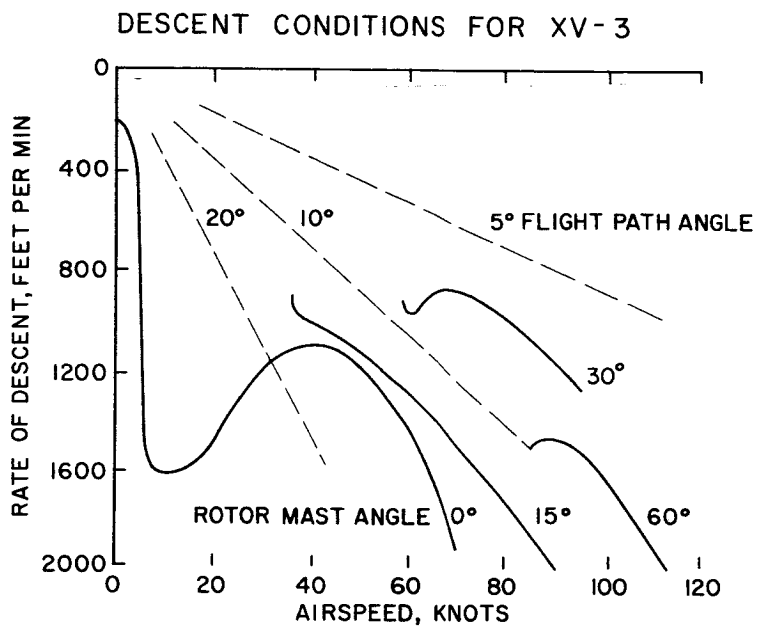


Figure 7

LIFT REQUIRED FOR FLARE IN TRANSITION

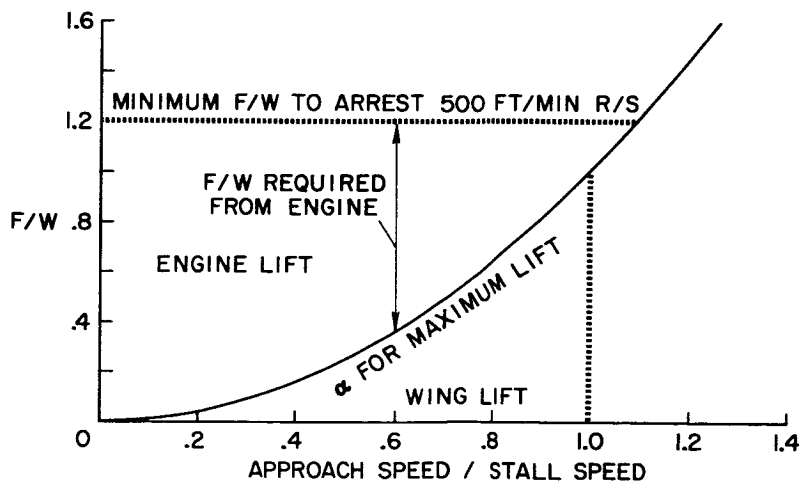


Figure 8

HANDLING QUALITIES EXPERIENCE WITH SEVERAL .

VTOL RESEARCH AIRCRAFT

By John P. Reeder

Langley Research Center

SUMMARY

All of the VTOL research aircraft discussed in this paper have successfully demonstrated conversion from hovering to airplane flight and vice versa. However, control about one or more axes of these aircraft has been inadequate in hovering flight. Furthermore, ground interference effects have been severe in some cases and have accentuated the inadequacy of control in hovering and very low speed flight.

Stalling of wing surfaces has resulted in limitation in slowdown and descending flight, particularly for the tilt-wing aircraft, which is a very rudimentary type. Minor modifications to the wing leading edge in this case have, however, produced surprisingly large and encouraging reductions in adverse stall effects.

Height control in hovering and in low-speed flight has proved to be a problem for the aircraft not having direct control of the pitch of the rotors. The other systems have shown undesirable time lags in development of a thrust change.

INTRODUCTION

The flight experience to be discussed has been acquired on VTOL research aircraft having four different types of rotor systems which provide vertical thrust for hovering and propulsion for forward flight. The aircraft are the Bell XV-3 with tilting rotors and a fixed wing, the Vertol VZ-2 with a tilting wing and flapping rotors, the Curtiss-Wright X-100 with tilting propellers and a very small fixed wing, and the Doak VZ-4 with tilting, ducted fans at the tips of a fixed wing.

Operation of the test-bed aircraft has, in general, been limited to light wind conditions. Also, all the aircraft have been power limited so that hovering flights have been considerably restricted. They have all demonstrated conversions from hovering to airplane flight and vice versa. The VZ-2 is the only one of the aircraft that has stability

augmentation systems. These provide damping about the roll and pitch axes. This paper discusses the aircraft without the system functioning.

Only significant areas of the handling qualities of the test beds pertinent to improved design of the next generation of VTOL aircraft are discussed in this paper.

STABILITY AND CONTROL

Photographs of the four VTOL research aircraft under discussion are presented in figures 1 to 4. The significant areas of the basic stability and control characteristics of these aircraft are summarized in table I. The presence of a letter in the table indicates which aircraft has a significant characteristic in the particular phase of flight indicated. This paper will discuss these characteristics in the various phases of flight.

Hovering

Figure 5 is a summary chart of hovering stability and control characteristics for the VTOL research aircraft. The parameters plotted, the ratio of angular velocity damping to inertia of the aircraft and angular acceleration capability of the control per inch displacement, were found to be important handling-qualities criteria in the evaluation of helicopters. The boundaries of desirable and unacceptable characteristics shown were obtained from flight tests with a variable-stability helicopter during hovering maneuvers and low-speed, precision, instrument-flight tasks. It is felt that the boundaries are applicable to the next generation of VTOL aircraft in lieu of better information.

The lateral or roll control of the VZ-4 aircraft in hovering is obtained by means of controllable inlet guide vanes. This control in its present stage has proved to be very inadequate, as indicated in figure 5. The other aircraft have tended to be too responsive to lateral control, but this is not considered a basic problem since the control power can be reduced.

Longitudinal stability and control of the VZ-2 aircraft in hovering without the pitch-rate damper has caused difficulty for the unindoc-trinated pilot. The basic aircraft has exhibited very low damping in pitch in hovering flight with no wind. Also, the longitudinal control is nonlinear and weak, and the control system does not permit exact positioning of the control for trim. When first trying to hover without the pitch damper, using hand and wrist motions for controlling, the pilot felt he was out of phase with an expanding oscillation. He quickly had

to convert to an arm and shoulder technique with which he could put in sufficient control at a higher rate. No further difficulty was experienced after this except that continuous controlling was necessary.

All the aircraft have deficiencies about the yaw axis in hovering. As shown in figure 5, they all show little damping and very weak control about this axis. However, the yaw axis is of least concern in hovering, particularly for a test bed, inasmuch as little hazard results from the lack of control. Of course, for an operational vehicle intended to perform precision maneuvers under all weather conditions, the yaw control requirements will have to be considerably greater than for these aircraft.

Experience has indicated that the length of time required in hovering prior to a landing is a direct function of the controllability of the aircraft; that is, the poorer the controllability, the greater the time required.

Accelerating Conversion

The power used in an accelerating conversion is more than that required for level flight. In the test-bed operation, it has most often been the maximum power available. During maximum-power operation of the VZ-2 aircraft in climb at a wing incidence angle of about 20° , an unstable Dutch roll oscillation with a period of about 4 seconds has been encountered. Although controllable, this oscillation was of concern to the pilot. The oscillation is thought to be due to the destabilizing effects of having the principal axis of inertia nose down with respect to the flight path. It is felt that such oscillations can be readily damped with simple rate stability augmentation systems.

Other problems encountered in accelerating conversions have been more critical in the decelerating conversion or descent phase and are discussed subsequently.

Cruise

In the cruise condition, which is considered to be airplane flight, the XV-3 aircraft has a poorly damped short-period pitching oscillation which becomes more poorly damped as rotational speed of the rotors is reduced. In rough air, rather large yaw disturbances have been observed to couple with the pitch oscillation to produce an annoying circular motion of the nose of the aircraft.

A short-period longitudinal oscillation is also evident in the VZ-2 aircraft, but to a lesser extent. In this case little undesirable

behavior results, but the damping is less than desirable. During one landing as an airplane, a gentle flare was started at 95 knots, but an uncontrollable tendency to balloon was immediately apparent. The approach was successfully continued to landing by using power alone as height control. The ballooning tendency might well have been a result of the poor damping in pitch.

Decelerating Conversion and Descent

During conversion, the X-100 aircraft develops a nose-up change in trim at high nacelle angles in slow forward flight due to a forward shift of resultant force on the propellers. The largest forward stick displacement to offset these moments is required at about 20 to 30 knots. At powers used in flight, however, a margin of control remained throughout this region of flight.

The VZ-4 aircraft develops a large nose-up trim change due to the ducts at duct angles of the order of 60° . In the original duct configuration, the moments were large enough to make full forward stick control necessary at about 20 to 25 knots in a level flight slowdown to hovering flight. Also, the trimmable stabilizer had to be set for full nose-down trim and the airplane still had to be allowed to pitch up to more than 15° angle of attack. The exit guide vanes, which are programed to offset the duct moments, now make it possible to traverse this region at a constant attitude with some margin of elevator control remaining.

In the case of these two aircraft (the X-100 and the VZ-4), the pitching-moment changes appear to the pilot as instabilities with respect to speed, which will be very undesirable during landing approaches, particularly under instrument conditions.

During all flight phases, the VZ-2 aircraft has static directional, or weathercock, instability over a range of left sideslip angles. In the cruise phase, this is probably due to the low dynamic pressure at the tail because of the high drag configuration. However, at higher wing incidence angles, strong cross flows may very well be present which may require research to establish a cure. Figure 6 shows pedal position plotted against sideslip angle from directional stability tests at two wing incidence angles. For the cruise condition (wing incidence angle of 9°), the instability exists over a much smaller range than at a wing incidence angle i_w of 40° . However, the pilot's impression is that the instability is worse at a velocity V of 100 knots than at a velocity of 40 knots because the angular acceleration is higher as divergence begins, corresponding to the higher dynamic pressure. At the lower speed, however, considerable use of control is required because of the reduced effectiveness of the control.

Landing

The limitations due to stalling that occur with the VZ-2 aircraft and, to some extent, with the VZ-4 aircraft during descent are discussed subsequently in this paper. However, one limitation of control for the VZ-2 aircraft exists during the last stages of a slow descent and landing as an STOL aircraft. At less than 30 knots, the directional control power is insufficient to correct adequately for even light crosswinds or gust disturbances. Although the longitudinal control also becomes too weak to adjust the attitude for a three-point landing within the ground-effect region below 30 knots, this weakness constitutes less of a problem than the directional one because the aircraft can be readily landed on the wheels.

FACTORS THAT INFLUENCE HANDLING QUALITIES

Some very important factors that influence the handling qualities of the VTOL research aircraft and emphasize their need for more adequate control are presented in table II. Table II is similar to table I with the phases of flight indicated as before. The factors to be discussed are tabulated on the left with the letters B, C, D, and V indicating which aircraft seem to have significant characteristics in the various phases of flight.

Ground-Downwash Interference Disturbances

Hovering.- Near the ground, the VTOL aircraft are subjected to severe recirculation airflows. The details of this problem are discussed in reference 1. Suffice it to say that the aircraft are greatly disturbed in this interference region. It has been difficult to pinpoint a height above the ground at which the disturbances cease, but it has been about 10 to 15 feet in the case of the test-bed aircraft. Above this height the aircraft are all fairly steady and free of vibration.

The XV-3 and X-100 aircraft suffer from erratic wing drooping and yawing in this interference region, the effect being stronger for the X-100 aircraft. Noticeably large lateral control displacements are required to offset the lateral disturbances, particularly for the X-100 aircraft. This may be significant inasmuch as these aircraft otherwise have powerful roll control. In yaw the aircraft cannot be controlled within 10° to 20° of a desired heading because of the very weak control, but this does not necessarily create a hazard in hovering flight.

The VZ-2 aircraft has not shown roll disturbances in hovering of which the pilot is particularly aware. However, it does suffer heavy buffeting and more abrupt and larger yaw disturbances than the XV-3 or X-100 aircraft. Translatory accelerations of the aircraft are also apparent. The yaw disturbances cannot always be controlled in this case either.

The VZ-4 aircraft does not suffer from buffeting, and the disturbances it suffers are not as abrupt as for the others. However, if lifted clear of the ground several feet, uncontrollable yawing and persistent lateral upsetting tendencies have been encountered. With the weak yaw control and, particularly, the weak roll control described previously, the unindoctrinated pilot may find himself unable to control the aircraft.

Accelerating conversion.- The effects of ground interference are intensified as the aircraft advances into the disturbances which it is forcing out ahead of itself. The speed range at which at least three of the aircraft encounter the most disturbance is from about 15 to 20 knots. Beyond this speed range the downwash field shifts aft, as it is for an airplane, and disturbances cease.

The disturbances in both roll and yaw for the XV-3 and X-100 aircraft are considerably greater under these conditions than for hovering, and it is very difficult to maintain lateral control and a heading in the direction of the desired track while advancing through this region. Yaw disturbances are greatly intensified for the VZ-2 aircraft also, and it is sometimes impossible to maintain heading closer than 20° to the track. Again, though, roll disturbances have not been particularly apparent to the pilot in this aircraft.

In none of these aircraft have appreciable pitch disturbances been noted by the pilot.

It is apparent that the aircraft should either climb through the critical altitude region as quickly as possible, power permitting, or operate as an STOL type and take off at a speed above that at which the disturbances disappear. It is not possible to avoid the most critical disturbance speed altogether by taking off vertically, however, because winds of about 15 knots will create the same situation as forward translation with calm winds.

In the final stages of a landing approach to a near vertical landing, the same behavior patterns just described happen in reverse. This behavior becomes more hazardous for the landing than for the take-off and acceleration phase.

Ground Effect on Power Required

The X-100 aircraft has exaggerated ground effect on power required up to heights of about 20 feet, whereas the VZ-2 aircraft, which has a similar rotor configuration, has essentially none. The X-100 aircraft has a covered fuselage with a flat bottom and rounded corners. The strong ground effect on lift probably comes largely from impingement of the recirculating flows on the bottom of the fuselage.

It has been noted that the X-100 aircraft settles rapidly toward the ground when upset in bank or pitch attitude in the ground-effect region. Also, at a speed of 15 or 20 knots while in a level attitude and after accelerating through the region of most intense disturbances, the aircraft rather suddenly settles toward the ground. This unusual settling behavior may be caused by a shift in the area of impingement of the upward flow under the aircraft due either to an attitude or a velocity change, thus resulting in a loss of lift on the fuselage. From the pilot's standpoint, the settling and the lateral upsetting moments that may occur are very undesirable. The implications are that in hovering in operational wind conditions or in traversing the interference flow region, the behavior of VTOL aircraft may be very unpredictable, depending on fuselage design and the sensitivity of downwash patterns to attitude or speed changes.

Adverse Stall Effects

The most critical regions of operation for some V/STOL aircraft are the decelerating conversion and descent. Stalling of lifting surfaces under these conditions is probable, leading to buffeting, uncontrolled-for motions, and general difficulty in handling the aircraft. The X-100 aircraft is notably free of disturbances and airframe roughness in these flight phases, at least away from the ground.

The VZ-2, a rudimentary tilt-wing aircraft, had serious stall-imposed limitations in its original wing configuration as shown in figure 7. The boundary shown on the right with heavy crosshatching is that for stall onset. At wing incidence angles between approximately 25° and 35° , enough power to climb had to be used if wing drop, heavy buffeting, and large yaw disturbances were to be avoided. Deceleration in level flight through about the same incidence range at rates great enough to require reduction of power to less than 350 horsepower had to be avoided for the same reasons. At higher wing incidence angles such as 40° , the stalling became symmetrical, and buffeting intensity was reduced because of lower speed so that a reasonable rate of descent could be attained for approach to a landing in smooth air. In rough air, the usable rates of descent were considerably reduced. Actually, the buffeting and poor directional

behavior in these descent conditions were tolerated only because lateral and longitudinal control were good and it was known that the behavior would be greatly improved by the addition of power for flareout and landing. Acceptable rates of descent below 35 knots, as indicated in figure 7, were reduced because of a lack of directional and longitudinal control. Approach speeds lower than 35 to 40 knots were not used for STOL landings because of inadequate directional and longitudinal control for the landing.

A modification was made to the leading edge of the VZ-2 wing which provided, effectively, about 6° of droop. This change so greatly improved the characteristics of the aircraft as indicated by the lower boundaries in figure 7 that serious stall limitations in descent and level-flight deceleration were essentially eliminated from the range of practical flight operation, at least at incidence angles up to 50° . With the modified wing, the aircraft has become, by comparison with the original configuration, a pleasure to fly.

Examination of limiting operating conditions in deceleration and descent for the VZ-4 aircraft at the Langley Research Center has not been completed. However, stalling of the outboard sections of the wing in level flight and descent at duct angles over about 30° has produced buffeting and alternate left and right wing dropping of generally small magnitude at moderate airplane angles of attack. Although it is possible to avoid the stalling by keeping the airplane angle of attack low enough, it may not be operationally practical to do so in steep descents. Also, if a vertical landing is to be made, the stall angle must be exceeded at some stage in the landing maneuver. Severe wing dropping has been experienced in this aircraft when the stall angle of attack has been slowly approached. The roll control was not adequate to keep the aircraft upright under these conditions.

Glide-Path Control

It has been generally assumed that operation of V/STOL types at low speed as required in a steep approach means operating on a steeply rising "backside" of the power-required curve. Operation in this region is generally found more difficult than operation above the speed for minimum power required because any speed change, whether due to attitude correction by the pilot, gusts, or power change, will result in deviation from the desired flight path if power adjustments are not made. Consequently, corrections to glide path are made primarily by power changes, a more complex technique than one where attitude corrections can be used. The need for this type of operation is particularly undesirable during instrument flight.

The power-required curves usually presented for the VTOL aircraft, which show a steeply rising variation below the speed for minimum power, are obtained with some parameter, such as fuselage attitude, constant and with the tilting elements varied to establish the trim speeds for the powers shown. However, this does not represent the characteristics the pilot appreciates during an approach. On the approach, particularly on instruments, the pilot would very probably use a fixed-tilt configuration.

Figure 8 shows results of tests with the VZ-2 aircraft at fixed wing incidence when speed is varied by attitude change. In this case there is no variation in power required so that difficulties of "backside" operation would, at least, be minimized. However, the flat curve is a function of the change in drag of the fuselage with angle of attack and is not apt to be so favorable on cleaner, future designs.

The power-required characteristics of the VZ-4 aircraft are shown in figure 9. The slope of the curve at constant duct angle is actually favorable for a range of speeds. Thus, the glide-path control on the approach is much less a problem than was supposed at an earlier stage. This characteristic is fundamental to the fixed-wing configuration as long as the wing remains unstalled.

Height Control

Good height control in hovering and landing is very important and is a function of how immediately and accurately the pilot can control the thrust. In the case of the XV-3 and VZ-2 aircraft, as for helicopters, the pilot has direct control of the rotor pitch and height control is not a problem.

For the other aircraft a change in propeller rotational speed or propeller governing must occur following throttle operation to obtain the desired thrust change. The time delay in these systems is large enough to force the pilot to operate the throttle very gingerly to offset his inability to anticipate the final result. There is a strong tendency for the unindoctrinated pilot to establish immediately an oscillation in height with the maximum thrust change dangerously out of phase with the pilot's desires. On the other hand, the experienced pilot finds it necessary to plan continually in advance to avoid situations in which large or rapid thrust changes may be required near the ground.

The requirement for a short-time constant in thrust response is unimportant well away from the ground and in forward flight. On the other hand, rotor-pitch governing is necessary in forward flight to prevent rotor and engine overspeeding or to prevent large power variations if governed by fuel-flow changes.

GENERAL CONSIDERATIONS

The operation of the tilting elements of all the aircraft has proved little more complex than the operation of flaps or speed brakes on an airplane. It has been quite natural to use the tilting components as a speed control at the low end of the speed range. All of the aircraft under discussion have a switch on the control stick for operation of the tilting elements. Thus, tilt is accomplished without necessity for removing the hands from any of the primary controls.

In the case of the XV-3 aircraft, a large speed range can be covered without tilting the rotor masts forward and without the necessity of large fuselage tilts because longitudinal rotor feathering is provided. This flexibility of control leaves an added decision up to the pilot as to how and when to use the rotor tilt.

The undesirable complexity of operation of these vehicles is encountered when additional factors such as trim surface settings, engine power, angle of attack, speed, or other things must be programmed in sequence with the tilting elements to convert successfully. Only one of these aircraft, the VZ-4, at present requires such programming, and then during the slow-down to hovering. The fact that all the aircraft do not require special techniques in conversion is, indeed, remarkable.

With regard to cockpit instrumentation, it is felt that presentation of angle-of-attack information to the pilot is not necessary for the tilt-wing aircraft. Since operation will probably involve partial stalling during some phase of flight, the stalling must always be "flyable." With fixed-wing types of V/STOL, however, it may be desirable or necessary to avoid stalling or to know when it is imminent. In these cases angle-of-attack instrumentation is necessary.

CONCLUSIONS

Handling qualities experience with the Bell XV-3, Vertol VZ-2, Curtiss-Wright X-100, and Doak VZ-4 aircraft have indicated that:

1. Hovering control is inadequate in some cases. However, guidance with respect to requirements for adequate control is available.
2. Ground interference on the VTOL aircraft can cause serious control problems and results in greater demands for control power than for helicopters.

3. The aircraft fly through conversion in both directions with remarkably few problems. Vibration arising from the rotor systems has been low for all of them. The VZ-4 and X-100 aircraft have been notably smooth in this respect.

4. Stalling of wing surfaces has provided some limitation, particularly for the VZ-2 aircraft, and to a lesser extent for the VZ-4 aircraft. However, the VZ-2 is a rudimentary form of tilt-wing aircraft, and known stall-alleviation principles will be applied in design of later configurations. Relatively simple methods of stall protection can be applied to the VZ-4 aircraft. The X-100 aircraft suffers no apparent stall problems.

5. Positive and accurate height control is very important in vertical take-offs and landings. Present experience indicates that a satisfactory system requires direct control of rotor pitch by the pilot in vertical flight, whereas governing systems will be necessary for forward flight.

6. During a critical maneuver such as conversion from an approach configuration to a vertical landing, the pilot should have to operate only the following controls: the stick, the pedals, the power lever, and a control for the tilting elements. It should not be necessary for the pilot to remove his hand from the stick or power lever during such a maneuver.

7. Angle-of-attack indication for the pilot is not necessary for the tilt-wing type but will be necessary for the fixed-wing types.

REFERENCE

1. Schade, Robert O.: Ground Interference Effects. (Prospective NASA Paper.)

TABLE I

STABILITY AND CONTROL SUMMARY FOR VTOL RESEARCH AIRCRAFT
PHASE OF FLIGHT

STABILITY OR CONTROL AXIS	HOVERING	ACCELERATING CONVERSION	CRUISE	DECELERATING CONVERSION	DESCENT	LANDING
LATERAL STABILITY CONTROL	D	V			D	D
LONGITUDINAL STABILITY CONTROL ADVERSE TRIM REQUIREMENTS	V V	CD	BV	CD		
DIRECTIONAL STABILITY CONTROL	BCDV BCDV	V V		V V	V V	V

B, XV-3
C, X-100
D, VZ-4
V, VZ-2

AIRCRAFT SYMBOLS IN TABLE INDICATE SIGNIFICANT AREAS.

TABLE II

FACTORS THAT INFLUENCE HANDLING QUALITIES OF
VTOL RESEARCH AIRCRAFT
PHASE OF FLIGHT

FACTOR	HOVERING	ACCELERATING CONVERSION	CRUISE	DECELERATING CONVERSION	DESCENT	LANDING
GROUND-DOWNWASH INTERFERENCE DISTURBANCES	BCDV	BCV				BCDV
GROUND EFFECT ON POWER REQUIRED	C	C				
ADVERSE STALL EFFECTS				DV	DV	
GLIDE-PATH CONTROL					DV	
HOVERING HEIGHT CONTROL	CD					CD

B, XV-3
C, X-100
D, VZ-4
V, VZ-2

AIRCRAFT SYMBOLS IN TABLE INDICATE SIGNIFICANT AREAS.

BELL XV-3 AIRCRAFT

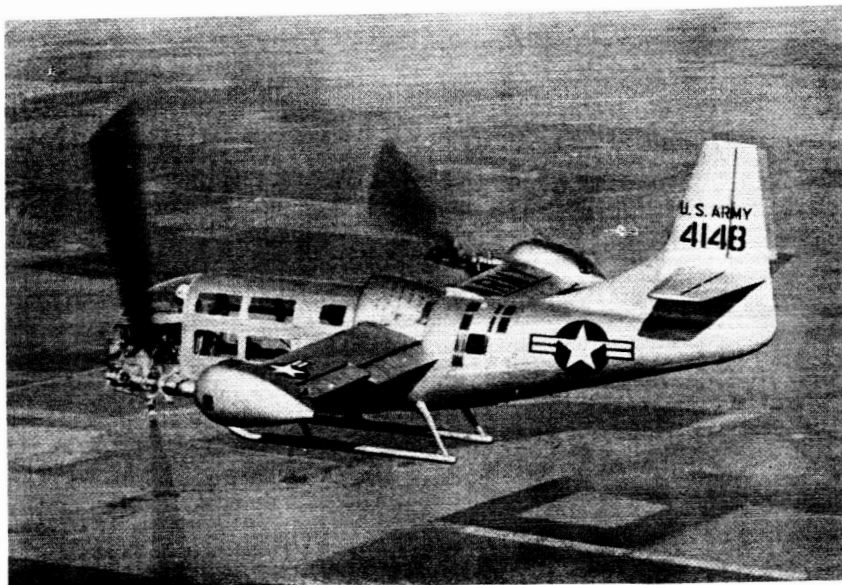


Figure 1

VERTOL VZ-2 AIRCRAFT

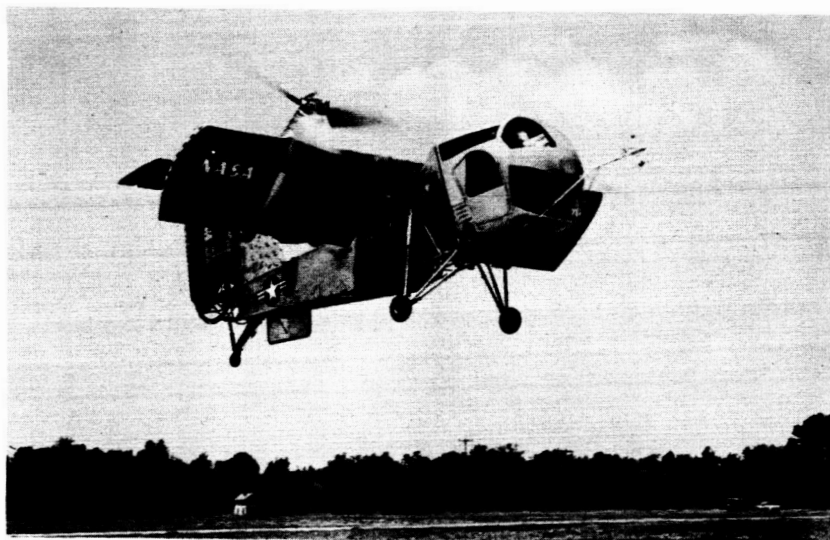


Figure 2

CURTISS-WRIGHT X-100 AIRCRAFT

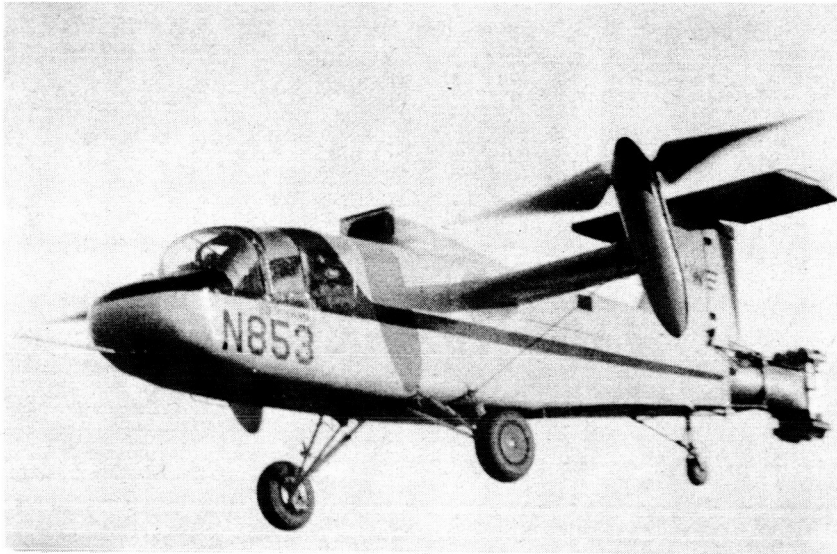


Figure 3

DOAK VZ-4 AIRCRAFT

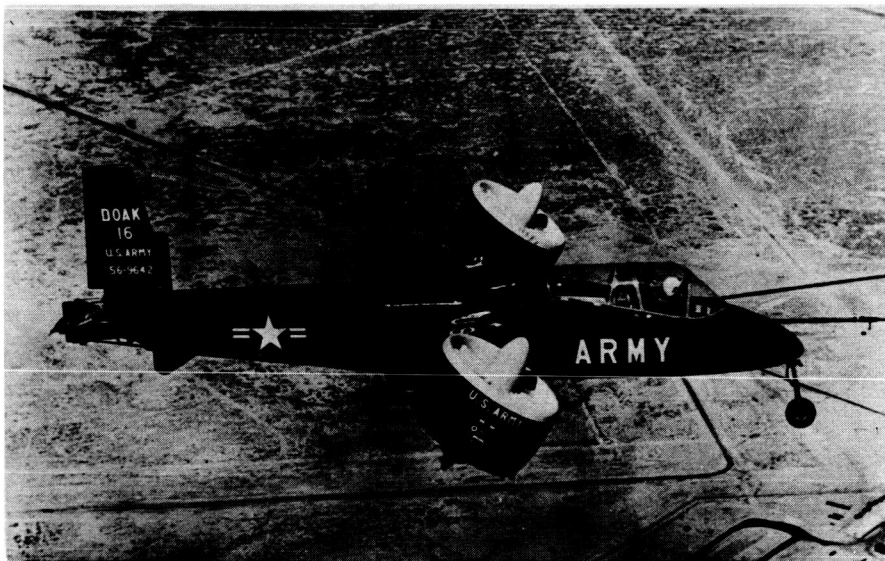


Figure 4

HANDLING QUALITIES OF VTOL RESEARCH AIRCRAFT
IN HOVERING

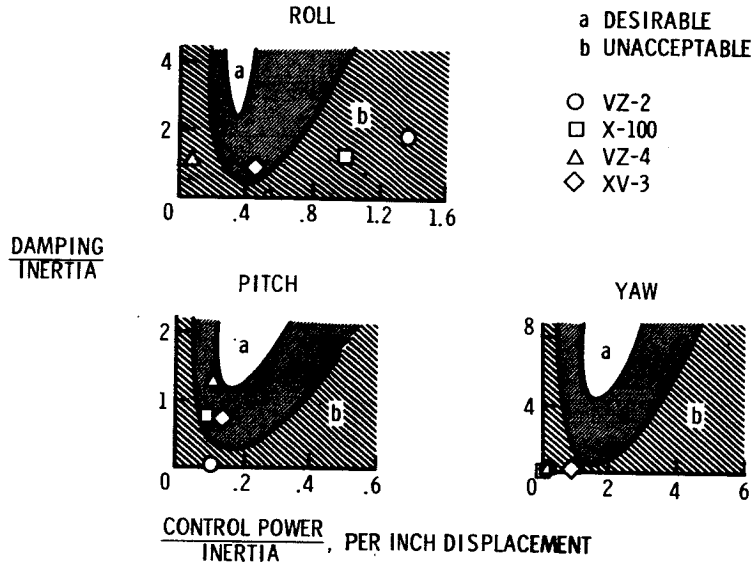


Figure 5

STATIC DIRECTIONAL STABILITY, VZ-2 AIRCRAFT

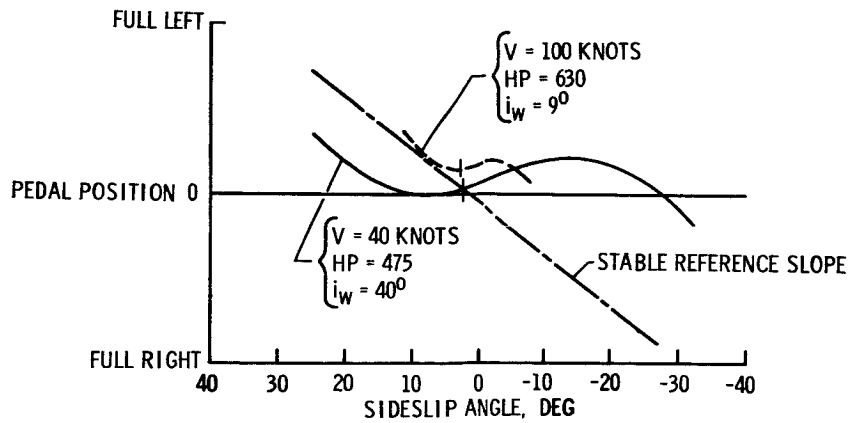


Figure 6

RATE-OF-DESCENT LIMITATIONS DUE TO STALLING,
VZ-2 AIRCRAFT

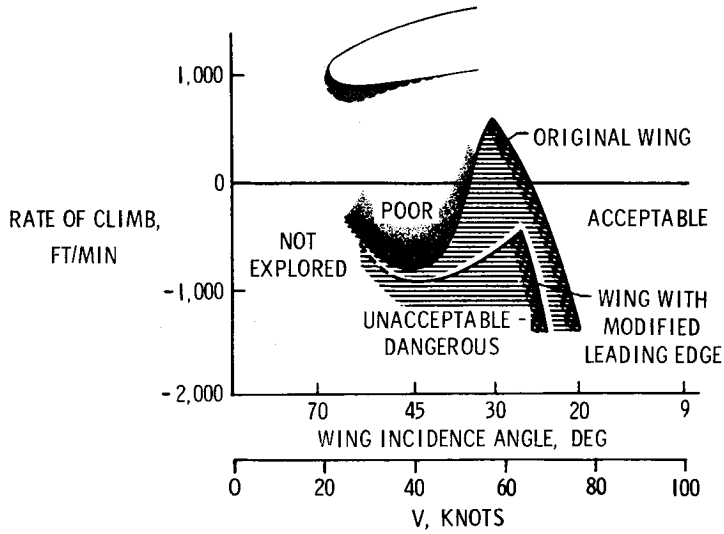


Figure 7

POWER REQUIRED FOR LEVEL FLIGHT, VZ-2 AIRCRAFT

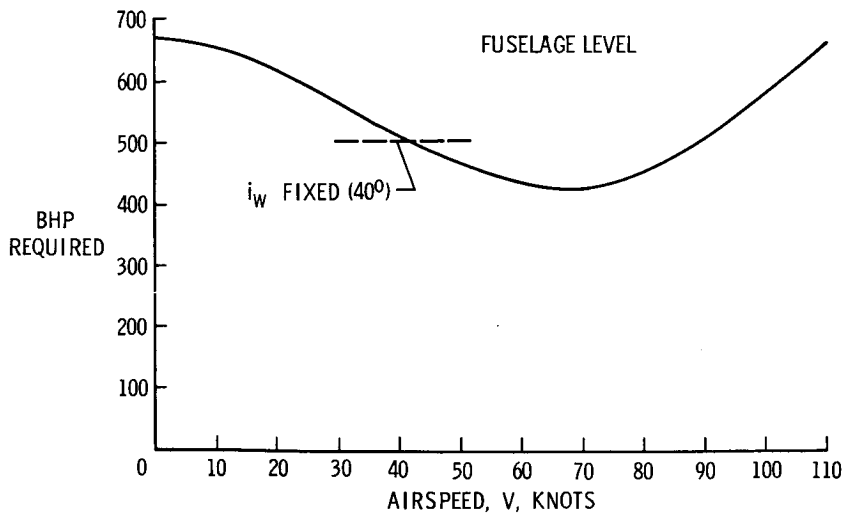


Figure 8

POWER REQUIRED FOR LEVEL FLIGHT, VZ-4 AIRCRAFT

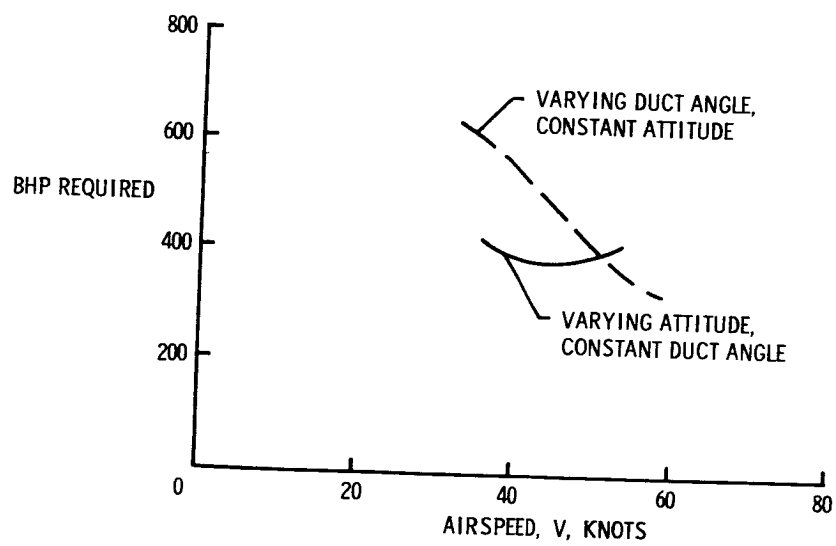


Figure 9

AERODYNAMIC OBSERVATIONS FROM FLIGHT TESTS

OF TWO VTOL AIRCRAFT

By F. B. Gustafson, Robert J. Pegg, and Henry L. Kelley

Langley Research Center

INTRODUCTION

The purpose of this paper is to help bridge the gap between pilot experience and wind-tunnel or theoretical results by presenting flight measurements of aerodynamic characteristics for two types of VTOL aircraft. The experience thus represented is interpreted in terms of design philosophy for improvement. The two aircraft to be discussed are the tilt-wing (VZ-2) and tilt-duct (VZ-4) test beds shown in figures 1 and 2. The gross weights and horsepowers of these two aircraft are about the same; the tilt-wing configuration uses tail fans for control at low speeds, whereas the tilt-duct configuration uses the exhaust jet. In addition to the data obtained by NASA test pilots, some data have been included which were obtained by the respective company pilots while the programs were being monitored by NASA.

SYMBOLS

V	airspeed, knots
α_f	fuselage angle of attack, deg
i_w	wing incidence referenced to fuselage reference line, deg
δ_d	duct angle, referenced to fuselage reference line, deg
β	angle of sideslip, deg

DISCUSSION

Four phases of research are discussed: effects of ground proximity, wing-stall phenomena, aircraft pitching moments, and power-required variations. Additional information is included in the appendix on control moments, static stability, trim changes, and oscillations.

The first point to be observed is that the approach to the ground can cause severe unsteadiness. Figures 3 and 4 show the behavior of the tilt-wing configuration in and out of ground effect, without any artificial stabilization, for a near-hovering condition. Note that the aircraft and control motions are moderate out of ground effect (fig. 3). For the aircraft in the region of ground effect (fig. 4), note that the aircraft and control motions are many times greater, with erratic angular velocity changes of about 10^0 per second and with frequent control motions of several inches. As has already been discussed in the paper presented by Robert O. Schade, the presence of the ground causes the slipstream to rebound and hit the tail surfaces, and this is at least a contributing cause to the instability. This problem can be expected to arise in practice for a variety of designs, especially when the aircraft are operated over uneven terrain.

The use of airframe design changes, such as larger tail rotors, to damp these motions would, unfortunately, be expected to increase the erratic moments from the rebounding flow and perhaps even to increase the motions. Therefore, the best recommendation that can be offered now is the use of artificial damping to minimize the piloting problem. This damping was used with considerable success in the test aircraft.

The tilt-duct aircraft has thus far given little evidence of this type of unsteadiness, but there are indications of lateral instability from flow reflected from the ground. Piloting difficulty at certain heights has occurred in roll. Unstable rolling moments equal to about $1/3$ of the available control moment have been indicated by rough measurements. Figure 5 shows a part of the mechanism of this instability. The aircraft was supported from a crane and was operated at fairly high power. Tuft grids were used to determine the flow paths shown. When the aircraft is banked, the upflow shifts to the wing which is already high. Since flow pressures as well as direction have a bearing on this problem, another check on the variation of moment with roll angle was made with most of the wing area removed. Unstable moments were no longer evident.

One step in the solution of such a problem would be the use of high-lift devices as a substitute for part of the wing area. Another step might be a modification to the planform.

The next topic of this discussion is the wing-stall phenomena; these effects have been mentioned in several papers. Figure 6 shows a sample flow pattern for the tilt-wing aircraft. Separation is indicated over a considerable area for this marginally acceptable flight condition. For the more extreme, unacceptable conditions, as shown in figure 7, the flow remained smooth over only a small area (near the tip at the leading edge).

The expedient of leading-edge droop as an approach to cleanup of the flow produced successive improvements in the flow for part-span and full-span coverage. Figures 8 to 10 show the successive shifts in rate of descent boundaries. Figure 8 is for the basic wing. The shaded area marked "poor" represents a region of difficult but feasible flight. The area beneath the solid lines is considered unacceptable; in fact, dangerous. The regions to the right and above are acceptable. Figure 9 shows the results for the outboard leading-edge-droop installation. Note that the peak of the boundary drops from climb at 500 feet per minute to just under level flight. In figure 10 for the full-span leading-edge droop, considerably more improvement is noted, with the peak down an extra 500 feet per minute; it is thus apparent that both inboard and outboard areas are important.

With leading-edge droop, not only were the "unacceptable" boundaries lowered, but flying in the "poor" areas was made far easier. Incidentally, the power required was reduced by an average of about 5 percent over this range of airspeeds with this approach to separation control.

These separation effects can be controlled either by high-lift devices and other approaches to flow control or by increasing wing area. Consideration of overall low-speed flying-qualities effects indicates that high-lift devices or flow control are preferable to a wing-area increase; in fact, wing-area decrease appears attractive if these flow-separation problems can still be handled. For example, two points are covered in more detail in the appendix; the undesirably high value of speed stability and the related short period of the longitudinal oscillations would (at low speeds) be aggravated by adding wing area and would be relieved by reducing it.

Further consideration is now given to leading-edge droop. It is not to be implied from one success with this device that a thorough understanding of this flow-separation problem has been attained. The leading-edge camber, as such, should not have been nearly so effective as is indicated, and the changed position of the leading edge relative to the propeller axis may have had a material effect on the results.

For the tilt-duct aircraft, this flow-separation problem is of far less concern, but interesting effects do occur for this type also (fig. 11). The duct angle for this test was 50° . This outboard flow separation was observed in level flight at a moderate wing angle of attack, about 7° , and is in keeping with other observations which indicated that the duct produced considerable upflow on the wing. This upflow is believed beneficial to performance, especially if flow separation can be minimized. Some adverse effects of the flow separation on flying qualities were noted, but some of these would be avoided if

the aileron action were irreversible. Both the flow separation and the effects on flying qualities increase with increased rate of descent. Rates of descent up to 1,200 feet per minute are usable as is, at approach speeds. To further improve the descent characteristics, and also to avoid rapid roll-off when aircraft stall is encountered, some form of flow-separation control, probably including leading-edge slots or the equivalent over the outer part of the wing, again appears desirable.

The nose-up pitching moments during decelerating flight are next considered. These moments have been a problem with successive types of low-speed aircraft for over 20 years and deserve specific and continued attention from designers. The tilt-wing configuration has shown a reasonable control margin in the recorded data, although pilots' comments indicate a problem in rapid decelerations at low speeds. Power-available limitations have prevented recorded data from being obtained on this point, but study of the control and trim characteristics points up the need for an increase in control moment available as one means of improvement.

For the tilt-duct aircraft, figure 12 shows a pitching-moment problem. These results are representative of a decelerating transition; the decrease in airspeed in this interval of approximately 1 minute was obtained by an increase in the duct angle as shown. The aircraft angle of attack is seen to increase. The important point is that the longitudinal stick position moves slowly forward and, at low speeds, is essentially full forward, even though the nose was allowed to rise. Records of this type will vary in detail but show, in effect, that pilots have at best roughly no control margin under generally favorable circumstances; whereas, if the aircraft is to be handled in gusts or is to make short landings, a decisive margin of control is needed, as is recommended in the paper by Robert J. Tapscott. For this case, the longitudinal-control power is, in its own right, high enough. It is therefore recommended that the moment be reduced at its source, namely, at the ducts. Both tunnel and flight measurements have shown the ducts to be the source of this moment, and the previous paper by Paul F. Yaggy and Kenneth W. Goodson covers this point in some detail. Since the problem arises in large measure from normal force at the duct lip, one major step appears to be to shift the duct so that the lip is closer to the pivot axis; this axis would remain near the wing quarter-chord line and the aircraft center of gravity. Current tests of this aircraft at Langley involve use of moment-offsetting vanes in the rear portion of the ducts, so linked as to change angle as the ducts are rotated relative to the fuselage. As was shown in the previous paper by Yaggy and Goodson, such vanes can logically be used to handle part of the moments. The use of the vanes as the only device is, however, primarily an expedient to permit more control margin under favorable conditions. Such

vanes should not be used in the future as the only device, because they will not relieve the pitch-up moments caused by gusts or by rapid maneuvers. Incidentally, the use of such vanes differentially is recommended as a powerful source of much-needed yaw control.

The final item for consideration is power required, relative to potential gains suggested by effects shown for varying the aircraft attitude at given wing or duct angle. This effect is relatively small, and also less fundamental in origin for the tilt-wing configuration, and therefore results for only the tilt-duct aircraft are presented. Figure 13 includes data that have been presented in the previous paper by John P. Reeder, which indicated the favorable flying-qualities significance of the short, constant-duct-angle curve. The added point to be made from figure 13 is that there is a large effect of attitude on power required at a given airspeed. The horsepower required is seen to be considerably less for the 10° -attitude curve than for the level-attitude curve ($\alpha_f = 0^\circ$). This power saving is shown not only as cruise flight is approached, where it would certainly be expected, but also at much lower airspeeds. Figure 11 showed separated flow over part of the wing at a moderate angle of attack; performance gains are shown in figure 13 to continue to higher angles of attack before large amounts of separation eventually limit the gains. It follows that use of high-lift devices, including flaps, should materially shorten take-offs and landings for the tilt-duct aircraft, since more load could be transferred to the wing without the aircraft getting too close to the angle for serious stall effects. Any increase in the usable length of the fixed-duct-angle curve obtained by such high-lift devices would also provide more freedom of piloting action in a steady approach at a fixed duct angle.

CONCLUDING REMARKS

Suggestions have been made concerning V/STOL design philosophy for taking greater advantage of favorable power-required effects and for dealing with the problems resulting from ground proximity, from flow-separation effects, and from pitching moments arising in decelerating flight. Perhaps the most general observation to be drawn from this material is the desirability, at this stage of development, of exploiting potential flying-qualities and performance gains by use of high-lift devices or by other ways of getting more lift from less wing area.

APPENDIX

MEASURED CHARACTERISTICS OF TILT-WING AND
TILT-DUCT CONFIGURATIONS

This appendix presents a number of additional measured characteristics of the VZ-2 and VZ-4 test aircraft. It should be noted that, except where otherwise stated, no automatic stabilization was used when the data presented were obtained.

Stability

Speed stability.- The speed stability variation of longitudinal-control position with airspeed for each of several fixed wing angles and constant power positions is shown in figure 14 for the tilt-wing aircraft. The steepness of the slopes at the low-speed wing settings indicates that large pitching-moment changes will be experienced with inadvertent changes in airspeed; for example, in gusty air and during longitudinal oscillations. Pilots' comments indicated that flatter slopes would result in more favorable flight characteristics.

Longitudinal oscillations.- Sample oscillations resulting from deliberate disturbances (longitudinal pulse input) on the tilt-wing aircraft are shown in figure 15. In the hovering configuration ($i_w = 85^\circ$), the response is essentially a simple, rapid divergence, though in a direction opposite to the input. At moderate speeds ($i_w = 40^\circ$), a lightly damped motion of undesirably short period is indicated. At cruise speeds ($i_w = 9^\circ$) the oscillation is well damped, but still of short period. It should be possible to improve the low-speed characteristics by reduction in speed stability (for example, by reduction of wing chord) and by increased damping of the aircraft.

The corresponding variation of the longitudinal oscillation period with airspeed is shown in figure 16.

Angular velocity response to longitudinal pulse inputs for the tilt-duct configuration are presented in figure 17 for duct angles of 7° , 20° , and 50° . In all of these conditions, pilots' comments indicated that the damping was very good, as confirmed by data presented in figure 17.

Static directional stability.- The static directional stability characteristics of the tilt-wing aircraft are shown in figure 18. The unstable (center) portion of the curves is believed to be caused, at least in part, by interference of the bifurcated exhaust pipe (and the exhaust flow) with the airflow over the vertical tail. Tuft surveys showed the portion of the tail behind the exhaust flow to be ineffective. Oval (flattened) tail-pipe assemblies have been designed and are expected to reduce this problem.

The static directional characteristics of the tilt-duct configuration are shown in figure 19. According to pilots' opinion, this plot is typical for a range of duct angles of at least 0° to 50° . The curve shows the static directional stability characteristics to be stable; however, at a left sideslip angle of about 8° there is a small region of instability as indicated by the curve.

Dihedral effect.- A positive dihedral effect is shown in figure 20 for the tilt-wing test bed. At the high end of the speed range, the tilt-wing aircraft exhibits a strong lateral static stability, whereas at lower speeds this effect is decreased.

A sample curve, showing the dihedral effect characteristics of the tilt-duct configuration, is presented in figure 21. Pilots' comments indicated that the dihedral effect was so strong, for a range of duct angles of at least 0° to 50° in right sideslip, that he ran out of aileron control before rudder control was exhausted.

Control

Control power.- Control moment per inch of stick deflection in the near hovering configuration for the tilt-wing aircraft was considered marginal in yaw, adequate in pitch, and excessive in roll. In the paper by John P. Reeder, values of control power are given for the tilt-wing and tilt-duct aircraft in the hovering configuration.

Angular velocities in roll.- Maximum roll velocities encountered in hovering flight on the tilt-wing test bed, according to existing criteria, are greater than is desirable. No reason was found for not reducing materially the control power in roll; an alternate solution, however, which would permit retaining the moment available, would be to use a damper on the control stick. In figure 22, the maximum roll rate per inch of stick motion is plotted as a function of trim airspeed.

Yaw fan thrust.- The yaw-fan thrust variation with pedal displacement for the tilt-wing aircraft is shown in figure 23. These nonlinear control characteristics (particularly those near neutral) are objectionable to the pilots in this case, as in past aircraft experience.

Trim

Longitudinal trim change with airspeed.- For fixed fuselage attitude of 0° and also for a fuselage attitude variation up to 10° , figure 24 shows the corresponding longitudinal stick position changes over flight range of the tilt-wing VTOL aircraft. The varying flight attitude is shown to require materially less change in longitudinal stick than the 0° fuselage flight attitude.

Wing angle of attack as a function of airspeed.- Figure 25 gives the variation of wing angle of attack of the tilt-wing aircraft with trim level-flight airspeed. Fuselage attitudes ranged from 0° to $\pm 10^\circ$; these variations did not introduce appreciable scatter.

Power Required

In figure 26, power required for level flight of the tilt-wing aircraft is given as a function of trim airspeed. The test points spotted below the power curve indicate the power required for the aircraft with full-span drooped leading edges on the wings.

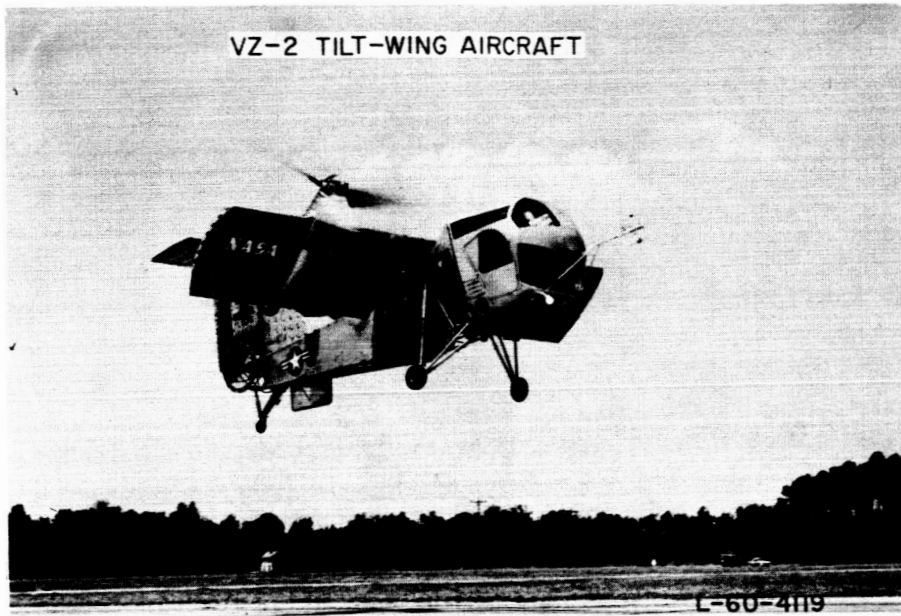


Figure 1

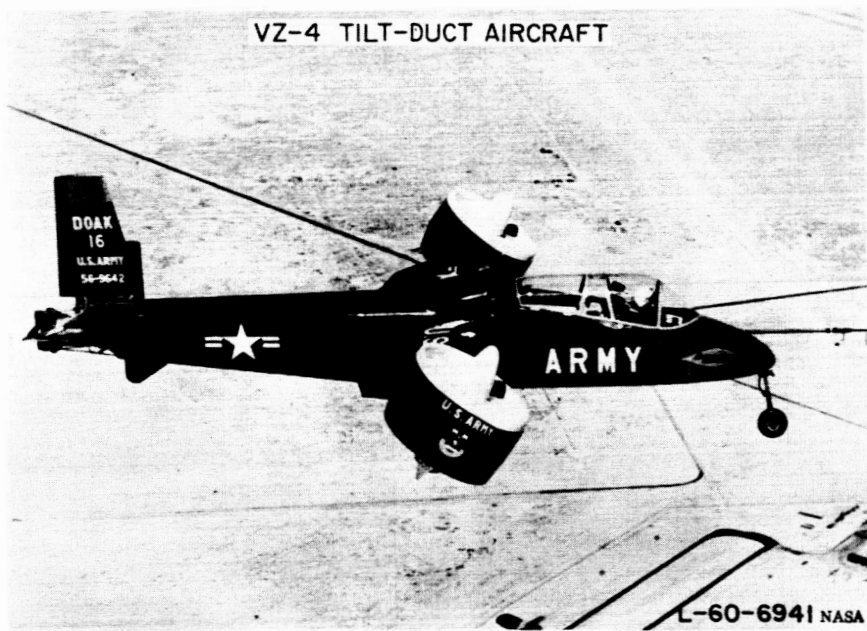


Figure 2

AIRCRAFT BEHAVIOR OUT OF GROUND-EFFECT REGION
TILTWING; NEAR HOVERING

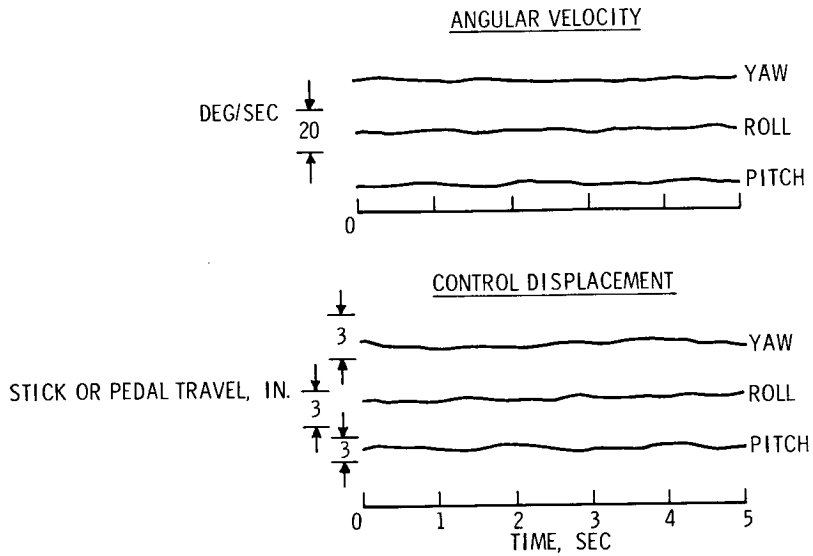


Figure 3

AIRCRAFT BEHAVIOR IN GROUND-EFFECT REGION
TILTWING; NEAR HOVERING

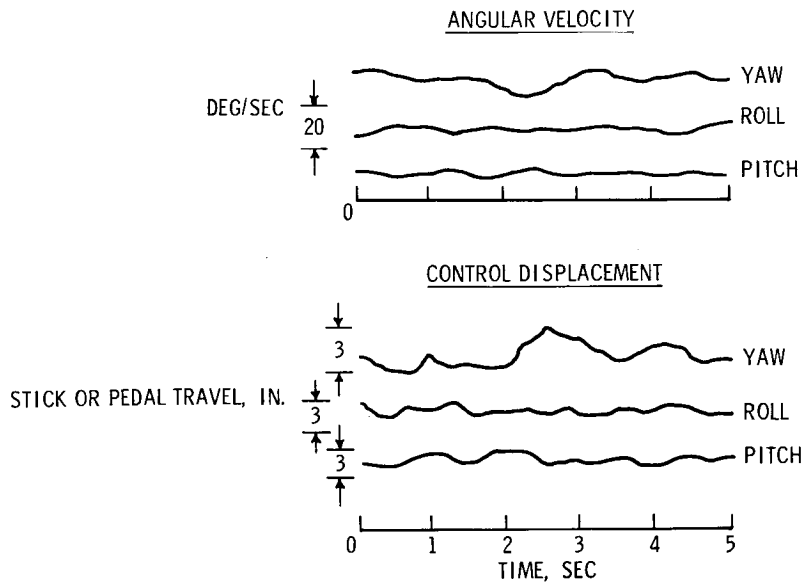


Figure 4

SOURCE OF DESTABILIZING GROUND EFFECT

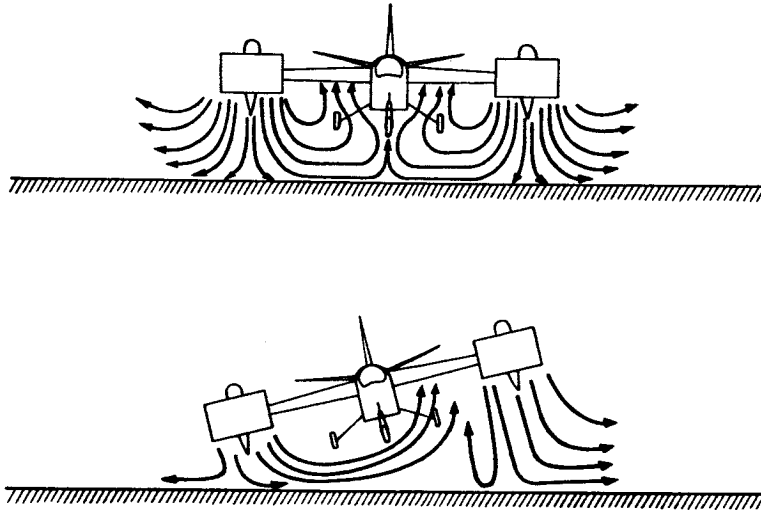


Figure 5

PARTIALLY STALLED WING
40° WING ANGLE

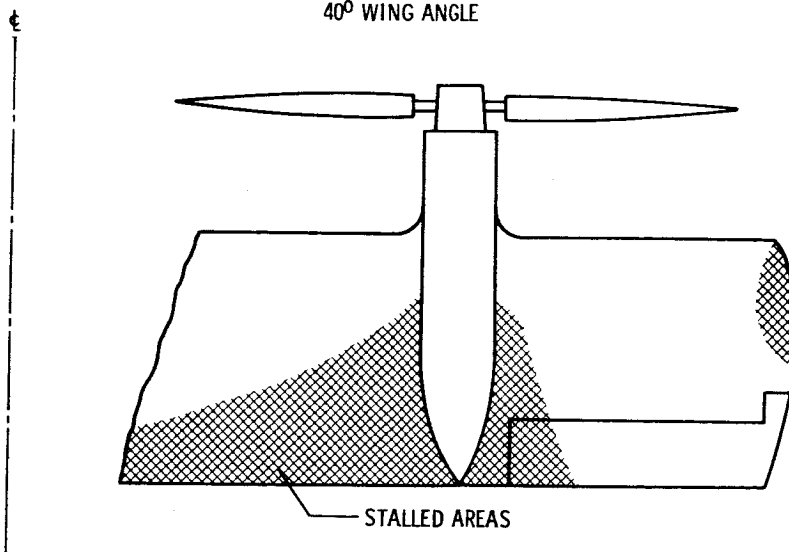


Figure 6

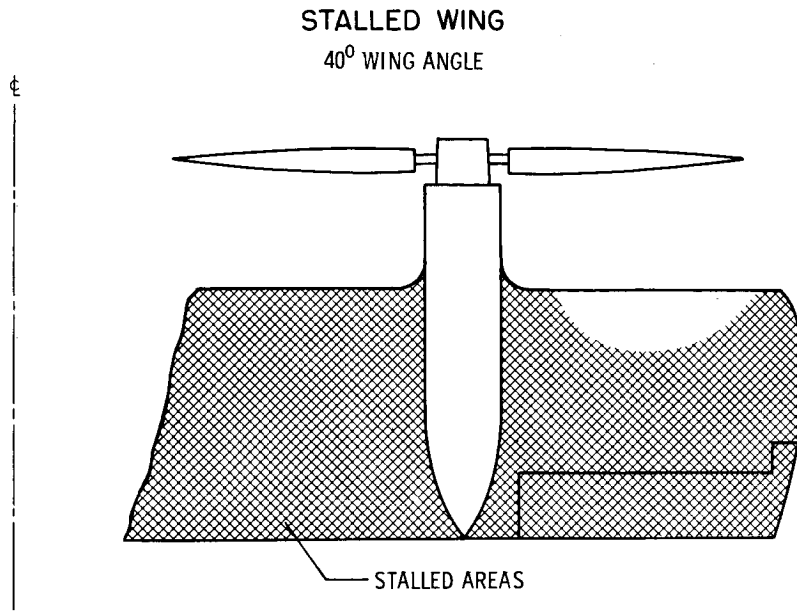


Figure 7

TILT-WING RATE-OF-DESCENT LIMITATIONS
BASIC WING

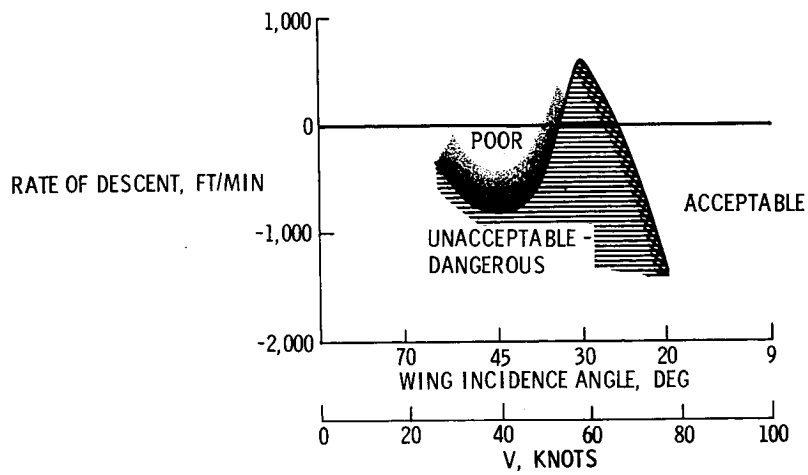


Figure 8

**RATE-OF-DESCENT LIMITATIONS
OUTER-PANEL LEADING-EDGE DROOP**

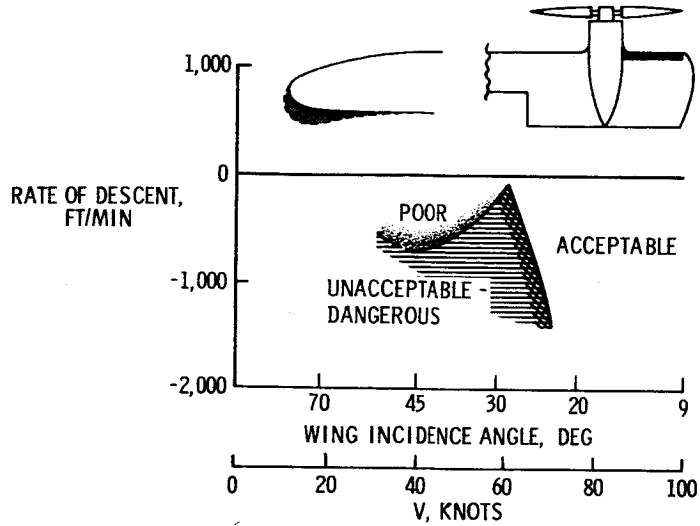


Figure 9

**RATE-OF-DESCENT LIMITATIONS
FULL-SPAN LEADING-EDGE DROOP**

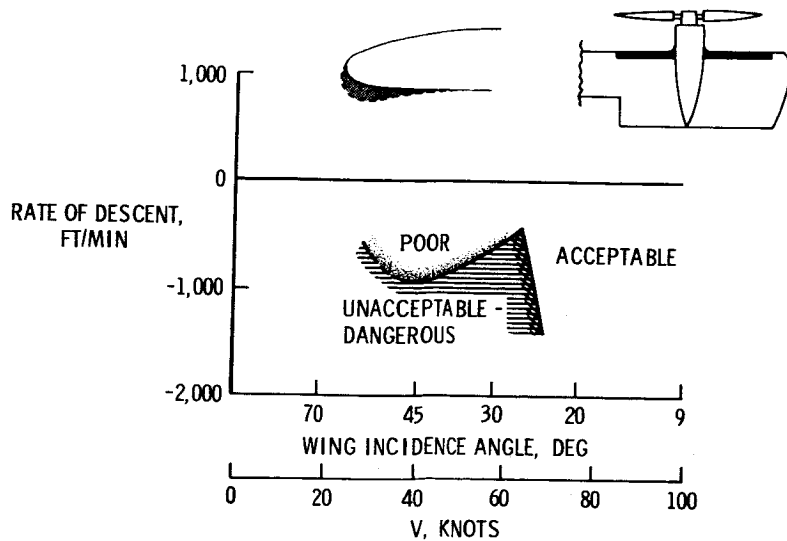


Figure 10

FLOW SEPARATION NEAR DUCT

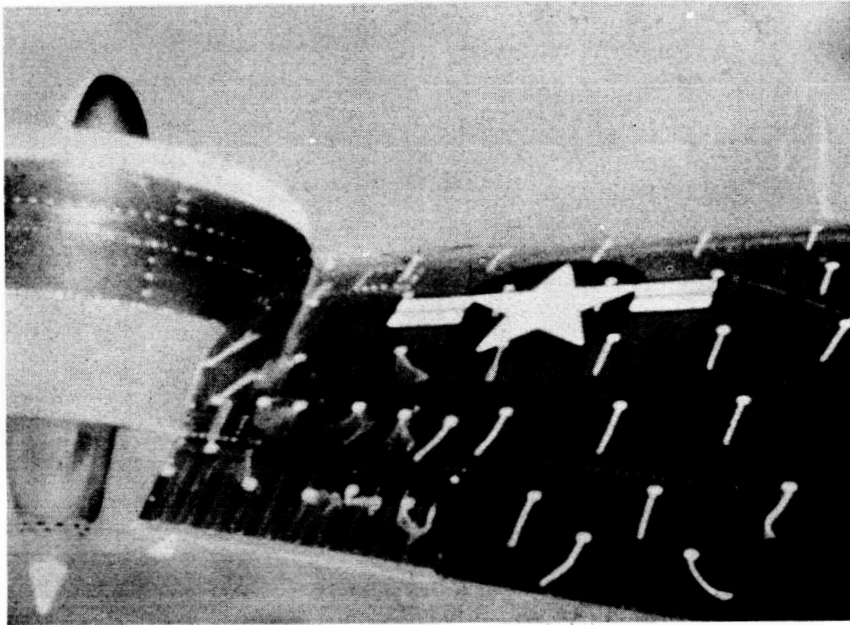


Figure 11

LONGITUDINAL CONTROL IN TRANSITION

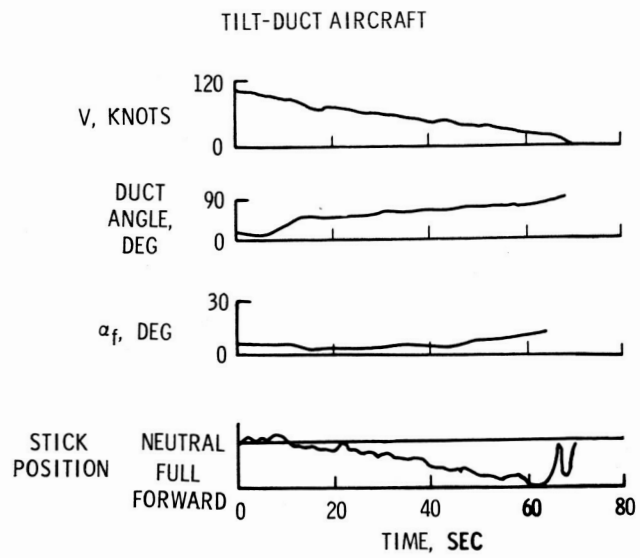


Figure 12

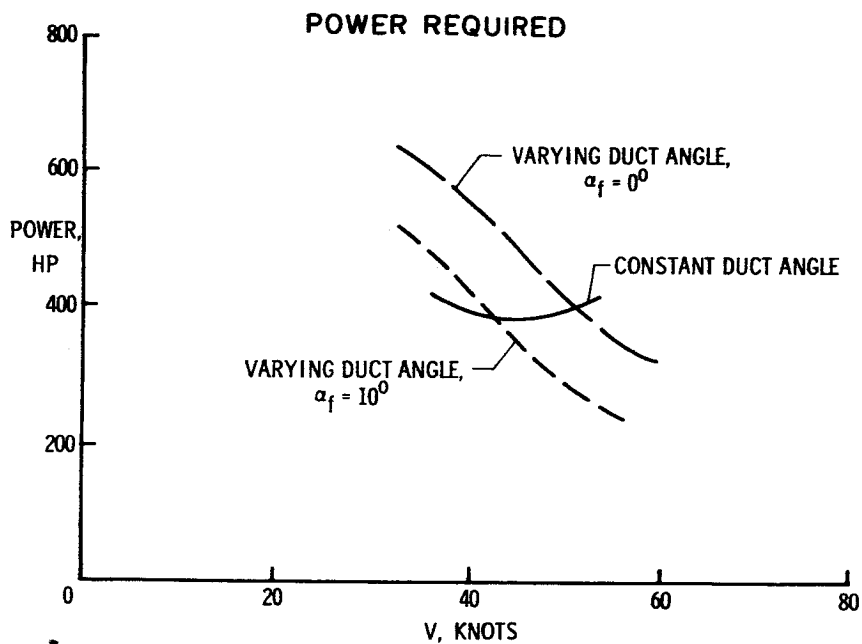


Figure 13

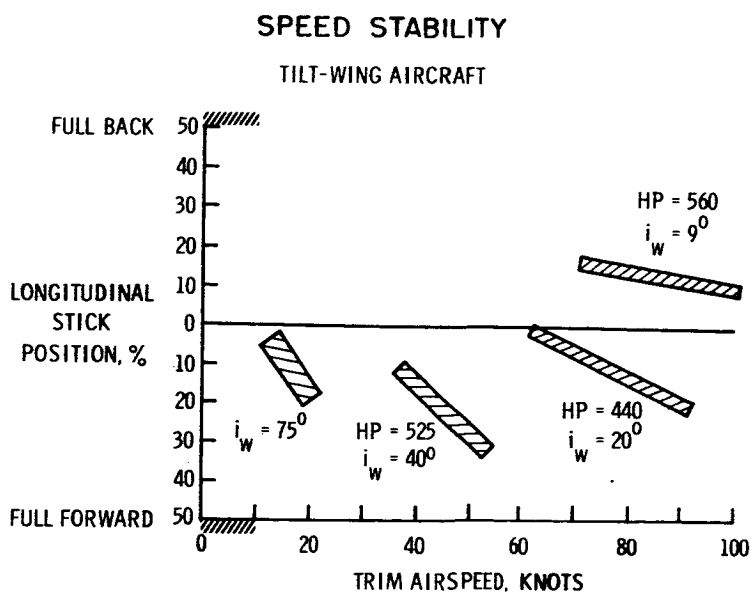


Figure 14

OSCILLATIONS DUE TO A PULSE INPUT
TILT-WING AIRCRAFT

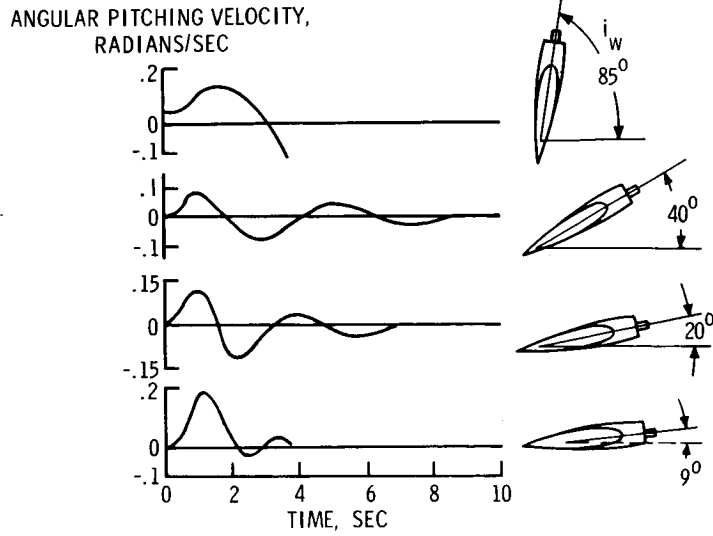


Figure 15

PERIOD OF LONGITUDINAL OSCILLATION
TILT-WING AIRCRAFT; APPROXIMATELY LEVEL FLIGHT

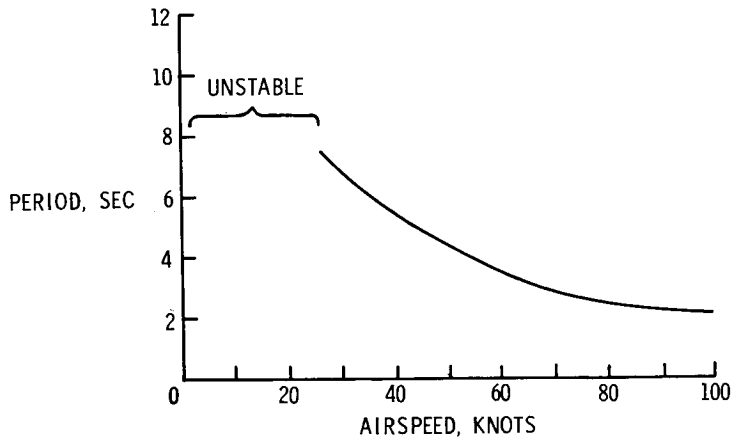


Figure 16

OSCILLATIONS DUE TO A PULSE INPUT

TILT-DUCT AIRCRAFT

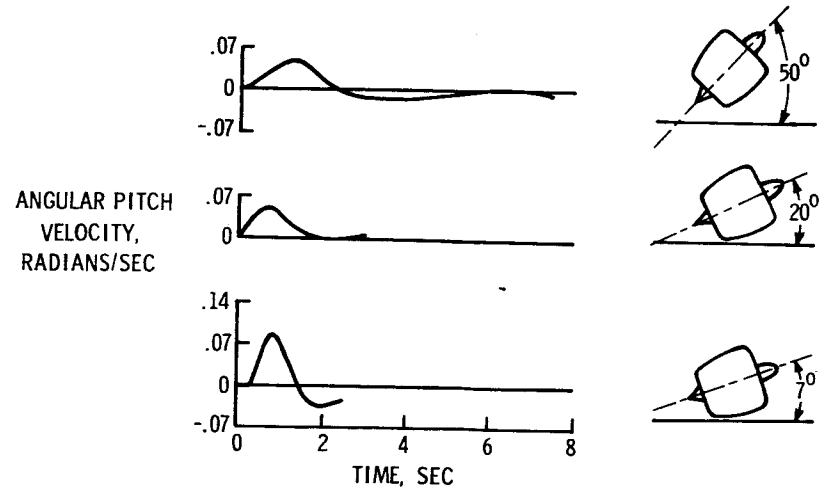


Figure 17

STATIC DIRECTIONAL STABILITY

TILT-WING AIRCRAFT

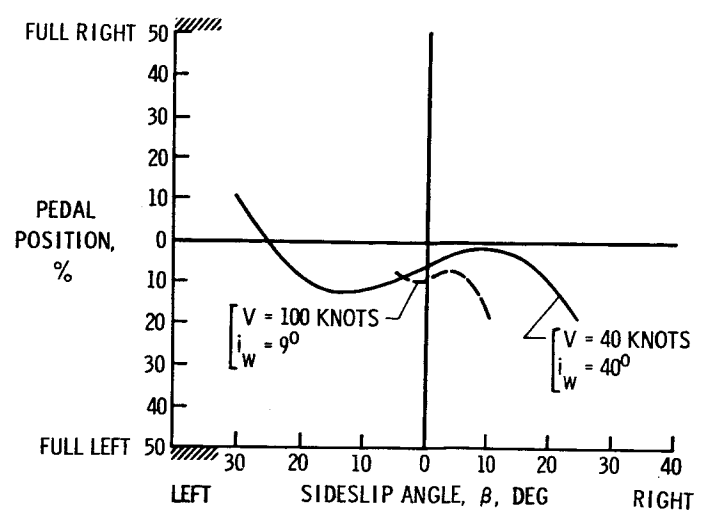


Figure 18

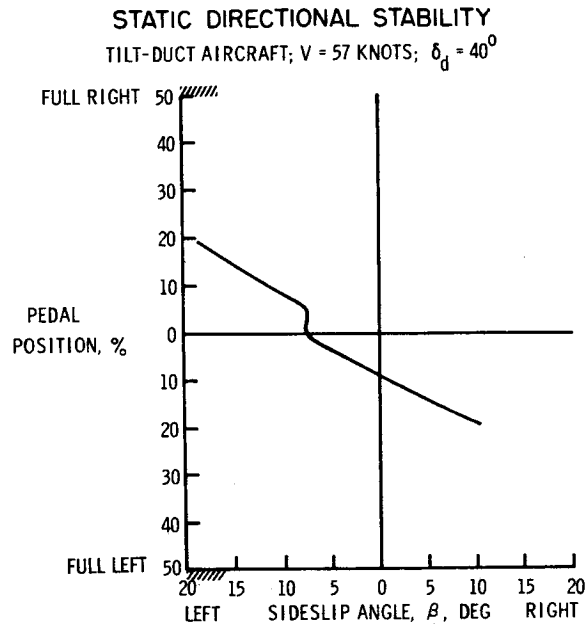


Figure 19

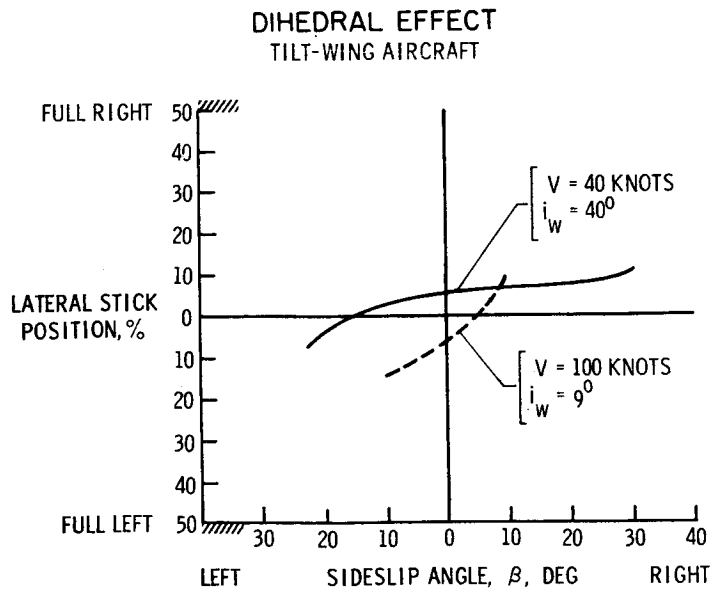


Figure 20

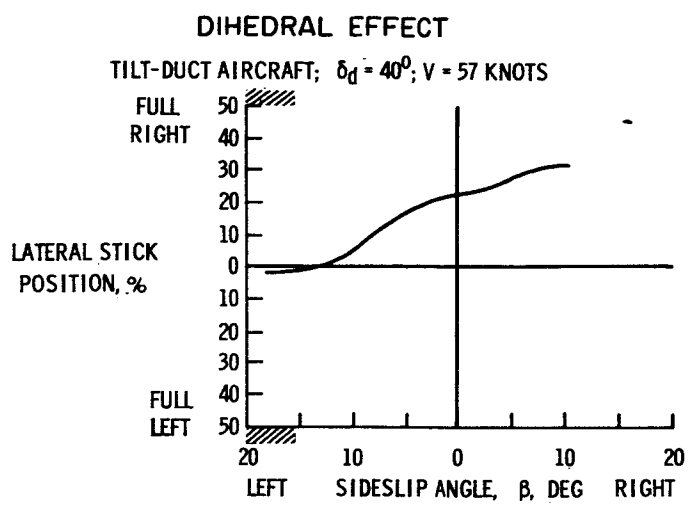


Figure 21

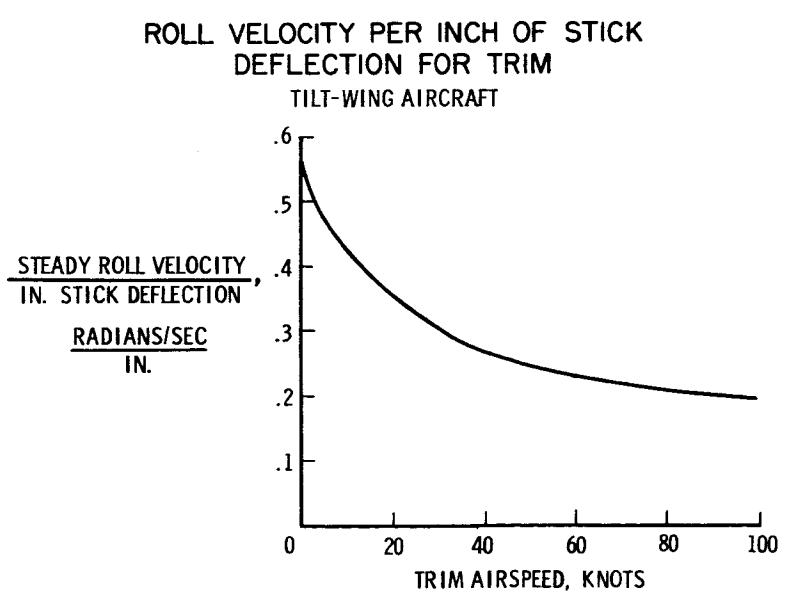


Figure 22

YAW-FAN THRUST AGAINST PEDAL DISPLACEMENT
TILT-WING AIRCRAFT

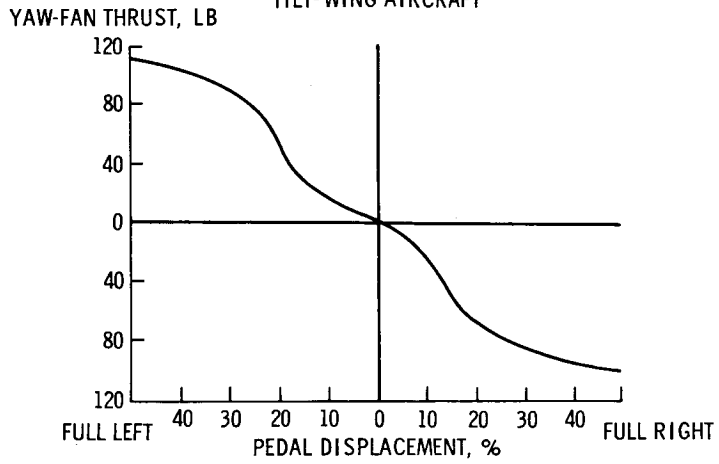


Figure 23

TRIM CHANGE WITH AIRSPEED

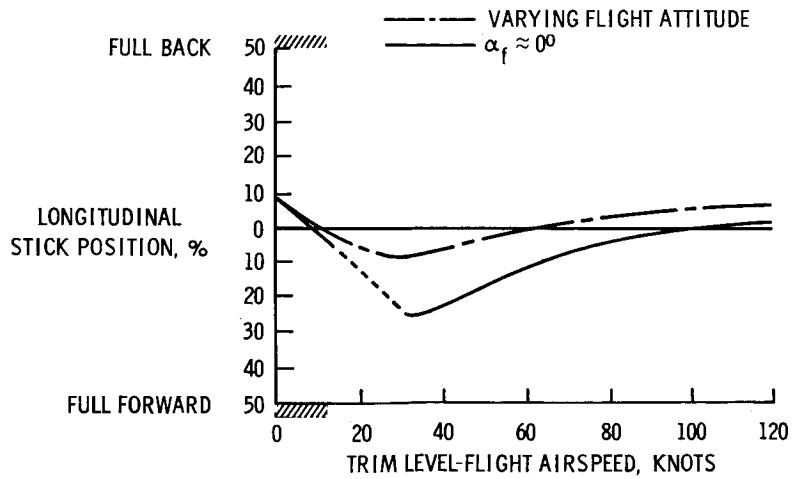


Figure 24

TRIM VELOCITY VARIATION WITH WING ANGLE OF ATTACK
TILT-WING AIRCRAFT; POWER FOR LEVEL FLIGHT

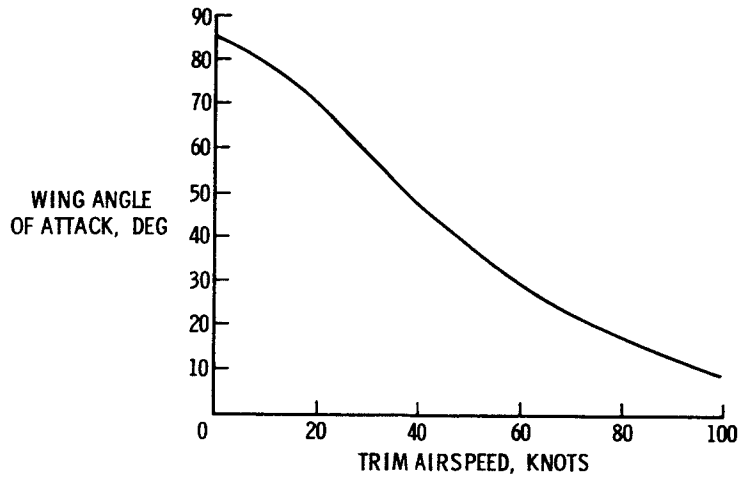


Figure 25

POWER REQUIRED
WEIGHT, 3,400 LB

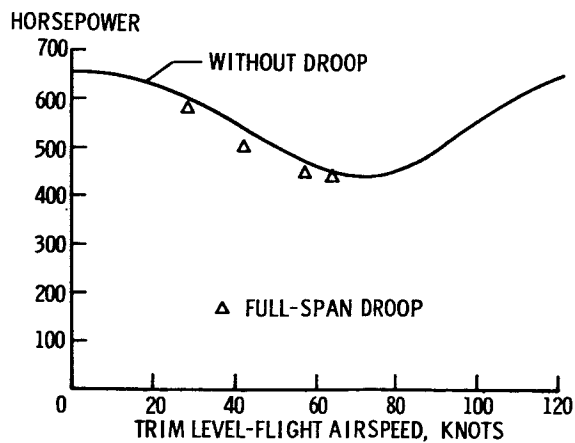


Figure 26

CHARACTERISTICS OF A DEFLECTED-JET VTOL AIRCRAFT

By L. Stewart Rolls

Ames Research Center

INTRODUCTION

Of the VTOL vehicles available for study only one incorporates characteristics similar to those which are typical of high subsonic or supersonic speed aircraft. This vehicle is the Bell X-14 which derives its vertical take-off capabilities from the vectored direct thrust of turbojet engines. Flight tests of this machine are being conducted at the Ames Research Center. Results have been obtained which have general applicability to VTOL research as well as to the specific type. This paper summarizes these results.

DESCRIPTION AND TESTS

Figure 1 is a sketch of the X-14, built by the Bell Aircraft Corporation, illustrating its important features. Two side-by-side mounted Armstrong Siddeley Viper ASV. 8 turbojet engines provide the thrust. The exhaust from each engine passes through cascade-type diverters. These diverters are controlled by the pilot and enable him to select any direction of the thrust vector from vertical to horizontal. In airplane flight, conventional aerodynamic controls are used to control the airplane; in hovering, reaction jets at the wing tips and at the tail supply the control. The air for these reaction controls is bled from the compressors of the turbojet engines.

The flight experience gained with the X-14 showed that operation of a deflected-jet VTOL airplane is feasible. Transitions could be performed fairly easily. The transfer of control from reaction nozzle to aerodynamic control was smooth. These flight tests did, however, point out problems associated with the deflected-jet type of VTOL vehicle which should be corrected to improve its usefulness. These problems are height control, coupling of reaction control moment to engine thrust, and gyroscopic coupling. Even though the X-14 lacked sufficient control power because of the limited amount of bleed air available, it was possible to examine these problem areas.

RESULTS AND DISCUSSION

The first problem to be considered is the height control. Operation of a deflected-jet VTOL vehicle is complicated because of the negative ground effect or ground suction associated with the jet exiting in the center of a flat plate. This ground effect means that a vertical thrust in excess of the weight of the airplane is required to accomplish the initial lift-off. As pointed out in a previous paper by Robert O. Schade this extra thrust is proportional to the distance the exhausting jet is above the ground. For the X-14, the excess thrust required to break ground contact is on the order of 12 percent of the airplane gross weight. Once the airplane becomes airborne, the pilot must cope with the problem of reducing this excess thrust to zero if he plans to hover at a fixed altitude. During hover, the throttle performs as an acceleration command control and the pilot has difficulty in arriving at an exact balance between the thrust and weight. This problem of establishing equilibrium between weight and thrust usually results in a roller-coaster ride for the pilot on his first few hovering flights in the airplane. At present, no method of overcoming this negative ground effect by aircraft modification except moving the jet away from the center of the vehicle is known.

The second problem is that of varying control power with varying engine thrust. Where the reaction nozzles are supplied air directly from the compressors of the lifting engines, the amount of control power available to the pilot is a direct function of the compressor airflow. The amount of control-power reduction with reductions in engine speed for the X-14 is shown in figure 2. It will be noted that this reduction is very severe. As was pointed out in the discussion of height control, the airplane hovers out of ground effect at less than full throttle; hence, the pilot never has full reaction control available in this flight condition. Also, as the flight continues, the amount available becomes less, because of the reduction in thrust as fuel is consumed. Normal hovering engine speeds are of the order of 93 to 97 percent and, as a result, control powers of about 90 percent of the maximum are available. However, momentary reductions in engine speed as low as 90 percent have been experienced, and, as a result, control power of only 70 percent of maximum is available.

Some relief from this problem could be gained if variable bleed could be designed into the system to allow more bleed air at the lower engine speeds and thus minimize the loss of reaction control power with the reduction in engine speeds. Variable-geometry jet exits could also be used to allow the pilot to monitor thrust and operate the engines at full speed.

The third problem area associated with the operation of a deflected-jet VTOL can be gyroscopic coupling. This coupling on the X-14 is between the pitch and yaw axes because of the horizontal engine axis. On a VTOL design with vertically mounted lifting engines, the gyroscopic coupling would be between the pitch and roll axes. On the X-14 this gyroscopic moment is of sufficient magnitude that, at rates of yaw greater than 15° per second, the pilot is unable to hold the airplane level with the existing amount of longitudinal control. Reducing the gyroscopic moment by reducing engine speed does not minimize the problem because of the attendant loss of control power. In order to make a deflected jet operational, it will be necessary to overcome the gyroscopic coupling. An automatic stabilization system will eliminate this problem provided there is sufficient reaction control available for both the pilot and the stabilization system. A failure of the stabilization system, however, might leave the pilot with an unacceptable airplane. The gyroscopic coupling problem might be eliminated or reduced with engines similar to the Bristol Siddeley BE-53 which employs two spools rotating in opposite directions.

Transition with the X-14 airplane presents no great problems. As with any fixed-wing VTOL airplane, as the wing approaches the stall angle of attack, some control difficulties may occur. With the X-14 the speed at which the wing stalls can be restricted to a speed where the dynamic pressure is low; thus, no large airplane motions result. If the pilot has sensitive airspeed, rate-of-climb, and angle-of-attack indicators, he is able to perform transition without difficulties and is able to avoid the stall region.

As a support to the general investigation of the handling-qualities requirements for operational V/STOL aircraft, it was felt that a variable-stability V/STOL airplane would be of great value. The X-14 possessed the unique feature that the reaction nozzles exert a pure moment on the airframe; hence, a variable-stability vehicle controlled with reaction nozzles would not be influenced by possible cross-coupling effects such as would result with aerodynamic controls. Also the loading and unloading of the fixed wing would afford an opportunity to investigate transition and STOL-type operations. The conversion of the X-14 to a variable-stability-and-control airplane was possible because of the greater bleed-air capabilities of the General Electric J85-5 engines. The J85-5 engines also furnished greater thrust at less weight than the Viper ASV. 8 engines originally installed in the X-14 and were adaptable to the existing diverter system.

The X-14 is shown in figure 3 as it will operate as a variable-stability-and-control airplane; only one engine is shown for clarity. The original reaction nozzles have been retained for the pilot's control and a parallel set of nozzles were installed to supply the variable-stability moments. This parallel arrangement of nozzles was

used to provide an effective margin of safety. Since the pilot's control nozzles supply a greater amount of bleed air than the variable-stability nozzles, the pilot has a direct mechanical overriding capability.

The variable-stability reaction nozzles are driven by servomotors which are controlled by a signal combining six possible airplane functions. The pilot is furnished a selector which enables him to vary the magnitude and sign of these input signals. The moments from these nozzles can be applied in the same direction as the pilot control moments to investigate increases in control power or applied in the direction to oppose airplane motion to investigate additional damping.

The ranges of damping and control power available with the modified X-14 airplane using both reaction-nozzle systems are illustrated in figure 4. In this figure, the shaded areas indicate the conditions of control power and damping which can be obtained when the available bleed air is divided among the axes on the basis of 55 percent for roll, 28 percent for pitch, and 17 percent for yaw. The solid curves indicate the control-power-damping characteristics which could be investigated if the maximum bleed air were used on only one axis, sufficient air being used on the other axes only to maintain approximately the same control as that of the original airplane. The boundaries for satisfactory, unsatisfactory, and unacceptable control characteristics discussed in a paper by Alan E. Faye, Jr., are shown in this figure for reference. The data points represent the original X-14 airplane. It will be noted that with the X-14 it will be possible to investigate ranges of characteristics from satisfactory to unacceptable in pitch and roll; however, in yaw its capabilities are somewhat less because of the higher moment of inertia about that axis. These reaction-control power and damping capabilities can also be imposed upon the airplane characteristics during transition. It will, for example, be possible at 40 knots (which is a speed approximately halfway through the transition) to change the airplane damping from zero to twice the aerodynamic damping available at that speed. Since the aerodynamic damping in roll and yaw is low, areas of control power and damping similar to those shown for hovering can be investigated through the transition.

The first tests conducted with the variable-stability-and-control system will be to investigate the control-power-damping requirements for satisfactory pilot opinion; this investigation is similar to that conducted by Alan E. Faye, Jr., on a moving-base simulator. In this investigation the reaction nozzles will be positioned by signals from rate gyros and control motions by the pilots.

X-14 VTOL TEST VEHICLE

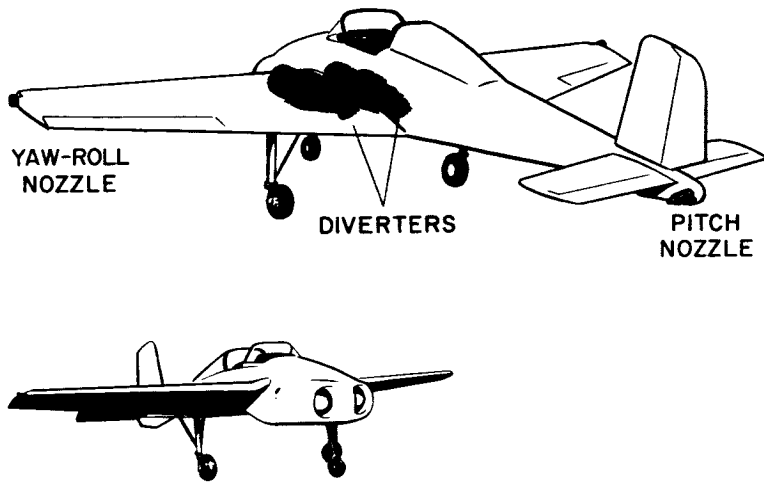


Figure 1

CONTROL POWER-ENGINE RPM RELATION

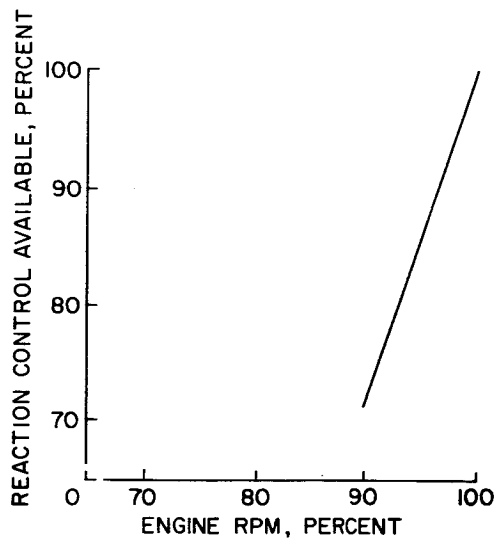


Figure 2

VARIABLE STABILITY VTOL VEHICLE

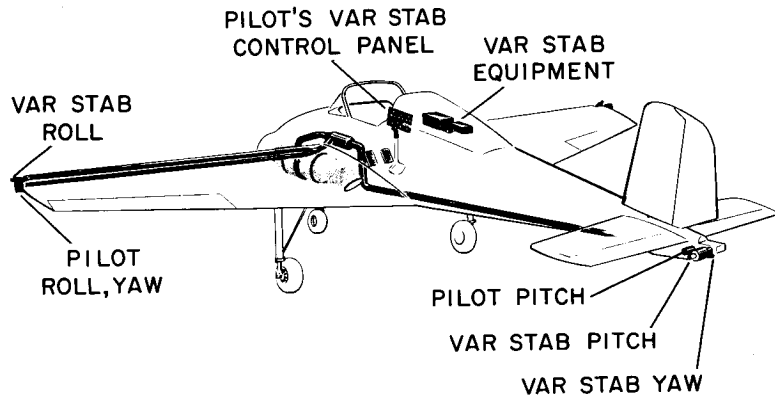


Figure 3

REACTION-CONTROL CAPABILITY OF VARIABLE-STABILITY AIRPLANE

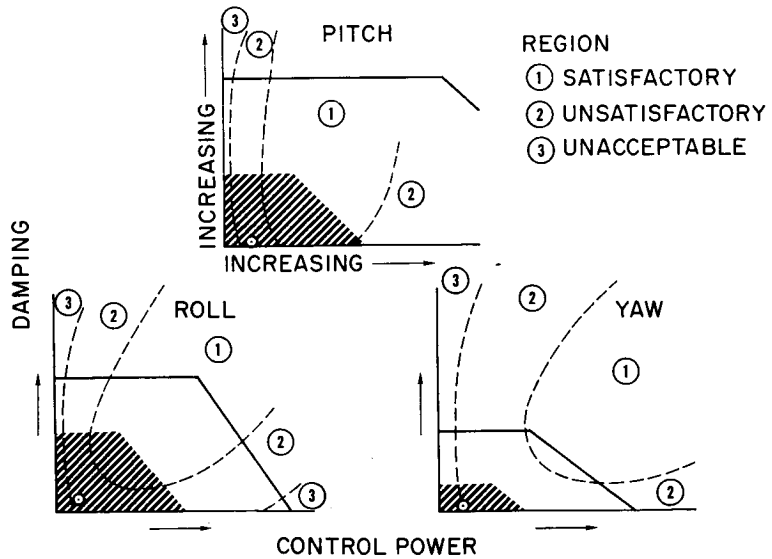


Figure 4

THE EFFECT OF BLADE FLAPPING ON THE DYNAMIC STABILITY
OF A TILTING-ROTOR CONVERTIPLANE

By Hervey C. Quigley and David G. Koenig

Ames Research Center

INTRODUCTION

The Bell XV-3 convertiplane has been extensively tested over the past several years. An investigation was conducted in the Ames 40- by 80-foot tunnel to study the effectiveness of a number of modifications to correct the wing-pylon oscillation which was evident on the initial flights of the airplane. This investigation, reported in reference 1, showed that the airplane could be flown through transition and gear-shifted to low prop-rotor rotational speed in airplane flight without serious airplane or rotor stability problems. A limited flight evaluation was performed by the Air Force Flight Test Center and is reported in reference 2. The flight evaluation explored the flight characteristics of the airplane from near hover to about 155 knots. Since the completion of the Air Force tests, the airplane has been flight-tested by the National Aeronautics and Space Administration at the Ames Research Center to explore further some of the problem areas noted in previous tests and to study general handling-qualities requirements for V/STOL aircraft. Much of the recent flight testing of the XV-3 has centered around the cruise configuration of the airplane in order to study the effect of the large flapping rotors on the handling qualities at cruising speed and above. This paper will deal with what is considered to be the one of the basic problems of the tilt-rotor concept in cruise when flapping prop-rotors are used for propellers. This problem can be divided into four separate but related problem areas:

- (1) The high blade-flapping amplitude with steady-state angles of attack and sideslip
- (2) The increase in flapping due to maneuvering
- (3) The prop-rotor normal force associated with pitching and yawing angular velocities of the airplane
- (4) The airframe vibration which accompanies airplane angular velocities

DISCUSSION

The low-disk-loading flapping rotors of the XV-3 (see fig. 1) are of the semirigid, teetering or seesaw, type construction and are driven by a 450-horsepower reciprocating engine in the fuselage. A gear shift is incorporated which permits the operation of the prop-rotors at either of two prop-rotor rotational speeds while maintaining maximum engine rotational speed. Blade flapping is designed into the rotor system to relieve the unbalanced moments across the rotor disk and to provide a means of controlling the aircraft longitudinally and directionally in hover and low-speed flight. The flapping rotor also provides damping about all axes at low airspeed and in hover. When the prop-rotor is converted into a propeller, the control provisions of the rotor are washed out and the blade-flapping function is to relieve the blade stresses that occur once per revolution.

The variations of the steady-state blade flapping angle with airspeed for the two prop-rotor rotational speeds used in this investigation are shown in figure 2. These data are for the masts tilted forward (cruise configuration). The airspeed range of the airplane in this configuration was from 100 to 140 knots. The low prop-rotor rotational speed gives the highest values of flapping and is the one of particular interest since this speed is used in airplane flight to attain the highest possible propeller efficiency. As airspeed is increased, the steady-state flapping decreases for both prop-rotor rotational speeds. Thus, it would appear that flapping should become less of a problem as speed is increased; however, any type of maneuver will introduce additional flapping. The flapping due to maneuvering in pitch at 130 knots airspeed is presented in figures 3 and 4 where the change in blade flapping due to angle of attack and due to pitch angular velocity are presented. The change in blade flapping angle due to angle of attack alone (fig. 3) is relatively small, but the blade flapping due to pitch angular velocity (fig. 4) can be quite large. A pitch angular velocity of only -0.2 radian per second results in a change in blade flapping angle of over 4° . In dynamic maneuvers, the change in blade flapping angle due to angle of attack and pitch angular velocity can add to give even higher blade flapping angles. The XV-3 is provided with a maximum available blade flapping angle of $11\frac{1}{2}$ which should prove adequate for any normal maneuver. It can be seen in figure 4 that the change in blade flapping angles is positive when the pitching angular velocity is negative; because of inertial effects, the prop-rotor disk is lagging the angular motion.

In evaluation flights of the airplane at high airspeeds, pilots have reported a condition in which the airplane oscillated about all axes simultaneously. An analysis of the time histories taken during

this maneuver has shown that it consisted of longitudinal and lateral-directional oscillations that were very lightly damped. The damping ratio and period for the two oscillations over the speed range that could be covered with this airplane are presented in figure 5. These data are for the low prop-rotor rotational speed. The longitudinal and lateral-directional oscillations are not directly coupled. They are at different frequencies and oscillations can be performed in either mode without exciting the other, but with such low damping it is easy to excite both modes at the same time. These damping ratios are much lower than are considered acceptable by any of the criteria for airplanes in cruise. Damping ratios of 0.34 for the longitudinal mode and 0.18 for the lateral-directional mode have been specified as the minimum allowable by military handling-qualities specifications. The damping ratios are not only low but also change appreciably over this relatively small airspeed range, approaching zero at the higher speeds. In examining the reasons for this low damping, the longitudinal mode will be discussed and a discussion of the lateral-directional mode would be similar.

Computations have shown that, if the prop-rotor contribution to damping were ignored, the airplane would have a higher damping ratio than was measured. The computed damping ratio and the measured values for the two prop-rotor rotational speeds tested are shown in figure 6. Since there is a large difference between computed and measured values of damping and also a significant difference between damping with high and low prop-rotor rotational speeds, a negative damping moment produced by the prop-rotors is indicated. This negative damping was also evident in the wing-tip pylon-position data obtained during the flight tests, which indicated that when the airplane had a nose-up pitching motion there was an "up" force on the prop-rotor hub proportional to the rate of pitch. The instrumentation was not sufficient to measure accurately the magnitude of this force. Due to the low tail volume of the XV-3, the force on the prop-rotor hub had a large effect on the dynamic stability of the airplane.

It was predicted in reference 3 that convertiplanes which use flapping prop-rotors would have this problem. Being consistent with helicopter theory, a flapping rotor is essentially a gyroscope and requires a couple across the rotor disk 90° out of phase with the angular motion of the airplane to make it precess and follow its shaft. (See ref. 3.) When airplane pitching motion is introduced, the prop-rotor disk lags the airplane angular motion until sufficient flapping is present to produce the necessary couple aerodynamically by increasing lift on one side of the disk and decreasing lift on the opposite side; thus, the increase in flapping due to airplane angular velocity. The change in aerodynamic force on a blade due to flapping can be resolved into two forces, one perpendicular and one parallel to the prop-rotor disk. These forces are shown schematically in figure 7. This sketch indicates that when the airplane is pitching down the components of the forces due to flapping

are forward and down on the inboard side, and rearward and down on the outboard side of the prop-rotor disk. For a constant prop-rotor rotational speed, Ω , the magnitude of the precessing force changes little with airplane flight conditions, but the in-plane force depends on blade angle. At low advance ratios, the blade angles are small; therefore, the in-plane force is small. However, at the high advance ratios, when blade angles are large, this force becomes sufficiently large to affect the dynamic stability of the airplane. It can be seen that the in-plane force is in the direction of the motion and produces a negative damping moment when the prop-rotors are in front of the center of gravity. The method in reference 3 of calculating these forces and moments was developed for helicopters in hover and low-speed flight and will require expansion to analyze damping moments due to flapping prop-rotors at high advance ratios.

The vibration which accompanies large pitch rates is also traceable to the in-plane force on the prop-rotor and shows up as an oscillatory force with a frequency of 2 cycles per rotor revolution. This vibration in the pilot's opinion was large enough to be a limiting factor on the maximum angular rates attainable. Since the in-plane forces and, therefore, the vibration are associated with flapping, the amplitude of the vibration is maximum when the blade flapping angle is maximum. The use of three or more blades on future prop-rotors should alleviate this type of vibration.

While the XV-3 convertiplane is the first VTOL aircraft to be plagued with these blade-flapping problems, they have been encountered in the past on a prototype STOL fighter equipped with flapping propellers mounted on the wing tips. These problems are largely attributable to the compromise required to maintain good hovering efficiency as well as high propeller efficiency in cruise which dictates the use of flapping prop-rotors at high blade angles in cruising and high-speed flight regardless of the disk loading. Solutions to these problems can be approached in several ways on future VTOL airplanes. Higher dynamic stability can be provided in the design of the airplane itself. To illustrate, lengthening the tail about 5 feet would increase the damping ratio of the XV-3 to 0.5 at 140 knots. Another solution would be to place the prop-rotors behind the center of gravity where the in-plane forces would provide positive damping. This would probably result in a pusher configuration. Alternatively, the magnitude of the in-plane forces on the prop-rotor hub could be reduced by supplementing the aerodynamic precessing couple by the use of offset flapping hinges, blade-flapping restraint springs, or other methods. However, there is little information available on the behavior of a prop-rotor at high advance ratios, and additional research is required to determine the optimum method of reducing the in-plane forces associated with this blade flapping and still maintain the desirable features of the light-weight prop-rotor system.

CONCLUDING REMARKS

At high advance ratios the prop-rotor blade flapping due to airplane angular velocity generates a force on the prop-rotor hub in a direction which reduces the dynamic stability of the airplane. This is a problem area that will be common to all prop-rotor configurations with flapping blades, and there is a need for additional research into the problems of flapping prop-rotors at high airplane flight speeds.

REFERENCES

1. Koenig, David G., Greif, Richard K., and Kelly, Mark W.: Full-Scale Wind-Tunnel Investigation of the Longitudinal Characteristics of a Tilting-Rotor Convertiplane. NASA TN D-35, 1959.
2. Deckert, Wallace H., and Ferry, Robert G.: Limited Flight Evaluation of the XV-3 Aircraft. AFFTC-TR-60-4, Air Res. and Dev. Command, U.S. Air Force, May 1960.
3. Amer, Kenneth B.: Theory of Helicopter Damping in Pitch or Roll and a Comparison With Flight Measurements. NACA TN 2136, 1950.

XV-3 CONVERTIPLANE



Figure 1

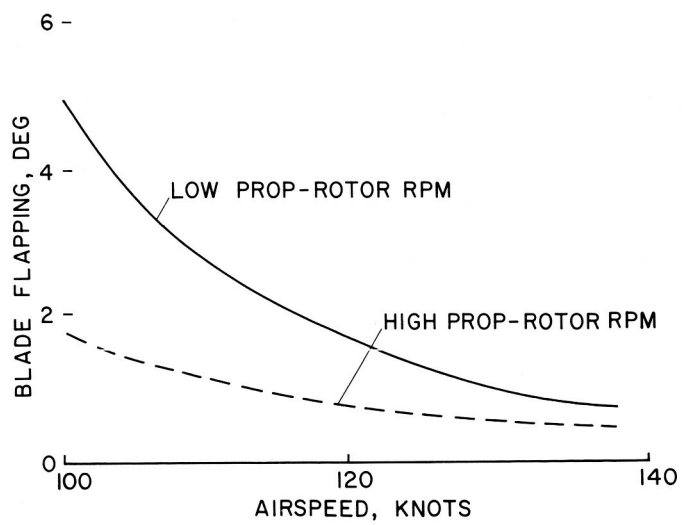
VARIATION OF STEADY-STATE BLADE
FLAPPING FOR AIRPLANE CONFIGURATION

Figure 2

CHANGE IN BLADE FLAPPING WITH
ANGLE OF ATTACK AT 130 KNOTS

PITCH RATE=0

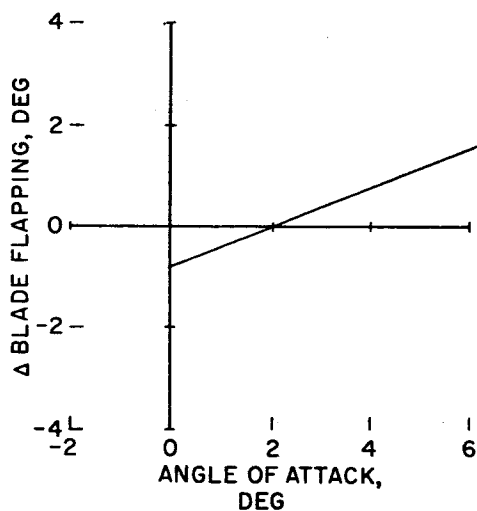


Figure 3

CHANGE IN BLADE FLAPPING WITH
PITCHING ANGULAR VELOCITY AT 130 KNOTS

ANGLE OF ATTACK = 2°

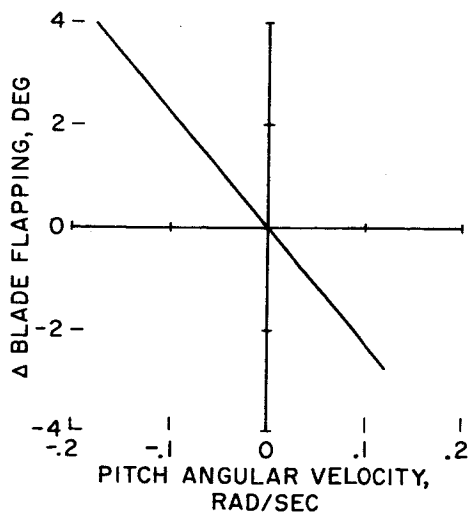


Figure 4

LONGITUDINAL SHORT-PERIOD AND LATERAL-DIRECTIONAL OSCILLATORY CHARACTERISTICS

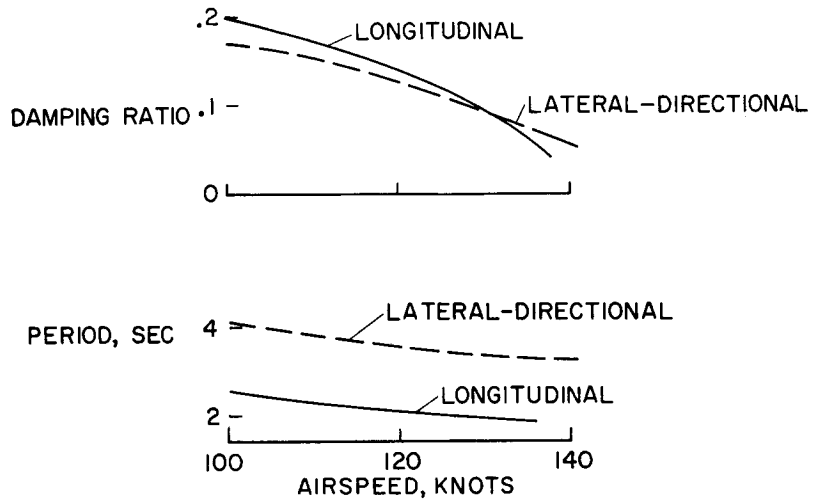


Figure 5

COMPARISON OF LONGITUDINAL SHORT-PERIOD CHARACTERISTICS

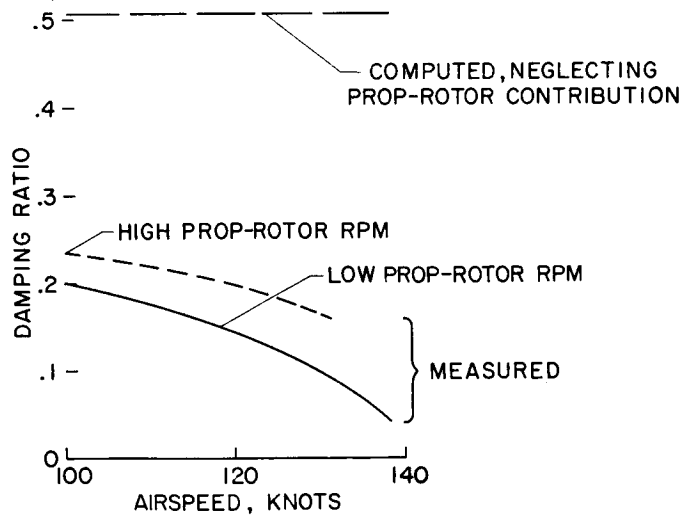


Figure 6

FORCES ON PROP-ROTOR BLADES
DUE TO PITCHING VELOCITY

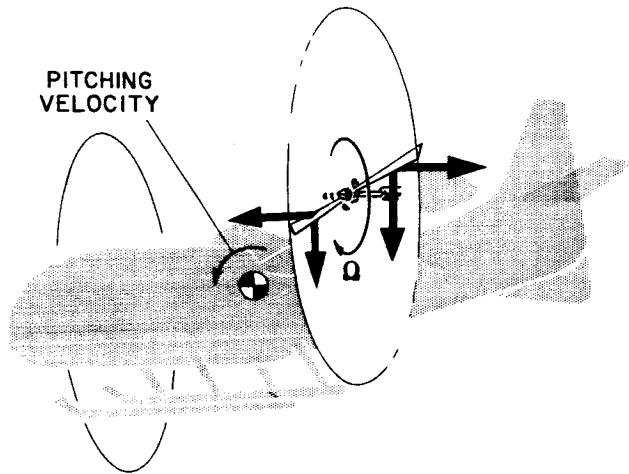


Figure 7

HIGHLIGHTS OF HANDLING QUALITIES CRITERIA FOR V/STOL AIRCRAFT

By Seth B. Anderson

Ames Research Center

INTRODUCTION

A major obstacle delaying the appearance of the operational V/STOL vehicle has been the lack of the formulation of handling qualities requirements. Past experience with airplanes and helicopters has brought out the need for handling qualities requirements to insure that these vehicles could carry out a mission in a safe and efficient manner. A similar but tentative set of handling qualities criteria have been proposed for V/STOL aircraft. These V/STOL criteria were arrived at from a broad background of flight results and pilots' comments from VTOL and STOL type aircraft, aircraft equipped with boundary-layer control, variable-stability aircraft, landing-approach studies, and flight simulators. The purpose of this paper is to point out the reasoning behind the handling qualities criteria for V/STOL vehicles.

DISCUSSION

In this paper only a few of the V/STOL criteria are discussed briefly. A more detailed description and a more complete discussion of the reasoning behind and the sources of information leading to all the V/STOL criteria are available in NASA Technical Note D-331.

Mechanical Characteristics of Control Systems

In regard to mechanical characteristics of control systems, flight experience has revealed the fact that in landing approach, V/STOL aircraft must be completely controllable by one man. In low-speed precision-type approaches, it was desirable for the pilot to use one hand to adjust the flight controls and the other hand to adjust the engine power to control the flight-path angle or rate of sink. In this regard, force values must be kept small for V/STOL aircraft and made equal for stick or wheel controls. This philosophy has been applied to such items as trim changes, stick-force gradients, and control for longitudinal and lateral performance. This suggests that a stick-type control could be used in a four-engine transport instead of a wheel.

Longitudinal Stability and Control Characteristics

Stick-fixed static stability.- Recent tests with variable-stability aircraft have indicated for some flight conditions that stick-fixed static stability is not required as long as stick force and dynamic requirements are met. For V/STOL airplanes, however, which are to operate extensively at low speeds, flight tests have indicated the desirability of stick-fixed stability in the transition and landing regions. In particular, a pitch-up is considered unacceptable if the instability occurs in the speed range below the speed for minimum drag. Flight experience in flying on the back side of the drag curve has indicated a particular need for stable, linear stick-fixed gradients in order to make satisfactory height adjustments along a desired flight path. It is to be noted that smooth steady flight is required throughout the speed range including maximum usable speed in rearward flight.

Control effectiveness in unaccelerated flight.- The desirability of having a margin in control effectiveness at each end of the speed range to cope with effects of longitudinal disturbances is well founded. The data in figure 1 illustrate this requirement. The question of how much margin is needed for V/STOL aircraft over the speed range has yet to be determined with the desired accuracy. As a start, a margin of at least 10 percent of the maximum attainable pitching acceleration in hovering has been suggested for VTOL operation.

Dynamic longitudinal stability (short period).- For airplanes, the short period and the phugoid modes have widely different periods and have not been coupled. At the low speeds of STOL operation, however, similar periods may exist for the two modes and the combined effect on the overall behavior of the aircraft must be considered. Considerable flight and simulator experience has made possible the establishment of more specific requirements for the dynamic behavior of aircraft. In figure 2 is shown a boundary of the short-period characteristics in terms of natural frequency and damping ratio. These data, which were obtained in the cruise flight configuration, can be used to define the limits in frequency and damping applicable to V/STOL aircraft maneuvering at the higher end of the speed range. Sufficient data are not available to define a boundary for landing approach. There are indications, however, from data obtained in landing approaches for a number of aircraft and from helicopter experience, that lower frequencies and less damping may be acceptable for the landing-approach configuration.

Control effectiveness in hovering.- The ability to position VTOL aircraft accurately and rapidly over a given spot is a primary consideration used to define control power. To insure that adequate longitudinal control power is available for VTOL aircraft for maneuvering during hovering, values for control power derived from Langley

tests of a variable-response helicopter have been used. The reasoning behind these requirements with particular reference to the effect of aircraft size is discussed in a subsequent paper by Robert J. Tapscott.

Acceleration-Deceleration Characteristics in Transition

The ability to accelerate and decelerate quickly in a safe and efficient manner at constant altitude or along a constant flight path is one of the important items affecting the utility of the VTOL vehicle. Although the vehicle must be able to accelerate rapidly, a limit on thrust rotation may be necessary to prevent wing stall on some configurations. On the other hand, deceleration should not be limited because of the necessity of maintaining high percent engine power to supply power for trim and maneuvering. In addition, it should be possible to decelerate rapidly without stalling or objectionable buffeting and it should be possible to prevent settling when slowing down to hover.

Control Effectiveness in Take-Off

For control effectiveness in take-off, experience in VTOL operation has shown that it is necessary for the longitudinal control, which may depend on the main engine, to be powerful enough to adjust the attitude of the airplane so that the thrust vector is directed as necessary to prevent fore or aft translation during run-up to maximum power.

Control Effectiveness in Landing

For control effectiveness in landing, the longitudinal control should be powerful enough to land the airplane under a variety of approach conditions. For example, in steep descents for which it may be necessary to reduce engine power significantly, the type of longitudinal control that derives its power, in part, from the main engine must be powerful enough at reduced engine thrust to obtain maximum lift or guaranteed landing speed in ground proximity.

Lateral-Directional Stability and Control Characteristics

Directional control power.- Directional control power in hovering should, from the flight safety standpoint, be less critical than roll control since directional rotation at touchdown is not as serious as side velocity. In spite of this, the directional control power desired from both moving-base simulator tests and variable-response helicopter tests was large in comparison with that required for either

pitch or roll. In this case the large amount of directional control power desired was felt to be due in part to the large magnitude of the heading changes desired by the pilot. In contrast to the small attitude changes of approximately 10° used in pitch or roll, heading changes of the order of 180° are frequently made in hovering maneuvers.

Lateral control power.- It is recognized that both control power and damping are important for satisfactory lateral characteristics. It is to be noted that, because of unsatisfactory lateral control, a number of VTOL test-bed aircraft have been damaged. The significance of the relationship of lateral control power to damping was shown initially for aircraft in NASA research in 1959. A summary of these results is plotted in figure 3 in terms of the initial rolling acceleration for full lateral control input and the damping expressed in seconds. A lower boundary for V/STOL aircraft in low-speed flight and hovering is included, also. These results, which include both flight and simulator tests, showed that pilot opinion deteriorated at low values of roll control power and at low values of damping. At high values of roll power there was a loss of control precision due to sensitivity.

As would be expected, the data showed that greater control power was demanded for maneuvers in cruising flight compared with that required for hovering or low-speed flight. In addition, the results indicated that, to avoid the feeling of stiff or sluggish aircraft, more control power was required as damping was increased. With regard to damping, simulator results indicated that values of the order of 4 seconds were considered satisfactory for hovering. Although a number of V/STOL aircraft are being flown with essentially zero damping, most of the flights have been conducted under still-air conditions by skilled test pilots. It is felt that for practical VTOL operation, a value not greater than 0.7 second for roll rate damping is necessary.

Stalling Characteristics

The stall requirements for airplanes which allow bank angles of 20° at the stall have been revised to be more stringent in the landing approach and landing. In this region, it is felt necessary to limit the maximum allowable uncontrolled rolling at the stall to the roll angle at which a wing tip, pod, or propeller may strike the ground when the aircraft is resting on the landing gear. Figure 4 illustrates these criteria. This philosophy, which extends from a variety of flight experience in landing approach, is intended to place a more practical limit on the allowable roll-off at the stall.

CONCLUDING REMARKS

A brief look at the reasoning behind a few of the V/STOL handling qualities criteria contained in NASA Technical Note D-331 has been presented. The need for meeting these requirements should be emphasized. It is noteworthy that the VTOL test-bed aircraft have been able to meet only a few of the criteria and, as a result, have been restricted to still-air flying. Many of the criteria require refinements which can be obtained only from operational experience with V/STOL aircraft. It is recognized that the criteria presented herein will be modified and added to as more information becomes available; however, it is felt that at the present time they can serve a useful function as a guide in writing specifications for an operational VTOL assault transport.

LONGITUDINAL CONTROL EFFECTIVENESS MARGIN

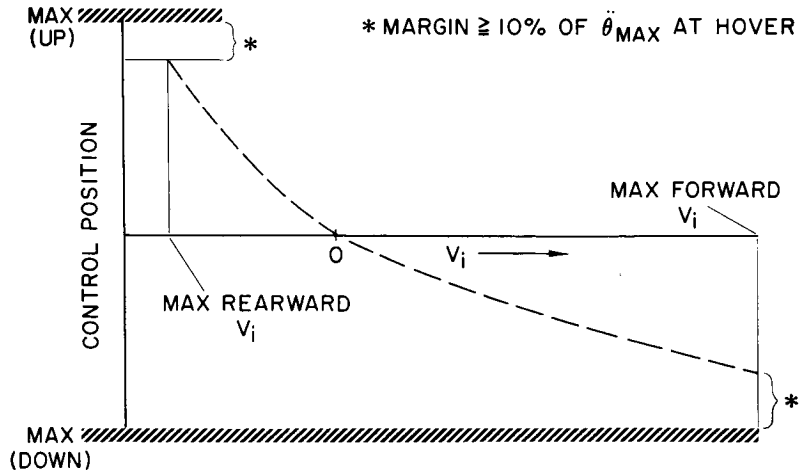


Figure 1

SHORT-PERIOD LONGITUDINAL CHARACTERISTICS

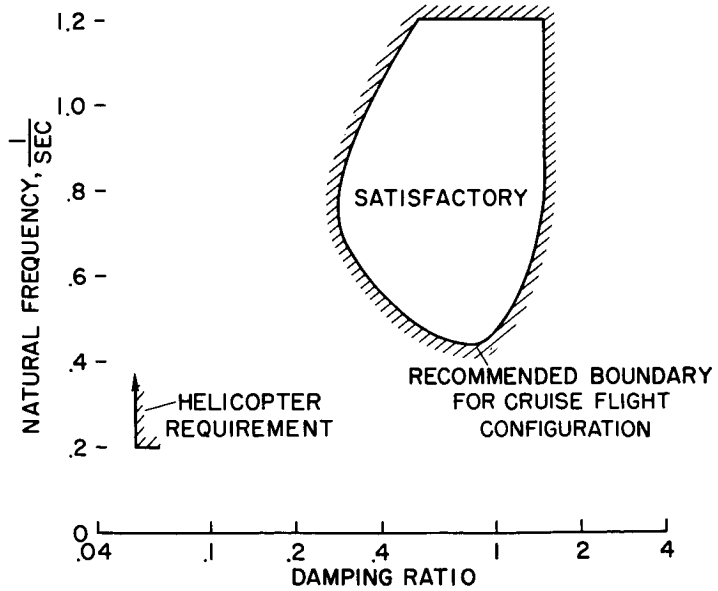


Figure 2

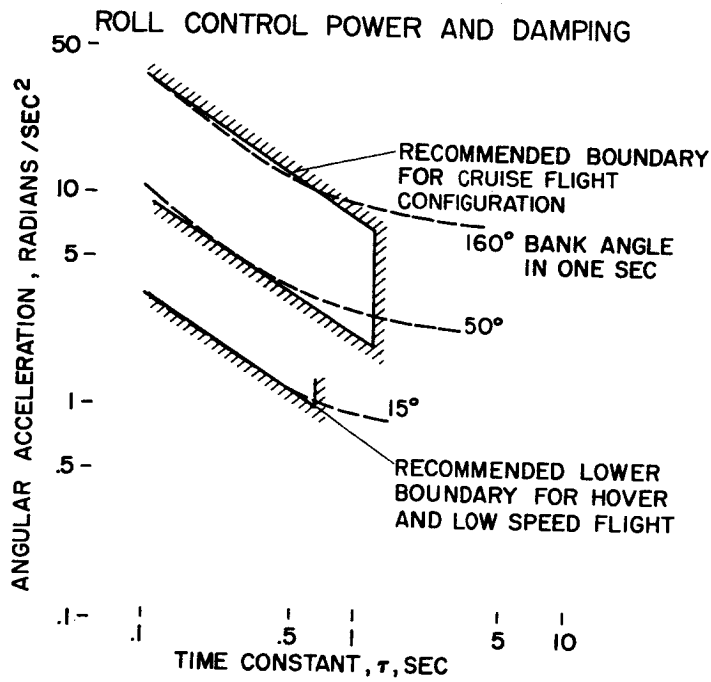


Figure 3

STALL CRITERIA

ALLOWABLE ROLL-OFF AT STALL LIMITED TO ROLL ANGLE AT WHICH A WING TIP, POD, OR PROPELLER MIGHT STRIKE THE GROUND

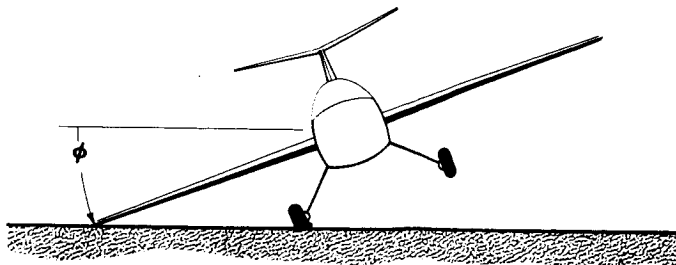


Figure 4

CRITERIA FOR PRIMARY HANDLING QUALITIES CHARACTERISTICS
OF VTOL AIRCRAFT IN HOVERING AND LOW-SPEED FLIGHT

By Robert J. Tapscott

Langley Research Center

INTRODUCTION

In establishing criteria for hovering and low-speed characteristics for the newer types of VTOL aircraft, one approach has been to draw upon helicopter criteria in this region. In certain cases, this approach would require some extension of the ranges of operating and design conditions for which the helicopter criteria were established. In other cases, the newer VTOL configurations have characteristics which are already within the ranges for which the earlier criteria have been established in helicopter studies. It is believed that this discussion will, to some extent, indicate the applicability of these criteria to the newer VTOL configurations. In addition, the experience obtained with the present generation of VTOL research aircraft will be drawn upon and criteria for several fundamental characteristics will be suggested.

SYMBOLS

t a given time

I, I_X, I_Y, I_Z moments of inertia

W weight of airplane

A, B constants representing coefficients of control power and damping expressions, respectively (table I)

AIRCRAFT CHARACTERISTICS DURING HOVERING AND LOW-SPEED FLIGHT

Initial Response to Controls

Probably the most significant of recent handling qualities criteria for low-speed and hovering flight relate to initial response to control

characteristics. Figure 1 illustrates such a response and the particular characteristics which are important. The control input is shown, for illustrative purposes, as a step input; the lower curve illustrates a typical buildup of the angular velocity of the aircraft in response to the control input. The first parameter of importance is characterized by the initial slope of the angular velocity curve. The second parameter is characterized by the time taken for the angular velocity to reach a given percentage of the resulting steady-state value. The response characteristics are determined, respectively, by the control power, or moment per unit control deflection tending to produce angular acceleration, and the angular-velocity damping, or moment proportional to and opposing the angular velocity, as illustrated by the diagrams at the top of figure 1.

In order to establish a criterion for these parameters, use has been made of pilots' comments and flight measurements for a range of aircraft sizes; however, the main basis has been the studies with the variable-response helicopter, in which these parameters could be adjusted over a range for trial in flight. Both statistical analysis of flight records and pilots' comments were used to get boundaries of the type shown in figure 2. Boundaries such as these, showing the degree of acceptability of various combinations of control power and damping, were determined for each aircraft control axis. The rather extensive data from which these boundaries were determined are published in reference 1 and will not be repeated herein. Most of this experience has been with lower than acceptable values, with at least one aircraft experiencing higher than acceptable values of roll control power.

These boundary-plot results were combined with other data for gross weights from 1,000 to 10,000 pounds and with more limited data and experience at a gross weight of 30,000 pounds. From this information a criterion for each axis was derived as a function of size; these criteria are shown in equation form in table I. These formulas give values of control power in terms of the number of degrees of angular displacement of the aircraft in a given time following a control input and angular-velocity damping in terms of $\frac{\text{ft-lb of moment}}{\text{radians/sec}}$. Each formula

has two constants, one to represent minimum characteristics for visual flight and another of higher value to represent the more stringent needs of instrument flight.

To satisfy control needs for the precision maneuvers or tasks, the total control - that is, inches of travel with the per inch values of control power specified for the respective axes by the formulas - should be at least ± 4 inches longitudinally, ± 3 inches laterally, and ± 3 inches for the pedals. It should be noted that these amounts of

total travel are the minimum necessary to satisfy precision maneuvering needs and any requirements for more gross maneuvering or for use of the primary controls for trim purposes during steady flight should be added to these values.

Variation of Response Parameters With Aircraft Size

With respect to the variation in response with size, permitted by the formulas given in table I, figure 3 shows, in general form, the variation of control power and damping, when the formulas are applied to a family of aircraft over a range of gross weights. The reduction, shown in figure 3, for control power and damping parameter as aircraft size increases is in keeping with previous airplane criteria. It has been suggested that constant angular acceleration be required over the size range to provide sufficient maneuverability of the larger aircraft; in this respect it should be noted that the reduction indicated for these parameters represents essentially constant angular-velocity capabilities over the entire size range.

In order to provide a somewhat more direct insight into what the reduction represents, the case of yaw has been considered where an angular acceleration produces a side force at points on the aircraft other than at the center of gravity. Figure 4 illustrates the variation with size of the side force at a given location - in this case, the front of the fuselage where the pilot is generally located. The solid curve shows that when the yaw criterion is applied, the side force due to yaw, for typical full pedal movement of 3 inches, would be essentially constant at about $\frac{1}{4}$ g regardless of the size of the aircraft. For comparison, the dashed curve shows that, when the higher values of control power, such as have been found desirable for aircraft at a gross weight of 5,000 pounds, are maintained as the aircraft size goes up, a side force on the order of 1g would result for full pedal deflections for even moderately larger sizes. From this it would appear that providing constant angular acceleration over the entire size range might result in characteristics that might be undesirable as well as very expensive, designwise, to get.

The exact form of the criteria formulas, however, needs more substantiation, particularly at the larger sizes.

Transition Characteristics

There are a few parameters for control during transition which appear likely to need specific attention in order to fill in the gaps in the previous criteria and to insure acceptable characteristics in this flight range. Table II presents three of these items.

Trim changes.- The first factor for trim changes has to do with the margin of control remaining between the amount used for trim and the amount available, to allow for disturbances and for maneuvering the aircraft with some decisiveness. In this respect it is recommended that a margin of at least 20 percent of the available control be demonstrated during transitions with a rate of acceleration or deceleration of $\frac{1}{4}$ g - that is, a rate of change of forward speed of at least $\frac{1}{4}$ g.

The second factor relates to the rate at which any permissible trim changes occur. If changes in trim occur so abruptly that the pilot cannot react fast enough to keep the aircraft from being out of trim over a short period of time, then even relatively small trim changes can become sources of considerable disturbance to the aircraft. Since the problem in this respect is one of reaction time or, in the case of instrument flying, of scanning plus reaction time, a proposed criterion would appear best related to the shortest period of time over which the required change in control position would have to be made. Thus the recommendation is that during the transition, again with at least a rate of change of forward speed of $\frac{1}{4}$ g, rates of stick movement to maintain trim be no greater than 1 inch per second. Expressed another way, this represents about a 1-inch change in trim stick position for any 5-knot change in airspeed during the conversion or transition with a rate of change of $\frac{1}{4}$ g.

Speed stability.- It appears desirable to place a limit on the maximum amount of speed stability. In the hovering and low speed range, the speed stability has direct bearing on the magnitude of the aircraft disturbance caused by horizontal gusts; it affects the oscillatory period and to some extent determines the usable speed range for fixed configuration of the lifting elements. In terms of the potential disturbance caused by inadvertent speed changes, it would appear desirable for a 10-knot gust, for example, to cause no greater disturbance than would a 1-inch control input. The tentative criterion, then, is to limit the maximum speed stability to that which would be represented by a slope of $\frac{1}{10}$ inch per knot on the curve of control position plotted against speed. Some experience with a VTOL aircraft with about this amount of speed stability at very low speeds has shown this to be about the limit for acceptable handling qualities.

Limitation on number of pilot-operated controls.- The next characteristic, that of the total number of pilot-operated controls, while not the most fundamental, appears to warrant some restrictions to avoid saturation of the pilot. In this respect five controls seem to be about the maximum tolerable. Counting the lateral, longitudinal, and directional controls and adding the power control, there are four controls for most VTOL aircraft. The addition of the control for the lifting-element angle or configuration change brings the total up to the limit

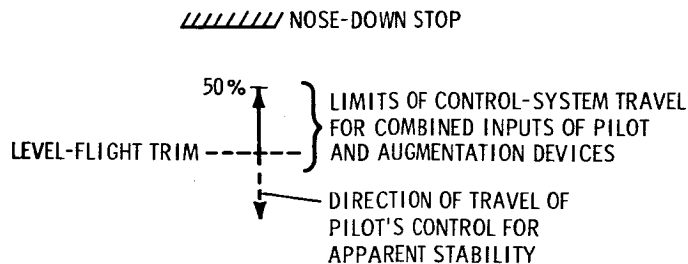
of five. It is of importance here to note that these five controls should be arranged in a manner such that the pilot is not required to release any control to manipulate another.

CRITERIA FOR USE OF STABILITY AUGMENTATION DEVICES

The characteristics which are judged necessary to insure adequate handling qualities have been discussed without regard to the mechanism by which these characteristics are obtained. In many cases the characteristics of VTOL aircraft, as well as of helicopters, invite the use of devices to provide some measure of the flying qualities parameters which are desired. As the reliability of available electronic components improves, such a procedure may become even more attractive. The basic problem exists, even for perfectly reliable devices, of insuring adequate control moment capability for the pilot and the devices. In particular, for those cases where automatic inputs into the primary control mechanisms must overcome unstable moments as well as generate the moments needed to provide the desired stability, some limitations must be observed to avoid catastrophic conditions. Table III shows the form of the criteria for the two most likely sources of difficulty when augmentation systems are used. The first is the situation where the basic airframe has static instabilities which must be overcome, and, second, the case where unstable damping moments must be overcome.

Static Instabilities

In order to insure some margin of control-system travel during maneuvering flight, it is recommended that, during specific test maneuvers, each of which would be selected to bring out the static characteristics, the combined inputs of the pilot and augmentation systems should utilize no more than 50 percent of the control moment remaining between the level flight trim position and the stops. The following sketch illustrates both the potential problem and the criterion by showing the control-system travel involved:



Consider the longitudinal axis where angle-of-attack instability would be the problem. The movement of the longitudinal control during a steady level turn is in the aft direction for apparent angle-of-attack stability. For the case where the apparent stability is provided by augmentation through the primary controls, the control system, after initially moving in the aft direction to initiate the maneuver, would move back past the trim position. The criterion, then, is that no more than 50 percent of the available travel should be used to provide the desired apparent stability and thus, in effect, limits the magnitude of the unstable moments of the airframe in relation to the available control moments. For the helicopter, a level-flight turn to design load factor at cruise speed is the designated critical maneuver for the longitudinal axis. For other VTOL configurations, flight conditions within the low-speed and transition region are likely to be more critical with respect to relative magnitudes of the available control moments and unstable airframe moments.

The criterion for control-system travel applies also to the roll and yaw axes with maneuvers involving sideslip to demonstrate the amount of control-system motion required to provide the apparent directional stability and the desired degree of dihedral effect or roll moment due to sideslip.

Unstable Damping

For the case where an augmentation system using the primary control mechanism must overcome unstable damping moments as well as provide the desired amount of stable damping moments, a similar control problem could result; a 50-percent rule similar to that discussed for the unstable static moments can be applied also by limiting the absolute value of any unstable damping moments of the airframe to 50 percent of the absolute value of the resulting stable moment.

CONCLUDING REMARKS

Although there are many gaps in the criteria presented, some of the major points with respect to characteristics at low speeds and the potential problem areas have been discussed. Criteria have been shown for the initial response characteristics, for some fundamental control characteristics in transitions, and for the use of devices to provide these characteristics. Although a lot remains to be done in this respect, it is believed that adherence to these minimum criteria will result in a good start toward obtaining vehicles with reasonable flying qualities.

REFERENCE

1. Salmirs, Seymour, and Tapscott, Robert J.: The Effects of Various Combinations of Damping and Control Power on Helicopter Handling Qualities During Both Instrument and Visual Flight. NASA TN D-58, 1959.

TABLE I
 CRITERIA FOR MINIMUM ACCEPTABLE CONTROL POWER
 AND ANGULAR-VELOCITY DAMPING

AXIS	ANGULAR-VELOCITY DAMPING, $\frac{\text{FT-LB}}{\text{RADIANT/SEC}}$	ANGULAR DISPLACEMENT IN GIVEN TIME FOR 1-INCH CONTROL DISPLACEMENT, DEG
VISUAL		
PITCH	$8(I_Y)^{0.7}$	$45/\sqrt[3]{W+1000}$ (1 SEC)
ROLL	$12(I_X)^{0.7}$	$27/\sqrt[3]{W+1000}$ ($\frac{1}{2}$ SEC)
YAW	$27(I_Z)^{0.7}$	$110/\sqrt[3]{W+1000}$ (1 SEC)
INSTRUMENT		
PITCH	$15(I_Y)^{0.7}$	$73/\sqrt[3]{W+1000}$ (1SEC)
ROLL	$25(I_X)^{0.7}$	$32/\sqrt[3]{W+1000}$ ($\frac{1}{2}$ SEC)
YAW	$27(I_Z)^{0.7}$	$110/\sqrt[3]{W+1000}$ (1SEC)

TABLE II
 CONTROL CHARACTERISTICS IN TRANSITION

CHARACTERISTIC	RECOMMENDED CRITERIA
TRIM CHANGES A. MARGIN B. RATE	AT LEAST 20% OF AVAILABLE CONTROL MOMENT SHOULD REMAIN AT A $\frac{1}{4}g$ RATE OF ACCELERATION OR DECELERATION TRIM CHANGE SHOULD NOT REQUIRE CONTROL MOVEMENTS AT A RATE GREATER THAN 1 INCH PER SECOND AT $\frac{1}{4}g$ RATE OF ACCELERATION OR DECELERATION
SPEED STABILITY	AT ALL TRIM CONDITIONS, SHOULD BE LIMITED TO A MAXIMUM STICK DEFLECTION OF 0.10 IN. /KNOT
NUMBER OF PILOT-OPERATED CONTROLS	SHOULD NOT EXCEED FIVE

TABLE III
CRITERIA FOR USE OF STABILITY AUGMENTATION DEVICES

AUGMENTATION USE	LIMITATION
TO OVERCOME AIRFRAME STATIC INSTABILITY	REQUIRES USE OF LESS THAN 50% AVAILABLE CONTROL-SYSTEM TRAVEL DURING SPECIFIED MANEUVERS
TO OVERCOME UNSTABLE DAMPING	AMOUNT OF UNSTABLE DAMPING MOMENT OF BASIC AIRFRAME SHOULD BE LESS THAN 50 % OF THE RESULTING STABLE DAMPING MOMENT

INITIAL RESPONSE PARAMETERS

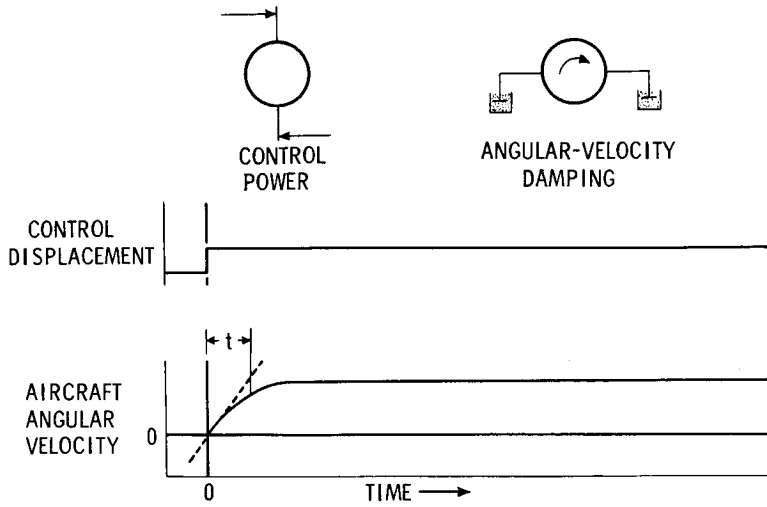


Figure 1

FORM OF BOUNDARIES

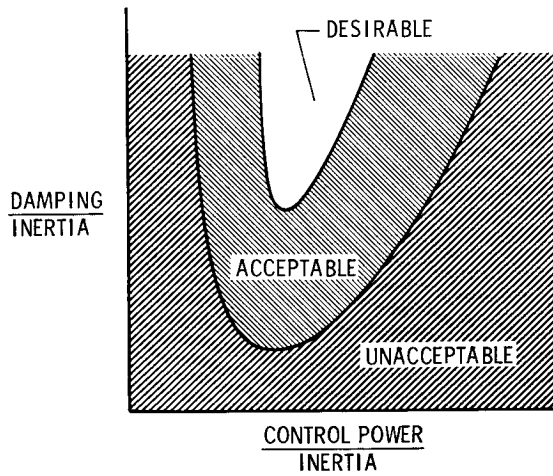


Figure 2

VARIATION OF RESPONSE PARAMETERS WITH AIRCRAFT SIZE

ANGULAR DISPLACEMENT, $A/\sqrt[3]{W+1000}$
 DAMPING/INERTIA, $B(I)^{-0.3}$

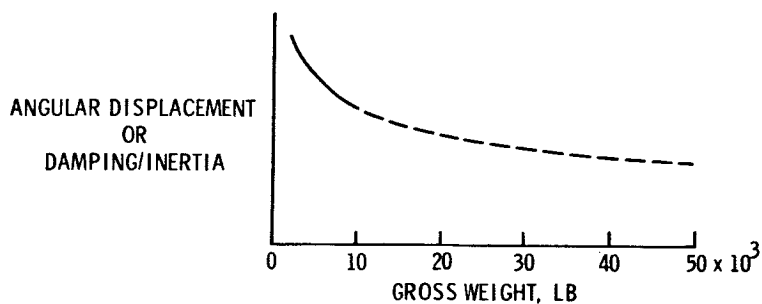


Figure 3

VARIATION OF SIDE FORCE DUE TO YAWING ACCELERATION WITH SIZE

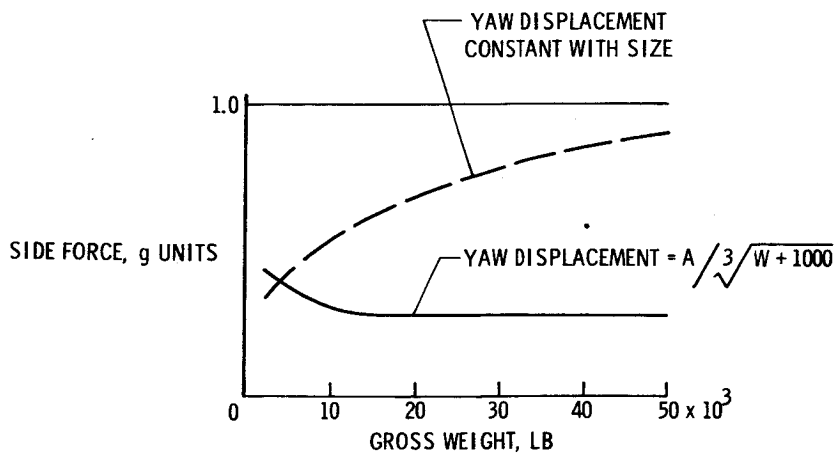


Figure 4

ATTITUDE CONTROL REQUIREMENTS FOR HOVERING DETERMINED
THROUGH THE USE OF A PILOTED SIMULATOR

By Alan E. Faye, Jr.

Ames Research Center

INTRODUCTION

The success of the VTOL airplane relies on the design of a safe and efficient vehicle with desirable handling qualities.

References 1 and 2 discuss VTOL handling qualities criteria with regard to providing desirable control characteristics in the hovering phase of VTOL flight. The purpose of this paper is to present the results of a simulator study conducted at the Ames Research Center for determining attitude control requirements for hovering, and to show that requirements obtained from simulator studies may be applied as criteria for flight.

Three NASA research pilots, with experience in hovering VTOL aircraft, participated in the simulator tests.

The results will be discussed in terms of control power and damping requirements for attitude control about all three axes: pitch, roll, and yaw. These requirements do not include the control necessary for trim while hovering, but represent the control required for maneuvering. Vertical translation or "height control" was not investigated.

Control requirements were first obtained about each axis separately, while the other two axes were held fixed. This allowed the pilot to devote his full attention to one control at a time. Next, the effect of controlling two axes simultaneously was determined by allowing freedom of motion about combinations of two axes, for example, the pitch and yaw axes. The reason for studying the controllability of two axes simultaneously is to show that the control requirements become more restrictive when multiple axes must be controlled, more nearly duplicating the actual hovering condition where simultaneous control of all axes is required.

Gyroscopic coupling was introduced that would result from mounting engines longitudinally, producing a couple between the pitch and yaw freedom of motion.

EQUIPMENT

The equipment used for the tests was the Ames two-degree-of-freedom motion simulator shown in figure 1. In this configuration, the cockpit was made to rotate about the pitch and yaw axes. Various arrangements of the cockpit drive system produced angular motions about any two axes simultaneously. A more detailed description of the drive system and performance of the simulator is given in reference 3. An instrument display of airplane attitude supplemented the visible outside world in the form of a gyro-horizon for pitch and roll attitude and a radio compass indicator for heading information. Analog computer equipment computed the proper airplane dynamic responses to drive the simulator and actuate the instrument presentation. The controls used in the cockpit had linear characteristics in that the variations of control power and control force with deflection were both linear. Additional mechanical characteristics of the control system are presented in table I.

TESTS

For a generalized "first look" at the attitude control requirements for hovering, the test conditions and scope were simplified, and are shown in table II. Although disturbances from gust and ground effects were not included as quantitative inputs to the simulator, since they constitute disturbances to the airplane which vary with different airplane configurations and VTOL concepts, the pilots included these effects qualitatively in making their evaluations. Visual flight conditions were assumed throughout the evaluation. Artificial attitude stabilization was not considered.

An effective means for evaluating hovering controllability was to require the pilot to make changes of attitude as rapidly as possible, without sacrificing ability to stabilize quickly on a desired attitude. Rapid changes in attitude are often required to maneuver over or around a point while hovering. In this study the attitude changes amounted to maximums of about 15° in pitch or roll and 30° in yaw. A 15° change of attitude in pitch or roll is equivalent to a change of forward or side acceleration of about $\frac{1}{4}g$. These are felt to be realistic accelerations for use in hovering maneuvers. The magnitude of the heading changes was indicated by Ames pilots to be representative for hovering and low-speed flight.

When controlling two axes simultaneously, attitude changes were made about one axis at a time, while attempting to maintain the other axis fixed.

RESULTS AND DISCUSSION

Single Axis

The results of the single-axis evaluation are presented first for the pitch degree of freedom in figure 2. The maximum control power is the pitching acceleration obtained with maximum control deflection. The area of negative damping corresponds to divergent airplane responses to control inputs.

In order to map the control boundaries shown, the Cooper Pilot Opinion Rating System was used, which is described in table III. (See ref. 4 for more complete description.) It is composed of rating numbers from 1 to 10 where a rating of 1 represents ideal characteristics and a rating of 10, catastrophic characteristics. A numerical rating of $3\frac{1}{2}$ represents the boundary between satisfactory and unsatisfactory regions and a rating of $6\frac{1}{2}$, the boundary separating the unsatisfactory and unacceptable regions. (See table III.) A reasonable interpretation of these boundaries is that the control system of a VTOL airplane must be designed so as to fall within this satisfactory area regardless of the amount of artificial augmentation devices necessary. However, failure of the augmentation devices must not result in a control system that falls outside of the unsatisfactory, into the unacceptable, region.

The line of optimum ratio, shown passing through the middle of the satisfactory area in figure 2, separates two regions for which there were different reasons for downgrading of pilot ratings. The test values to the right of the optimum ratio resulted in excessive control sensitivities, which caused overcontrolling of the airplane. The test values to the left of the optimum ratio represented insufficient control power, inasmuch as the responses were felt sluggish. Therefore, the optimum ratio indicates the best amount of control power for a given level of damping, and vice versa.

The roll and yaw control boundaries are shown in figures 3 and 4 with damping and control power coordinates similar to the previous figure. Again, note the regions that are satisfactory, unsatisfactory, and unacceptable. As in the evaluation of pitch controllability, pilot comments defined the existence of the line of optimum ratio for roll and yaw, shown passing through the satisfactory regions.

A plot of the pitch, roll, and yaw boundaries that are between the satisfactory and unsatisfactory regions (numerical rating of $3\frac{1}{2}$) is presented in figure 5 in order to compare the relative magnitudes and shapes of the boundaries for the three axes. Notice the similarity between the boundaries for the roll and yaw axes. Both of these boundaries enclose roughly the same satisfactory region, and neither boundary extends down into the negative-damping area. The pitch axis, on the other hand, differs from both roll and yaw in that the magnitudes of control power and damping values enclosed by the pitch boundaries are roughly one-half those of roll and yaw, and the satisfactory region surprisingly tolerates some negative damping.

Some speculation may be offered for these differences in magnitude. The pilots appeared to be more sensitive to pitching accelerations than roll or yaw accelerations. For example, they rarely used control angular accelerations greater than 1 radian/sec² in pitch, whereas roll and yaw accelerations of 3 and 5 radians/sec², respectively, were used frequently, when desirable control characteristics existed.

Combined Two Axes

The results of controlling two axes simultaneously will be discussed for the roll-yaw and pitch-yaw degrees of freedom. Time did not permit study of the pitch-roll combination nor the complete remapping of roll-yaw and pitch-yaw boundaries.

The controllability boundaries that result from the simultaneous control of the roll and yaw axes are presented in figure 6. The dashed lines represent the resulting shifts of the single-axis boundaries when the roll and yaw axes were combined. Only the small portion of the boundaries shown was mapped, and with the controls harmonized. The controls were felt to be harmonized when equivalent control power and damping values for each boundary were combined; for example, a point on the single-axis $3\frac{1}{2}$ roll boundary was combined with the equivalent point on the $3\frac{1}{2}$ yaw boundary, and so on, for other boundaries. For points taken along the line of optimum ratio, figure 7 shows the comparison of pilot rating for combined roll-yaw axes plotted against pilot rating for single-axis control. The 45° line of perfect agreement would result if there were no difference between single-axis and two-axis controllability ratings. For good control systems rated at about 2, the effect of combining axes is small in terms of pilot rating, but increases as the system is deteriorated to a rating of 6 or 7.

However, the resulting shift of boundaries is much larger for the $3\frac{1}{2}$ boundary than for the $6\frac{1}{2}$ boundary. This greater shift is caused by a steeper gradient of pilot rating near the $6\frac{1}{2}$ boundary than near the $3\frac{1}{2}$ boundary. This shifting or shrinking of single-axis boundaries is to be expected, since the additional task of controlling another axis divides the pilot's attention.

The importance of control harmonization became apparent when the control power and damping about one axis were held constant at a satisfactory single-axis value, while the control power and damping about the other axes were varied. For example, roll control power and damping values, located at a point on the single-axis $3\frac{1}{2}$ boundary, were held constant while allowing the yaw control system to deteriorate from a point on the $3\frac{1}{2}$ boundary to one on the $6\frac{1}{2}$ boundary. This caused the roll-control rating to deteriorate from a single-axis $3\frac{1}{2}$ to a combined-axes 6, or a change in rating of $2\frac{1}{2}$, compared with a change of about 1, for harmonized controls. If disharmonious control systems were to be evaluated, there would appear to be a sizable effect on the reshaping of these boundaries. The pitch-yaw combination of axes resulted in shifts of the single-axis boundaries similar to those shown in figure 7 for roll and yaw. These shifts moved the satisfactory boundary for pitch controllability to a point well above the zero-damping level, out of the area of negative damping.

Gyroscopic Coupling

Gyroscopic coupling effects will now be considered for coupling between the pitch and yaw axes. This coupling would result from engines or rotating masses whose spin centerlines are parallel to the longitudinal axis of the airplane. A representative ratio of moment of inertia in pitch to moment of inertia in yaw of $3/4$ was assumed, which is an average value for six different VTOL vehicles.

Shown in figure 8 are the pitch-axis and yaw-axis control boundaries with several lettered points along the line of optimum ratio and one point away from the line. These are some of the control power and damping values used in evaluating gyroscopics. Point (A) represents good control characteristics whereas points (B) and (C) represent

progressively poor control characteristics. Point (D) is included to illustrate the effects of moving away from the line of optimum ratio.

The effect of gyroscopic coupling on the pilot rating at each of the lettered points is presented in figure 9. The ordinate is the angular momentum of the rotating masses divided by the moment of inertia in pitch, with units of per second (the same as the units for damping). The abscissa is the pilot rating, which represents an "overall" rating since control inputs affect motion of the airplane about both axes. The levels of gyroscopics shown are for several existing VTOL airplanes and one hypothetical airplane, to represent realistic values.

First, a good control system - point (A) - is considered. The combined-axis rating with no gyroscopic coupling is a satisfactory rating of $2\frac{1}{2}$. The gyroscopic effects became unsatisfactory when a gyroscopic value of about 1 was reached, and unacceptable at about 5. For control systems (B) and (C), the controllability became unacceptable at somewhat lower gyroscopic values, as would be expected. It should be pointed out here that control systems (B) and (C) characterize a low value of damping and zero damping, respectively. The point away from the line of optimum ratio, shown as (D) in figure 8, appeared to tolerate higher levels of gyroscopic coupling than points (A), (B), and (C), as shown in figure 9. This is surprising, considering that point (D) represents a high sensitivity where one would expect the overcontrolling tendency to aggravate the gyroscopic effects.

A level of gyroscopic coupling is shown in figure 9 that may exist in a hypothetical, 35,000-pound, deflected-jet VTOL vehicle using existing jet engines. If this airplane were provided with control system (A), an artificial decoupling device must only reduce the gyroscopic couple from a value of 2 to a value of 1 to improve the system to satisfactory. However, if provided with control system (B), all the gyroscopic moments must be decoupled and further control improvements made before the system will become satisfactory. It appears, therefore, that for a given vehicle with a gyroscopic problem, there is a design compromise of the distribution of available reaction control force between providing good control power and damping, and decoupling the gyroscopic moment with an automatic decoupling device. Of course the most desirable solution to a gyroscopic problem is to eliminate it by designing a vehicle with counterrotating masses that will cancel the precessional gyroscopic moments.

Flight Simulator Comparison

A comparison is made in figure 10 between simulator and flight-determined pilot ratings for the roll degree of freedom. The results for a number of VTOL vehicles are plotted in this figure for comparison with the single-axis boundaries. The actual flight-determined pilot ratings for each vehicle are listed in figure 10 in tabular form. These flight ratings are compared in figure 11 with pilot ratings predicted from the single-axis boundaries, and with the previously shown roll-yaw combined-axis curve. Notice that the pilot ratings obtained in flight are higher in magnitude than those predicted from single-axis results by an amount very similar to the increases which resulted from combining two axes. Similar increases in pilot ratings were noted for the pitch and yaw degrees of freedom when comparing flight results with simulator results. These flight points substantiate the expected shifts of single-axis boundaries when more than one degree of freedom must be controlled. Some preliminary tests have been conducted on the Ames three-degree-of-freedom motion simulator, of simultaneous control of three axes (pitch, roll, and yaw). The resulting control requirements for three degrees of freedom were identical to those obtained for two degrees of freedom. This indicates that little or no change can be anticipated in the two-axis boundaries previously discussed when the additional third degree of angular freedom is added for the special case where controls are harmonized.

Several of the test VTOL vehicles have low values of roll control power making them almost unacceptable in roll. For the yaw degree of freedom, none of the test VTOL vehicles had sufficient control power and damping and all were unacceptable.

Ideal Design

Ideally, the VTOL airplane should be designed to fall well within the satisfactory region of the single-axis boundaries, preferably near the line of optimum ratio. Designing at or near the optimum ratio allows for variations of control power and damping that might result from changes in gross weight of a given airplane. For example, an airplane with a long-range mission could have an appreciable change in gross weight. Assuming that reaction control forces vary with the lifting forces of the airplane or gross weight, and that the moments of inertia vary with gross weight, there could be sufficient changes in maximum control power or damping to make the airplane unacceptable if it were designed right on or near the satisfactory boundary. Designing near the optimum ratio, well into the satisfactory area, also avoids the somewhat "fuzzy" boundary area which has been shown to be variable, depending upon disturbing influences such as combined

axes, control harmonization, and so on, not to mention the possible effects of nonlinear control characteristics.

CONCLUSION

It appears that a simulator study of attitude control requirements for hovering has established realistic boundaries for the control about each of the three axes, one at a time, under ideal conditions. Controlling attitude about two axes simultaneously with and without control harmonization, and with the addition of gyroscopic coupling, indicates shifts of the original single-axis boundaries to more restrictive values. Further modification of these boundaries may occur when control of all axes is presented the pilot, with gusts and nonlinearities included. The gyroscopic couple between the pitch and yaw freedom of motion resulted in a rapid deterioration of controllability with increasing amounts of gyroscopic couple, especially when the damping was reduced to low values. A comparison of simulator controllability results with flight indicates good correlation between two-degree-of-freedom simulator results and all-axes results obtained in VTOL airplanes.

REFERENCES

1. Anderson, Seth B.: An Examination of Handling Qualities Criteria for V/STOL Aircraft. NASA TN D-331, 1960.
2. Tapscott, Robert J.: Criteria for Control and Response Characteristics of Helicopters and VTOL Aircraft in Hovering and Low-Speed Flight. Paper No. 60-51, Inst. Aero. Sci., Jan. 1960.
3. Creer, Brent Y., Stewart, John D., Merrick, Robert B., and Drinkwater, Fred J. III: A Pilot Opinion Study of Lateral Control Requirements for Fighter-Type Aircraft. NASA MEMO 1-29-59A, 1959.
4. Cooper, George E.: Understanding and Interpreting Pilot Opinion. Aero. Eng. Rev., vol. 16, no. 3, Mar. 1957, pp. 47-51, 56.

TABLE I.- CONTROL SYSTEM CHARACTERISTICS

1. Linear control gain
2. Constant force gradients
 - (a) Pitch = 3 lb/in. of stick travel
 - (b) Roll = 2 lb/in. of stick travel
 - (c) Yaw = 10 lb/in. of pedal travel
3. Maximum control deflections
 - (a) Pitch = ± 6 inches of stick travel
 - (b) Roll = ± 5 inches of stick travel
 - (c) Yaw = ± 3 inches of pedal travel
4. Effects of nonlinearities neglected
 - (a) Deadbands
 - (b) Friction
 - (c) Hysteresis
 - (d) Time lag

TABLE II.- HOVERING SIMULATION

1. Test conditions
 - (a) Still air: No gust disturbances
 - (b) Out of ground effect: No self-generated disturbances
 - (c) Visual flight conditions
 - (d) No artificial attitude stabilization
2. Scope
 - (a) Single axis: One degree of freedom of motion
 - (b) Combined axes: Two degrees of freedom simultaneously
 - (c) Gyroscopic coupling between pitch and yaw motions

TABLE III.- COOPER PILOT OPINION RATING SYSTEM

Operating conditions	Adjective rating	Numerical rating	Description	Primary mission accomplished	Can be landed
Normal operation	Satisfactory	1	Excellent, includes optimum	Yes	Yes
		2	Good, pleasant to fly	Yes	Yes
		3	Satisfactory, but with some mildly unpleasant characteristics	Yes	Yes
Emergency operation	Unsatisfactory	4	Acceptable, but with unpleasant characteristics	Yes	Yes
		5	Unacceptable for normal operation	Doubtful	Yes
		6	Acceptable for emergency condition only ¹	Doubtful	Yes
No operation	Unacceptable	7	Unacceptable even for emergency condition ¹	No	Doubtful
		8	Unacceptable - dangerous	No	No
		9	Unacceptable - uncontrollable	No	No
	Catastrophic	10	Motions possibly violent enough to prevent pilot escape	No	No

¹Failure of a stability augments.

AMES TWO-DEGREE-OF-FREEDOM MOTION SIMULATOR

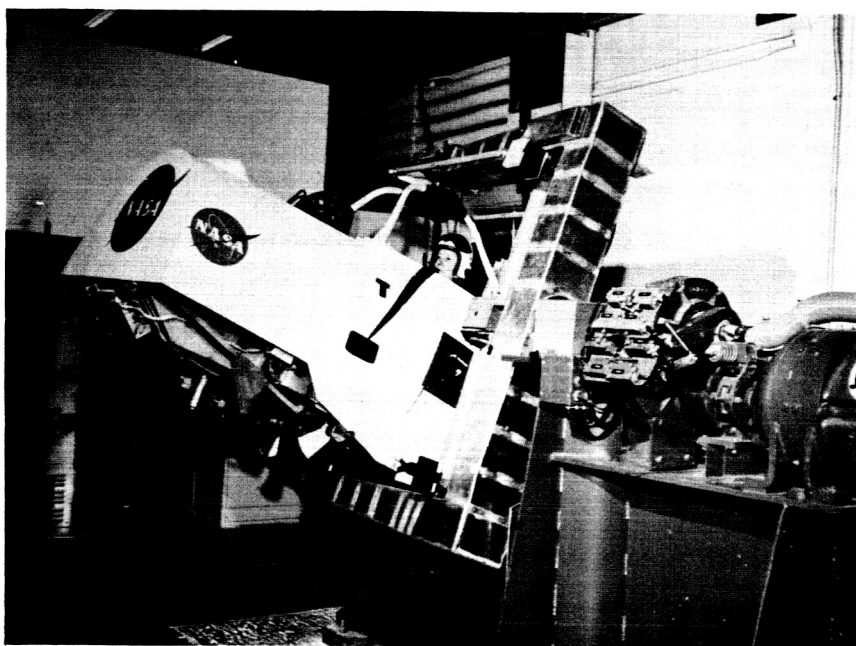


Figure 1

PITCH CONTROL BOUNDARIES (SINGLE AXIS)

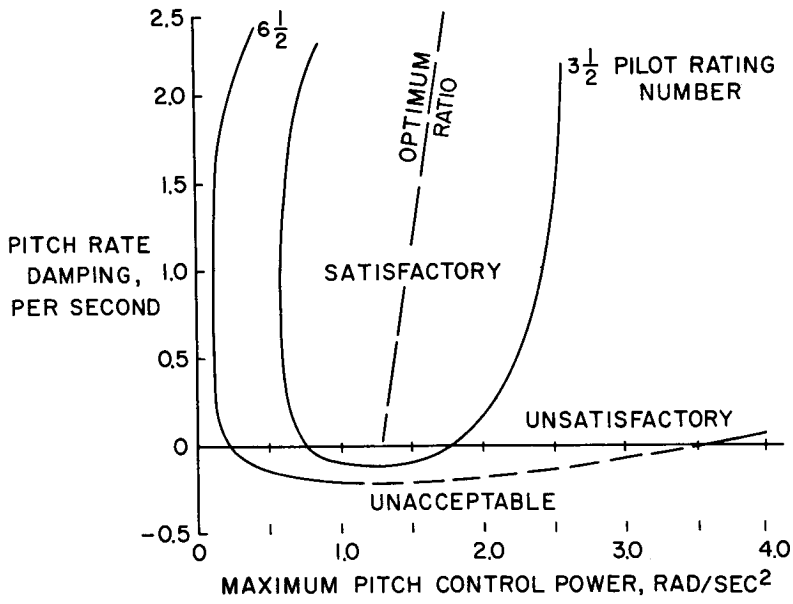


Figure 2

ROLL CONTROL BOUNDARIES (SINGLE AXIS)

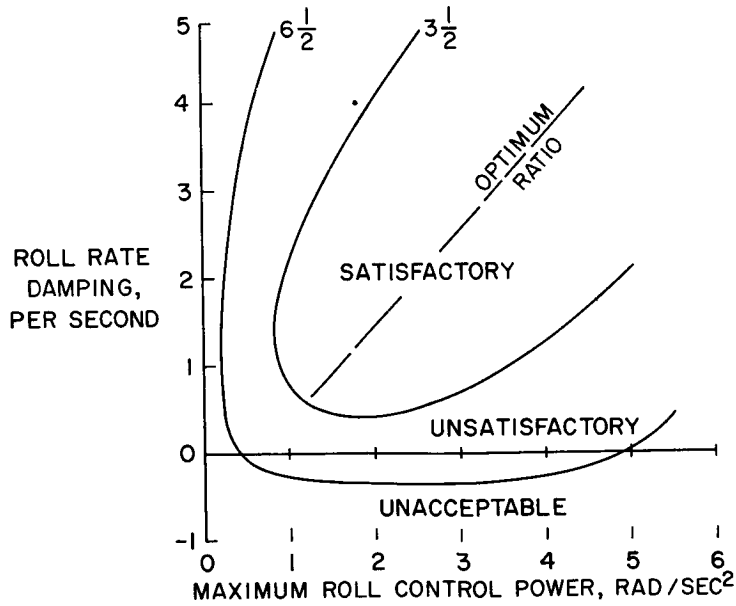


Figure 3

YAW CONTROL BOUNDARIES (SINGLE AXIS)

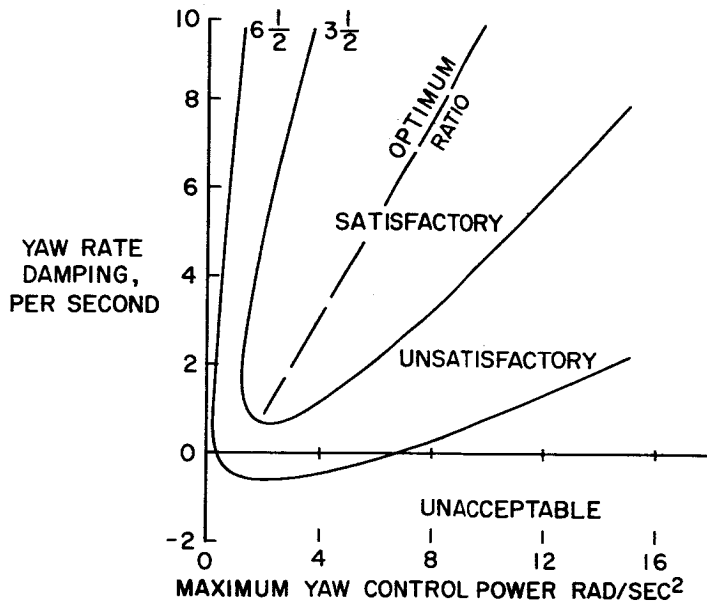


Figure 4

COMPARISON OF PITCH, ROLL AND YAW BOUNDARIES

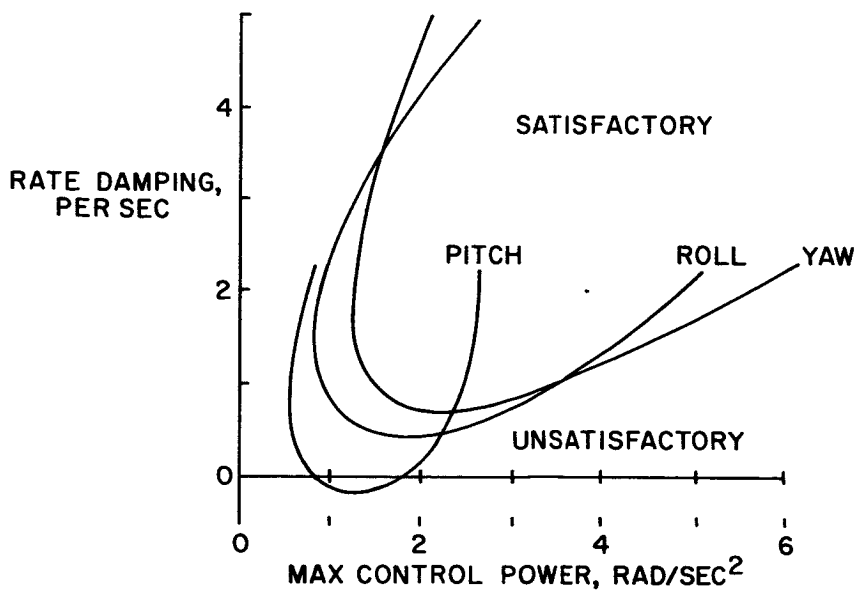


Figure 5

COMBINED ROLL-YAW BOUNDARIES

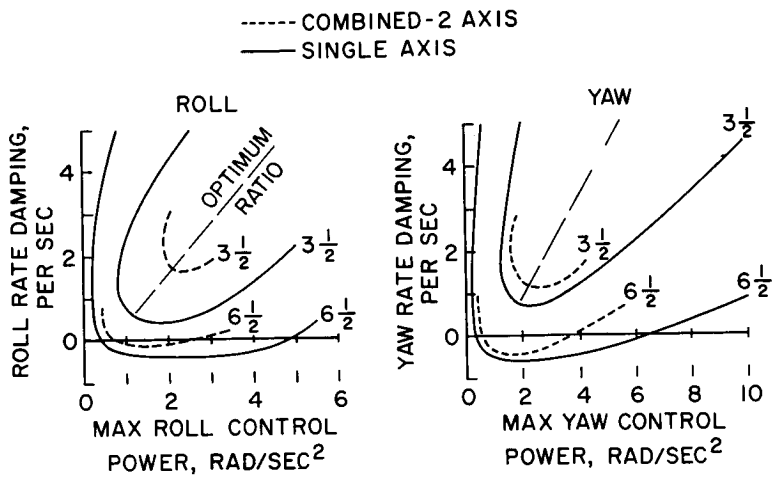


Figure 6

COMPARISON OF PILOT RATING OF CONTROLLABILITY
 FOR ONE AND TWO AXES
 OPTIMUM RATIO

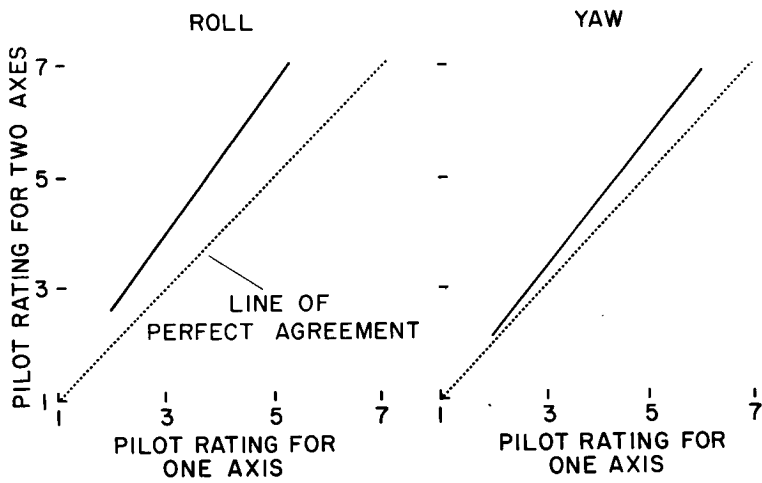


Figure 7

TEST CONDITIONS FOR GYROSCOPIC COUPLING
(SINGLE AXIS BOUNDARIES)

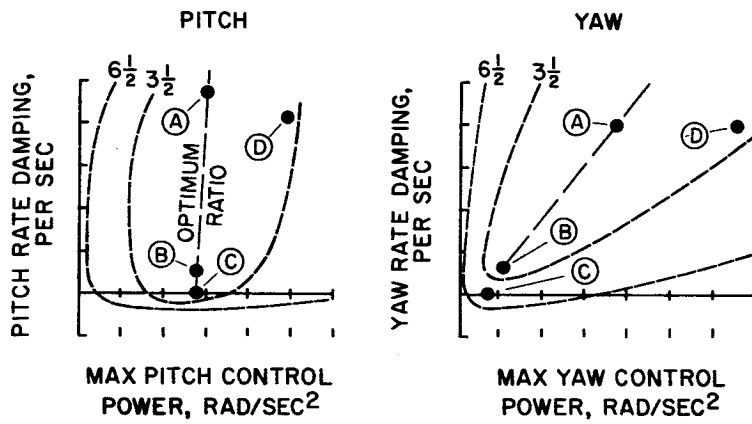


Figure 8

EFFECTS OF PITCH-YAW GYROSCOPIC COUPLING
ON PILOT RATING

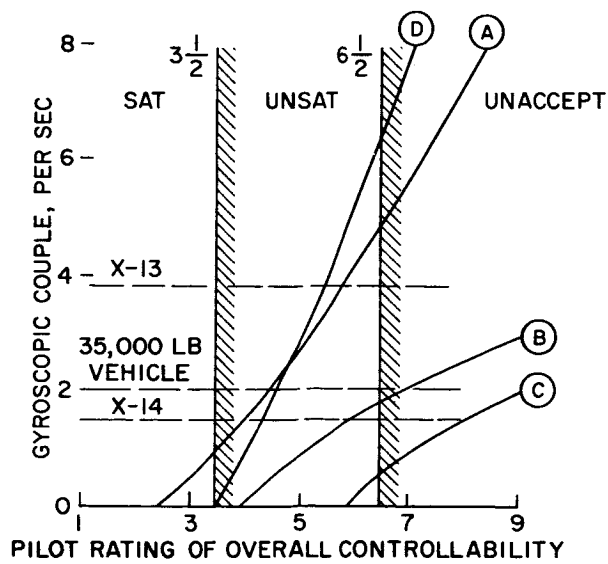


Figure 9

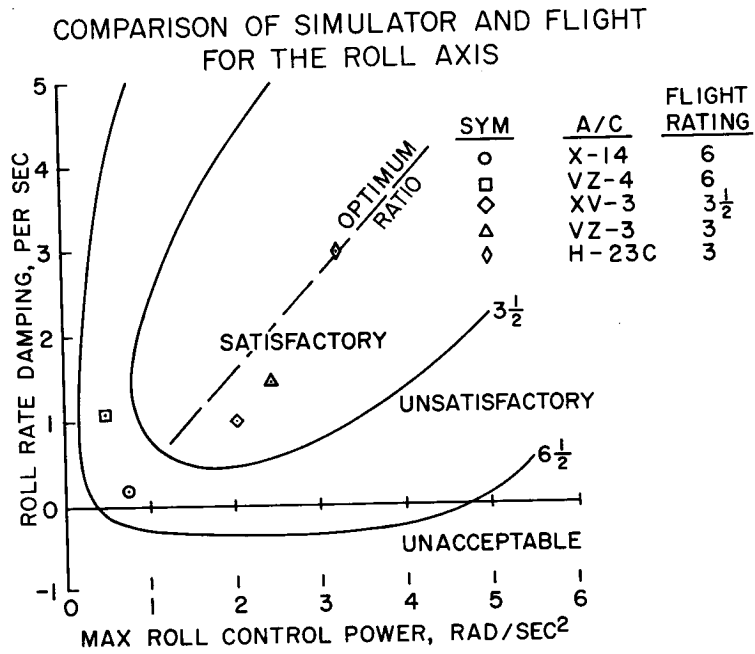


Figure 10

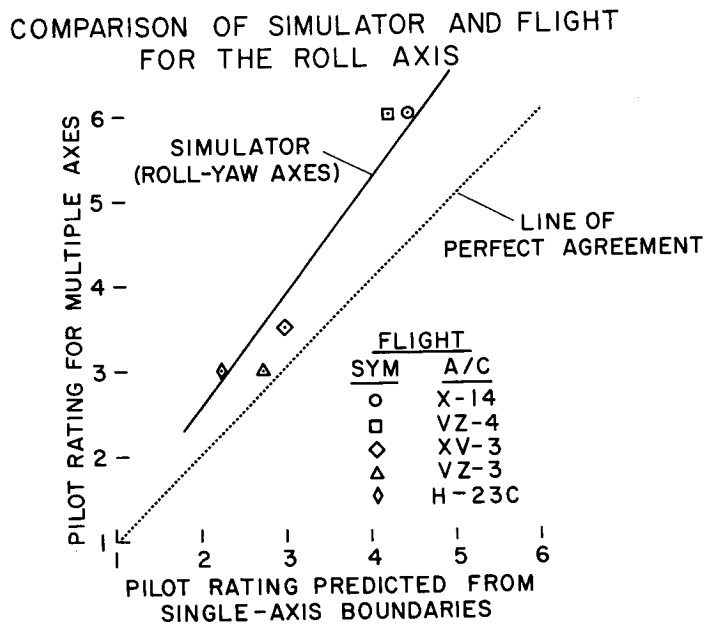


Figure 11

THE USE OF PILOTED SIMULATORS IN THE STUDY OF VTOL FLIGHT

By Donovan R. Heinle

Ames Research Center

INTRODUCTION

The value of flight simulators in the study of control problems associated with piloted vehicles is widely recognized and their use is becoming more widespread. Simulation devices are useful not only in the area of research but are also applied to design and development work. General experience with simulators other than training devices is still relatively limited and their capabilities are not as well defined as is desirable. Thus, it appears that a continual review of the state of the art is necessary in order to assure proper and efficient use of the available equipment. This paper will describe some of the simulation studies done at the Ames Research Center and delineate some of the philosophy that is considered important in the planning and executing of flight simulation work. The discussion is illustrated by simulations applicable to VTOL aircraft performed on the cockpit with two degrees of freedom of motion described in the previous paper by Alan E. Faye, Jr.

Since the results of simulation depend on the interpretation of pilot opinion, the factors to be discussed which affect the simulation and the pilot are

- (1) The experience of the personnel, particularly the pilot's ability to correlate and calibrate the simulation with recent flight experience
- (2) Mechanization in which is covered the field of cockpit size and shape, control placement, and instrument panel
- (3) Degrees of freedom represented by the mathematical equations used to define the motion of the airplane up to six degrees of freedom, which information is fed back to the pilot generally by visual means
- (4) Cockpit motion with reference to providing real motion cues to the pilot, usually in rotation about the axes of pitch, roll, and yaw

DISCUSSION

In order to examine the process by which a simulation program is developed, figure 1 presents a block diagram of the components and information flow of a fully developed piloted simulator. The heart of the system is the analog computer which, using vehicle aerodynamic and mass characteristics, computes the vehicle motion resulting from input disturbances. The vehicle motion can be examined at the output of the computer to study the effect of the inputs.

The complication in obtaining a simulator capable of truly representing the flight vehicle in all aspects may be greater than that of obtaining the vehicle itself. The real value of the simulator lies in the ability to limit its capabilities to the study of important problems while ignoring the unimportant ones. Thus, unlike the aircraft, the complete system is unnecessary and great simplification can result with no significant loss in the success of the study.

In all cases, use should be made of the full capability of the computer to examine the problem. Without undue complication, it is possible to examine the response of the vehicle to standard control commands. Such studies can be as simple as the response to a control surface pulse or as complicated, for instance, as response to a throttle pulse involving engine response, propeller governing response, and slipstream effect on the vehicle characteristics. The only limitation to such a study is the degree of detail of data applicable to the vehicle. If the vehicle were to be operated completely in the automatic mode such as with a space-vehicle control system, then the results obtained would suffice. However, if the piloting requirements or performance are to be studied then the outputs of the computer should be used to command visual motion displays as in the top loop or to command real motion feedback as in the bottom loop. (See fig. 1.) The visual cues and/or real motion can be presented to a pilot and he can supply the command inputs to the computer. In this manner, closed-loop operation with the pilot in the loop is achieved.

For the piloted vehicle the question to be answered is whether the vehicle response characteristics are compatible with the pilot's requirements. Examination of the responses obtained without the pilot in the loop may show cases which would be considered acceptable. For example, smooth subsidence of motion following a disturbance or absence of motion cross coupling between axes may be taken as evidence that the pilot will find the vehicle characteristics acceptable. In general, however, decisions based on the examination of analog-computer motion traces alone tend to be conservative. The human and particularly the skillful pilot is a highly adaptive control mechanism and can cope with many systems which might otherwise appear hopelessly deficient. To take advantage of this

skill requires that the pilot be brought into the system to aid in studying critical areas to avoid penalizing the design unduly.

Since the simulation results are dependent upon the pilot's reactions to the vehicle characteristics and he has to voice an opinion, the pilot must bring to the simulation a basis of knowledge about the task and characteristics being studied. The simulator cannot duplicate all of the experiences of flight but it can provide hints of what the flight would be like and, from these hints, the pilot must extrapolate to actual flight. This requires mental gymnastics by the pilot and he should have recent flight experience in the task being performed or a related task to be successful in the mental correlation. The interpretation of the pilot opinion given is quite important and it is felt that the simulation engineer with an understanding of pilot opinion procedure enhances the reliability of the results.

Mechanization of the cockpit assumes importance as soon as the pilot is included in the loop. It is not necessary to duplicate everything; but the controls and instruments essential to the problem need to be placed correctly. With fixed-cockpit simulation, it must be realized that the pilot receives all his information visually from the instruments and they must be adequate. Control-system characteristics should be reasonable as far as the feel to the pilot is concerned. An unrealistic breakout force or dead band in the control stick, for instance, has been found to have definite influence on the pilot's opinion of given characteristics.

With the pilot in the loop and surrounded by a cockpit that appears to him to represent the airplane, it must be decided what information is to be given him through his visual cues, the instruments, to obtain useful data. It is obvious that these instruments could be used to present to the pilot information showing motion about all axes. Some of these instruments would be required to substitute for motion cues and thus would be of a type not generally necessary or familiar to the pilot. Generally it is the opinion that it is impossible to absorb and act on the six-degree-of-freedom information presented in this way. The pilot's visual capacity to absorb the information becomes saturated and even relatively trivial problems may not be handled. It then becomes necessary to reduce the simulation to fewer degrees of freedom and possibly to divide the problem into portions for study. Thus it may be necessary to include only one degree of rotational freedom and one or two degrees of translational freedom in the simulation. If the problem can be restricted in this way, then the pilot has a firmer basis for judging the vehicle dynamics. If the problem cannot be simplified and more degrees of freedom are required, it is the conclusion that the pilot opinion will be unduly conservative if the visual cues are in the form of instrument presentation.

A more recent and less explored form of visual presentation is that of using television or motion-picture projection to present the pilot with an outside world which moves in relation to the vehicle response as a result of his control commands. Such a presentation extends the ability of the pilot to absorb more visual information by allowing him to use his peripheral vision to pick up movement while concentrating on instruments or other objects. Although experience with these systems is limited, it is the opinion that this type of presentation will substitute for motion of the simulator cockpit where low accelerations are expected to be imposed on the pilot in the real vehicle. If this proves to be true, then certain six-degree-of-freedom cases can be studied without motion of the pilot.

From studies made on a fixed-cockpit simulator, certain conditions will appear to be unacceptable or uncontrollable to the pilot and the question arises whether or not motion cues would supply information enabling the pilot to revise his opinion. In addition, some problems must be studied which require more degrees of freedom to be simulated than are acceptable in the fixed-cockpit case. In general, it can be stated that the degrees of freedom which can be analyzed by the pilot satisfactorily increase directly as degrees of freedom of real motion feedback are added and may add to those acceptable in a visual sense. For example, two degrees of angular motion freedom provided could enable the pilot to analyze three degrees of angular freedom (one by visual presentation) and two degrees of linear freedom (both by visual presentation). The nature of the problem will specify the particular motion freedom required in addition to the visual presentation. In VTOL aircraft the linear accelerations on the pilot are fairly low and rotary motions therefore will usually be more pertinent to the simulation.

In the foregoing discussion a rough guide has been presented of the procedure to decide what parts of the block diagram (fig. 1) will be included and how complicated they will get. Each step in increased sophistication is made only when an unacceptable flight condition is found which is suspected to be the result of inadequate simulation. Thus for each step, the number of problems to be studied tends to reduce and the sophisticated simulation becomes directed at specific problems. Consequently, the simulation may remain simpler than first thought necessary.

Now that some of the factors influencing piloted simulation studies have been discussed, their use is illustrated by some specific examples.

The first of these was the study of transition characteristics of the deflected-slipstream vehicle. In figure 2 is the range of flight conditions studied from 0 to 55 knots. From the wind-tunnel tests, the variation of angle of attack with airspeed was determined for several flap deflections. Any point on any of the curves represents a steady level flight condition. The upper boundary is fixed by the wing stall

and control available to balance the pitching moments. The lower boundary is imposed by the structural limits of the flap. From wind-tunnel results alone, it would be concluded that the vehicle could operate in this region. Prior to flight the transition was studied using a fixed-cockpit simulation. The pilots found it very difficult or impossible to complete the transition. To check on whether the omission of motion cues caused this result, the simulation was repeated with pitch and roll motion of the cockpit added. With these motion cues, the pilots were able to explore the transition region and establish a comfortable transition boundary which with the flap limit boundary designated a corridor through which the aircraft could be flown by careful attention to flaps, speed, and angle of attack. The gray area was to be avoided because it was too near the upper boundaries to allow sufficient control. Subsequent flight experience supported the pilots' conclusions regarding this corridor.

In reviewing the results of this simulation, the need for cockpit motion was readily apparent. Without cockpit motion, it became very difficult to perform the transition, even in the limited three-degree-of-freedom case of longitudinal mode only, because of the multiplicity of quantities which had to be monitored. The addition of roll and yaw calculation to give six-degree-of-freedom simulation made the task impossible and it was necessary to add pitch and roll motions to the cockpit to achieve satisfactory pilot performance.

A second example of the effect of motion feedback can be illustrated in some results obtained from the simulation of a large tilt-wing vehicle in hover. The study was concerned with the roll control and the simulation was limited to three degrees of freedom including roll and vertical and lateral translation. The pilot was given the tasks of lifting off into hover, of landing, and of moving laterally. Some conditions were compared with the cockpit fixed and with it moving in roll. As the characteristics became worse, a definite difference appeared as shown in figures 3 and 4. Figure 3 presents representative time histories of the roll-control position, rolling velocity, and lateral velocity for fixed-cockpit simulation and figure 4 shows the same quantities for the moving cockpit. The erratic movements and larger lateral velocities of the fixed-cockpit simulation are compared with the more regular movement and lower lateral velocity with the roll motion feedback. Even in this simple case, the pilot found the added motion cues in roll to be an aid since they gave him a more realistic picture of the onset of lateral velocity. He remarked that he found it possible to remove his hand from the control stick for brief periods of time with the moving cockpit and still regain control - something he could not do with the cockpit fixed.

This example illustrates that fixed-cockpit studies alone tend to be conservative. It emphasizes that, when a pilot finds he can cope with a problem on a fixed-cockpit simulator, the problem can probably be

considered unimportant. However, when he cannot cope with the problem even where visual saturation is not suspected, serious consideration must be given to increasing the realism of the simulation to obtain valid pilot opinion.

The next two examples are of the study of specific operational problems which demonstrate the ability of simulation to familiarize the pilot with new characteristics, help him to explore limiting or boundary conditions without endangering the aircraft, and aid in development of techniques to handle an unusual situation. Motion of the cockpit was used in both of these cases to give the pilot a truer picture of the flight problem and to provide a more realistic environment of simulator operation.

The first of these was the study of attitude control in hover of a deflected-jet airplane. The reaction control power of this aircraft is low about all axes and the rotary damping is negligible. The simulation, making use of the pitch and roll motion of the cockpit, served to help the pilots learn what to expect and how to handle this type of hovering; it is somewhat akin to balancing yourself on a ball on a smooth surface.

This airplane also has the problem of gyroscopic coupling due to the engine rotating mass causing cross coupling between the axes of motion. This coupling appears in the pitch mode due to yaw movement. Gyroscopic coupling can be predicted and was recognized as a possibility early in the program; early flight tests confirmed this. Because of the inadvisability of exploring the limits of this region with the airplane itself, the simulator was used. With the simulator the pilot could explore the coupling region, determine approximately what the airplane limit should be, and calibrate himself to avoid this limit. Figures 5 and 6 have typical simulation records of this coupling. It should be pointed out that the pilot must supply his own damping, for the vehicle has little of its own. Values of yawing velocity, pitch control, and pitch angle are shown. Figure 5 shows the results of an attempt to hold a rate of yaw of approximately 5° per second. It can be seen that the yawing velocity in the first part of the figure varies between 5° and 8° per second. At the same time the pilot finds it necessary to use 50 to 80 percent nose-up pitch control to keep the pitch angle near zero. As the pilot reverses yaw control he requires nose-down pitch control to keep the pitch angle at a reasonable value. Figure 6 shows an attempt to hold a higher yawing velocity and it can be seen that an average rate of around 12° per second was held. Here full pitch control was necessary. From this study, the pilot selected the values of yawing rate to which he would restrict himself depending on the reaction control available. Some amount of margin of control is required by the pilot to handle disturbances and for maneuvering. In a previous paper, L. Stewart Rolls discusses this particular problem.

An investigation involving another deflected-jet aircraft studied the control problems due to the longitudinal dynamic characteristics in transition. Since only the longitudinal mode was being studied, the simulation was limited to three degrees of freedom and the cockpit moved in pitch only. The pilots went through a typical familiarization with the characteristics which were representative of the unaugmented stability or emergency case. The solid lines on figure 7 represent the variation of engine thrust with speed at three values of angle of attack for steady level flight as determined from the wind tunnel. Steady flight should be possible in the area above and to the right of the curve for $\alpha = 15^\circ$. The pilots found on the simulator that steady flight was possible in this region. With the requirements that altitude for transition from forward speed to hovering be held constant and that it be performed expeditiously, the initial transitions were attempted with low engine thrust for deceleration into the region of higher angles of attack before increasing engine thrust for lift. This type of deceleration ended in an uncontrollable pitch-up as indicated by ① (fig. 7). A second attempt with slightly higher thrust ended the same way. Eventually it was found that the only feasible way of performing the transition was to move the diverter full down at a high enough speed to obtain good aerodynamic control and immediately increase engine thrust to 100 percent to obtain maximum reaction control power. The angle of attack was held slightly negative through most of the speed range to balance the excess lifting thrust.

This example demonstrates the value of simulation studies in interpreting wind-tunnel results as applied to new types of vehicles. Only in this way is it possible for the pilot to experiment with new techniques for a new vehicle. Simulation studies of this type are required to obtain a clear definition of the maneuvering requirements of VTOL vehicles as set by dynamic conditions rather than by static conditions.

The pilot still considers these simulation devices to be poor substitutes for flying but they can be a powerful tool in the investigation of flight problems. The simulator will become more important in the future when flight testing may not be available and most or all of the problems will have to be solved before the vehicle leaves the ground.

CONCLUDING REMARKS

This paper has discussed some of the factors affecting piloted flight simulation and the use of simulators in the study of flight techniques. Related pilot flight experience and engineer simulator experience enhance the reliability of simulation data. Proper cockpit mechanization is an important aid to the pilot in his correlation with the flight vehicle and with the task or problem being studied. Increased

degrees of freedom in computation add to the realism of simulation but may be superfluous. Cockpit motion is an aid to the pilot in providing him with cues that otherwise must be interpreted visually.

BLOCK DIAGRAM OF PILOTED SIMULATOR

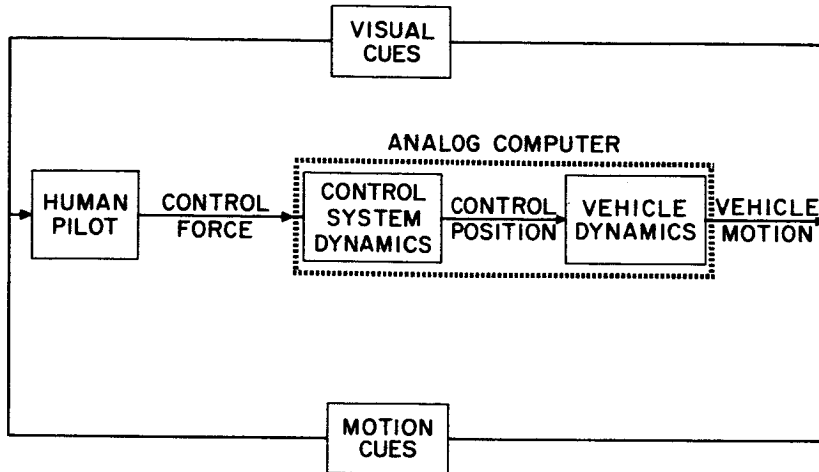


Figure 1

TRANSITION BOUNDARIES OF DEFLECTED SLIPSTREAM AIRCRAFT FROM SIMULATOR STUDIES

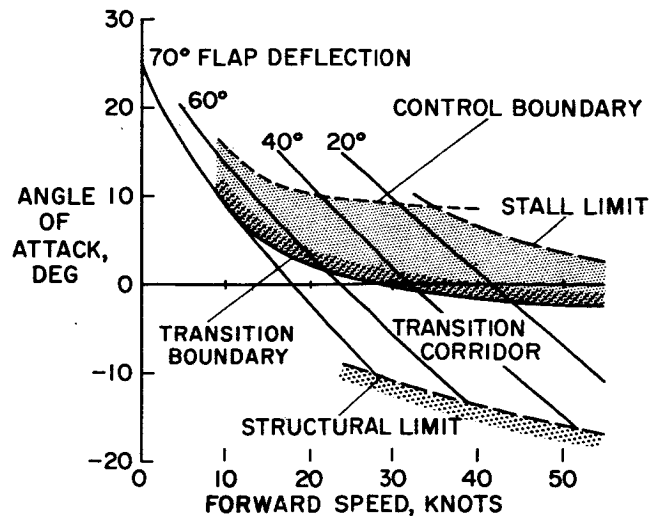


Figure 2

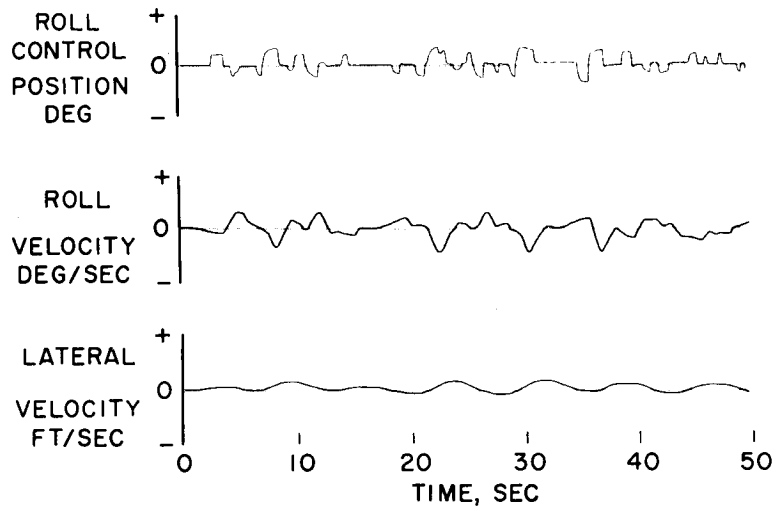
LATERAL CONTROL IN HOVER
FIXED COCKPIT

Figure 3

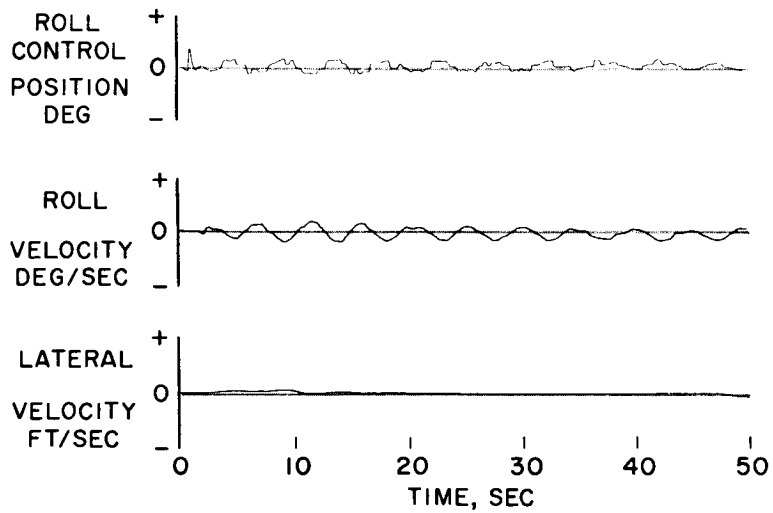
LATERAL CONTROL IN HOVER
MOVING COCKPIT

Figure 4

TIME HISTORY OF GYROSCOPIC COUPLING
SIMULATION AT LOW YAW RATE

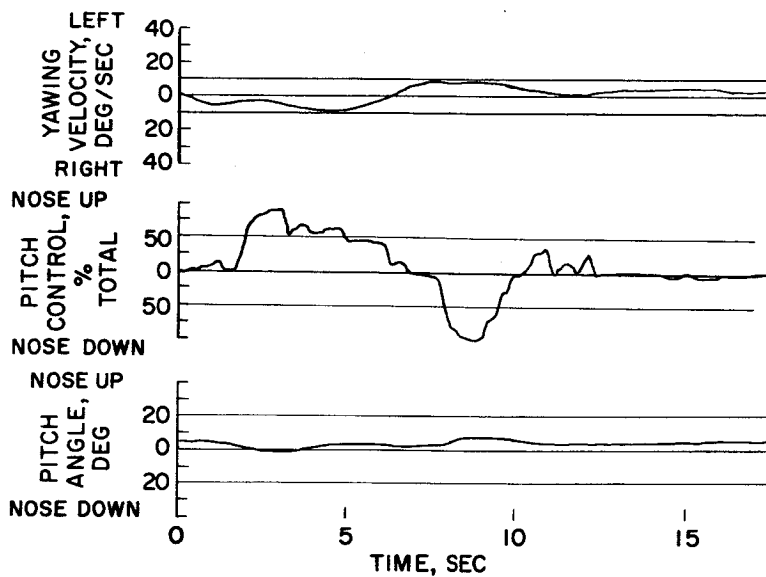


Figure 5

TIME HISTORY OF GYROSCOPIC COUPLING
SIMULATION AT HIGH YAW RATE

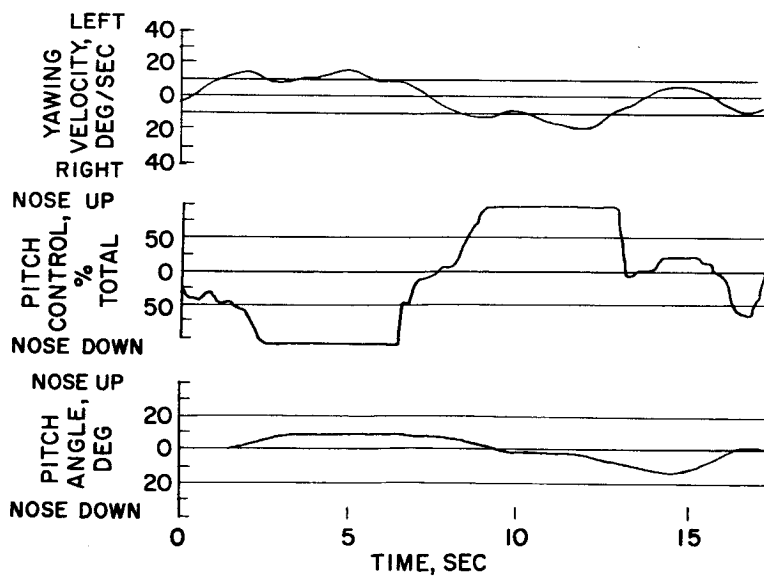


Figure 6

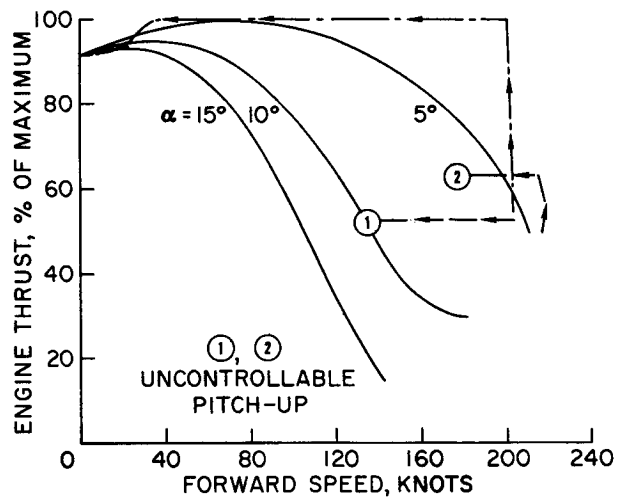
SIMULATOR TECHNIQUE IN TRANSITIONS
FROM FORWARD SPEED TO HOVER

Figure 7

OPERATIONAL ASPECTS OF V/STOL AIRCRAFT

By James B. Whitten

Langley Research Center

VTOL aircraft have the capability of performing a wide variety of military and civil missions. In performing these missions some operational limitations, particularly in the low-speed flight regions, will exist. This paper will discuss some operational aspects of ground handling, take-off and transition, engine-out characteristics, and instrument approaches and landings.

Several mission profiles that might be used for V/STOL aircraft are shown in figures 1 and 2. The mission profiles for military transports are shown in figure 1 as a solid line for a logistic mission and as a dashed line for an assault mission. The mission profile for a civil transport was established to utilize the airspace not used now by conventional aircraft in terminal areas. (See fig. 2.) Examination of these and other profiles indicates that the main areas of operational interest will be ground handling, take-off, transition and initial climb, and approaches and landings.

Ground handling will require careful consideration of the slipstream velocities which will vary with types of V/STOL aircraft from below 80 mph to over 1,000 mph. When this slipstream velocity is vertical, severe ground erosion as well as recirculation of debris causing foreign object damage is likely to occur unless operations are restricted to clean hard surfaces. If taxiing is done in the fully converted or cruise configuration to avoid ground erosion, operational limitations will be similar to those for current conventional aircraft having comparable slipstream velocities.

In order to discuss take-off, the turbulent air regions created by the high slipstream velocities must be considered first. As shown in figure 3, the vertical take-off will be in the highly turbulent region from lift-off until an altitude of 15 to 25 feet is attained and will probably require a stability augmentation system to correct for the erratic disturbances due to the rough air. The STOL take-off (fig. 3) can be scheduled for take-off at a conversion angle and at an airspeed where the major part of turbulent region is behind the aircraft and not affecting its flight behavior. This speed may be considerably above the optimum take-off speed, depending on the configuration, and some penetration of the turbulent region may be required even for STOL take-offs.

Figure 4 can be used to consider transition procedures typical of the power required for a four-engine tilt-wing VTOL. The dashed line shown for power available, drawn at 1.2 times the power required for hovering, was estimated to be an adequate margin to provide height control for hovering in rough air and to provide a reasonable margin of power for initial acceleration to forward flight. This margin was selected on the basis of previous experience with helicopters and one of the VTOL test beds. Dashed lines are also shown in figure 4 for three-, two-, and one-engine operation. Thus, level flight can be maintained at a speed below 20 knots with one engine out, at 35 knots with two engines out, and at about 60 knots with three engines out. The dashed line labeled overload indicates the effects of high temperatures and high altitudes or military overloads on performance capabilities. The aircraft in the overloaded condition must now have about 20 knots for take-off and about 30 knots for level three-engine flight.

For take-offs where obstacle clearance is not a problem, vertical take-offs would only be made if a short ground run were not possible (over water, rough ground, etc.). The procedure to be followed would be vertical lift-off, conversion close to the ground to a configuration where at least a 200- to 300-ft/min rate of climb would be possible with three engines, climb to a safe altitude, and then completion of conversion to speed for best climb. The STOL take-off would differ only in that the acceleration to a three-engine safety speed would be on the ground. This procedure allows the pilot to accelerate to a safe speed even under instrument conditions and avoids configuration changes in the critical portion of flight close to the ground.

To estimate distances, an average acceleration rate to safe three-engine speed that is usable by the average pilot under both visual and instrument conditions must be established. Most present transport acceleration values are from $1/10$ to $3/10$ g. Modern jet fighter rates can be in excess of $1/2$ g. For both of these, however, take-off speeds are high and the pilot has ample time to anticipate rotation and take-off speeds. For V/STOL aircraft with considerably lower take-off speeds and the additional requirements for properly scheduling conversion angle with airspeed and varying power to control altitude, a maximum acceleration value of about $1/4$ g is usable operationally. Figure 5 shows the distances required at this acceleration for different values of three-engine safety speed. Using the four-engine VTOL of figure 4 this would show a requirement of about 100 feet for the VTOL aircraft or 200 feet for the overload or STOL aircraft.

For some military operations where vertical take-off and climb-out of very restricted areas will be required, it is necessary to evaluate the hazard involved if an engine fails abruptly. In discussing this, it is assumed that the engines are geared to the lifting and control systems

in such a fashion that failure of one engine does not result in large changes in trim or reduction of control power. Figure 6 shows a comparison of the estimated ground contact regions of a four-engine-propeller VTOL and a four-engine helicopter. These regions define combination of altitude and airspeed that would require more than average piloting skill to avoid ground contact if an engine failed. The comparatively small area of the VTOL may be explained by reference to figure 7. The vertical lines on the right of each region in figure 6 are drawn at the speed at which each machine could fly level with three engines. Figure 7 shows that this would be about 20 knots for the VTOL and 30 knots for the helicopter. The upper sloping lines in figure 6 are determined by the power available for acceleration which is greater at each speed for the VTOL. It is interesting to note that in figure 7 the VTOL has a rather large range of speeds available even for two- or one-engine operation, and that the helicopter has a narrow range with two engines and cannot fly level with one.

Since military missions operate, at present, vertically into restricted areas, it can be assumed that the hazard involved with the VTOL can be accepted and will be less than for present aircraft.

The cruise portion of the VTOL flight will be conducted at the same altitudes as present jet fighter and transport aircraft. This may create problems of traffic control since they will be operating at speeds several hundred miles an hour slower than the turbojet aircraft.

It is sometimes suggested that the last thousand feet or so of an approach be made vertically. Under visual flight conditions, this is certainly possible with due consideration of the ground contact region just discussed. However, even visually, this is not too practical due to the high fuel consumption in vertical flight and the difficulty in accurately controlling the flight path. In instrument flight, at present, vertical letdowns are not possible without completely automatic guidance and control.

The establishment of an operational VTOL instrument-approach system depends on a number of factors. Among these are aircraft-performance and handling-qualities limitations, obstruction-clearance requirements, ability of the pilot to follow the guidance system, and community acceptance.

An investigation of approach-angle limits with a helicopter has indicated some of the problem areas associated with low-speed, steep, instrument approaches which will be common to all types. First, the rate of turn for small bank angles is high and g forces in maneuvers are low. This results in requiring a more rapid scan, more concentration,

and a higher degree of proficiency than for conventional approaches. Second, at lower speeds, the helicopter and VTOL aircraft will be flying at speeds on the back side of the power-required curve. This requires adjustment of the rate of descent by power changes rather than attitude and results in slower corrections for deviations. Third, wind effects, both crosswind and wind shear, are considerably more difficult to compensate for at low speeds.

A typical steep instrument approach as shown in figure 8 can be conveniently considered in two parts. The first part might be called the acquisition and stabilization portion and consists of that portion from level flight until breakout. The second part starts at breakout and includes the transition to hovering and landing. A typical flight path is shown by the dashed line in figure 8. Results of the previously mentioned steep instrument-approach investigation indicated that for the first phase, about 90 seconds would be considered a minimum operational time for stabilization on the glide path, and 25 knots a minimum speed considering wind and piloting problems. Current developments in pictorial and analog instrument displays, Doppler ground speed presentation, and omni-angle approach systems may allow lower approach speeds in the future. Research programs to investigate these systems are currently programmed. If an initial altitude of 1,000 feet is specified for noise or traffic control purposes, this will result in speed-angle relationships as shown in figure 9. Speeds below 25 knots are shown for reference. Only those speed-angle combinations in the usable region are considered operational at present. This indicates that a maximum approach angle at 25 knots would be about 15° and that at 80 to 100 knots, the maximum approach angle would be about 5° .

The second phase starting at breakout is a visual phase which involves visual recognition of ground or light patterns, transition to hovering configuration, and landing. To establish a minimum time, current conventional aircraft minimums may be considered first. At present for the approach speeds and runway visual-range minimums, the pilot has about 9 seconds along the glide path to recognize his portion, align the aircraft with the runway, and arrest the rate of descent before contact. This 9 seconds includes about 3 seconds for recognition, evaluation, and decision and 6 seconds to alter the flight path and arrest descent. Speed is usually held about constant and configuration changes are usually minor or are not made at all. Since the VTOL pilot will have the additional problem of completing the conversion, a more appropriate time for VTOL might be about 12 seconds. Figure 10 shows the approach-speed—approach-angle relationship for two breakout heights based on this 12-second flare phase. The operational combinations are again shown as usable regions. This shows that the ceiling has a considerable effect on permissible approach angles, particularly at lower speeds (at 25 knots a 100-foot ceiling at 11° and a 200-foot ceiling

at 21°). Also, at 90 knots and 100 feet, ceiling approach angles are about the same as current ILS glide slopes at $2\frac{2}{3}^\circ$.

Figure 11 shows a summary plot of approach-angle ceiling limitations based on combined limitations of the acquisition and flare phases shown in figures 9 and 10. It can be seen that at the low speed of 25 knots a ceiling as low as 50 feet can be operationally feasible at angles appreciably above current ILS approach angles. It is also apparent that an omni-angle approach system would greatly improve VTOL approach capabilities. The break in the curve at about 140 feet is a limit from the acquisition phase.

Turbulence, crosswinds, and wind shear make the steep angle, low-speed approaches more difficult than the standard 3° approach at conventional aircraft speeds. On some occasions during the steep approach program, when ground winds were 10 knots or less the winds at an altitude of 1,000 feet were in excess of 25 knots and low-speed approaches were not possible. On other approaches heading corrections required to maintain the localizer course were as high as 60° at 800 to 1,000 feet and 5° to 10° at 100 to 200 feet due to wind shift and wind shear effects. For the majority of approaches, however, in smooth air or with light turbulence the limits of figure 11 are considered to be operational limits.

In summary, operational introduction of VTOL types appears feasible with minimum disruptions of present practices and procedures. Effects of high slipstream velocities must be carefully considered in the establishment of ground taxiing, take-off, and landing areas. Partial power operation of VTOL's will probably be somewhat safer than for comparable helicopters. Steep instrument approaches will be limited to a minimum speed of 25 knots and a maximum angle of 15° until improved instrumentation permits lower speeds.

MISSION PROFILES FOR MILITARY TRANSPORTS

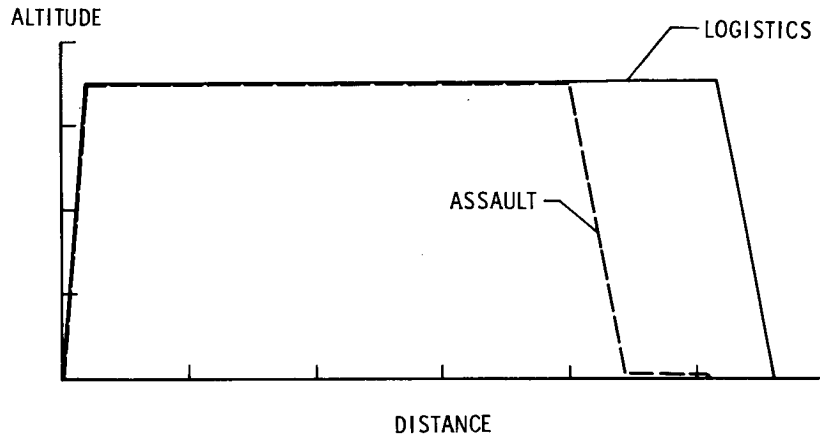


Figure 1

MISSION PROFILE FOR CIVIL TRANSPORT

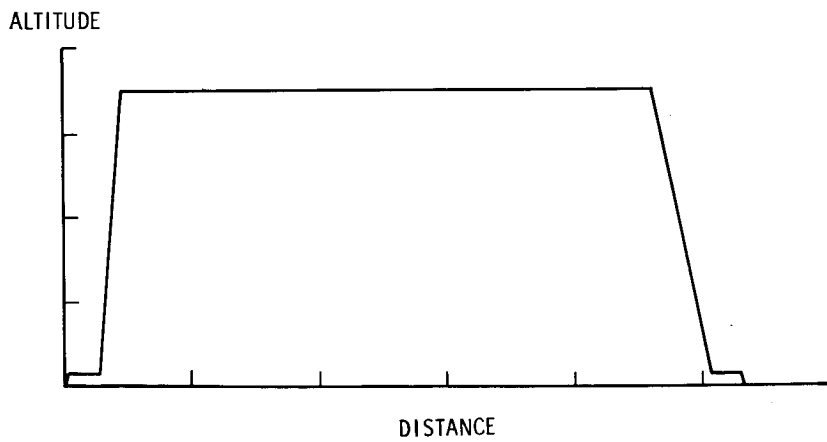


Figure 2

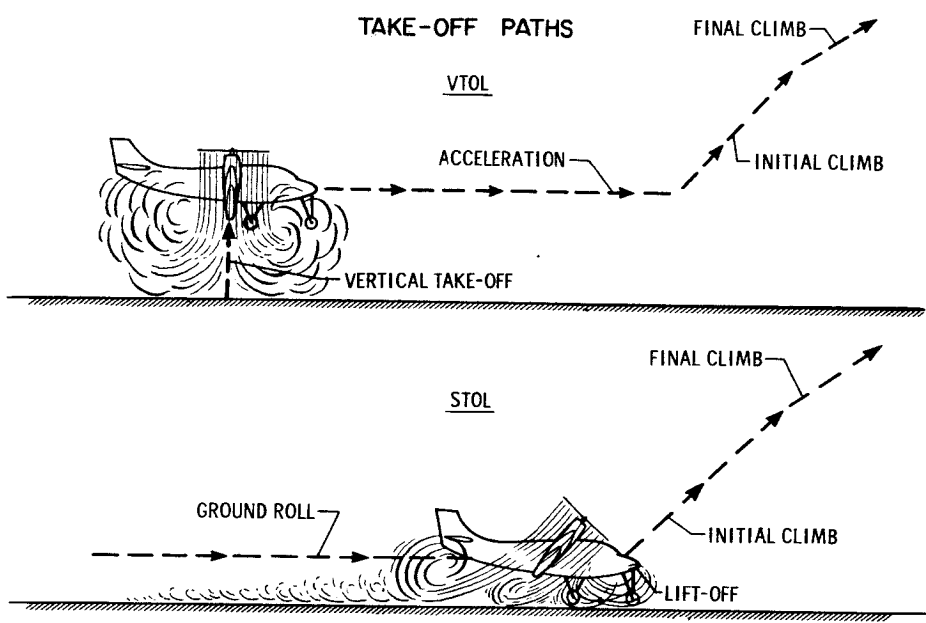


Figure 3

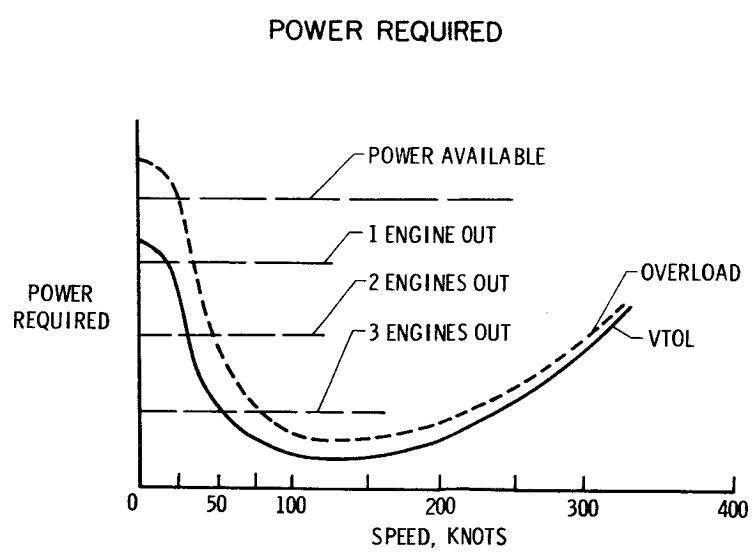


Figure 4

ACCELERATION DISTANCE AT $\frac{1}{4} g$

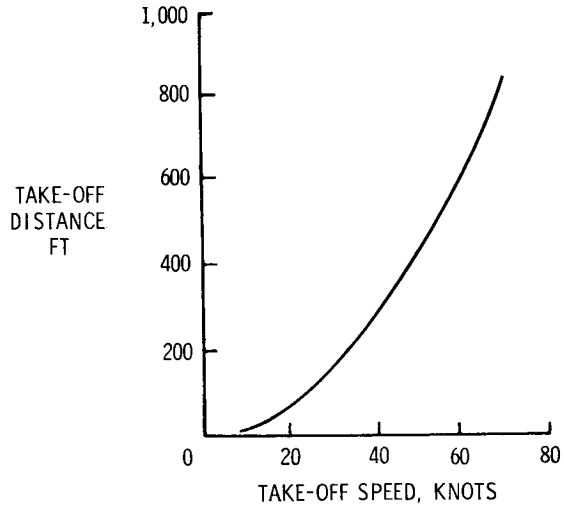


Figure 5

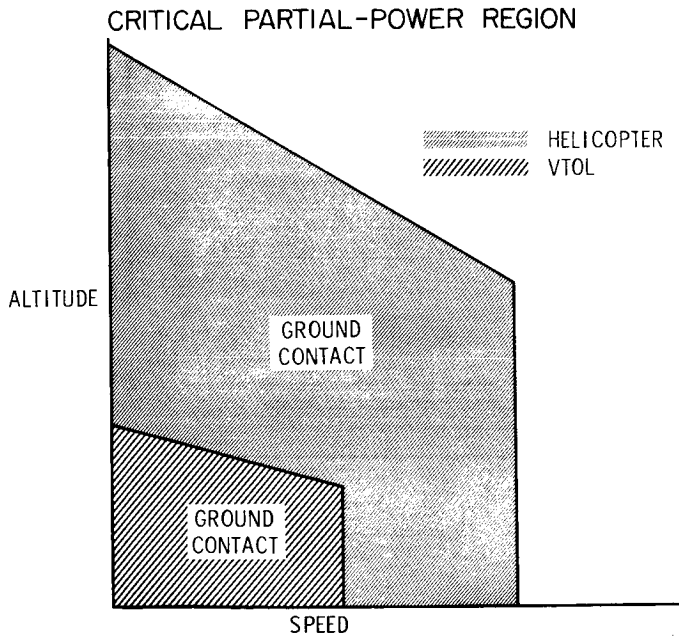


Figure 6

COMPARISON OF POWER REQUIRED FOR HELICOPTER AND VTOL

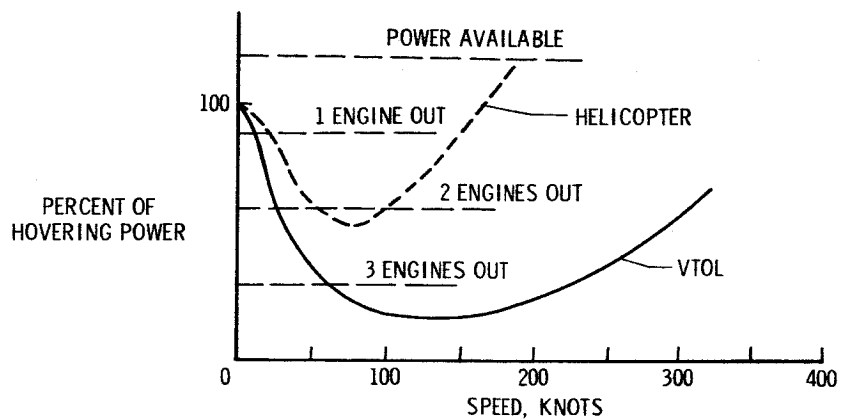


Figure 7

INSTRUMENT APPROACH

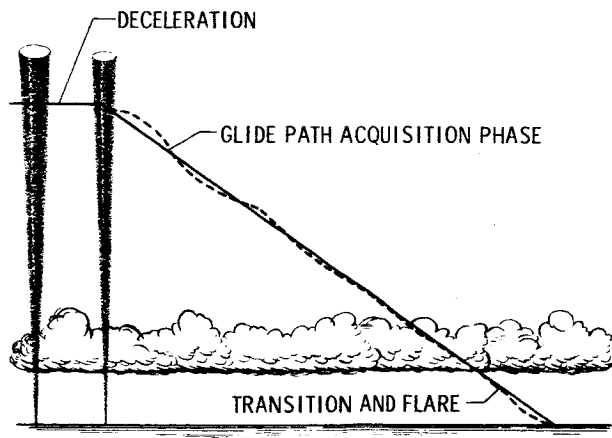


Figure 8

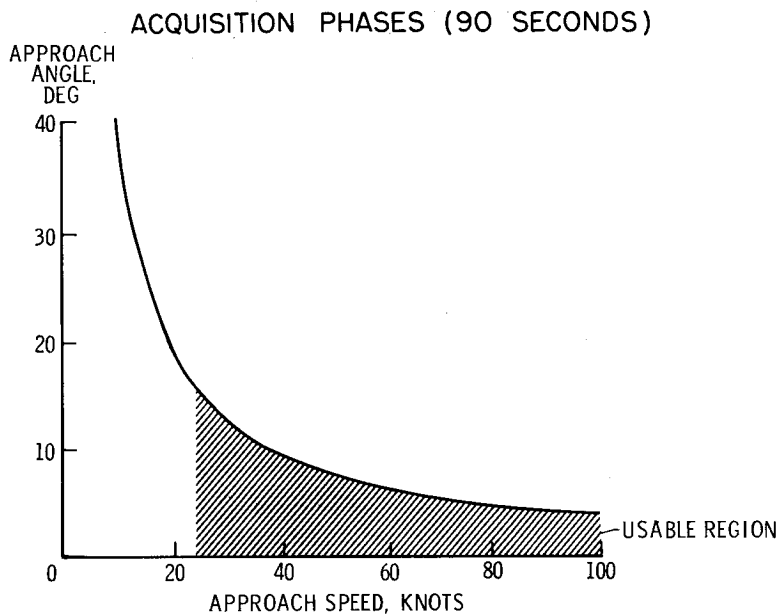


Figure 9

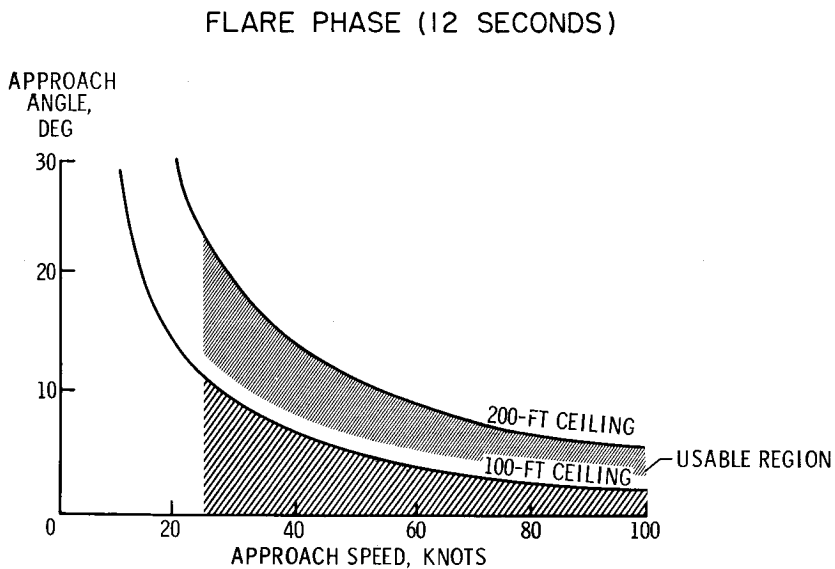


Figure 10

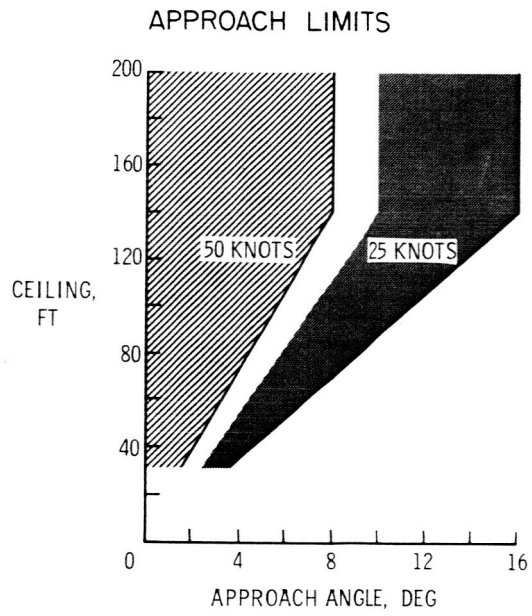


Figure 11

OPERATING PROBLEMS OF V/STOL AIRCRAFT IN
STOL-TYPE LANDING AND APPROACH

by Robert C. Innis and Curt A. Holzhauser

Ames Research Center

INTRODUCTION

Considerable effort has been expended in the past, both in this country and abroad, to develop conventional type aircraft with short-take-off-and-landing performance. A number of these airplanes have utilized high thrust-to-weight ratios to achieve good take-off performance but have relied on low wing loadings and conventional high-lift devices to obtain short landing distances. Although these aircraft can be designed to meet specific requirements in regard to take-off and landing performance, they are relatively inefficient in high-speed cruise flight and derive few benefits from the large amount of power that is available to them during the landing approach. In fact, in order to achieve the shortest landing distance over a given obstacle with these vehicles, the approach must be conducted at idle power. This deprives the pilot of much of his ability to adjust the touchdown point during the approach and places considerable reliance on his judgment of when and where the approach should be commenced. Although this type of operation has often been referred to as STOL, it does not meet the definition used herein which refers to STOL operation in terms of a specific operational flight regime rather than in terms of the performance capabilities of a particular airplane.

Recent studies conducted by the NASA as well as by individual aircraft companies have been directed towards harnessing a portion of this available power to use in augmenting lift during the landing approach as well as during take-off. These are exemplified by the models and aircraft shown in figure 1. Both the two-propeller and four-propeller models shown on the left have been tested in the Ames 40- by 80-foot tunnel with various forms of boundary-layer control (BLC) applied to both the highly deflected trailing-edge flaps and the drooped ailerons. The aerodynamic characteristics have been reported in references 1, 2, and 3. The airplane at the upper right, the Stroukoff YC-134A, has been flight tested at the Ames Research Center. At the lower right is the BLC version of the Lockheed C-130B which has been flight tested by Lockheed Aircraft Corporation. All of these vehicles utilize propeller slipstream effects in conjunction with BLC to develop high lift coefficients. In addition to determining the

feasibility of STOL operation of these large airplanes having a gross weight of 50,000 to 100,000 pounds, it was desired to find out the problem areas that may result by flying at the relatively low speeds with considerable power being applied. Although the test vehicles represent conventional transport-type airplanes, the results of the tests are also felt to be applicable to the VTOL vehicle operating in an overload condition or at a thrust-to-weight ratio of less than 1 such as might occur with a partial power loss. It is the purpose of this paper to review the results that have been obtained to date, to point out the limitations, and to show how some of these limitations can be coped with to obtain further improvements.

RESULTS AND DISCUSSION

A generalized plot of the STOL operating envelope of an aircraft which derives a portion of its lift capabilities from engine power is presented in figure 2. These characteristics are quite similar to those of the aircraft in figure 1. In figure 2, steady-state flight-path angle is plotted as a function of velocity for various values of engine power. This is represented on the figure by the series of solid lines, each of which is labeled with its corresponding amount of power in terms of the percentage of total power available. In this particular example, 100-percent power represents a thrust-to-weight ratio of about 0.4. The broken lines on the figure indicate the angle of attack that corresponds with each combination of power and airspeed in steady nonaccelerated flight. This envelope is bounded on three sides by the aerodynamic and performance capabilities of the airplane. The boundary on the lower left represents the stalling speed and illustrates its variation with engine power for this particular vehicle. The maximum steady-state glide angle, the bottom boundary, is of course limited by the aerodynamic lift-to-drag ratio of the airplane at idle power. The upper line represents the maximum attainable climb angle in this configuration with full power.

It is important to point out the control technique that is required of the pilot when he is operating in this STOL flight region. Changes in angle of attack have at best little effect on flight-path angle. In fact it can be seen from the figure that the steady-state flight-path angle resulting from changes in angle of attack may be in the opposite direction from that to which the pilot is accustomed. This is known as a "region of reversed command" or the "back side of the drag curve." Attempting to control flight-path angle by use of the elevator while in this region can lead to a rapid divergence in speed; therefore, the pilot tries to maintain a relatively constant angle of attack while he controls his approach-path angle by use of power

changes. This method of control is not difficult; however, it requires that the pilot keep one hand on the throttles while controlling attitude and angle of attack with the other. Because of this, it is felt that the flight-control systems of STOL aircraft should be designed for one-hand operation. In addition, the thrust response to throttle movement should be smooth and rapid.

In addition to these aerodynamic and performance boundaries, there are certain limitations imposed by the pilot in order that the approach may be conducted in what he considers a safe manner. The areas that are avoided are indicated in figure 3 by the shaded region superimposed on the STOL envelope.

The first of these limitations is represented by the vertical line in the upper left-hand portion of the figure. This is the minimum airspeed at which it is possible to perform a satisfactory wave-off. Current Civil Air Regulations specify that a 1.8° climb gradient must be available in this configuration with all engines operating. It was found that under ideal conditions, with a clear unobstructed path available for climbout, Ames research pilots have considered a climb gradient of less than 1° to be acceptable; however, this would be considered acceptable only for an emergency situation. Perhaps a more practical solution to the question of satisfactory wave-off performance should consider any obstacles which would have to be cleared during climbout.

The second limitation is imposed by the proximity to the stall. This is represented by the diagonal line which runs roughly parallel to the stall boundary. The stall in this case is considered to be defined by either a sudden loss of lift or a rapid deterioration of stability or control characteristics. Previous research at Ames on jet fighter-type airplanes has indicated that the pilots were willing to approach at speeds as low as 1.1 times the power-on stall speed; however, when the stall speed is less than 100 knots, it has been found that a fixed margin, rather than a fixed percentage above the stall, is desirable. This provides protection against finite variations in approach speed due to pilot distractions or disturbances such as gusts. If the stall speed remained constant as power was varied, a margin of 10 knots above the stall would represent a realistic minimum. However, when the lift coefficient and hence stall speed are greatly affected by engine power, as is the case with these vehicles, use of airspeed during the approach becomes less useful. The pilot must turn to something more consistent to protect against inadvertent stall. Reference to the angle-of-attack indicator in the Stroukoff YC-134A proved to be most satisfactory for this purpose as the pilot could maneuver or manipulate the throttles as much as he wished and still be assured that he was maintaining a safe margin from the stall. During the landing evaluation of the YC-134A, the pilots chose to approach at an

angle of attack which corresponded to about a 10-knot margin above the stall speed for any desired power setting. Another limitation occurs as the approach angle becomes steeper, the pilot's ability to flare the aircraft at constant power. In executing this flare it has been found that the pilot will not normally use more than 85 percent of the maximum lift coefficient that is available. The assumption that the flare is made at constant power is based on the current practice of designing and locating the engine control system, which has rendered the addition of power during the approach impractical.

In the discussion of steep approaches, the question quite naturally arises as to what is the maximum rate of descent that the pilot will tolerate prior to the flare. Most certainly as sink rate increases in magnitude, the errors associated with estimating it and in estimating the ability to arrest it become greater. These errors, of course, detract from the safety of the operation, and, if large enough, can lead to disaster. There is little quantitative data on the ability of the pilot to arrest these high sink rates. It is of interest to note that during the steepest approaches that were conducted with the YC-134A, which were about 10° with 1700 feet/minute rate of descent, the ability to flare was considered marginal.

The remaining area which is indicated as being avoided by the pilot reflects his demand for ability to control flight-path angle. Since power is being used as the primary flight-path control, the pilot desires a portion of it to be held in reserve; therefore, he will not consciously choose to approach in a condition where he does not have this reserve. Again previous research involving jet fighter airplanes has indicated a minimum available thrust-to-weight ratio of about 0.1 to be limiting. Additional research is necessary, however, to determine whether this value is applicable to this type of aircraft. The combination of all these limitations can rather severely limit the scope of the STOL operating envelope. It is of interest, therefore, to see if this envelope can be expanded by deviating from the current operating techniques. For example, an aircraft that is limited by the ability to wave off could be improved if the pilot were willing to accept a configuration change such as reduced flap deflection in order to accomplish a wave off. Such a change, however, would have to be carefully programed in order to avoid undesirable trim changes or a loss of lift. Another way in which the envelope could be expanded is the use of power to assist in flaring the airplane during steep approaches. This would not only eliminate the excess speed required during the approach for the flare, but would also reduce the stalling speed as the flare was accomplished. Such a technique has been used quite successfully on a jet fighter-type airplane which incorporated boundary-layer control on a highly deflected trailing-edge flap.

Using the limitations indicated in figure 3 as a guide, minimum approach and touchdown speeds can be predicted for an STOL vehicle at various values of approach angle. It is obvious that for a vehicle of this type, the lowest touchdown velocity and consequently the shortest ground roll will be achieved from an essentially flat approach where maximum advantage is taken of the lift augmentation to reduce the stalling speed. Unfortunately, however, consideration must be given to obstacles which have to be cleared in the approach path; therefore, a realistic value for the landing distance of an STOL airplane must take into account the air distance required to clear such an obstacle. This air distance, of course, becomes smaller as the approach path is steepened. However, the reduced power required for a steep descent results in a higher stall speed and consequently a higher touchdown speed which increases the ground roll. It therefore appears desirable to determine if an optimum approach angle exists which will result in the shortest total distance over a given obstacle. By combining the air distance required for the approach and flare with the ground roll resulting from the corresponding touchdown speed, the total distance can be calculated. Figure 4 presents the results obtained with the YC-134A for the landing distance over a 50-foot obstacle. The solid curve indicates the calculated variation in the air distance required for the approach and flare as the approach angle is steepened. The calculations are based on the method outlined in reference 4. The circled points are values obtained from flight tests by a Fairchild Flight Analyzer from three representative approaches. It is of interest to note that the flight approach speeds corresponding to the various glide angles shown in figure 4 were 84 knots for 5.6° and 97.5 knots for 8.7° and 9.5° . To obtain the total distance, the calculated ground roll has been added assuming two different values of braking coefficient. The short-dashed curve on the right corresponds to the ground roll that might be obtained if wheel brakes only were used for deceleration. The long-dashed curve is representative of the use of reverse thrust in addition to wheel braking. It can be seen that an optimum angle does exist and also that this angle shifts to a steeper value if the greater braking coefficient is assumed. It is important to note, however, that relatively small gains were realized with the YC-134A at approach angles greater than about 4° . To the pilot, this means that he can approach at a reasonably shallow angle with a moderate rate of descent and still obtain near maximum performance. This shallower approach affords much better control of both sink rate and touchdown point.

Comparing the total landing distances over the range of approach angles provides a convenient method of evaluating STOL operation and the relative merits of various high-lift devices. Using the foregoing discussion as a guide, the reductions in landing distances indicated to be possible were examined. The results calculated from the wind-tunnel tests are summarized in figure 5. The curve on the right

represents the total landing distance of the vehicles with two propellers assuming that the approach is conducted in a conventional manner at 1.3 times the power-off stall speed. The improvement that is made possible by adopting the STOL technique (i.e., using power to augment lift) is apparent. The effect of increasing the trailing-edge flap effectiveness to provide more lift augmentation was also examined. Increasing the trailing-edge flap effectiveness by applying BLC produces higher power-off lift coefficients. Increased lift coefficients result in larger induced-drag coefficients which necessitate more thrust for a given glide angle. This in turn provides a larger benefit from the slipstream. With BLC applied to the trailing-edge flap and aileron, the maximum lift coefficient is limited by airflow separation from the leading edge of the wing, even on the 17-percent-thick wing used in the tests. Tests in the wind tunnel have demonstrated that the leading-edge stall can be delayed by the use of a plain nose flap. The improvements that would be expected from adding a leading-edge nose flap with blowing are also shown in figure 5. The calculations presented in figure 5 were based on a conventional transport-type airplane having a wing loading of 45 pounds per square foot and a thrust-to-weight ratio of about 0.4. It was shown that by applying STOL techniques to this airplane and utilizing the lift augmentation obtained from the propeller slipstream effect on a highly effective flap, the total landing distance can be reduced by more than half. Improvements of this order can be expected for similar aircraft having wing loadings ranging from 30 to 60 pounds per square foot. The curve on the left of figure 5 (BLC on the leading edge and the trailing edge) represents what is felt to be about the minimum attainable landing distance for a vehicle of this type without resorting to much of the complexity and expense associated with the true VTOL vehicle. In order to obtain further significant gains, the installed thrust-to-weight ratio would have to be increased significantly. This in turn would lead to the requirement of interconnected propulsion systems with propellers of opposite rotation. The low approach speeds involved would rule out the use of aerodynamic control surfaces and a more sophisticated control system would have to be included.

In the remainder of the discussion some problems are considered which are associated with STOL operation of relatively conventional aircraft not possessing features required by true VTOL aircraft. It is important to point out that the limitations which were outlined previously are approached only if the aircraft possesses satisfactory handling qualities. Experience with the YC-134A has tended to emphasize increasing importance of certain stability and control characteristics in STOL operation as opposed to conventional landings. For example, as the speed is reduced and the thrust coefficient is increased, the longitudinal stability in pitch of the airplane is reduced because of the change in downwash characteristics at the horizontal tail. The importance of maintaining a constant angle of attack during STOL

approaches has been pointed out previously. This is particularly true if the approach is being conducted on the back side of the drag curve. Any reduction in the tendency of the airplane to return to trim angle of attack following disturbance could greatly complicate the pilot's control task and should be avoided if at all possible. The trim change that occurs with power must also be examined in this light. Both of these stability parameters are influenced by the location of propellers as well as by the position of the horizontal tail. If good stability cannot be obtained by a judicious choice of airplane geometry, stability augmentation should be considered in the design of the vehicle.

During the flight tests of the YC-134A, it was noted that with high power a buildup in sideslip occurred as the stall was approached and straight wing level flight was maintained. This required nearly full lateral and directional control and of course was objectionable. By banking the airplane slightly to the right these control requirements were greatly reduced. The wind-tunnel tests indicate that these side forces do not result from inplane propeller forces or from airflow separation, but rather from the flow field produced by corotating propellers. The use of four rather than two propellers did not reduce the severity of this problem.

Another problem that must be given serious attention is that of losing an engine. The minimum control speed of STOL aircraft must be examined in the approach configuration as well as the take-off condition. Figure 6 illustrates the severe reduction to the STOL operating envelope that can occur unless the pilot chooses to ignore the minimum control speed. This is indicative of results obtained with the YC-134A. With one engine out the area above the line is unusable to the pilot because he is unable to maintain control. The loss of control may result from a lack of lateral control power, as well as directional control power, because of the reduced lift on the side with the inoperative engine. This implies that if an engine were lost on the YC-134A during an approach that was shallower than about 6° there would be no alternative but to land short, unless sufficient altitude remained to make a configuration change. If the approach were planned for a flight path steeper than 6° , sufficient power could be added on the good engine to reach the intended touchdown spot. If reverse thrust is not considered for deceleration, there would be little reduction in landing performance. Although the use of boundary-layer control on both lateral and directional control surfaces can increase their effectiveness and thereby reduce the minimum control speed, the landing problem is not completely alleviated. Loss of an engine will reduce the upper boundary of the STOL envelope by the percentage of power represented by the inoperative engine; therefore, the pilot may still be forced to accept the fact that he is committed to land because of the inability to wave off.

It has been found that reducing speed by the use of high thrust coefficient will also decrease directional stability. The low directional stability in combination with the low airspeed results in a lateral directional oscillation that is easily excited and has quite a long period. Its presence in the YC-134A was quite objectionable even though the damping of the oscillation meets the current military specification in cycles to damp to half amplitude. This suggests that the parameter time to damp to half amplitude might be a better criterion when oscillations of long period are involved. It is quite possible that STOL aircraft may require the use of a yaw damper at low speed in order to obtain satisfactory lateral directional characteristics.

It is obvious that as speed is reduced, the control power afforded by aerodynamic surfaces deteriorates rapidly. This situation can be alleviated to some extent by the application of BLC to the surfaces. Figure 7 shows the maximum rolling acceleration obtained with the YC-134A by using drooped ailerons with area suction, and when complemented by spoilers. These accelerations are compared with the value required to obtain a bank angle of 15° at the end of 1 second. (See ref. 5.) The drooped ailerons plus spoilers were considered satisfactory by the pilots down to about 80 knots, whereas the drooped ailerons without spoilers were unsatisfactory at the same speed. Also shown in this figure is the rolling acceleration that would be expected with blowing applied to the ailerons. It is felt that the increase in effectiveness should be sufficient to provide satisfactory control for maneuvering down to a somewhat lower airspeed. However, in order to obtain further increases in control power, it would be necessary to immerse the ailerons or spoilers in the propeller slipstream or to use differential propeller thrust.

CONCLUDING REMARKS

In this paper the operating envelope of an STOL aircraft has been examined, and limitations have been pointed out which the pilot must consider when choosing his minimum approach speed. Flight and wind-tunnel tests have demonstrated the ability of transport-type airplanes to utilize propeller slipstream effects in conjunction with conventional high-lift devices to obtain short landing distances. These tests indicate that the landing distance can be halved. To realize this reduction a thrust-to-weight ratio of the order of 0.4 will be required. To obtain further significant gains would require much higher thrust-to-weight ratios and would lead to the complexity and expense of the VTOL vehicles. The problems reviewed in the paper would be, in the main, also representative of those of a large overloaded VTOL aircraft operating in an STOL manner with comparable thrust-to-weight ratios.

REFERENCES

1. Weiberg, James A., Griffin, Roy N., Jr., and Florman, George L.: Large-Scale Wind-Tunnel Tests of an Airplane Model With an Unswept, Aspect-Ratio-10 Wing, Two Propellers, and Area-Suction Flaps. NACA TN 4365, 1958.
2. Griffin, Roy N., Jr., Holzhauser, Curt A., and Weiberg, James A.: Large-Scale Wind-Tunnel Tests of an Airplane Model With an Unswept, Aspect-Ratio-10 Wing, Two Propellers, and Blowing Flaps. NASA MEMO 12-3-58A, 1958.
3. Weiberg, James A., and Page, V. Robert: Large-Scale Wind-Tunnel Tests of an Airplane Model With an Unswept, Aspect-Ratio-10 Wing, Four Propellers, and Blowing Flaps. NASA TN D-25, 1959.
4. Lovell, J. Calvin, and Lipson, Stanley: An Analysis of the Effect of Lift-Drag Ratio and Stalling Speed on Landing-Flare Characteristics. NACA TN 1930, 1949.
5. Anderson, Seth B.: An Examination of Handling Qualities Criteria for V/STOL Aircraft. NASA TN D-331, 1960.

REPRESENTATIVE STOL VEHICLES

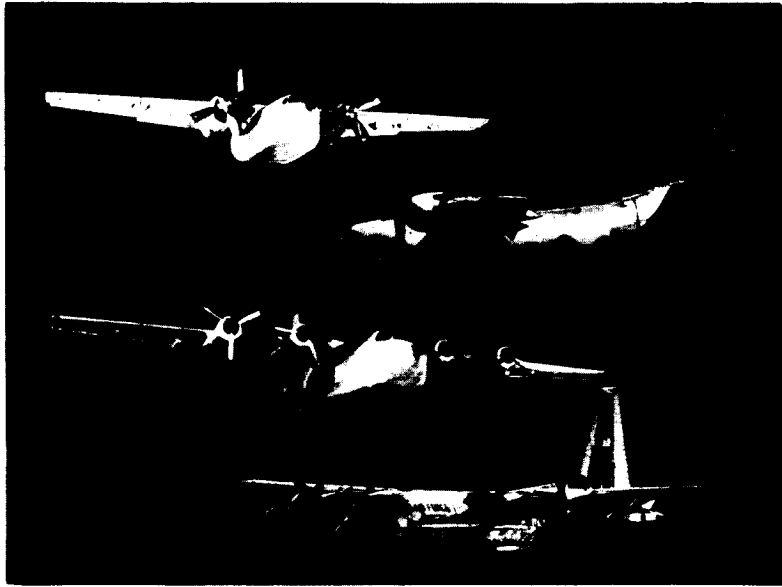


Figure 1

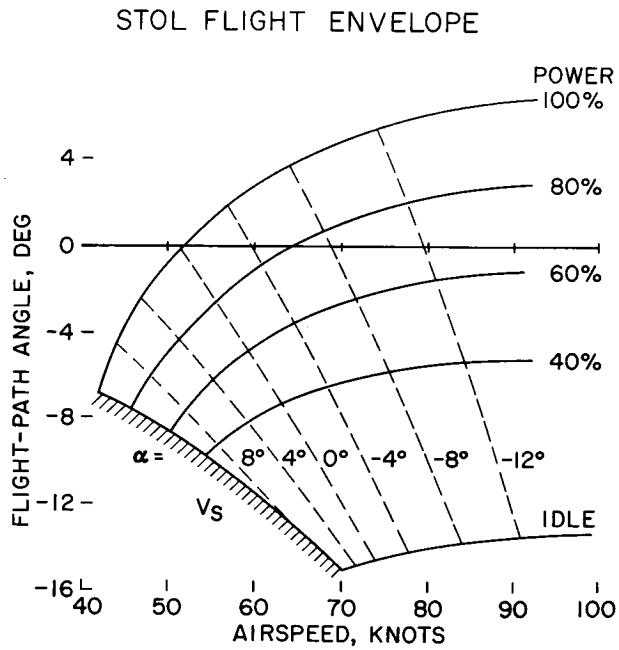


Figure 2

LIMITATIONS IMPOSED BY THE PILOT

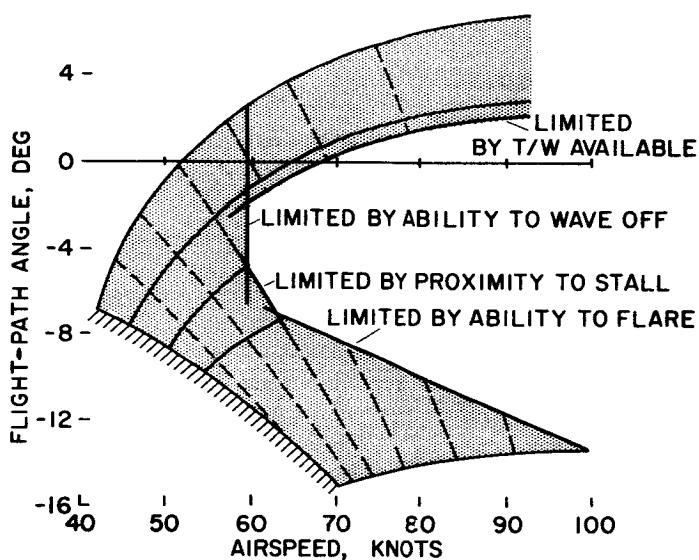


Figure 3

EFFECT OF FLIGHT-PATH ANGLE ON TOTAL LANDING DISTANCE

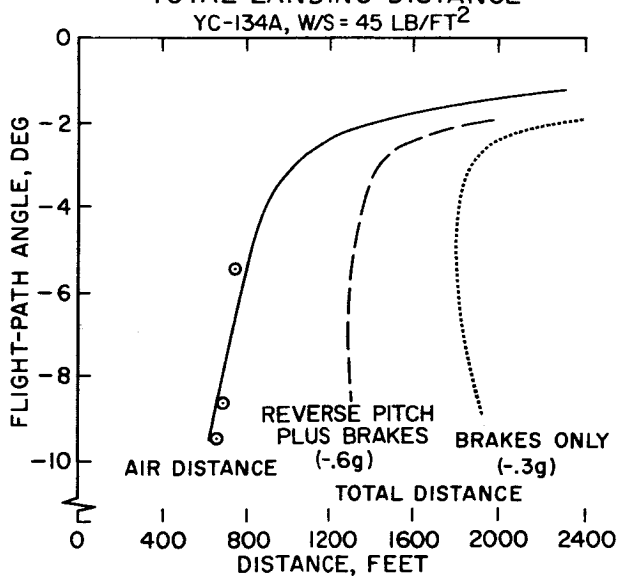


Figure 4

EFFECT OF USE OF HIGH-LIFT DEVICES
ON TOTAL LANDING DISTANCE

W/S = 45 LB/FT², BRAKES ONLY

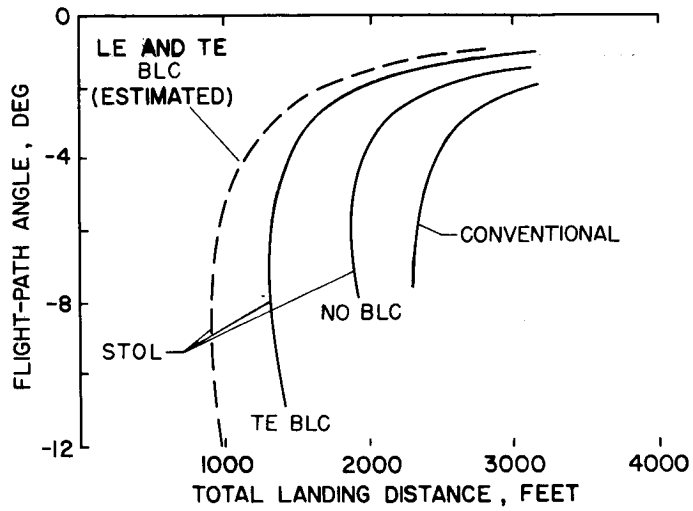


Figure 5

LIMITATIONS DUE TO ONE ENGINE INOPERATIVE

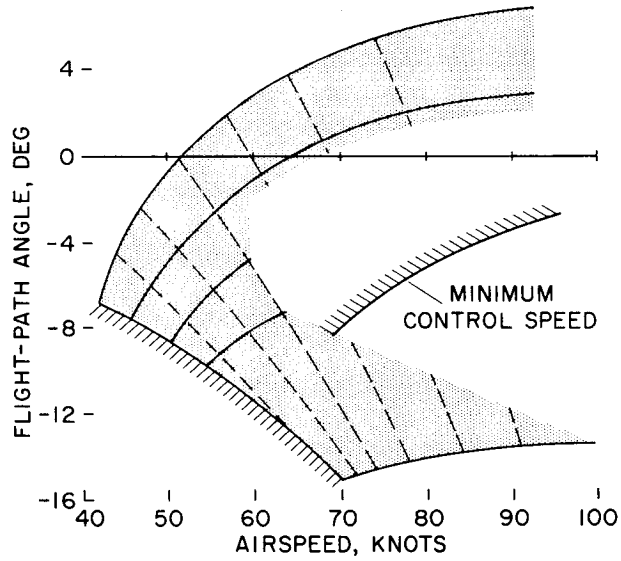


Figure 6

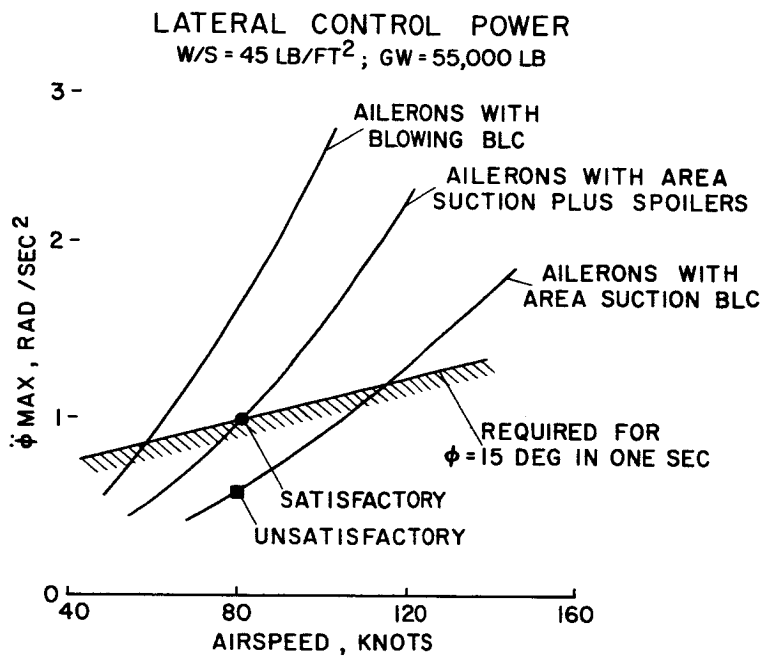


Figure 7

CONSIDERATIONS OF THE EFFECT OF VTOL DOWNWASH
ON THE GROUND ENVIRONMENT

By Thomas C. O'Bryan

Langley Research Center

This paper will consider VTOL downwash from the standpoint of ground erosion and movement of objects to determine the present status of the downwash problem.

The first problem which will be considered is the erosion effect of the downwash. Figure 1 indicates the dynamic pressure required to start erosion for a number of ground surfaces. This information is a summary of small-scale erosion tests reported in reference 1 except for the example of loose crushed rock at 19 lb/sq ft. This example was obtained from an incident with the Vertol VZ-2 operating over an area covered with loose rock which resulted in damage to the airplane. All data shown in figure 1 were obtained with the use of cold jets. Since sod withstands erosion at dynamic pressures up to 1,000 lb/sq ft, operation of jet VTOL aircraft over this surface would appear feasible. Landings of the Bell X-14 and Short S.C.1 on sod have, in fact, verified this feasibility. Experience indicates, however, that hot jets operating over sod would eventually burn off the grass and dry out the soil with resulting erosion.

The most serious effect of erosion arises when the dynamic pressure is sufficient to dig a crater in the ground, a condition which is usually imminent once erosion starts. The crater not only represents a source of material to be recirculated, but in addition, the sides of the crater provide a path for the eroded material to be projected vertically into the rotor.

In addition to the crater problem, eroded material moving radially may encounter large enough objects on the surface of the ground to project them vertically into the rotor or onto the airframe.

The flow field around a hovering aircraft determines the extent of the area to which these considerations apply. A schematic illustration of the flow field is shown in figure 2. The presence of the ground turns the flow from a vertical to a horizontal direction, and it is this flow of air parallel to the ground which is of concern. Measurements of the dynamic pressure of the outward flow of air were made with a vertically traversing pitot head at several radial distances from the center of the rotor. The height of the rotor above the ground varied from about

1/3 diameter to 1 diameter, so the effect of rotor height on the flow field is not considered significant.

Typical results of these surveys for a 35-foot rotor are shown in figure 3. Shown in this figure is the variation of the ratio of dynamic pressure to disk loading $\frac{q}{T/A}$ with height above the ground measured in diameters h/D . The data indicate a general geometric similarity of the profiles and a decrease in maximum dynamic pressure as distance from the rotor is increased. Inasmuch as these profiles indicate that the height of this sheet of air is nearly constant, momentum considerations would indicate that this decrease in dynamic pressure with increase in distance from the rotor would be expected because as the radial distance (the distance in all directions from the center of the rotor) increases, the circumference of the sheet of air increases linearly with distance. Therefore the flow area increases and continuity requires that the velocity must decrease. From these considerations it would be expected that the dynamic pressure would decrease inversely as the square of the radial distance.

A typical decay of the maximum dynamic pressure with increase in distance from a rotor x/D is shown in figure 4. Here the ratio of the maximum dynamic pressure divided by the disk loading is plotted as a function of the radial distance for a full-scale 9.5-foot rotor and for a 28-inch-diameter model and is compared with the calculations based on the previous considerations. The actual decay is somewhat more rapid than this simple estimate as a result of the mixing of the flow with the still air above it and the friction with the ground beneath as the flow moves away from the source.

These results have been presented nondimensionally; in the practical case it is of interest to compare the actual q at a given distance from the aircraft for different disk loadings. To facilitate this comparison model data have been scaled to full-scale disk loadings. In figure 5 the decay of maximum dynamic pressure of the air flowing along the ground is compared for two 40,000-pound-gross-weight configurations, one with a disk loading of 10 lb/sq ft and the other at half the diameter with a disk loading of 40 lb/sq ft. The main feature to be noted here is that at a reasonable distance from the center the maximum dynamic pressure is equal for the two rotors. Except in the near vicinity of the aircraft dynamic pressure is a function of gross weight or thrust and not a function of disk loading. Moreover as indicated by the sketch at the top of figure 5, the sheet of air flowing along the ground is thinner for the smaller rotor. Figure 6 shows the distribution of dynamic pressure with height above the ground for the two rotors at a distance of 72 feet from the center. The greater depth of the flow for the large rotor indicates that in these regions where dynamic pressure

is equal for the two rotors the large-diameter low-disk-loading machines would produce larger overturning moments to objects under its influence than would the smaller diameter high-disk-loading rotor. However, in the area in the immediate vicinity of the aircraft the erosion problems that may be encountered are a function of disk loading.

The discussion so far has dealt with single-rotor configurations. When multiple rotors are used, interactions can exist which bring in other considerations. Figure 7 is shown in order to discuss the effect of the flow at the plane of symmetry that exists when the flow from two rotors meet. The first point to be made is that the resulting vertical flow of air under the fuselage provides a path for the products of erosion to be recirculated. An example of this is the Vertol VZ-2 incident mentioned previously. In this case the loose rock was projected by the flow into the open fuselage, as well as into the propellers with considerable resulting damage to the machine. It is expected that the situation would have been less severe in the case of a closed fuselage.

Another feature of the flow in the plane of symmetry is that for short distances ahead of and behind the airplane the meeting of the two slipstreams results in an increase in the dynamic pressure of the airflow parallel to the ground. Figure 8 illustrates this effect using model data scaled to full-scale disk loadings. Here is shown the contour line for a constant dynamic pressure of 8 lb/sq ft around a two-propeller configuration. This increase in dynamic pressure shows up as the peak in the contour line ahead of the nose. Also shown is the contour line for a constant dynamic pressure of 8 lb/sq ft that would be obtained with a single rotor of the same disk loading. It can be seen that for practical purposes there is little difference between these contours. Thus the effects of the interaction of these two flows are confined to the immediate vicinity of the airplane.

CONCLUSIONS

In conclusion, ground erosion becomes a serious problem as disk loading is increased, and operating experience is needed to define the tolerable limits.

The problems associated with increased disk loading are confined to the immediate vicinity of the aircraft. Except for this area in the vicinity of the aircraft the dynamic pressure of the outward flowing sheet of air is dependent only on the gross weight of the aircraft. Furthermore, the thickness of this outward flowing sheet of air decreases directly with decreases in the diameter of the slipstream.

REFERENCE

1. Kuhn, Richard E.: An Investigation To Determine Conditions Under Which Downwash From VTOL Aircraft Will Start Surface Erosion From Various Types of Terrain. NASA TN D-56, 1959.

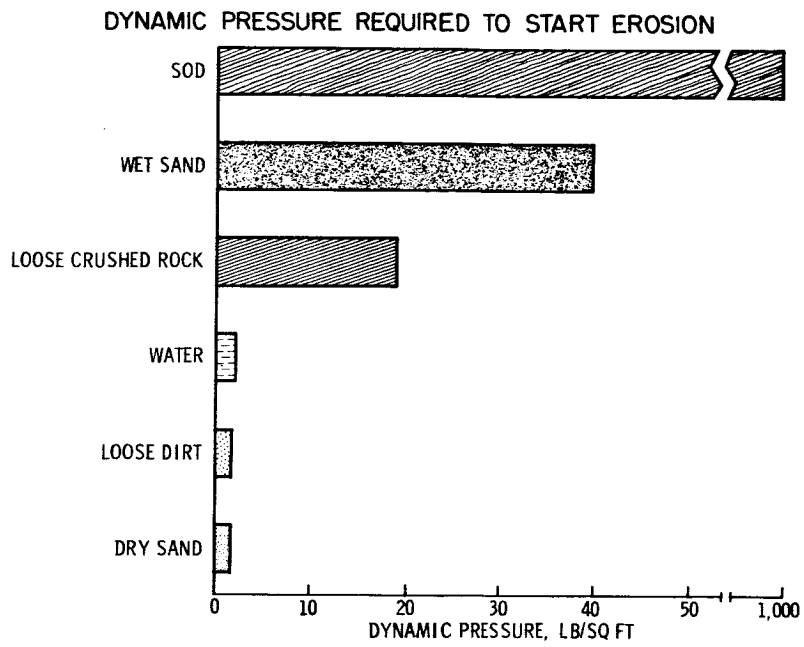


Figure 1

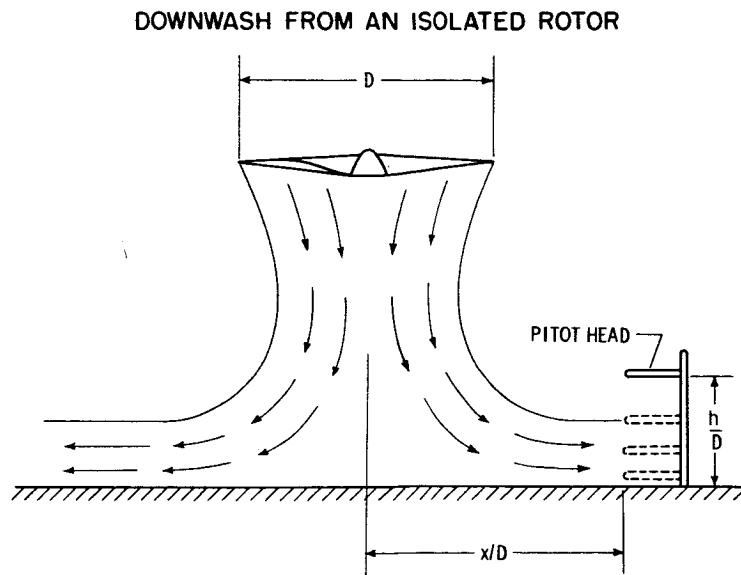


Figure 2

DYNAMIC-PRESSURE PROFILE FOR ISOLATED ROTOR MEASURED ON RADIAL LINE FROM CENTER OF ROTATION

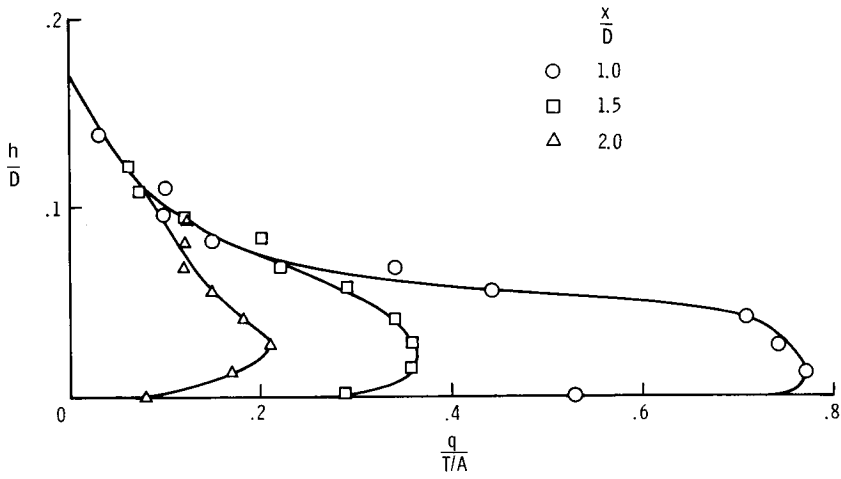


Figure 3

COMPARISON OF ESTIMATED AND MEASURED DYNAMIC-PRESSURE DECAY

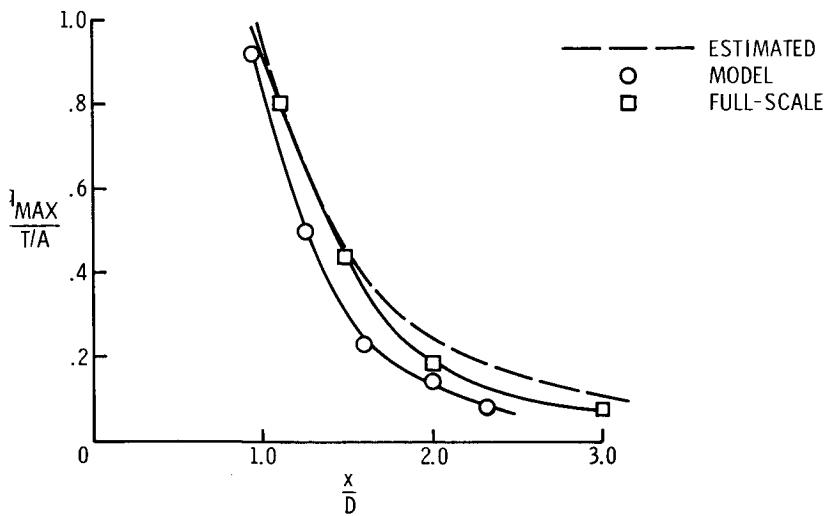


Figure 4

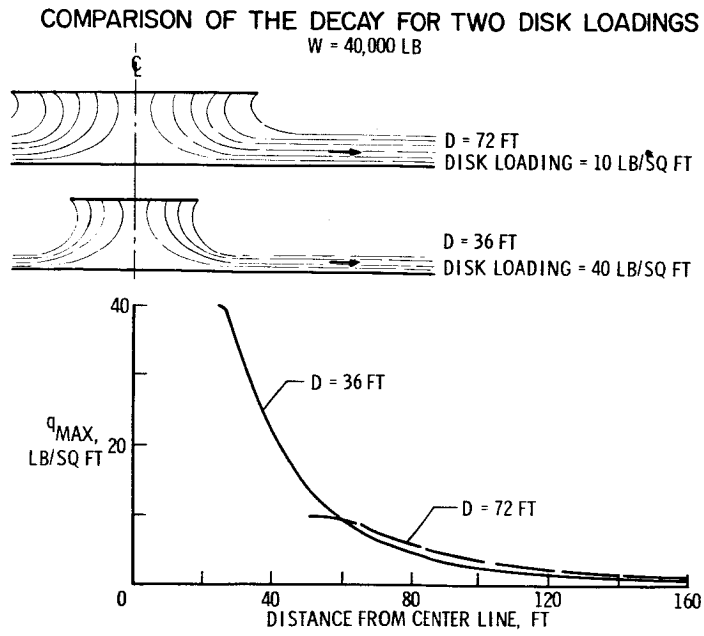


Figure 5

THICKNESS OF DYNAMIC PRESSURE PROFILES
 $W = 40,000 \text{ LB}; x = 72 \text{ FT}$

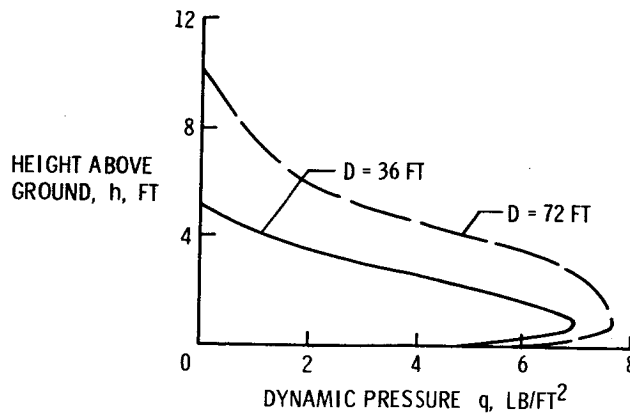


Figure 6

THREE-DIMENSIONAL SLIPSTREAM PATTERN

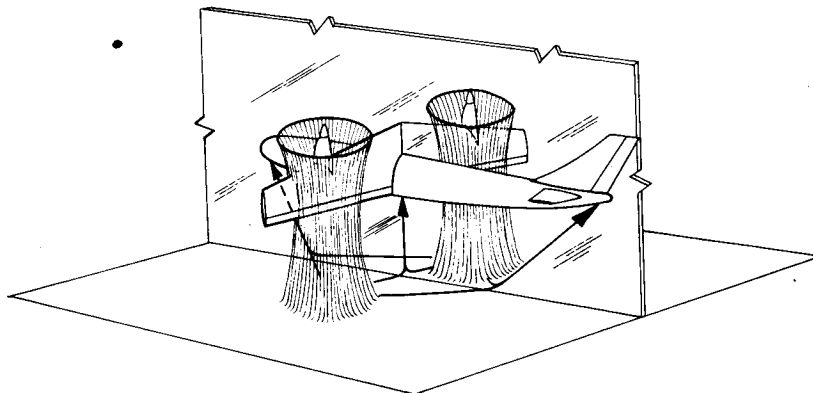


Figure 7

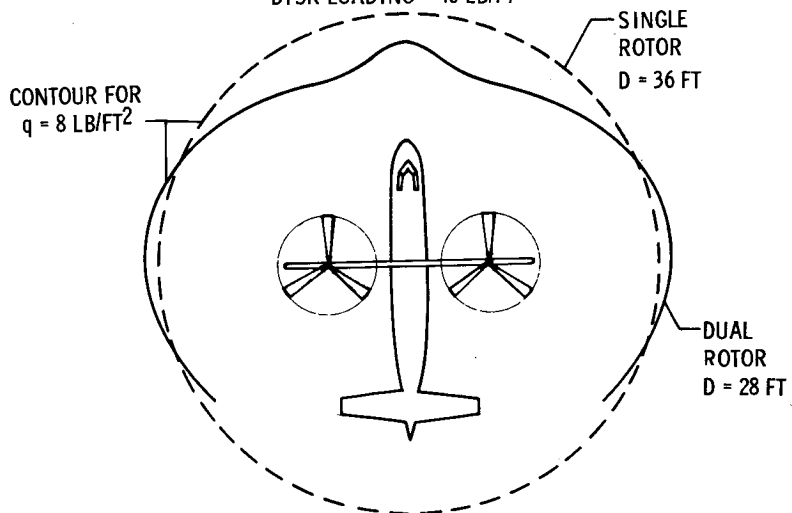
GROUND DYNAMIC PRESSURE CONTOUR
FOR HOVERING VTOLDISK LOADING = 40 LB/FT^2 

Figure 8

NOISE CONSIDERATIONS IN THE DESIGN AND OPERATION
OF V/STOL AIRCRAFT

By Domenic J. Maglieri, David A. Hilton,
and Harvey H. Hubbard

Langley Research Center

SUMMARY

Available propulsion-system noise data have been applied to the problems of design and operation of V/STOL aircraft. In particular, considerations have been given to minimizing adverse community reaction for operations between airports and to minimizing detection due to noise for military missions.

For minimizing adverse community reaction, configurations incorporating low-blade-loading rotors, low-tip-speed propellers, or turbofan-type engines are judged to be most satisfactory. For minimizing detection, consideration must be given to minimizing the noise of the generating airplane, having maximum background noise in the vicinity of the observer, and operating the aircraft at minimum altitude.

INTRODUCTION

References 1 and 2 are examples of the many papers which have dealt with proposed configurations and operating practices of V/STOL aircraft. Based on available experience for other types of aircraft, it is believed that the noise problems of V/STOL aircraft will be closely related to their design as well as to the manner in which the aircraft are operated. In the present paper, discussions are included on the noise characteristics of the various propulsion systems and aircraft configurations of interest for V/STOL missions. Design variables and operating conditions affecting the noise generated by this type of vehicle are first discussed from the standpoint of minimizing adverse community reaction and then brief attention is given to the problem of avoiding detection for special military missions.

RESULTS AND DISCUSSION

Effect of Design Variables and Operating Conditions

Assessment of community reaction.- For the purposes of assessing community reaction, the calculated quantity perceived noise level (in PNdb) rather than sound pressure level is used as a basis for comparison. (See ref. 3.) The use of this concept can be discussed with the aid of figure 1. Shown in the figure are sound pressure levels in various frequency bands for propeller and turbojet noise spectra having equal overall sound pressure levels of 100 decibels. It can be seen that the frequency content differs, the greater high-frequency content being associated with the turbojet spectrum. In the perceived-noise-level calculation procedure, the higher frequencies are weighted more than the lower frequencies. For the examples shown in figure 1, this results in a value of 113 PNdb for the turbojet spectrum as compared with a value of 107 PNdb for the propeller spectrum. In order to attach some significance to the difference in the perceived noise levels of the two spectra, a 6-PNdb difference corresponds roughly to a factor of 2 in distance, at least for distances significant for landing and climbout operations. For instance, in the example cited the turbojet aircraft would need to be about twice as far from an observer to be judged equally noisy. The use of the PNdb concept with regard to airport community reaction has been verified, particularly for spectra such as those for propeller and turbojet aircraft. (See ref. 3.) For the purposes of this paper, the PNdb concept is also applied to helicopter noise spectra for which very little experience is available.

Propulsion-system noise generation.- Because of their configurations and the speed ranges in which they are operated, the main sources of noise of V/STOL aircraft are the propulsion systems. As an indication of the types of V/STOL configurations considered and the relative noise-producing characteristics of each, figure 2 has been prepared. In this figure is presented a bar-graph comparison of the perceived noise levels of four types of possible V/STOL configurations; namely, the pure helicopter, two jet-engine lifting types (turbojet and turbofan), and the tilt-wing turboprop. It is assumed that each of these vehicles is capable of carrying a 9,500-pound payload. The data are estimated for an observer station on the ground with the vehicles in full transition in a 10° climbout condition at a distance of 500 feet. This distance of 500 feet was chosen for convenience; however, it is believed that the conclusion would not be markedly different for other distances significant for climbout operations. It can be seen from the extent of the bar graphs in the figure that there is a wide range of perceived-noise-level values depending upon the V/STOL configuration considered. There is also a range of noise levels for each configuration and the

values depend on the range of performance variables. The effects of these variables (blade loading, jet-exhaust velocity, propeller-tip Mach number, etc.) on the perceived noise levels are shown in figures 3, 4, and 5 for the same operating conditions of figure 2 and are discussed in some detail in the following sections.

Helicopter rotors: It is generally realized that for conventional helicopters the exhaust noise of the reciprocating engines is one of the main noise sources. However, it is believed that in a properly designed turbine-powered helicopter, the engine noise can be reduced to the point where it can be assumed that the main source of noise is due to the shedding of vortices from the rotor. (See ref. 4.) The data of figure 3 indicate the nature of this rotor-noise problem and the variables that are significant in noise generation. Perceived noise levels are plotted as a function of blade loading for a range of rotor-tip speeds. It can be seen that the perceived noise levels decrease with decreasing tip speed and with decreased blade loading. The shaded region indicates combinations of rotor-tip speeds and blade loadings that are of current practical interest. For such designs a sizable reduction in tip speed might not be feasible because of the proximity to stall. A more promising approach to reducing the noise would be to decrease the blade loading by the use of additional rotor solidity.

Measurements have indicated that helicopter rotor noise fluctuates in amplitude at a rate corresponding to the blade passage frequency. (See ref. 4.) In the application of the PNdb concept to helicopter rotor noise, no attempt has been made to account for this phenomenon. It is thus believed that the PNdb values for the helicopter of figures 2 and 3 may be lower than they would be if this amplitude modulation effect were properly accounted for.

Jet engines: In the case of the jet-powered V/STOL aircraft, the noise is due to the mixing of the jet exhaust with the ambient air and the nature of this problem is illustrated in figure 4. (For example, see refs. 5, 6, and 7.) Perceived noise levels are shown on the vertical scale as a function of the average jet-exhaust velocity. Data are included for a range of velocities significant for conventional turbojet engine operation (nonafterburning), turbojets with afterburning, and the turbofan engine. It can be seen from the curve that jet velocity has a very strong influence on jet-exhaust noise production and accounts for a wide range of noise levels. Also, it can be seen that the higher noise levels are associated with the high jet-exhaust velocities of the turbojet engines with and without afterburning.

The portion of the curve corresponding to the turbojets without afterburning has been fairly well established, based on present-day operating experience. The use of suppressors of the type now available

results in noise reduction of the order of 4 PNdb. (See refs. 3, 7, 8, and 9.) The present trend, however, is toward the turbofan engine with its large potential noise reduction due to its inherent low jet-exhaust velocity. (See refs. 6 and 7.) Experience with the earlier version of the turbofan engine indicates that the PNdb values are generally higher than those presented in figure 4. These higher noise levels are believed to be due to the combined effects of fan noise and incomplete mixing of the primary and secondary air. (See ref. 6.) Recent advances have been made toward improving the noise characteristics of these engines (ref. 7), and it is believed that the noise levels will finally approach those represented by the turbofan curve shown in figure 4.

Propellers: In the case of turbopropeller aircraft, particularly for the case where compressor and accessory noises are minimized, the main noise source is the propeller. The nature of the propeller-noise problem is illustrated in figure 5. Perceived noise levels are plotted as a function of propeller-tip Mach number M_t for various numbers of blades. The curves have been estimated assuming four propellers of 17-foot diameter absorbing a total of 8,500 horsepower. (See ref. 10.) It is seen that noise may be reduced by either reducing the propeller-tip Mach number or by increasing the number of blades, or both. Most of the proposed high-powered vehicles incorporate four-blade propellers, and it is felt that an increase in the number of blades would result in relatively small noise reductions in addition to lending added complexity. Noise reduction might be more practically achieved by reducing propeller-tip Mach number.

It should be realized that substantial noise reductions for any of the propulsion systems discussed are usually accompanied by performance penalties and these would have to be evaluated for any particular configuration under consideration.

Ground noise patterns.- In order to discuss some of the operational practices that are useful in controlling the noise patterns on the ground, a tilt-wing V/STOL airplane incorporating a turbopropeller propulsion system and capable of carrying a 9,500-pound payload will be used as an example in figures 6, 7, and 8. Such an aircraft as this would have the capability for a wide variety of take-off profiles, two of which are illustrated for comparison in figure 6. As illustrated, the pilot would have the option of throttling back in power and tip speed and still be able to climb at a 10° geometric angle or of maintaining full take-off power and climbing at a 20° geometric angle. In the 20° climb-out condition, the airplane would not be in full transition to the forward flight configuration in order that the floor angle in the cabin could be maintained at an acceptable value for the passengers.

The 105-PNdb ground noise contour patterns for take-off have been calculated for the two cases illustrated in figure 6, and these results are plotted in figure 7 along with comparable data for a conventional propeller-driven transport airplane having a gross weight of about 130,000 pounds. (See ref. 3.) The 105-PNdb contour was arbitrarily chosen as a basis for comparison and may not necessarily be an acceptable level in all communities near airports for this type of operation on a round-the-clock basis. Regardless of the PNdb level chosen to be acceptable, it is felt that the conclusion would not be significantly changed. It can be seen that the reference contour line for the conventional airplane extends out laterally from the flight track approximately 1,600 feet in each direction and extends about 12,000 feet from the point of lift-off. The contours for the V/STOL aircraft extend out to about the same distance laterally but both are foreshortened considerably in the longitudinal direction. It can also be seen that the extent of the ground pattern for the V/STOL aircraft is minimized when the climbout is made at the lower angle. This latter result arises because of the lower horsepower required and because of the additional beneficial effects of a reduction in tip Mach number from 0.76 to 0.61.

Similar data are plotted in figure 8 for the landing approach configuration of the V/STOL aircraft at a 6° geometric angle. Data are shown for a given power rating but for two different propeller-tip Mach numbers M_t , and the results are again compared with available data (ref. 3) for a conventional present-day propeller transport aircraft. It can be seen that at the higher tip Mach number the ground contour extends farther laterally and longitudinally than the corresponding ground contour for the conventional aircraft. At the lower propeller-tip Mach number, however, the resulting ground contour encompasses less area than that for the conventional airplane and extends a shorter longitudinal distance.

Based on a knowledge of the basic noise characteristics of the various V/STOL aircraft of figure 2 and the manner in which they would be operated (ref. 2), some ground noise contours have been calculated for both the landing and take-off conditions. The results for these calculations for the 105-PNdb ground noise contours are presented in table I. In these calculations, a 6° approach angle and a 10° climbout angle were assumed. The sketch at the top of table I includes a runway and it has been assumed that landing and take-off are accomplished in the same direction. The dimension l is the total longitudinal distance covered by the 105-PNdb contours and the dimension w is the maximum lateral extent. The distances l and w are given in the table for the various V/STOL configurations considered. It will be noted from the results of reference 2 that for the approach angles considered for the V/STOL configuration the associated approach speeds are

considerably lower than those for present-day propeller and jet transport aircraft. In the calculations for table I, 3 PNdb have been added to the perceived noise levels for a given operating condition for each halving of the approach speed in an attempt to account for the associated longer duration of noise exposure. Also included in table I are the distances associated with the operation of a conventional propeller airplane of reference 3. These distances are considered to be representative of current experience.

It can be seen from table I that the smaller distances are associated with the V/STOL turboprop and helicopter and that the larger distances are associated with the jet-powered vehicles. The data also indicate that the noise patterns associated with V/STOL aircraft do not exceed in extent those of a conventional present-day propeller transport aircraft. This result suggests that from a noise standpoint, V/STOL aircraft could probably operate satisfactorily into and out of conventional airports. If, however, operations are proposed for smaller area short-haul terminals, then the ground distances involved may constitute a serious problem in land acquisition.

It should be noted that in the case of operation of V/STOL aircraft which are sensitive to wind direction so that take-off and landing operations may have to be accomplished in many directions, the term w may not be significant and the term λ would apply in all directions. An additional problem, not discussed in this paper but which may be of concern in the operation of V/STOL aircraft, is the generally higher noise levels anticipated within the terminal areas.

Detection of Aircraft by Means of Noise

The detection of aircraft by means of noise is of particular concern for military vehicles such as V/STOL aircraft which might be used in special tactical missions. Recently, some studies have been made to determine how far a propeller airplane could be detected by hearing. (See ref. 11.) Based on this experience some estimates have been made of the detection distances of a four-engine V/STOL turbopropeller aircraft of 6,000 horsepower and having a propeller-tip Mach number of 0.53. The basic concepts involved are illustrated in figure 9. The noise levels in the various frequency bands are shown for the airplane at various distances and also for two assumed background noise spectra at an observer station - one associated with the noise of a residential area of a city and the other (the lower curve) with that of a quiet countryside (ref. 11). The data for the top dashed curve were estimated for the aircraft at a distance of 500 feet. The data for the aircraft at the other distances were calculated based on the values for 500 feet and by including atmospheric propagation losses (ref. 12).

It can be seen that the atmospheric losses attenuate the high-frequency parts of the spectra at a more rapid rate than the low-frequency parts.

For the purposes of this discussion it is assumed that detection is possible when any portion of the airplane noise spectrum lies above the background noise spectrum. For the conditions of a background noise corresponding to a residential city area, this detection distance is approximately 50,000 feet, and it appears that the frequency band of 300 to 600 cps is most significant in this particular case. For some special cases where the noise has distinctive characteristics, detection may be possible at greater distances. It should be noted that this detection distance is a function of the three main variables; namely, the background noise conditions at the observer station, the noise characteristics of the airplane, and the noise propagation phenomena involved. The manner in which detection distance is affected by each of these variables, zero wind being assumed, is shown in figures 10 and 11.

As previously noted, the atmospheric propagation losses are a significant part of the detection problem. There are also significant effects of terrain, and these effects are illustrated in figure 10. Shown in the figure are combinations of altitude and horizontal distance for which detection is possible, that is, areas within the curved boundaries. It has been found that when the elevation angle measured from the observer to the airplane is 7° or greater, atmospheric effects are significant and this determines the shape of the boundary curve, in this case above an altitude of about 3,000 feet. At lower elevation angles, terrain effects become significant and they determine the shape of the lower portion of the boundary curve (ref. 11). The dashed-line boundary corresponds to conditions of open terrain, whereas the solid-line boundary corresponds to conditions of heavily wooded terrain. The shaded region between these curves is thus an indication of the order of magnitude of the effects of the type of terrain. The effects of terrain, therefore, are such that they greatly reduce the distances over which detection is possible for low elevation angles.

The manner in which the background noise level and engine operating conditions may affect the detection distances is indicated in figure 11. Boundary curves are shown for areas where detection is possible for the case in which the condition of heavily wooded terrain is assumed. The lower boundary curve indicates the detection distances for the aircraft at the high-speed cruise condition for a background noise corresponding to a residential area of a city. For the same background noise level, reducing the power and propeller-tip Mach number results in the middle boundary curve. It can be seen that this low-speed cruise condition generally results in large reductions in the detection distances at a given altitude. Assuming this low-speed cruise condition and an increase in the background noise level of about 10 db to a level representing city

traffic leads to further reductions in the detection distances, as indicated by the boundary curve at the left.

The manner of operation of the aircraft and the background noise conditions at the observer station are seen to have rather large effects on the detection distances for the intermediate range of airplane altitudes. However, if the airplane is operated at minimum altitude, the range of detection distances is seen to be relatively small for the wide range of operating conditions and background levels assumed.

It should be noted that the actual detection distance in the presence of wind will be either less than or greater than those indicated in figure 11, depending on whether the observer is upwind or downwind, respectively, of the generating aircraft. (See ref. 11.)

L
1
4
3
0

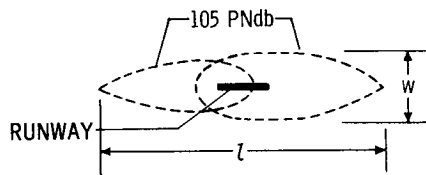
CONCLUDING REMARKS

Operating procedures and design concepts in the interest of noise reduction for several V/STOL aircraft have been discussed from the standpoint of minimizing adverse community reaction for commercial operations and avoiding detection for special military missions. For minimizing adverse community reaction, configurations incorporating low-blade-loading rotors, low-tip-speed propellers, or turbofan-type engines are judged to be most satisfactory. For minimizing detection, consideration must be given to minimizing the noise of the generating airplane, having maximum background noise in the vicinity of the observer, and operating the aircraft at minimum altitude.

REFERENCES

1. Kuhn, Richard E.: Review of Basic Principles of V/STOL Aerodynamics. (Prospective NASA paper.)
2. Staff of Langley Research Center: A Preliminary Study of V/STOL Transport Aircraft and Bibliography of NASA Research in the VTOL-STOL Field. NASA TN D-624, 1961.
3. Bolt Beranek and Newman Inc.: Studies of Noise Characteristics of the Boeing 707-120 Jet Airliner and of Large Conventional Propeller-Driven Airliners. Prepared for The Port of New York Authority, Oct. 1958.
4. Hubbard, Harvey H., and Maglieri, Domenic J.: Noise Characteristics of Helicopter Rotors at Tip Speeds up to 900 Feet Per Second. Jour. Acous. Soc. of America, vol. 32, no. 9, Sept. 1960, pp. 1105-1107.
5. North, Warren J., Callaghan, Edmund E., and Lanzo, Chester D.: Investigation of Noise Field and Velocity Profiles of an Afterburning Engine. NACA RM E54G07, 1954.
6. Greatrex, F. B.: By-Pass Engine Noise. Preprint No. 162C, Soc. Automotive Eng., Apr. 1960.
7. Gordon, Bruce J.: The Noise Control Efforts of Engine Manufacturers. Flight Propulsion Div., General Electric, Nov. 15, 1960.
8. Withington, Holden W.: Silencing the Jet Aircraft. Aero. Eng. Rev., vol. 15, no. 4, Apr. 1956, pp. 56-63, 84.
9. Anon.: Evaluation of Noise for Flight Operations of the Douglas DC-8 Jet Airliner With JT4A-9 Engines and Daisy-Ejector Suppressors. Rep. No. 656, Bolt Beranek and Newman Inc., Consultants in Acoustics, Oct. 26, 1959.
10. Hubbard, Harvey H.: Propeller-Noise Charts for Transport Airplanes. NACA TN 2968, 1953.
11. Hubbard, Harvey H., and Maglieri, Domenic J.: An Investigation of Some Phenomena Relating to Aural Detection of Airplanes. NACA TN 4337, 1958.
12. Parkin, P. H., and Scholes, W. E.: Air-to-Ground Sound Propagation. Jour. Acous. Soc. of America, vol. 26, no. 6, Nov. 1954, pp. 1021-1023.

TABLE I
EXTENT OF GROUND CONTOURS



CONFIGURATION	l , MILES	w , MILES
HELICOPTER	1.2	0.3
TURBOPROP	1.5	.6
TURBOFAN	3.0	.8
TURBOJET	4.0	1.0
CONVENTIONAL PROP	4.5	.7

COMPARISON OF PERCEIVED NOISE LEVELS FOR
TWO SPECTRA HAVING EQUAL OVERALL SPL

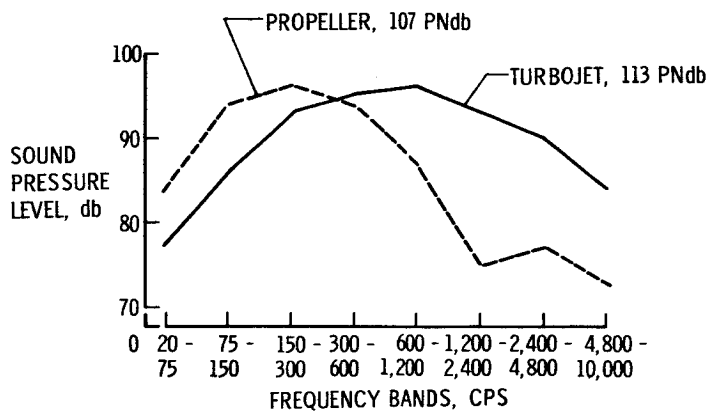


Figure 1

RANGE OF NOISE LEVELS OF V/STOL CONFIGURATIONS
PAYLOAD = 9,500 LB

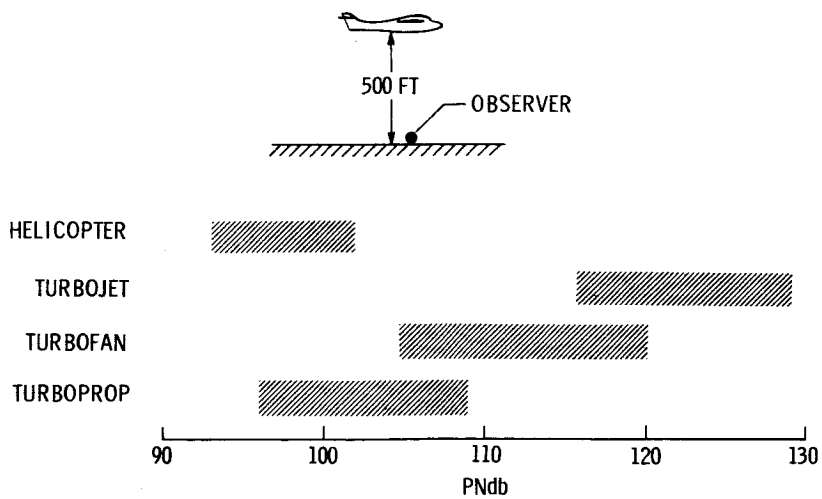


Figure 2

NOISE CHARACTERISTICS OF HELICOPTER ROTORS

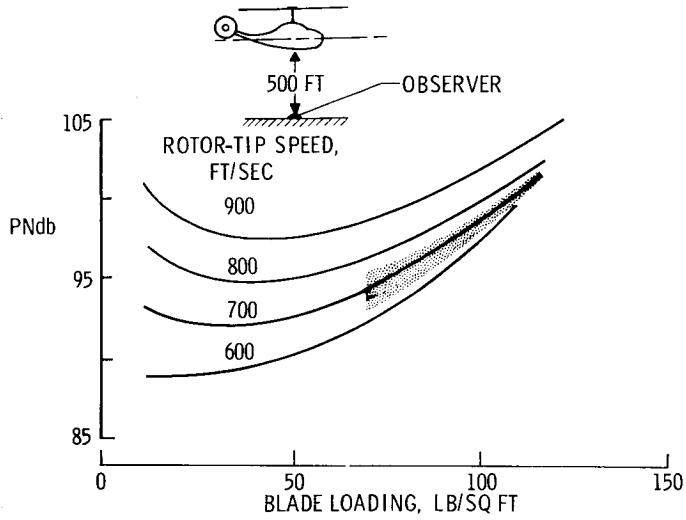


Figure 3

EXHAUST NOISE FROM JET ENGINES

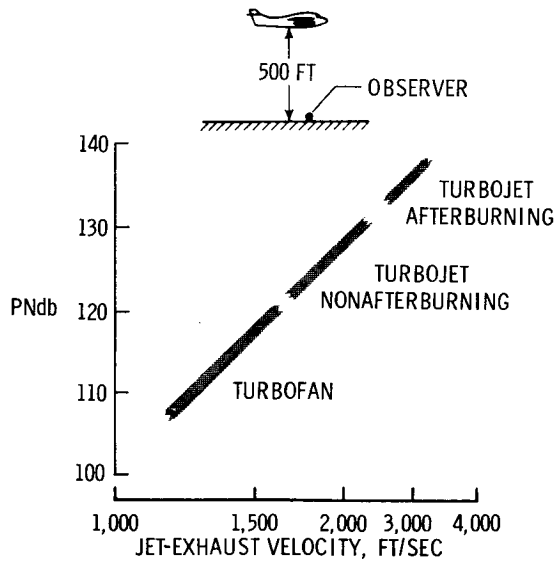


Figure 4

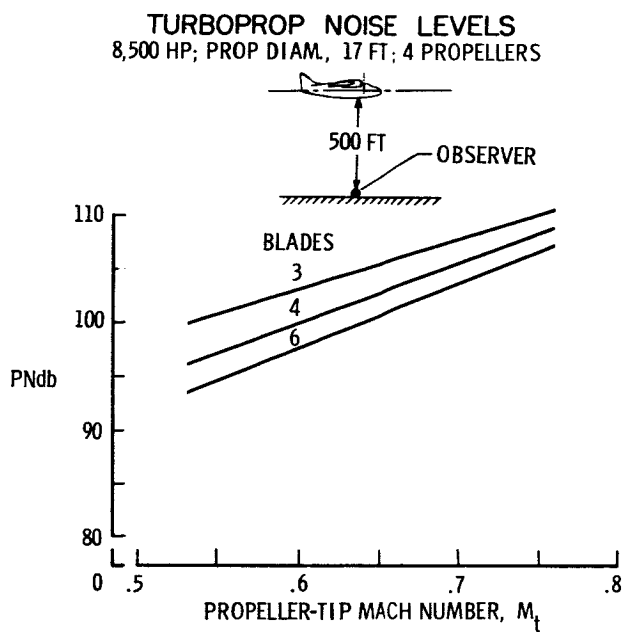


Figure 5

TURBOPROP V/STOL AIRCRAFT TAKE-OFF PROFILES

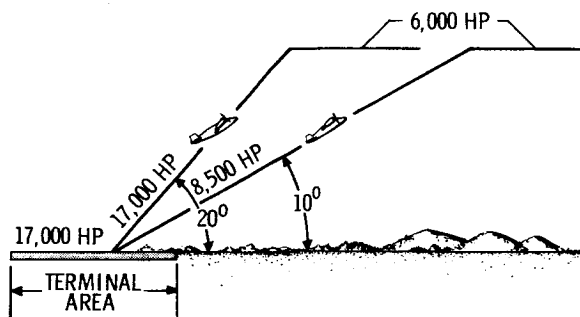


Figure 6

GROUND NOISE CONTOURS FOR TAKE-OFF

105 PNdb

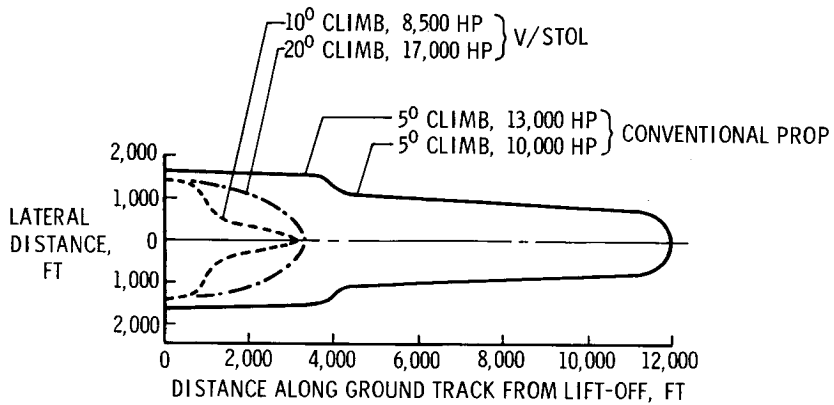


Figure 7

GROUND NOISE CONTOURS FOR LANDING

105 PNdb

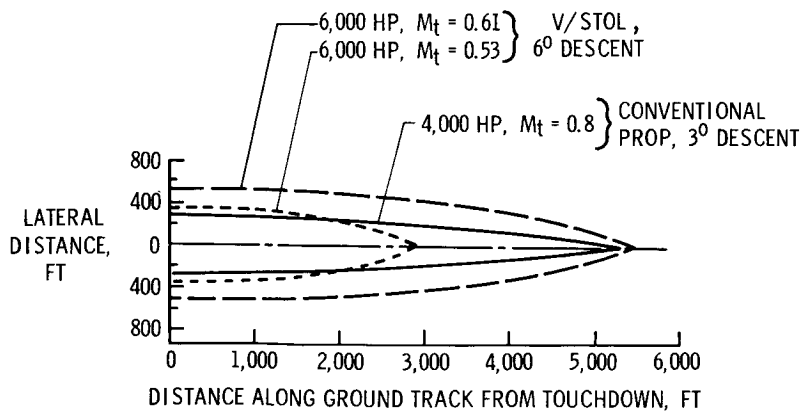


Figure 8

NATURE OF DETECTION PROBLEM FOR V/STOL TURBOPROP AIRPLANE

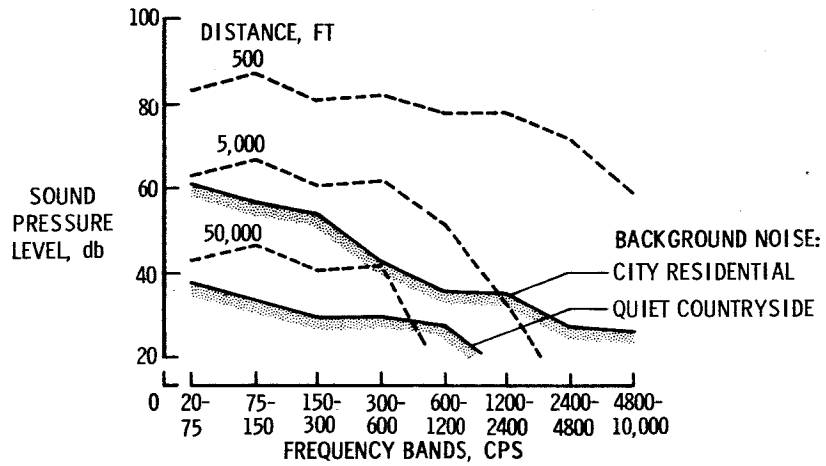


Figure 9

DETECTION DISTANCE FOR V/STOL TURBOPROP AIRPLANE EFFECT OF TERRAIN

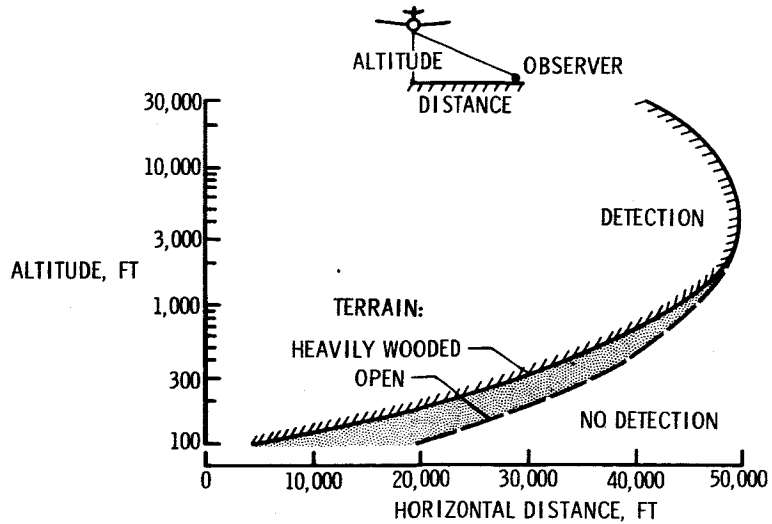


Figure 10

DETECTION DISTANCE FOR V/STOL TURBOPROP AIRPLANE
EFFECTS OF BACKGROUND NOISE AND ENGINE OPERATING CONDITIONS

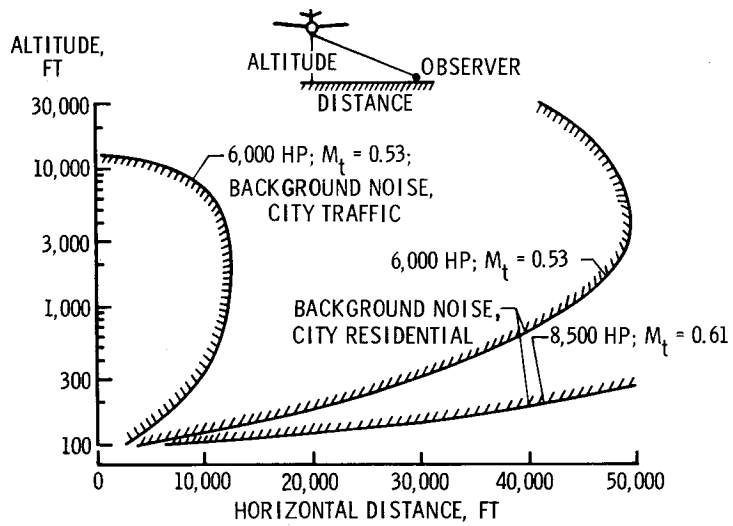


Figure 11

SOME RECENT STUDIES IN STRUCTURAL DYNAMICS
OF ROTOR AIRCRAFT

By George W. Brooks and Milton A. Silveira

Langley Research Center

SUMMARY

This paper presents a summary of four recent studies relating to the structural-dynamics problems of rotor-powered aircraft. The first study concerns the measurement by means of dynamic models of the forces and moments at the hubs of various rotor configurations. The results of this study show that the periodic components of the forces and moments are highly dependent on both the rotor configuration and the flight condition.

The second study treats the problem of resonance amplifications of rotor-blade stress and shows that by using multiple flapping hinges or flex-joints it is possible to control the natural frequencies of the rotor blade so that conditions of resonance between the frequencies of the aerodynamic input forces and the natural frequencies of the lower blade modes are avoided for all rotor speeds.

Two studies of the stability of rotor aircraft are also discussed. One of these involves the mechanical instability or ground resonance of rotorcraft wherein the rotor support in each of two mutually perpendicular directions in the rotor plane is represented as a multiple-degree-of-freedom system in contrast to the system having a "single" degree of freedom normally used in helicopter analysis. The consideration of the rotor support system as a two-degree-of-freedom system predicts additional unstable ranges of rotor speed not predicted by former analyses. The other instability treated is propeller whirl for which the significant motions are the pitching and yawing motions of the propeller disk which are coupled together by gyroscopic forces. The effect of the significant variables on the instability is presented and shows that the speed at which the instability occurs can be increased by increasing the relative stiffness of the propeller in the pitch and yaw directions or by increasing the effective structural damping of the nacelle.

INTRODUCTION

The importance of structural-dynamics problems in the development and use of rotor-powered aircraft is well recognized, and the interest

in these problems continues as the state of the art is advanced. Although it is necessary to reevaluate the problems as major developments in performance or changes in configuration occur, the basic situation remains that these aircraft are subjected during flight operations to a variety of aerodynamic loads and load distributions and they may encounter several types of instability such as ground resonance, propeller whirl, and flutter.

In the design of these aircraft to minimize the response of the structure to the loads imposed in flight and to avoid instabilities, it is necessary to know the nature and magnitudes of the applied loads and to define and control the system characteristics such as component natural frequencies.

This paper will briefly discuss some aspects of four recent studies relating to structural-dynamics problems of rotor-powered aircraft. These include: (1) the determination of the force and moments at the hubs of various rotor configurations; (2) the use of multiple flapping hinges to control the natural frequencies of rotor blades; (3) the effect of additional degrees of freedom in the rotor support on the mechanical stability of rotors; and (4) the effect of stiffness and damping on the gyroscopic whirling stability of propellers.

SYMBOLS

a_1	radial location of first flapping hinge, ft
a_2	radial location of second flapping hinge, ft
a_3	radial location of third flapping hinge, ft
b_a	normalized imaginary part of root of characteristic equation $b_a = \frac{b}{\omega_r}$
F_{VIB}	vibratory component of axial force, lb
F_{STEADY}	steady component of axial force, lb
g	structural damping coefficient
N	integer number
R	rotor radius, ft

V	forward velocity, ft/sec
V_d	reference forward velocity, ft/sec
α	rotor angle of attack, deg
θ	collective pitch angle of rotor blades, deg
μ	tip-speed ratio, $\frac{V \cos \alpha}{\Omega R}$
ϕ	propeller pitch angle, deg
ψ	propeller yaw angle, deg
ω_n	natural frequency of nth mode of rotor blade, radians/sec
ω_r	reference frequency, radians/sec
Ω	rotational frequency, radians/sec
Ω_a	normalized rotational frequency, Ω/ω_r

RESULTS AND DISCUSSION

A Study of the Periodic Forces and Moments at the Rotor Hub

This section of the paper treats the variations of the forces and moments at the hub of various rotor configurations.

A wind-tunnel investigation has been conducted with the use of model rotors on a dynamic balance which is capable of measuring the steady and periodic components of the forces and moments about three mutually perpendicular axes through the hub as shown in figure 1. The forces and moments were measured over a range of operating conditions for four rotor configurations which included a two-, three-, and four-blade flapping rotor and a two-blade teetering rotor. All rotor configurations employed identical blades with a chord of 2.06 inches and a solidity of 0.02 per blade. The blades were scaled to possess dynamic properties representative of those in current use. The rotor diameter was 66 inches. The variables studied included collective pitch angles of 0° , 3° , and 6° ; rotor angles of attack of -10° , -5° , 0° , and 5° ; and variations of rotor speeds and tunnel speeds to encompass a range of tip-speed ratios from 0 to 0.45.

The measured loads were harmonically analyzed to determine the magnitudes and frequencies of the periodic components. Some typical samples of these data are presented in figures 2 and 3 for a collective pitch angle of 3° and a rotor angle of attack of -5° .

The Nth harmonic vibratory components of the axial force for N-blade flapping rotors are plotted as a function of tip-speed ratio in figure 2. The ordinate is the ratio of the vibratory force to the steady force measured at that tip-speed ratio, and data are presented for the two-, three-, and four-blade flapping configurations. Figure 3 presents a comparison of similar data for the two-blade flapping and teetering configurations. These initial results indicate that the vibratory forces increase slightly as the tip-speed ratio increases from zero and then decrease before rising sharply at the higher tip-speed ratios. In general, the data show that the variation of the vibratory forces with μ exhibits trends which are similar to the measured vibration trends on rotorcraft, and that the magnitudes of the vibratory forces are highly dependent on both the flight condition and rotor configuration.

The Use of Multiple Flapping Hinges or Flex-Joints to Control the Natural Frequencies of Rotor Blades

An analytic study has been conducted to investigate the control of the natural frequencies of rotor blades by means of multiple flapping hinges and this section of the paper will present some of the results of that study. A typical rotor frequency diagram for a conventional blade is shown in figure 4. The frequencies of the applied aerodynamic forces and the natural frequencies are presented as a function of rotor speed. The frequencies of the aerodynamic forces are indicated by the straight lines which radiate from the origin, and the natural frequencies of the flapping and first two elastic modes are shown by the dashed lines. For helicopter operation, the rotor speed is restricted to a rather narrow range during normal operation, and the primary problem is to design the blade so that the natural frequencies and aerodynamic input frequencies are as widely separated as possible at these rotor speeds in order to minimize resonant amplifications of blade bending stresses. For some types of V/STOL aircraft, it may be desirable to vary the rotor speed over a significant range to provide optimum performance. An examination of figure 4 shows that it is virtually impossible to vary the rotor speed of a conventional blade without encountering resonance involving some of the modes.

In order to obtain greater control over the natural frequencies and to minimize the resonance problem, a study has been made of a rotor blade which employs "rigid" segments connected by multiple flapping hinges or

flex-joints as shown in figure 5. This figure also presents the frequency diagram for such a blade. The use of multiple flapping hinges permits the natural frequencies of the lower modes at any rotor speed to be placed between the frequencies of the harmonic excitation forces as shown. A wide range of control over these frequencies is available by choice of number of hinges, hinge location, and mass distribution of the segments. For a blade having N flapping hinges, the first N natural frequencies will be multiples of the rotor speed as shown here, and thus the natural frequencies of these modes are fixed relative to the aerodynamic input frequencies at all rotor speeds. In general, the investigation is primarily concerned only with the lower harmonics of the aerodynamic loading, and there seems to be little necessity for more than three hinges. Figure 6 shows the variations in natural frequencies obtainable for a rotor of uniform mass distribution with three flapping hinges where the most inboard hinge is located at 4 percent of the radius ($a_1 = 0.04R$). The first natural frequency is independent of the outboard hinge locations. The locations of the second and third hinges may be selected so that the natural frequencies of the second and third modes of the blades may be fixed as desired relative to the rotor speed. For example, the frequencies for the case shown in figure 5, where the blade natural frequencies are 2.5 and 5.5 times the rotor speed for the second and third modes, respectively, were obtained by selecting $a_2 = 0.4R$ and $a_3 = 0.64R$.

The results of this study show that the blade natural frequencies can be widely varied or controlled by using multiple flapping hinges or flex-joints.

A Study of the Mechanical Instabilities of a Rotor on a Support Having Two Degrees of Freedom

Mechanical instability, commonly called ground resonance, first became a problem with the autogiro, and continued to be a major problem for many types of helicopters. It was found that this instability is not dependent on aerodynamic forces; the energies involved are stored in the rotor by virtue of its rotation. The designs of autogiros and helicopters are such that the balance of mass and spring forces necessary to produce the instability occurs only when the aircraft are in partial or total contact with the ground. However, when rotors are mounted on flexible wings, as in the case of some current and proposed VTOL and STOL aircraft, the instability may occur in flight and result in serious accidents. For the autogiro and the helicopter, the structure which supports the rotor may generally be considered as a system having a "single" degree of freedom in each of the two mutually perpendicular directions in the rotor plane as analyzed in references 1 to 3. For V/STOL configurations, however, the rotor support has at least two degrees of freedom in

any horizontal direction, one of which represents the mass and stiffness of the rotor mount relative to the wing, and another of which represents the mass and stiffness of the wing relative to the fuselage.

A study has been conducted to determine the mechanical instabilities of two-blade teetering rotors applicable to V/STOL aircraft such as shown in figure 7. The degrees of freedom considered in this analysis involve motions which are parallel to the plane of the rotor and include blade chordwise bending, shaft bending, and wing bending and torsion. This analysis differs from previous well-known analyses in that the rotor support is represented as a two-degree-of-freedom system, rather than by a system which has a "single" degree of freedom as treated in reference 1 and in other papers.

A typical stability diagram for the system studied is presented, in a rotating coordinate system, in figure 8. The imaginary parts of all roots of the system (where it is assumed that any characteristic motion is represented by $X = X_0 e^{\lambda_a t}$, where $\lambda_a = a_a + ib_a$) are plotted as a function of the rotor speed. Both the abscissa and ordinate are normalized by dividing through by a reference frequency. The complete system has six degrees of freedom, five of which are coupled and the other uncoupled. The uncoupled mode is that of the antisymmetric chordwise bending mode of the blades. The coupled modes involve motions of the blades, hub, and rotor support system (wing). The natural frequencies are the purely imaginary roots and are shown as the solid lines. This frequency diagram shows that there are five regions (shaded) where one or more of the roots become complex. Further analyses show that the real part a_a of one of these roots in each case is positive, indicating instability. Three of the regions, in which the instabilities are divergent oscillations, are indicated by the vertical shading. This instability is commonly referred to as ground resonance. Two other regions of instability are also indicated by the lightly shaded areas. The motions involved with these instability regions are purely divergent. Each of these two regions is bounded by two so-called critical speeds.

A comparison of the results of this study with those of previous analyses is shown in figure 9. The figure shows that the inclusion of the additional degree of freedom in the rotor support introduces an additional region of pure divergence bounded by two additional critical speeds. Two additional regions of divergent oscillations are also encountered.

All of the mechanical instabilities discussed are subject to control by the inclusion of damping in the system. Both damping of the hub relative to the wing, and of the wing relative to the fuselage, were investigated to determine the effect of damping on the mechanical

instabilities. Figure 10 shows the manner in which the regions for divergent oscillations vary with damping. The damping, in percent critical, is the same for the two uncoupled components (i.e., hubs on wing) and is plotted as a function of rotor speed. As the damping is increased from zero, the width of the first and third instability regions increases, whereas the width of the second region decreases. However, it should be pointed out that the magnitudes of the unstable roots diminish in all cases. As the damping is further increased, all unstable speed ranges close and ultimately disappear.

The results of this study show that the mechanical instability problem for V/STOL aircraft may be substantially different than that for autogyros and helicopters, in that additional degrees of freedom of the system lead to additional possibilities for instability. The use of damping is effective in the elimination of these instabilities; however, from a practical standpoint, the difficulty of obtaining sufficient damping in the wing must be considered.

A Discussion of the Whirling Instability of Propellers

This section of the paper will present a brief introductory discussion of another type of instability called propeller whirl which might be of concern to V/STOL aircraft. As shown in figure 11, the propeller disk undergoes pitching and yawing motions as a result of shaft pitching and yawing relative to the wing, shaft bending, and wing torsion. Gyroscopic forces couple the pitching and yawing motions together, and when the aerodynamic forces are included, an instability can arise.

This instability was recognized many years ago (ref. 4); however, the stiffness levels of airplane engine installations were so high that the instability was of no real concern and further considerations of the problem vanished. Recently, the requirements for increased vibration isolation has led to softer engine mountings. These requirements, coupled with the larger overhangs of power-plant installations and higher flight speeds, have resulted in reduced margins for propeller whirl instability. It is also likely that the rigidity of movable rotor-wing systems such as used on some V/STOL aircraft might be relatively low, and it is therefore important that these systems be examined to be sure that they are stable in this respect.

Some results which have been obtained from studies of conventional aircraft propellers are shown in figure 12. These results give a broad insight into the phenomena and indicate some of the significant variables involved. Further details on the solution of the problem for some specific configurations are given in reference 5. Figure 12 shows the effects of damping and stiffness on the velocities at which whirl instability is encountered. The structural damping coefficient g , which represents

some mean value of the damping of the pitch and yaw motions of the propeller, is plotted as a function of the ratio of velocity to a reference velocity. For the case presented in figure 12, the ratio of damping in the pitch and yaw directions is unity and an increase in g represents an equal increase in damping of the pitch and yaw motions. Curves which separate the stable and unstable regions are presented for different values of relative effective stiffness of the shaft at the propeller hub. This stiffness also corresponds to some mean value of the stiffnesses in the pitch and yaw directions. For the case presented in figure 12 the stiffness is assumed to be equal in the pitch and yaw directions. However, for cases where the stiffness is not equal in the two directions, the trends would still be similar to those shown. In a general study the effects of the various individual parameters should be investigated.

The figure shows that, for a given stiffness level, the instability may be encountered at a low forward speed if the structural damping is low. However, with a small increase in damping, the speed at which the instability occurs is increased substantially. Conversely, for a given value of damping, represented by a horizontal line on the figure, the speed at instability may be substantially increased by increasing the stiffness. This stiffness of course reflects both the stiffness of the propeller shaft and of the wing support structure. Another variable of importance, not shown on this chart, is the effective pivot point. The stability is generally increased as the pivot point is moved rearward. From the standpoint of V/STOL applications, the effect of flapping hinges on this phenomenon may also be significant and should be examined.

CONCLUDING REMARKS

Some recent studies in structural dynamics of rotor aircraft have been reviewed in this paper. The results of these studies are as follows:

1. The results obtained during the measurement of the forces and moments at the rotor hub for various dynamic model rotor configurations indicate that the vibratory components of these forces and moments are dependent upon both the rotor configuration and on the flight condition. A few samples of data are presented which show that the levels of the vibratory forces increase as the tip-speed ratio is increased from zero, and then decrease slightly before rising sharply at the higher tip-speed ratios.

2. The natural frequencies of rotor blades can be controlled by the use of multiple flapping hinges or flex-joints. For a blade having N flapping hinges, the first N natural frequencies will be multiples of the rotor speed. By proper selection of hinge locations, the

frequencies of the rotor blade can be placed between the aerodynamic loading frequencies for all rotor speeds thus reducing resonant amplification of blade stresses.

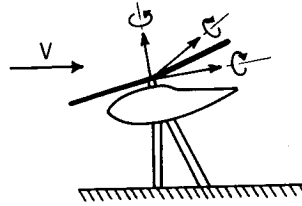
3. The mechanical instability of a rotor may be substantially different from the results of former analyses when considering an additional degree of freedom in the rotor support system.

4. The whirling instability of propellers is dependent upon the structural damping and relative stiffness of the system. The speed at which the instability occurs is increased by increasing either the damping or stiffness of the system.

REFERENCES

1. Coleman, Robert P., and Feingold, Arnold M. (With Appendix B by George W. Brooks): Theory of Self-Excited Mechanical Oscillations of Helicopter Rotors With Hinged Blades. NACA Rep. 1351, 1958. (Supersedes NACA TN 3844.)
2. Deutsch, M. L.: Ground Vibrations of Helicopters. Jour. Aero. Sci., vol. 13, no. 5, May 1946, pp. 223-228, 234.
3. Leone, Peter F.: Mechanical Stability of a Two-Bladed Cantilever Helicopter Rotor. Jour. Aero. Sci., vol. 23, no. 7, July 1956, pp. 633-638.
4. Taylor, E. S., and Browne, K. A.: Vibration Isolation of Aircraft Power Plants. Jour. Aero. Sci., vol. 6, no. 2, Dec. 1938, pp. 43-49.
5. Reed, Wilmer H. III, and Bland, Samuel R.: An Analytical Treatment of Aircraft Propeller Precession Instability. NASA TN D-659, 1960.

SCOPE OF INVESTIGATION OF PERIODIC FORCES AND MOMENTS AT ROTOR HUB



ROTOR CONFIGURATIONS

- 4-BLADE } FLAPPING
- 3-BLADE } FLAPPING
- 2-BLADE } FLAPPING
- 2-BLADE TEETERING

VARIABLES

- COLLECTIVE PITCH ANGLE, $\theta = 0^\circ, 3^\circ, 6^\circ$
- ROTOR ANGLE OF ATTACK, $\alpha = -10^\circ, -5^\circ, 0^\circ, 5^\circ$
- TUNNEL VELOCITY } $\mu = 0$ TO 0.45
- ROTOR SPEED }

Figure 1

Nth HARMONIC OF AXIAL FORCE OF N-BLADE FLAPPING ROTOR

$\theta = 3^\circ; \alpha = -5^\circ$

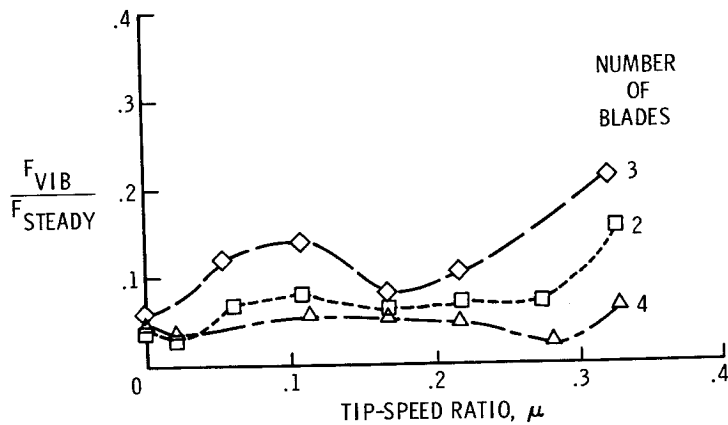


Figure 2

SECOND HARMONIC OF AXIAL FORCE FOR 2-BLADE ROTOR

$$\theta = 3^{\circ}; \alpha = -5^{\circ}$$

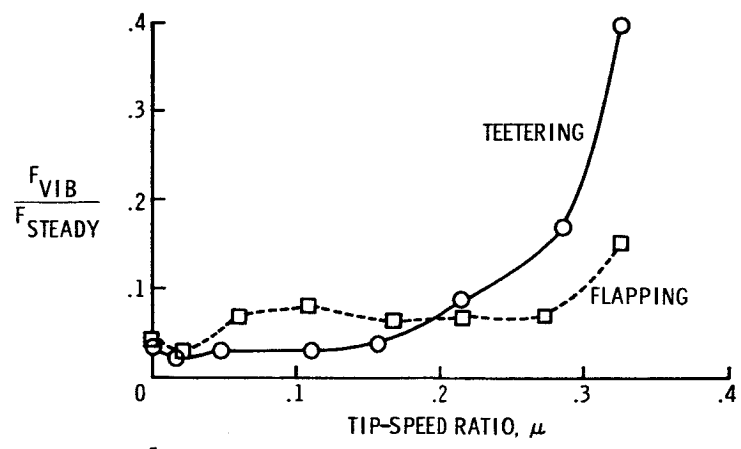


Figure 3

BLADE FREQUENCY DIAGRAM CONVENTIONAL BLADE

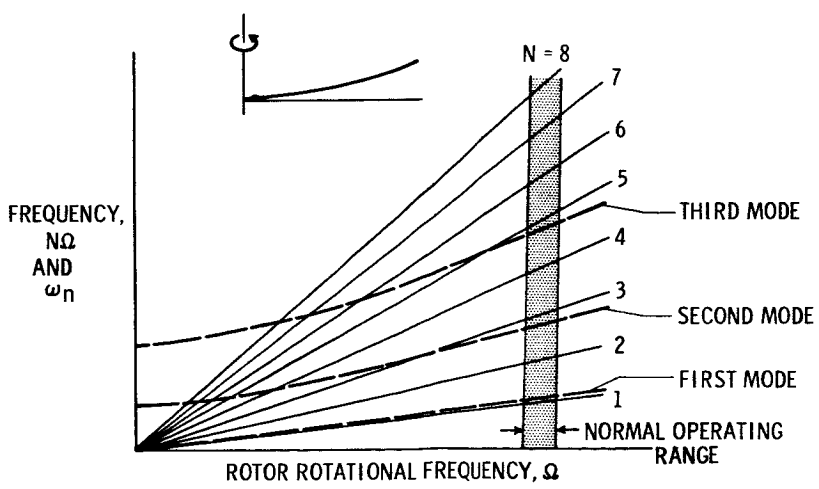


Figure 4

BLADE FREQUENCY DIAGRAM

MULTIPLE-HINGE BLADE

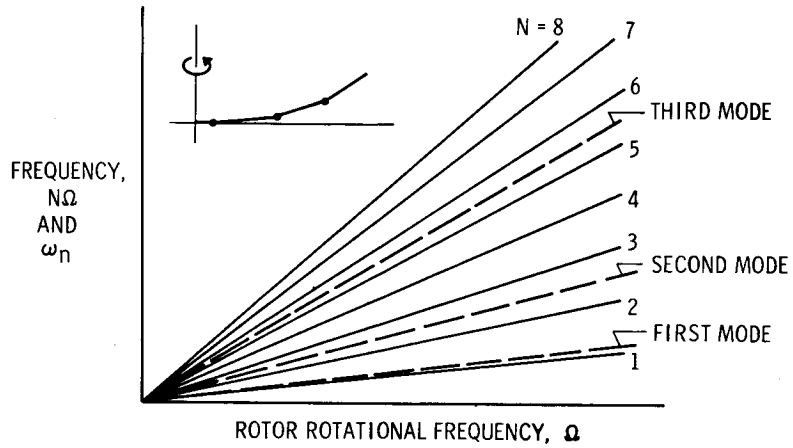


Figure 5

VARIATION OF NATURAL FREQUENCIES OF 3-HINGE RIGID-SEGMENT BLADE WITH HINGE LOCATIONS

$a_1/R = 0.04$

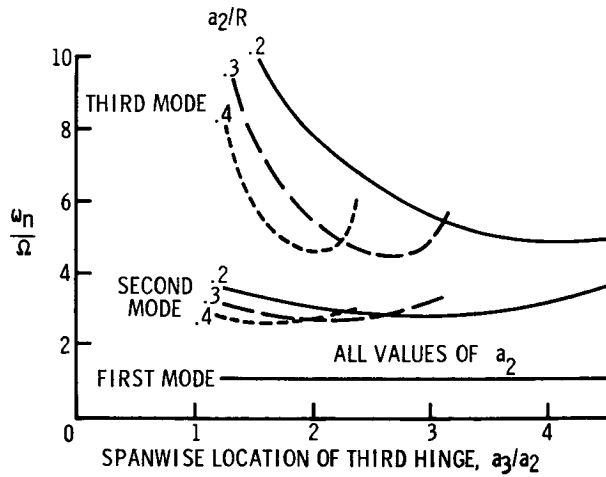
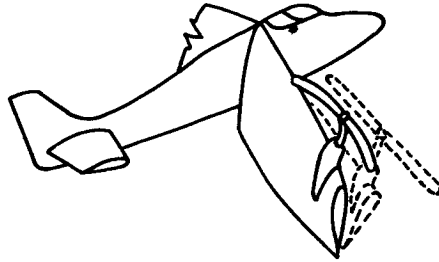


Figure 6

MECHANICAL INSTABILITY OF ROTORCRAFT
AERODYNAMIC FORCES UNNECESSARY



SIGNIFICANT MOTIONS ARE PARALLEL TO ROTOR PLANE:

1. BLADE CHORDWISE BENDING
2. SHAFT BENDING
3. WING BENDING AND TORSION

Figure 7

MECHANICAL INSTABILITIES AND NATURAL FREQUENCIES OF
2-BLADE ROTOR ON 2-DEGREE-OF-FREEDOM SUPPORT

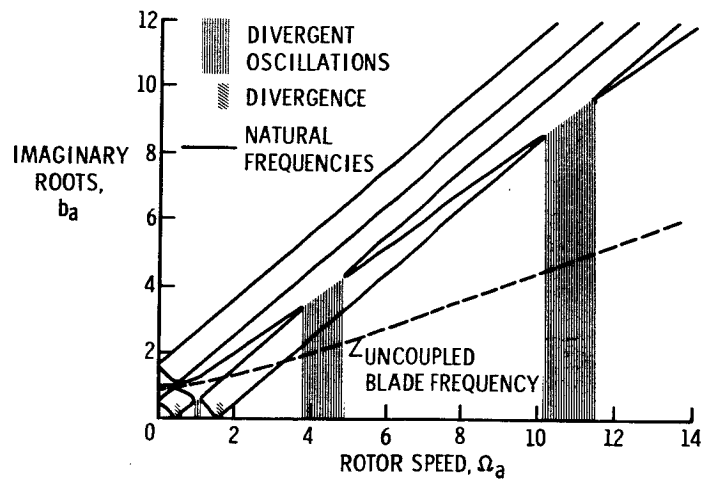


Figure 8

MECHANICAL INSTABILITY

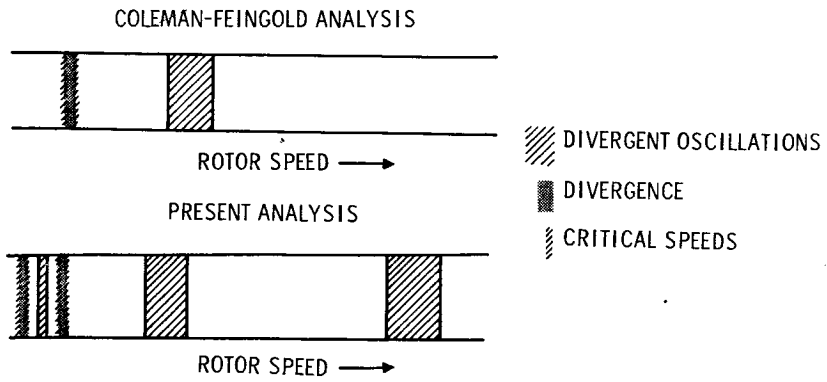


Figure 9

EFFECT OF DAMPING ON DIVERGENT OSCILLATIONS

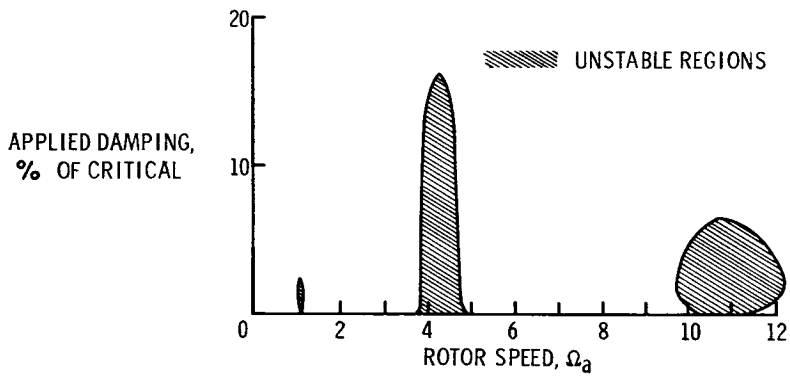
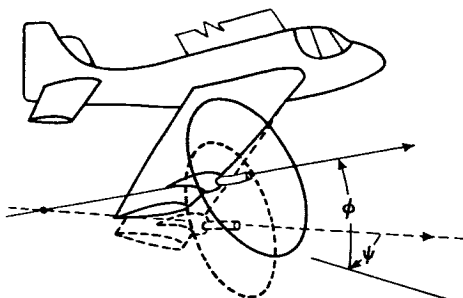


Figure 10

WHIRLING INSTABILITY OF ROTORCRAFT
AERODYNAMIC FORCES NECESSARY



SIGNIFICANT MOTIONS ARE GYROSCOPIC MOTIONS OF ROTOR:

1. SHAFT PITCHING AND YAWING
2. SHAFT BENDING
3. WING TORSION

Figure 11

WHIRLING INSTABILITY

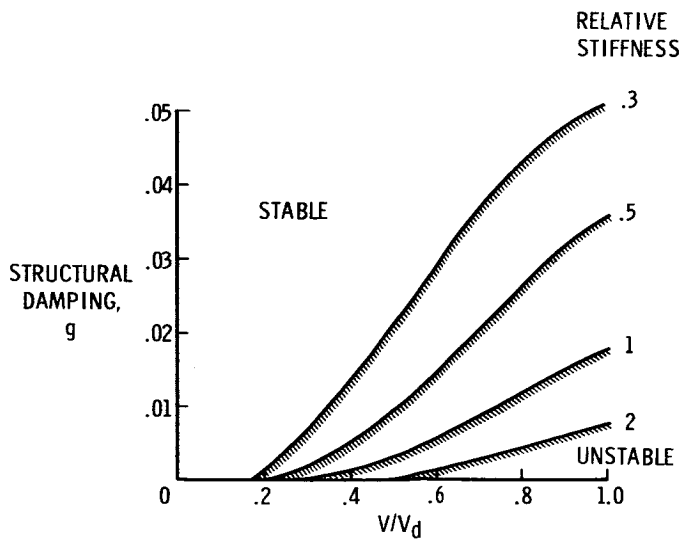


Figure 12

STRUCTURAL-LOADS SURVEYS ON TWO TILT-WING
VTOL CONFIGURATIONS

By John F. Ward

Langley Research Center

SUMMARY

The results of two structural-loads surveys are summarized. The first loads program discussed concerns the airframe vibratory loads encountered during flight tests of the VZ-2 tilt-wing VTOL aircraft throughout the operational range from hover to cruise flight. The primary sources of airframe vibration were wing-stall buffeting and tail buffeting in descents. The second loads program discussed concerns the initial results of a structural-loads survey conducted as part of the wind-tunnel test of a large-scale tilt-wing research model. This loads program deals with the steady wing loads measured throughout simulated transition from hover to cruise.

INTRODUCTION

This paper deals with the results of structural-loads surveys which were included as part of two of the VTOL research programs recently conducted at the Langley Research Center. These loads surveys were undertaken to investigate the nature of structural loadings associated with V/STOL aircraft incorporating the tilt-wing concept.

The first loads program that is discussed concerns the VZ-2 tilt-wing VTOL flight test aircraft. The principal result of this investigation was the determination of the character and relative magnitudes of vibratory loads that were encountered by the tilt-wing aircraft throughout the operational range from hover to cruise. Attention was focused on vibratory loads inasmuch as a number of limiting flight conditions were established, to a significant extent, on the basis of the severity of the airframe vibratory loads encountered.

The second loads program discussed concerns some of the initial results of a structural-loads survey conducted in conjunction with the wind-tunnel test of a large-scale, tilt-wing V/STOL model.

SYMBOLS

M	moment
M _{CRUISE}	steady bending moment in cruise (tunnel tests)
M _{HOVER}	steady bending moment in hover (tunnel tests)
M _{VIB}	vibratory bending moment (flight test)
M _{STEADY,CRUISE}	steady bending moment in cruise (flight test)
M _{VIB,CRUISE}	vibratory bending moment in cruise (flight test)
r	radial station
R	radius of rotor
V	free-stream velocity
α_w	wing angle of attack referenced to free-stream direction

FLIGHT INVESTIGATION OF VZ-2 AIRCRAFT

Test Procedures

Structural loads were monitored during the VZ-2 flying-qualities program at the Langley Research Center. This program included operation of the test-bed aircraft in the following flight conditions: hovering, transition, high-speed cruise, descents, and STOL operation. The program also included the investigation of the effects of a wing leading-edge modification installed to improve the aircraft behavior with regard to wing stalling limitations. With few exceptions, the flight program was conducted with incremental load factors less than $\frac{1}{4}g$, and rough-air conditions were avoided.

The airframe structural loads were monitored through the use of strain-gage bridges and a recording oscillograph. Figure 1 shows the test aircraft and the location of five strain-gage-bridge installations that will be referred to in this paper. In this figure the wing is shown in the hovering position. The locations of the strain-gage bridges used to monitor airframe vibratory loads are indicated in the figure; these gages measured horizontal- and vertical-tail bending moment, wing normal and chordwise bending moment, and wing-support-tube load. The main-rotor-blade flapwise vibratory bending moments were monitored by a strain-gage installation at the 48-percent blade radius.

Flight Results

Figure 2 illustrates some sample time histories of the output from the strain-gage installations shown in figure 1. These traces indicate the relative magnitude of airframe vibratory loads at three flight conditions. The wing angle of attack as given in this figure and used throughout this paper is defined as the angle between the wing-chord plane and the free airstream. The vibratory loads in the hover and cruise condition are of low magnitude. The condition shown for wing angle of attack of 60° was for a descent at 1,500 feet per minute. The buildup of vibratory load, in this case, was the maximum encountered in the flight program. The point illustrated is that the flight condition for maximum airframe vibratory load is the descent condition at high wing angles of attack. A 4.5-cycle-per-second frequency predominates in the traces for the vertical-tail bending, the wing support tubes, and the wing bending moment. From the relative deflection of the strain-gage traces and from the results of a simple ground check, this frequency appears to correspond to the fuselage torsional mode of vibration. The predominance of this mode is probably due to the fact that the large empennage is cantilevered from a rather flexible tubular fuselage.

The vibratory component of wing normal bending moment and vertical-tail bending moment is discussed in more detail so as to indicate the variation of airframe vibrations with wing angle of attack. Figure 3 presents the variation of the vibratory component of wing normal bending moment with wing angle of attack for level flight. The amplitude of the vibratory moments are referenced to a single value of the steady or mean wing normal moment measured in cruise. In the hover condition there is an increase in the magnitude of the wing vibratory load as the aircraft enters the ground-effect region. This region corresponds to wheel heights below approximately 20 feet. The effects of drooping the wing leading edge are indicated in the region of wing angle of attack of 30° . Without the drooped leading edge, wing-stall buffeting caused vibratory loads of 15 percent of the steady moment in cruise. After addition of wing-leading-edge droop the intensity of the vibratory loads induced by wing-stall buffeting reduced to 5 percent of the steady moment in cruise.

At stall onset the wing vibratory loads are induced by wing buffeting and are random in nature. At angles of attack above 40° , the wing vibratory loads, including the loads encountered in the ground-effect region, are primarily periodic at 4.5 cycles per second. The character of the vibratory loads at wing angles of attack above 40° indicates that the unsteady loads that are present are exciting the fuselage torsion mode of oscillation.

The buildup of the vibratory component of wing normal bending with rate of descent is presented in figure 4. The data in this figure and all subsequent figures for the VZ-2 aircraft were obtained with the drooped leading edge. The rate of descent is given in this figure to denote the flight condition in which the vibratory moment was encountered. The cut-off of the various curves at high wing angles of attack was due to the fact that unacceptable levels of pitch- and yaw-control roughness and airframe vibrations were encountered. The deterioration of pitch and yaw control suggests flow breakdown over the tail surfaces at high wing angles of attack and high rates of descent. In the descents the vibratory component of wing normal bending was periodic at 4.5 cycles per second just as was true in level flight at wing angles of attack above 40° .

Figure 5 illustrates the variation of vertical-tail vibratory load with wing angle of attack at various rates of descent. The vibratory component of vertical-tail bending moment is referenced to the magnitude of the vertical-tail vibratory moment measured in the steady cruise condition. As indicated in figure 5 there was a buildup of vertical-tail vibratory load in ground effect. The buildup of the vibratory load with rate of descent shows the same trend as the wing vibratory load presented in figure 4. The maximum values of vertical-tail vibratory loads were encountered at the limiting flight condition with unacceptable pitch and yaw control and airframe vibration. The character of the vibration was again a 4.5-cycle-per-second oscillation throughout the angle-of-attack range.

The large buildup of vertical-tail vibrations and the deterioration of pitch and yaw control at high wing angle of attack and high rates of descent suggest that the flow over the tail surfaces becomes increasingly unsteady and erratic as the descent rate increases for a given wing angle of attack. Figure 6 presents the buildup of tail vibratory load, at $\alpha_w = 60^{\circ}$, as a function of rate of descent. This figure is merely a cross plot of data from figure 5. A significant parameter which reflects the nature of the flow conditions in the descents is the rotor slipstream velocity. The calculated values of rotor slipstream velocity at the rates of descent investigated are indicated in this figure. The decreasing values of rotor slipstream velocity are a result of the reduced horsepower at the increased descent rates.

Figure 7 illustrates an estimate of the flow situation at the flight condition in which the maximum airframe vibrations were encountered. This situation corresponds to the end point on the curve of figure 6 with a wing angle of attack of 60° , rate of descent of 1,500 feet per minute, and a rotor slipstream velocity of 80 feet per second. The free-stream velocity for this flight condition was 70 feet per second.

The flow situation that develops at limiting rates of descent is the result of a number of contributing factors. A few of the more significant of these factors are suggested as follows. As the rotor slipstream velocity is decreased, the local wing angle of attack increases until stalling occurs. With the onset of stall, wing buffet loads develop so that airframe vibrations are induced. As the stalling spreads over the wing, the flow breakdown results in turbulence behind the wing-rotor combination. At the high wing angles of attack and high rates of descent, this turbulence is carried back over the tail surfaces inducing tail buffeting and loss of control effectiveness. The unsteady flow impinging on the tail surfaces contains a wide spectrum of input frequencies and therefore excites the fuselage mode at 4.5 cycles per second. There are many other factors contributing to the unsteady flow over the tail, such as fuselage interference, rotor slipstream turbulence, and engine-exhaust effects. These effects are probably secondary with respect to the flow breakdown induced by flying a stalled wing ahead of the tail during the descent.

Regardless of the details of the flow conditions which cause the airframe vibrations and control roughness that limit the rates of descent that may be achieved, the basic problem lies with the stalling and flow breakdown over the wing-rotor combination. This flow breakdown plays a dual role in introducing airframe vibrations and control roughness during descents. The direct effect of wing stall is reflected in wing buffeting loads at the onset of stall. The second and perhaps more significant effect takes place at higher wing angles of attack where the turbulent flow from the wing-rotor combination is carried back over the tail surfaces and leads to severe tail buffeting and deterioration of pitch and yaw control.

In the design of tilt-wing aircraft that are to be capable of achieving steep descents, it will be necessary to minimize the effects of wing stall, wing and rotor slipstream turbulence, and tail buffeting. Wing-stall onset can be delayed by employing high-lift devices such as slats and flaps. The effects of wing-rotor slipstream turbulence on tail buffeting can be minimized by properly locating the tail surfaces with respect to the path of the wing and rotor wake for the operational descent conditions. In this regard it will also be possible to draw upon the results of the research on tail buffeting already accomplished in connection with the development of the conventional airplane.

Up to this point, discussion has dealt with airframe vibrations in general. Figure 8 deals with the main-rotor-blade one-per-revolution vibratory moment variation with wing angle of attack in level flight. In this figure the magnitude of the blade flapwise bending moment is expressed as a ratio of the constant value of the blade vibratory moment measured in the cruise condition. As indicated in the figure, the magnitude of the one-per-revolution load increases to a maximum at

a wing angle of attack of 45° . This peak at an intermediate wing angle of attack is the result of the presence of relatively high free-stream dynamic pressure and unsymmetrical flow conditions at the rotor disk.

The VZ-2 loads survey indicated that the maximum airframe vibratory loads encountered occurred in descents at high wing angles of attack and were a result of tail buffeting induced by flow breakdown over the wing and rotor combination. Also, the maximum rotor-blade vibratory loads encountered occurred in level flight at intermediate wing angles of attack. These results suggest that, for the tilt-wing aircraft, the transition region between hover and cruise will require close attention in regard to fatigue-life substantiation.

TUNNEL-MODEL INVESTIGATION

This part of the discussion deals briefly with some of the initial results from the structural-loads survey conducted as part of the aerodynamic performance investigation of a large-scale tilt-wing V/STOL model. This investigation was conducted in the Langley full-scale tunnel. The complete results of the wind-tunnel investigation, which includes simulated accelerating and decelerating transition with various flap settings, are not presently available.

Test Procedures

The semispan of the configuration of the large-scale model is indicated in frontal view in figure 9 and in planform view in figure 10. The complete details of the configuration are given in reference 1, which presents results of ground effects on this same model. The wing structural loads were measured at the wing root with the strain-gage-bridge installation illustrated in figures 9 and 10. The strain-gage bridges were installed and calibrated according to the procedures outlined in reference 2. The wing loads measured included wing bending moment and shear in the normal and chordwise directions and wing torque. The outputs of these strain-gage bridges were monitored on a recording oscillograph throughout the wind-tunnel investigation.

Tunnel Test Results

Figures 9 and 10 illustrate the variation of the wing normal and chordwise bending moment through the angle-of-attack range from hover to cruise. These data are for unaccelerated transition with zero flap deflection. These loads are the steady moments due to aerodynamic loading on the wing during simulated steady-level-flight transition. The lift

was held constant throughout the transition and was equal to an aircraft weight of 3,500 pounds.

In general, the data indicate no abrupt change in spanwise centers of pressure. The shift of lift from the stalled wing to the propellers is indicated by the reduction in wing normal moment and the corresponding increase in chordwise moment at wing angle of attack of 45° . One other point is the presence of a wing normal moment in hover which is 30 percent of the value for cruise. This positive normal moment is due to the cambered wing acting in the high velocity propeller slipstream. To date no unusual structural loading problems have been noted, and it is expected that it will be possible to provide detailed structural-loads data for accelerating and decelerating flight throughout the transition range.

CONCLUSIONS

From a structural-loads survey of the tilt-wing VZ-2 aircraft in flight and preliminary results of a large-scale tilt-wing model in a wind tunnel, the following conclusions are indicated:

1. The flight-loads survey of the VZ-2 indicated that the primary sources of airframe vibratory loads are wing and tail buffeting. The vibratory loads result from wing buffeting at stall onset and from impingement of the separated flow from the stalled wing on the tail surfaces. The airframe vibratory loads encountered reached the maximum at high wing angles of attack during low-power descents with reduced rotor-slipstream velocities.
2. The addition of a leading-edge modification tended to reduce the intensity of the wing vibratory loads associated with the onset of wing-stall buffeting.
3. The rotor-blade one-per-revolution vibratory loads reached the maximum at intermediate wing angle of attack in consequence of the combination of relatively high free-stream dynamic pressure and unsymmetrical flow conditions at the rotor.
4. The initial wind-tunnel results of the structural loads survey of the large-scale tilt-wing model indicated no unusual behavior as regards the steady-wing loads during transition from hover to cruise.

REFERENCES

1. Huston, Robert J., and Winston, Matthew M.: Data From a Static-Thrust Investigation of a Large-Scale General Research VTOL-STOL Model in Ground Effect. NASA TN D-397, 1960.
2. Skopinski, T. H., Aiken, William S., and Huston, Wilber B.: Calibration of Strain-Gage Installations in Aircraft Structures for the Measurement of Flight Loads. NACA Rep. 1178, 1954. (Supersedes NACA TN 2993.)

L
1
4
3
2

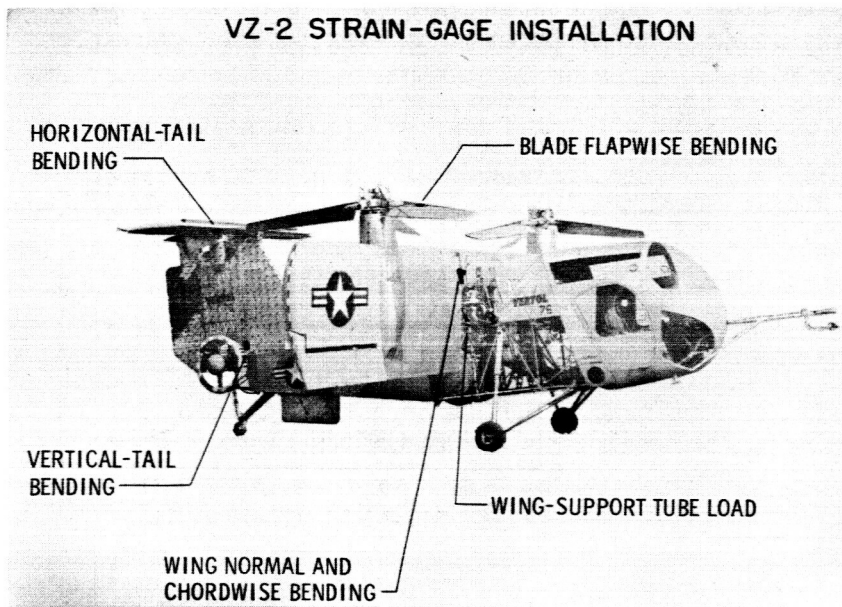


Figure 1

VZ-2 AIRFRAME VIBRATORY LOADS

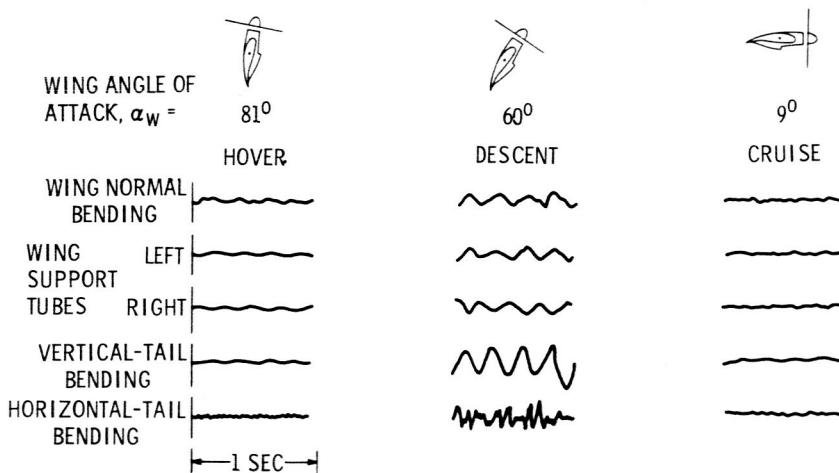


Figure 2

VIBRATORY COMPONENT OF WING NORMAL BENDING MOMENT
LEVEL FLIGHT

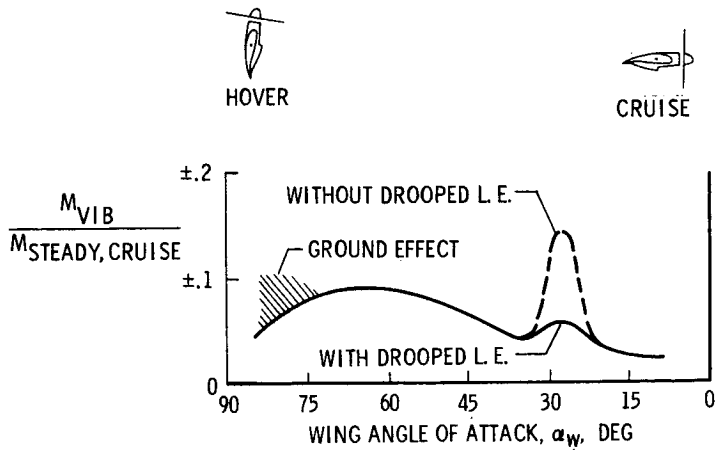


Figure 3

VIBRATORY COMPONENT OF WING NORMAL BENDING MOMENT

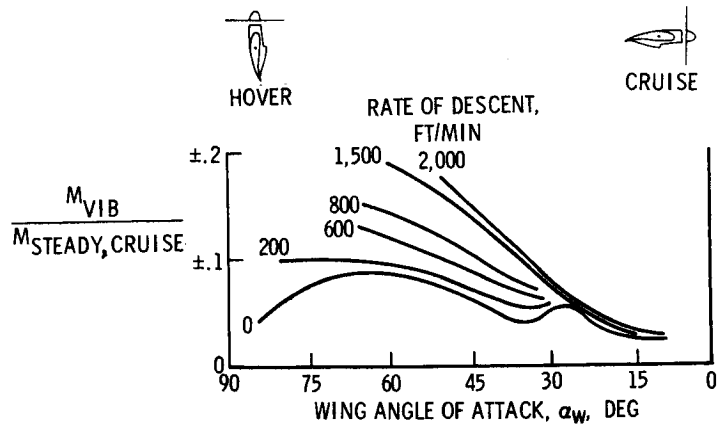


Figure 4

VIBRATORY COMPONENT OF VERTICAL-TAIL BENDING MOMENT

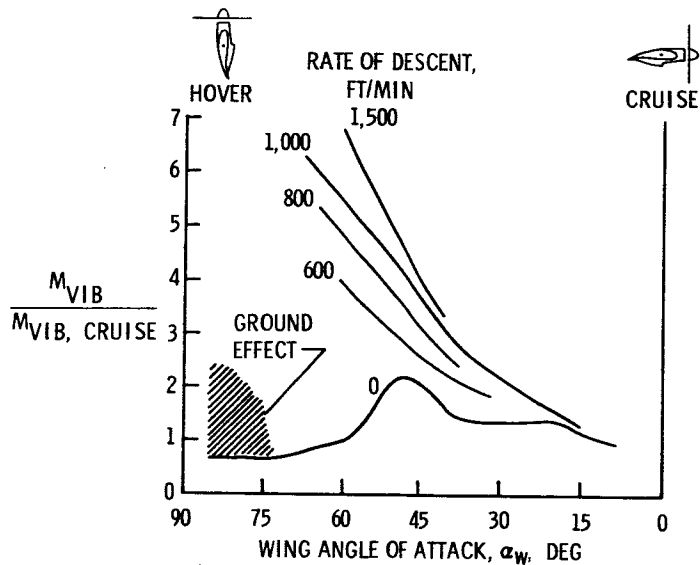


Figure 5

VIBRATORY COMPONENT OF VERTICAL-TAIL BENDING MOMENT

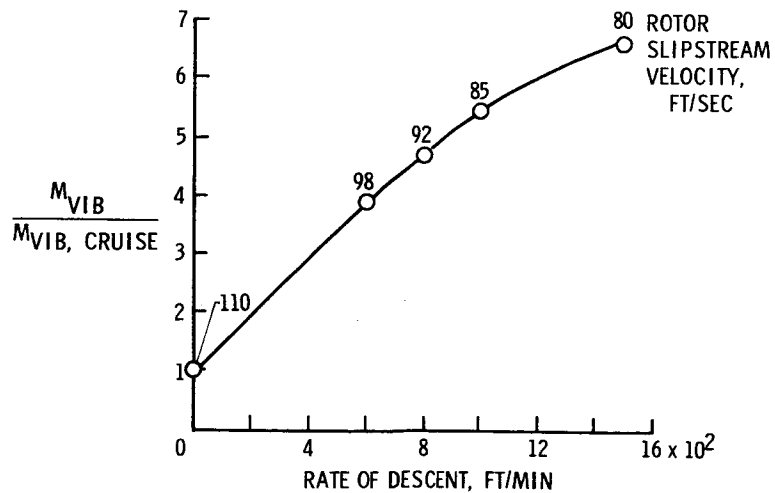
 $\alpha_w = 60^\circ$ 

Figure 6

FLIGHT CONDITION FOR MAXIMUM AIRFRAME VIBRATORY LOADS

RATE OF DESCENT = 1,500 FT/MIN

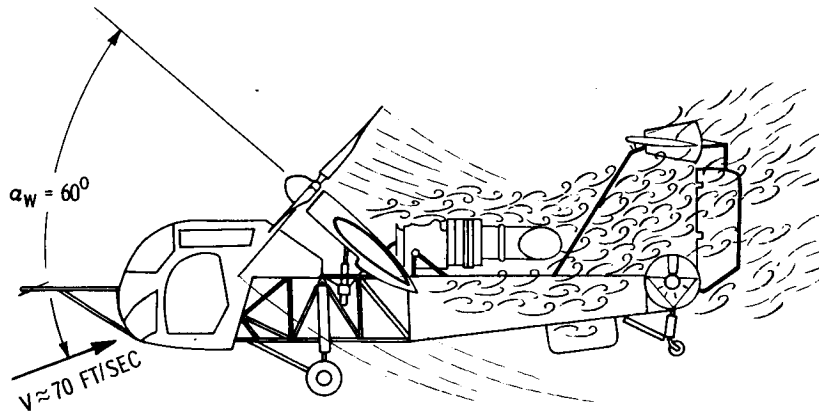


Figure 7

VIBRATORY COMPONENT OF MAIN-ROTOR
BLADE FLAPWISE BENDING MOMENT

LEVEL FLIGHT

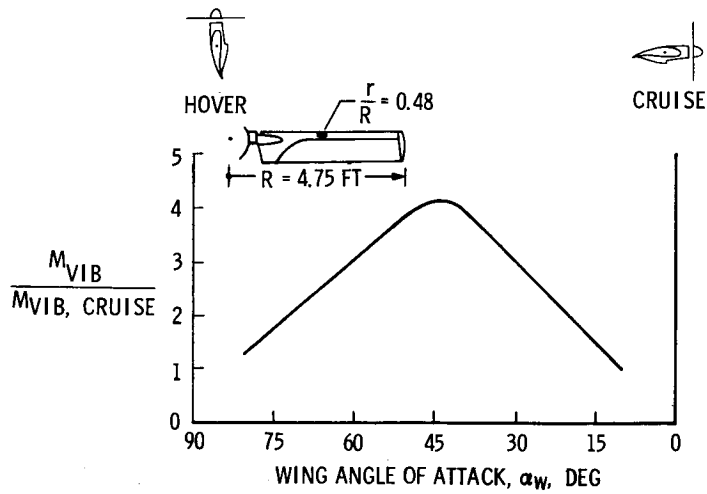


Figure 8

VARIATION OF WING NORMAL BENDING
MOMENT DURING TRANSITION

STEADY LEVEL FLIGHT

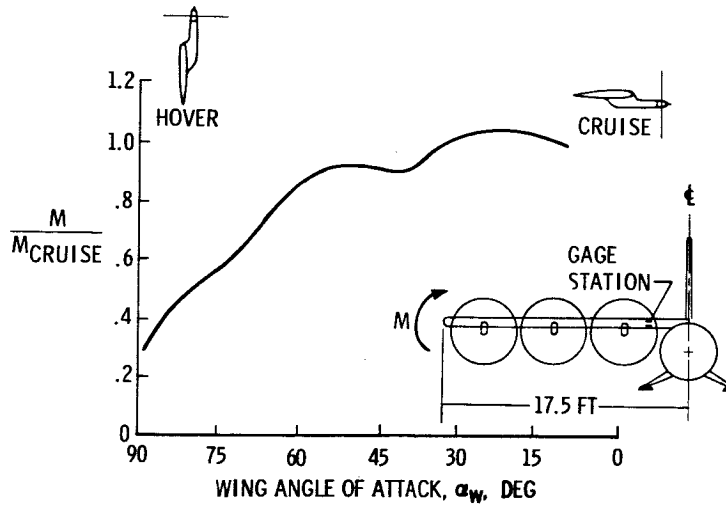


Figure 9

VARIATION OF WING CHORDWISE BENDING
MOMENT DURING TRANSITION

STEADY LEVEL FLIGHT

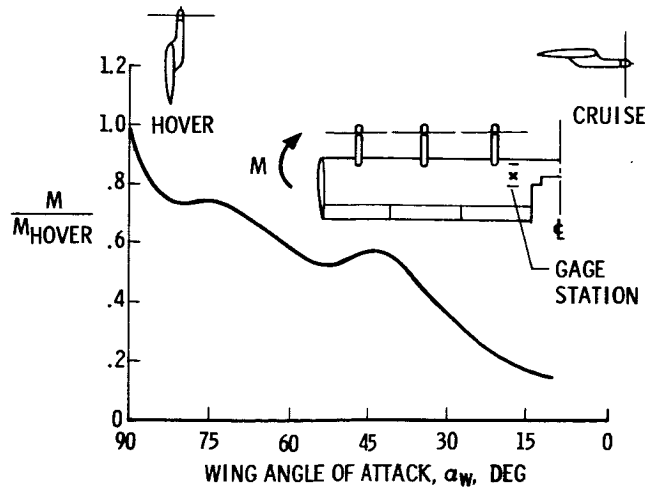


Figure 10

SUMMARY OF ROTOR-BLADE VIBRATORY-LOAD STUDIES

By LeRoy H. Ludi

Langley Research Center

The rotor-powered aircraft is directly associated with fatigue since the rotor is subjected to alternating aerodynamic loadings during all flight regimes. These alternating loadings on the rotor can produce periodic loads on the various components of the helicopter which could severely limit the service life of these components because of fatigue. In order to enable prediction of a satisfactory service life for these components, it is necessary to know which conditions result in the most severe periodic loads so that they may be investigated during prototype testing. Examples of conditions which require investigation are as follows:

- (1) Level flight throughout speed range
- (2) Retreating-blade stall
- (3) Landing approaches
- (4) Partial-power descents
- (5) Droop-stop pounding on the ground
- (6) Atmospheric turbulence
- (7) Moderate maneuvers
- (8) Transition
- (9) High-speed level turns
- (10) Pull-outs from autorotation
- (11) Autorotation at high forward speed with high rotor speed

The loads in these conditions in combination with the amount of time spent in the conditions are the basic factors in a rational determination of the fatigue life of a structure. In order to determine experimentally the information on the relative severity of the periodic moments encountered by a rotor blade during the conditions listed previously, a program utilizing the helicopter shown in figure 1, equipped with strain gages at 14 percent and 40 percent of the radius on one of the blades, was undertaken. These locations were chosen to give a maximum amount of information on the blade moments and were considered adequate for this investigation even though stress surveys usually involve more locations. The results are of general interest in that the flight conditions, which resulted in the most severe rotor-blade loads are defined. The conditions numbered 1 to 5 in the previous list were found to produce the more severe blade loads and will be discussed in more detail. Additional information on all the conditions listed previously can be obtained from references 1 to 4.

Before going into the results of the rotor-blade vibratory-load studies, it is interesting to see how much time a helicopter actually spends in its various operating airspeed ranges under continued operational use as shown in figure 2. The information in this figure is a result of a continuing study of operating experiences being obtained from both civil and military operations. Published information on surveys of helicopter operating conditions is contained in references 5 to 8. Figure 2 shows the percent of total time spent in the various speed regimes as a function of the ratio of forward velocity V to the maximum forward velocity V_{MAX} . The maximum forward velocity is determined from the pilot's handbook for the particular configuration. The distribution represents the complete flight profile of climb, en route, and descent for a helicopter in both a civil application as shown by the solid line and a military application as shown by the dashed line. As can be seen from the figure, the airmail operation tends to concentrate the major percentage of total time at speeds beyond 65 percent of V_{MAX} . The military operation, in this case pilot training, tends to shift the major percentage of total time toward the lower speeds. In fact, the military operation did not spend any time above 87 percent of the maximum speed. These results show that the entire speed spectrum must be checked for large moments, particularly when the helicopter has a dual mission. The high-speed end of the spectrum, where the large percentage of time spent and the expected increased moments are combined, is extremely important in fatigue-life calculations.

In order to illustrate how the rotor-blade vibratory moments are affected by forward speed, figure 3 shows the variation of measured vibratory moments as a function of the ratio of forward velocity to maximum forward velocity. The measured vibratory moments at any speed M are divided by the measured vibratory moments at cruise speed M_{CRUISE} . Cruise speed for this helicopter is 60 percent of its maximum velocity, and the vibratory moments at cruise speed are used as a reference for most of the following figures. The moments shown in figure 3 are flapwise bending moments at 40 percent and 14 percent of the blade radius and torsional moments at 14 percent of the blade radius. The torsional moments on the blade, while not as critical as bending moments in determining the fatigue life of the blade itself, are of prime importance in control-system design. In figures 3 to 8, amplitude and revolution or cycle are defined as shown in the small inset in figure 3. It can be seen that the trends for all three moments are similar. The buildup in moment value at 25 percent of the maximum forward speed is caused by the transition region, which is the region between hovering and the speed for minimum power and is characterized by a change in airflow through the rotor. As the speed increases above 70 percent of V_{MAX} , retreating-blade stall becomes

more responsible for the increased moments. At 95 percent of V_{MAX} , the highest speed achieved during this investigation, the flapwise bending moments at 40 percent of the blade radius had increased to twice the cruise value while the torsional moments at 14 percent of the blade radius had increased to $3\frac{1}{4}$ times the cruise value. The trends indicate that the use of turbine engines and the resultant higher ratio of cruise speed to maximum forward speed will produce very high moments that must be accounted for during fatigue-life calculations.

An additional problem which arises as a result of high-speed flight is increased periodic control loads in high-performance prototype helicopters. The increased periodic control loads, a result of increased torsional moments caused by retreating-blade stall, have seriously restricted the normal operating limits of these prototypes. The effect of stall on the torsional moments is illustrated in figure 4. In this figure, the torsional moments at the various forward speeds M are divided by the torsional moment at the speed which first produced a retreating tip angle of 12° M_{STALL} and plotted against increasing forward speed. The open symbols represent unstalled conditions, and the solid symbols represent stalled conditions. It can be seen that the moments increase at a fairly shallow rate until the retreating tip angle of attack exceeds the stall angle; then, they increase rapidly. Moderate penetration into stall results in ratios that are still fairly small while extreme penetration results in ratios of almost 3. These increased vibratory torsional moments illustrate the fact that careful consideration must also be given to control-system loads during high-speed flight in order to avoid operating limitations.

At the other end of the speed spectrum, there are flight conditions which were found to produce severe periodic rotor-blade moments that would be of interest in the design of the various rotorcraft components. Landing approaches and partial-power descents at zero or low forward speeds resulted in moments that were the highest encountered during the investigation. The maximum vibratory moments experienced by the rotor blade during a landing approach are shown in figure 5. In this figure, the inboard blade moments M are divided by the cruise moment M_{CRUISE} and plotted as a function of the forward speed ratio during the approach. Since the results obtained during the landing-approach tests are not readily repeatable, the moments in this figure represent the maximum values obtained during the investigation. Since there is scatter in this type of maneuver, the amount of scatter in the area of most interest is indicated by the shaded area and is discussed in detail later. In general, figure 5 shows that flapwise bending moments as high as 5.75 times the cruise moments are encountered during

the approach. These increased moments in the landing approach are believed to be caused by a change in the airflow similar to that which occurs during the transition region.

The effect of partial-power descents on the maximum vibratory moments encountered by a rotor blade is shown in figure 6. In this figure, the ratio of the inboard flapwise moments is shown as a function of the rate of descent, for two values of forward speed (0 and 28 knots). Since the moments at a particular rate of descent also are not readily repeatable, the moments plotted in the figure represent the maximum moments encountered in the various descents. As in figure 5, the amount of scatter during the partial-power vertical descents is shown by the shaded area. Figure 6 shows that inboard moments 6.8 times the cruise moments are obtained during partial-power descents at zero forward speed. Because of the random character of the flow during the vertical descents, control was generally poor and required large movements of the controls to maintain steady conditions. As forward speed is increased to 28 knots, the moments peak at a lower rate of descent and reach a lower numerical value than those encountered in vertical descents. At the higher forward speed, control is generally improved and smaller control movements are needed to hold steady conditions. The partial-power vertical descents were found to produce the highest vibratory moments of all the conditions investigated.

Since the moments encountered during partial-power descents have a random character, the degree of conservatism involved in using the maximum moments during a partial-power vertical descent, with the assumption that the maximum moments occurred during the entire time for a fatigue-life determination, was considered. An indication of the random nature of the moments encountered during a partial-power vertical descent is given by the distribution shown in figure 7. In this figure, the ratio of the inboard bending moments is plotted as a function of the percent of total cycles in the various bending-moment ranges. Figure 7 shows that the maximum moments shown in figure 6 occur only during 1 percent of the cycles and, therefore, might be too conservative if used exclusively. Furthermore, other conditions such as high-speed flight, where the maximum moments might be above the endurance limit and occur during a larger percentage of time than the maximums in partial-power descents, must not be neglected in any rotor-blade finite life assessment.

In addition to the flight conditions investigated, static droop-stop pounding, where the blade impinges on a mechanical stop due to flapping during rotor operation on the ground, also produced some additional moments which were of interest. Static droop-stop pounding, even though artificially produced for these tests, can inadvertently occur during rotor operation on the ground in strong, gusty winds or in ground

taxiing. In fact, some cases of droop-stop pounding in the air have been reported. The potential ability to produce droop-stop pounding moments that are higher than maximum flight moments, if the pounding is allowed to progress, is illustrated in figure 8. Here the inboard flapwise moments during droop-stop pounding M are divided by the maximum flight moments $M_{\text{FLIGHT,MAX}}$ (in this case, those encountered in partial-power vertical descent) and plotted as a function of the change in longitudinal cyclic pitch $\Delta B_{1,s}$. The cyclic pitch at which droop-stop pounding first occurs is used as a reference. In general, the figure shows that the moments increase linearly with cyclic control; therefore, the moments would also increase with increasing flapping angle. This trend indicates that if the design and the operating circumstances should produce large down flapping, such as fuselage clearance often allows, very high moments will result. Even though the moments during droop-stop pounding occur at a low frequency, they can become very important from a fatigue standpoint if the magnitude of these moments follows the trend shown in the figure. The moments in the figure are felt to be an indication of the rate of increase of moment with control displacement if droop-stop pounding is inadvertently permitted, at least for a blade with uniform spar and uniform mass.

Utilization of the moments illustrated in the figures and the moments encountered during the other flight conditions investigated, in conjunction with the results of helicopter operating surveys which illustrate the amount of time spent in various flight conditions, permitted rough sample fatigue-life calculations to be made for the rotor blade. One calculation, utilizing just two of the flight conditions that produced the highest moments, was made. The fact that these moments occur during the entire time in this flight condition was assumed. The blade fatigue life under these conditions was approximately 775 hours. A second calculation, utilizing all the flight conditions that produced moments above the endurance limit and more accurate distributions of the times spent during these flight conditions, was made. The blade fatigue life under these conditions was approximately 1,510 hours. These results illustrate the necessity for an accurate evaluation of the number of flight conditions which result in the most severe periodic loads and of the time spent in each condition to be used in a fatigue-life determination for the blade in order to provide a safe blade life without undue penalties.

The results of the rotor-blade vibratory-load study indicate that severe rotor-blade loads can be expected to occur during high-speed level flight, landing approaches, partial-power descents, and droop-stop pounding during rotor operation on the ground. In addition, retreating-blade stall can cause increased torsional moments which cause increased control loads. In the future design of rotorcraft, these severe rotor-blade loads must be accurately accounted for in component fatigue-life

determinations so that undue limitations will not seriously restrict the operational usage of the rotorcraft.

REFERENCES

1. Ludi, LeRoy H.: Flight Investigation of Effects of Atmospheric Turbulence and Moderate Maneuvers on Bending and Torsional Moments Encountered by a Helicopter Rotor Blade. NACA TN 4203, 1958.
2. Ludi, LeRoy H.: Flight Investigation of Effects of Retreating-Blade Stall on Bending and Torsional Moments Encountered by a Helicopter Rotor Blade. NACA TN 4254, 1958.
3. Ludi, LeRoy H.: Flight Investigation of Effects of Transition, Landing Approaches, Partial-Power Vertical Descents, and Droop-Stop Pounding on the Bending and Torsional Moments Encountered by a Helicopter Rotor Blade. NASA MEMO 5-7-59L, 1959.
4. Ludi, LeRoy H.: Flight Investigation of Effects of Additional Selected Operating Conditions on the Bending and Torsional Moments Encountered by a Helicopter Rotor Blade. (Prospective NASA Paper.)
5. Crim, Almer D., and Hazen, Marlin E.: Normal Accelerations and Operating Conditions Encountered by a Helicopter in Air-Mail Operations. NACA TN 2714, 1952.
6. Hazen, Marlin E.: A Study of Normal Accelerations and Operating Conditions Experienced by Helicopters in Commercial and Military Operations. NACA TN 3434, 1955.
7. Connor, Andrew B., and Ludi, LeRoy H.: A Summary of Operating Conditions Experienced by Two Helicopters in a Commercial and a Military Operation. NASA TN D-251, 1960.
8. Connor, Andrew B.: A Summary of Operating Conditions Experienced by Three Military Helicopters and a Mountain-Based Commercial Helicopter. NASA TN D-432, 1960.

TEST HELICOPTER



Figure 1

DISTRIBUTION OF OPERATING AIRSPEED

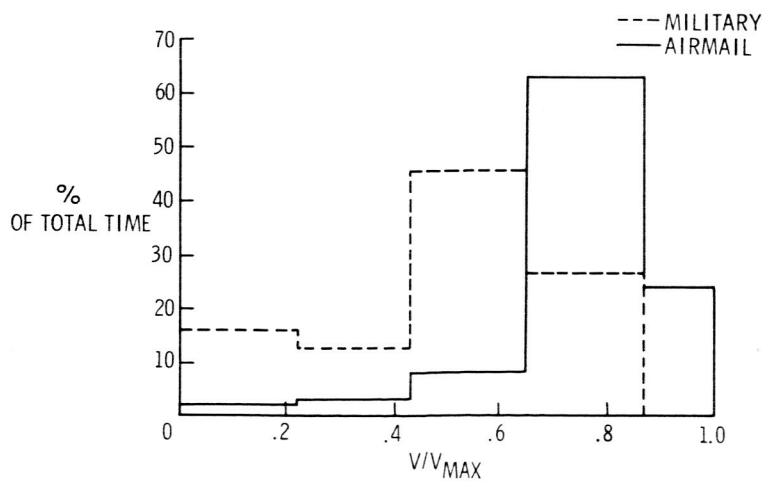


Figure 2

EFFECT OF FORWARD SPEED ON VIBRATORY MOMENTS

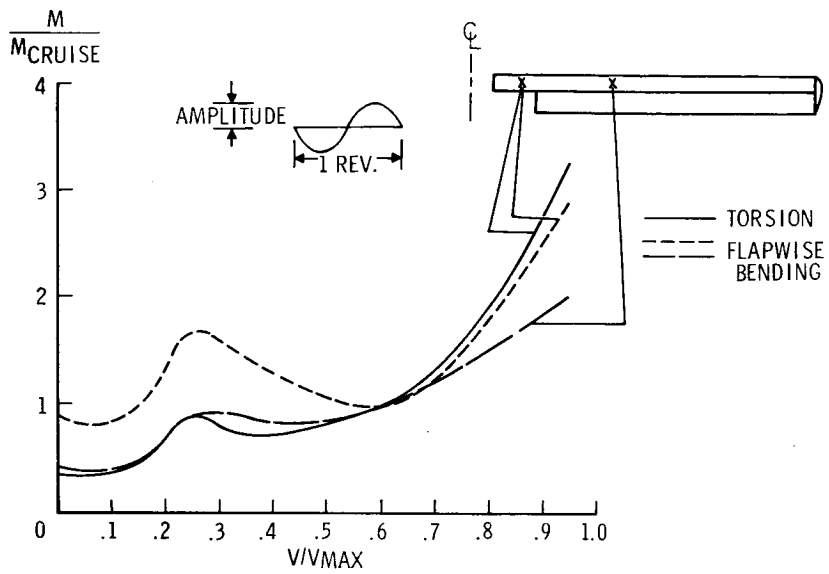


Figure 3

EFFECT OF RETREATING-BLADE STALL ON TORSIONAL MOMENTS

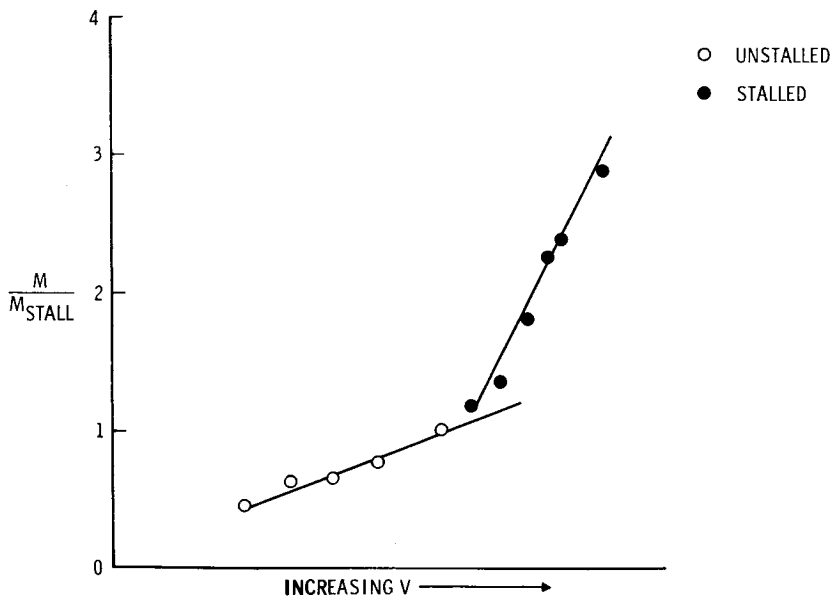


Figure 4

INBOARD FLAPWISE MOMENTS DURING LANDING APPROACH

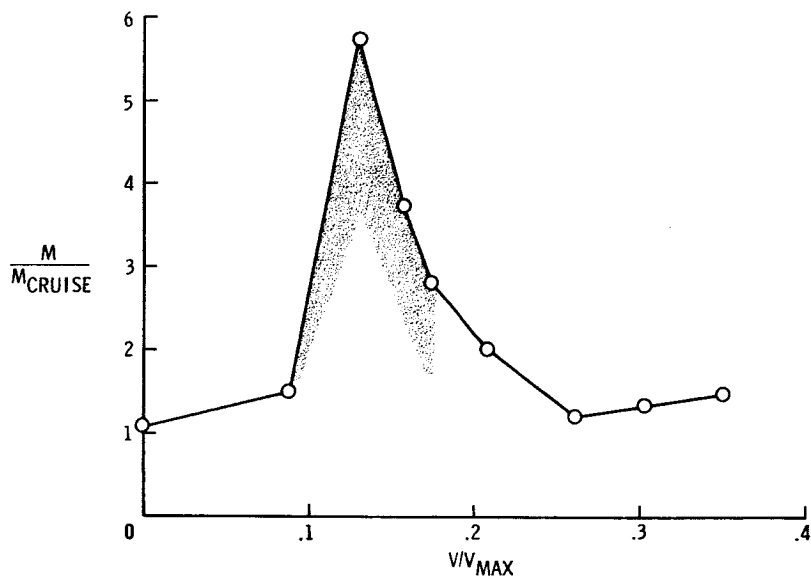


Figure 5

INBOARD FLAPWISE MOMENTS DURING PARTIAL-POWER DESCENTS

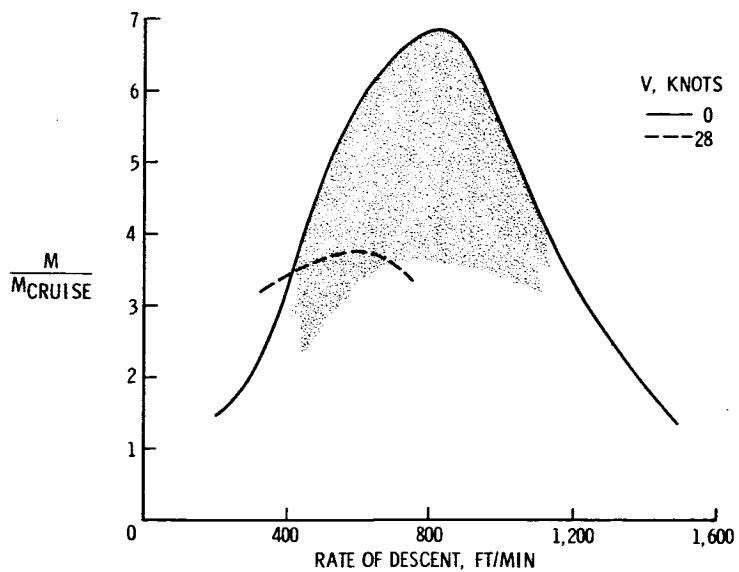


Figure 6

DISTRIBUTION OF INBOARD FLAPWISE MOMENTS DURING
PARTIAL-POWER VERTICAL DESCENT

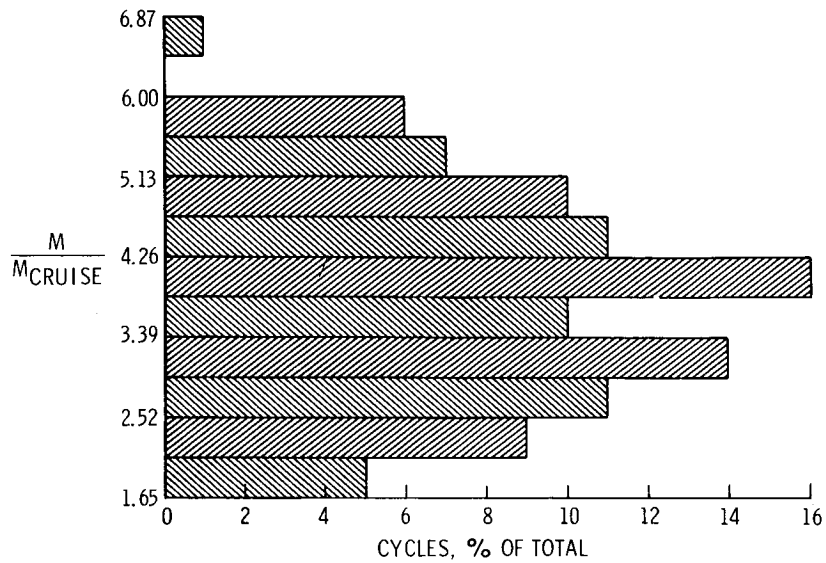


Figure 7

INBOARD FLAPWISE MOMENTS DURING DROOP-STOP POUNDING

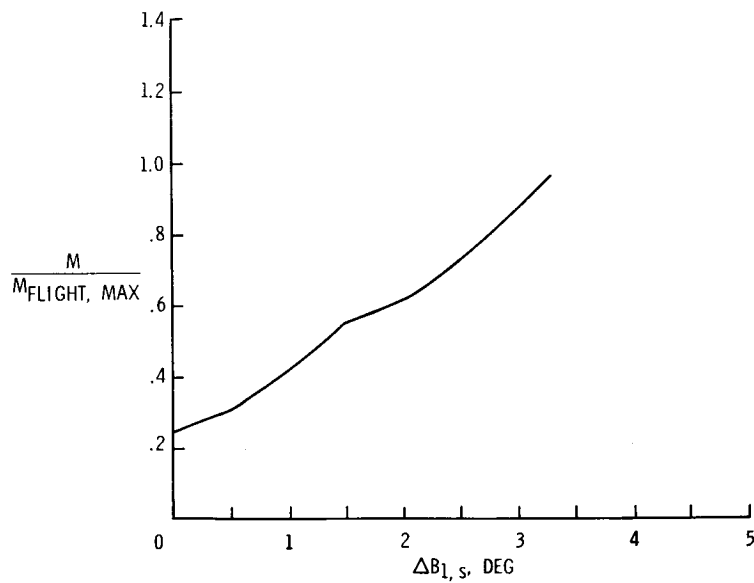


Figure 8

FACTORS IN EVALUATING FATIGUE LIFE OF STRUCTURAL PARTS

By Walter Illg

Langley Research Center

SUMMARY

Three facets of fatigue testing are discussed in relation to problems involved in evaluating the fatigue life of structural parts. These facets are variable-amplitude loading, fatigue-crack propagation, and equivalent fatigue loading. Experimental test results are included to support conclusions.

INTRODUCTION

In the interest of safety and according to regulations, it must be shown that an aircraft structure has a practically infinite life or a safe life must be established. At present, theory alone is not sufficient to evaluate the fatigue characteristics of a structural part. The only alternative is testing. Simple laboratory specimens are unsuitable because of the many factors which must be simulated from the full-scale parts. At the present stage of fatigue knowledge, testing the actual part is the only sure way to evaluate the fatigue life of a piece of aircraft structure. In this paper some recent NASA research, which sheds light on a number of factors that are involved in any evaluation of the fatigue life of structural parts, is discussed.

SERVICE LOADING

The first problem in testing is how to load a specimen to simulate service loading. A record of actual stresses encountered in flight can be obtained with the use of strain gages at critical points. The record will depend a great deal upon how the aircraft is used. In the event the same vehicle is to be used for more than one type of mission, the flight record to be used in testing should be from that mission which provides the severest load conditions. Each type of mission will include a variety of maneuvers, such as taxiing, take-off, and climb, which have characteristic load histories. The record should include sufficient samples of all phases of the aircraft's mission to give an accurate picture of the extremes and probabilities of occurrence of all loads.

It may or may not be possible to combine the loads from different phases, depending on the mean load. Schedules for phases having widely different mean loads should not be combined. In the case of the helicopter, the mean load in the blade for all phases will be practically identical since it is dependent upon rotor angular velocity which is essentially constant. The parts in other aircraft, however, will generally be subjected to varying mean loads.

It would be very satisfying if the exact flight-loading patterns could be reapplied to the part in question in the laboratory; however, the cost of such a procedure would be prohibitively high. On the other extreme, cycling continuously at a single load range has been shown to be incapable of reproducing all the effects of the varied flight loadings. For instance, fatigue tests of transport wings (ref. 1) indicated that more cracks were initiated under variable amplitude than under constant amplitude, and the crack which finally caused failure was in a different location for each type of loading.

VARIABLE-AMPLITUDE TESTING

Since constant-amplitude loading is unrealistic and exact flight-loading duplication is impractical, a compromise must be adopted. One solution is to translate the flight record into a load program composed of discrete steps which adequately represent the actual loads and which can be handled in the laboratory. Figure 1 illustrates how a step-loading schedule may be used to simulate a continuous spectrum. The smooth curve is a representative stress spectrum found from actual service conditions during one major phase of operations. The discrete levels shown are chosen so that they represent a number of equal stress intervals. The best number of steps to use has not been definitely established. In NASA work at the Langley Research Center, eight steps are generally used, and possibly no fewer than six should ever be used.

As figure 1 implies, all loads are assumed to cause fatigue damage. Even though the lowest load step lies below the fatigue limit, it is nonetheless important. One reason is that, after a crack appears, the stress-concentration factor increases, and the lowest step may contribute to crack propagation. For this reason, the test schedule should include loads below the fatigue limit. As mentioned before, a similar schedule will be obtained for each major phase of operation of the aircraft. The various test schedules should be applied in the same proportion that is expected to occur in service.

Once the magnitude and number of load steps have been determined, the sequence of application must be considered. Tests on simple specimens

under variable-amplitude loading have been conducted, and one discovery has been the effect of the sequence of loading on the life. Figure 2 shows the relative effect of three loading sequences on the fatigue life of the specimens tested (ref. 2). Each of these patterns depicts a different sequence of applying the same eight loads the same number of times, each on the same type of simple specimen. The loading pattern was repeated until failure occurred. The life for the random sequence is given a value of 1 for purposes of comparison. Note that the lo-hi sequence gave the shortest life while the hi-lo sequence gave the longest life. The life obtained with the random sequence fell between the other two. Thus, by change of sequence the results changed by a factor of 4.

In general, service loading of aircraft is of a random nature, in which case, the laboratory test loads should be applied in random order. Special cases may require other sequences to simulate the loading. The number of cycles in each block (fig. 2) should be chosen so that the specimen will survive at least 10 blocks.

FATIGUE-CRACK PROPAGATION

Under the application of any load schedule, the failure will take place in two stages; the first stage is the period before a crack is initiated, and the second stage is the period during which the crack is propagated to failure. The interval between crack initiation and part failure can be very important to an aircraft operator. Fatigue damage is first visible during this interval in the life of a part. During this time, the strength of the part decreases in a manner as shown in figure 3. The dashed line represents the maximum repeated load encountered in service. The solid line indicates the load which the cracked part can still carry. As the crack grows, the strength decreases until the part can no longer withstand the applied load, and failure occurs. This interval between crack initiation and failure provides an opportunity to inspect a part for fatigue damage. Two properties of the part must be known to make it possible to set up a realistic inspection interval. The first property is the rate of crack propagation under expected stresses, and the second property is the crack length at which the residual strength equals the load and the part fails.

Prediction of the rates of crack propagation in simple specimens at constant-amplitude loading is possible. Figure 4 shows some results for 2024-T3 sheet specimens tested with the ratio of minimum stress to maximum stress in a cycle R always at zero (ref. 3). The data for many tests fall on a continuous curve when the rate of crack propagation is plotted against a stress parameter which involves the local stress at the tip of the crack. The dashed line represents a semiempirical

expression used to correlate the data shown. The same curve may be used to estimate the rate of crack propagation at other stresses and for other size specimens. Crack propagation under variable-amplitude loading is currently being investigated to understand more fully crack growth under service-type loading.

The second property of the part which must be known (the residual strength as a function of crack length) has also been investigated for simple specimens. Some results are shown in figure 5 for 2024-T3 material (ref. 4). Note the sharp decrease in strength for small crack lengths. The solid line represents a theory for predicting strengths for any crack length. This theory is based on a stress concentration at the tip of the crack. When the local stress at the tip of the crack reaches the ultimate strength of the material, the specimen will fail. When the part is reasonably simple, this kind of data from simple specimens can provide a fairly good estimate of the number of cycles which the part can endure after a crack appears. For complicated structures, the part itself would have to be tested to obtain all crack-rate data and residual-strength data. In any case, the part should be tested to check the estimates made. From this information, an inspection interval could be calculated which would make it reasonably certain that a crack would be discovered before failure occurred. For the method to be practical, the probable locations of cracks must be known and easily accessible. Of course, in the event that the inspection interval is found to be too short, the parts must be discarded before a crack appears.

EQUIVALENT FATIGUE LOADING

In the course of an investigation of crack propagation, it may sometimes be desirable to substitute one loading ratio R for another, while maintaining identical rates of crack propagation. This procedure might be desired for practical reasons such as testing machine capability. Extreme care must be exercised in choosing an equivalent load. The following discussion illustrates how conventional methods for finding equivalent loads can result in invalid crack-propagation test data. The illustrative problem involves changing from a loading at $R = 0$ to a loading at $R = -1$.

The conventional method of finding equivalent fatigue loads is indicated in figure 6. The fatigue failure curves for unnotched specimens are plotted for the two load ratios $R = 0$ and $R = -1$. The ordinate is the maximum cyclic load and the abscissa is the total life. The conventional method requires the determination of the load level at $R = -1$ which gives the same life as the original load level at $R = 0$. However, the conventional method is invalid when dealing with the crack-propagation portion of fatigue tests.

Figure 7 shows the rates of fatigue-crack propagation for the two load ratios $R = 0$ and $R = -1$ (ref. 3). The material is 7075-T6 aluminum-alloy sheet. One set of tests was run with the minimum cyclic load held at zero ($R = 0$), and the other set of tests was run with the mean load held at zero ($R = -1$). These data show that, for the same maximum cyclic stress, the rates of crack propagation were the same even though the load range for $R = -1$ was twice that for $R = 0$.

In a recent investigation of the crack propagation in a full-scale helicopter rotor blade, the conventional method was used to change from a service loading at $R = 0$ to a test loading at $R = -1$. Since figure 7 indicated that in simple specimens the maximum cyclic stresses for similar cracking rates at $R = 0$ and $R = -1$ are the same, axial-load fatigue tests on small portions of the blade were performed to check the results of the full-scale test. One specimen was subjected to service loading and another specimen was subjected to the stresses that were used in the full-scale test. The results of these tests are shown in figure 8. The loading at $R = -1$, the so-called equivalent loading, gave a much smaller rate of crack length than did the service loading.

The result, then, of using an equivalent load obtained in the conventional manner, was that the full-scale test not only did not yield the answer that was sought but also gave a misleading indication of comparatively slow crack growth.

CONCLUDING REMARKS

It has been shown that many factors enter into the determination of the safe life of a structural component subjected to fatigue loading.

It is preferable to test actual parts because of the multitude of items which must be duplicated in simple specimens to make a valid test.

Variable-amplitude testing is preferred to constant-amplitude testing. The number of load steps for a given schedule should probably not be less than six. The sequence of loading should be random for most cases. The number of cycles per block should be such that at least 10 blocks will be survived by the part.

Loads below the fatigue limit should be included since they can affect the life of the part.

Inspection for cracks during the service life of an aircraft can improve its safety. When the procedure discussed in this paper for determining an inspection interval is used, the following properties must be ascertained:

- (1) The probable location of fatigue cracks
- (2) The rate of growth of all fatigue cracks
- (3) The length of the crack at which the residual strength is no longer greater than expected loads

When the rates of crack propagation are investigated, great care should be taken in determining equivalent loads if they are to be used.

REFERENCES

1. Whaley, Richard E.: Fatigue Investigation of Full-Scale Transport-Airplane Wings - Variable-Amplitude Tests With a Gust-Loads Spectrum. NACA TN 4132, 1957.
2. Naumann, Eugene C., Hardrath, Herbert F., and Guthrie, David E.: Axial-Load Fatigue Tests of 2024-T3 and 7075-T6 Aluminum-Alloy Sheet Specimens Under Constant- and Variable-Amplitude Loads. NACA TN D-212, 1959.
3. McEvily, Arthur J., Jr., and Illg, Walter: The Rate of Fatigue-Crack Propagation in Two Aluminum Alloys. NACA TN 4394, 1958.
4. McEvily, Arthur J., Jr., Illg, Walter, and Hardrath, Herbert F.: Static Strength of Aluminum-Alloy Specimens Containing Fatigue Cracks. NACA TN 3816, 1956.

SIMULATION OF CONTINUOUS STRESS SPECTRUM BY USE OF REPRESENTATIVE STRESS STEPS

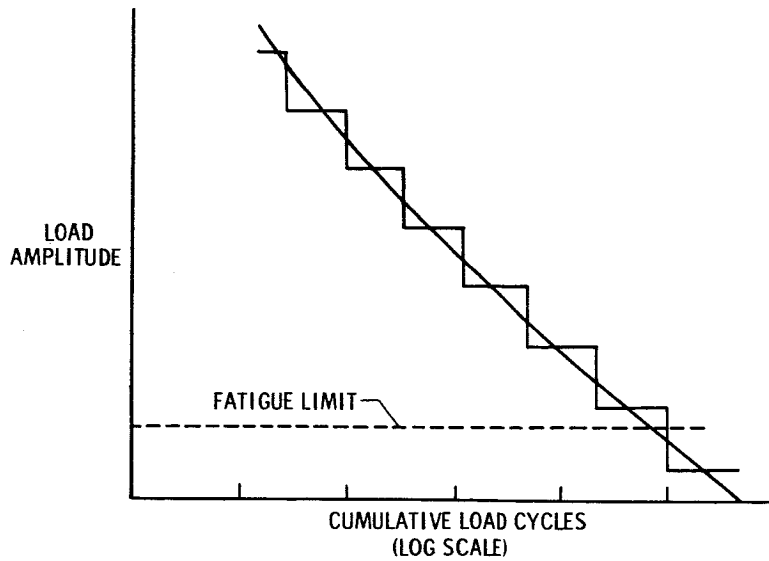


Figure 1

EFFECT OF TEST SEQUENCE ON FATIGUE LIFE

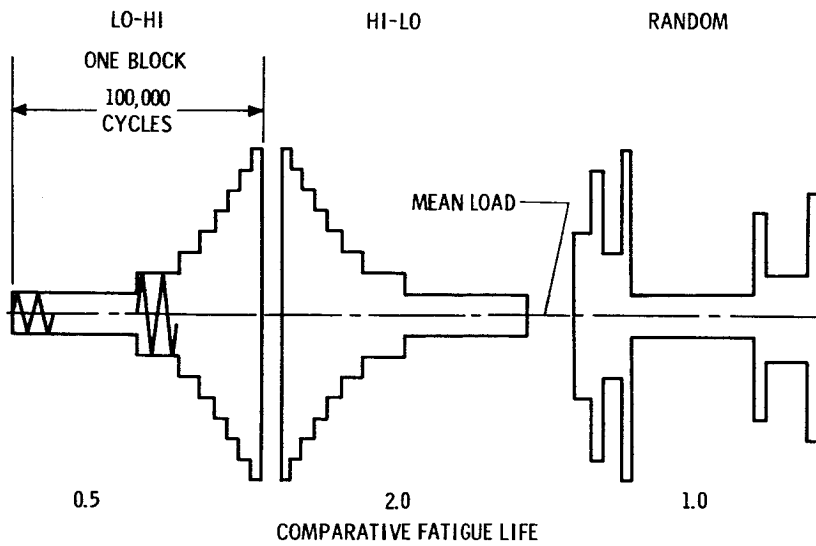


Figure 2

STRENGTH REDUCTION DUE TO CRACK PROPAGATION

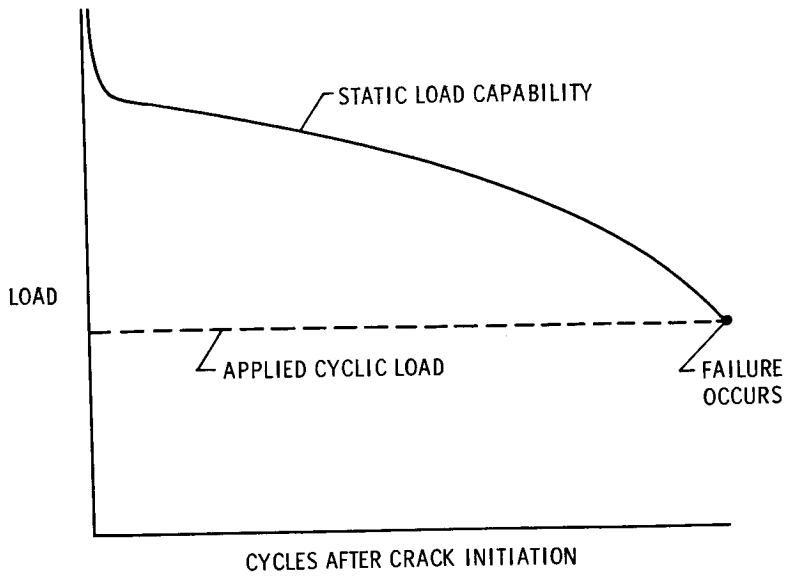


Figure 3

RATE OF FATIGUE - CRACK PROPAGATION IN 2024-T3 SHEET
 $R = 0$ (MINIMUM STRESS = 0)

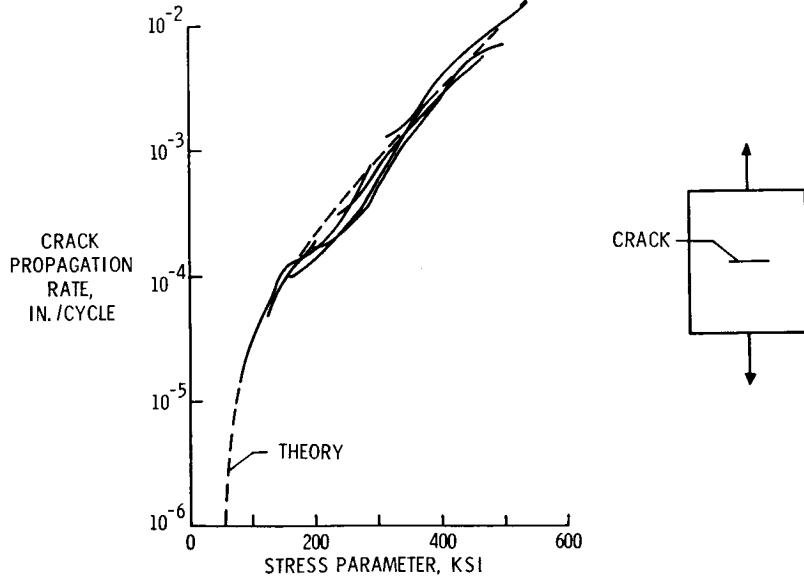


Figure 4

STATIC STRENGTH OF 2024-T3 SHEET
CONTAINING FATIGUE CRACK

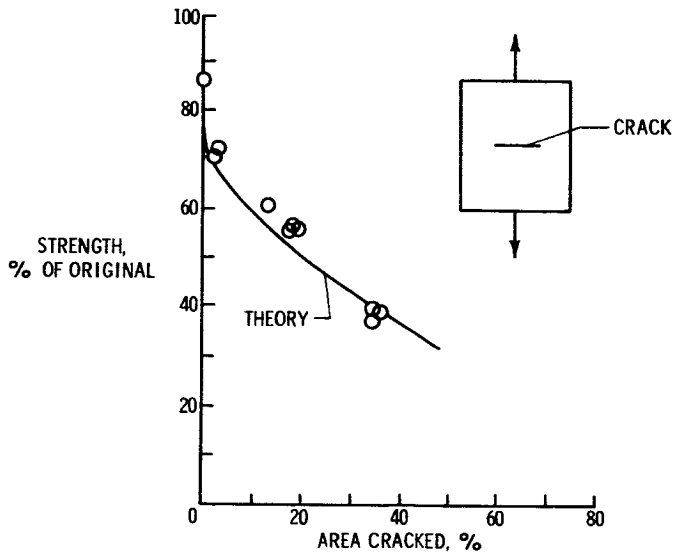


Figure 5

METHOD FOR DETERMINING EQUIVALENT LOADING
SIMPLE-SPECIMEN FAILURE CURVES

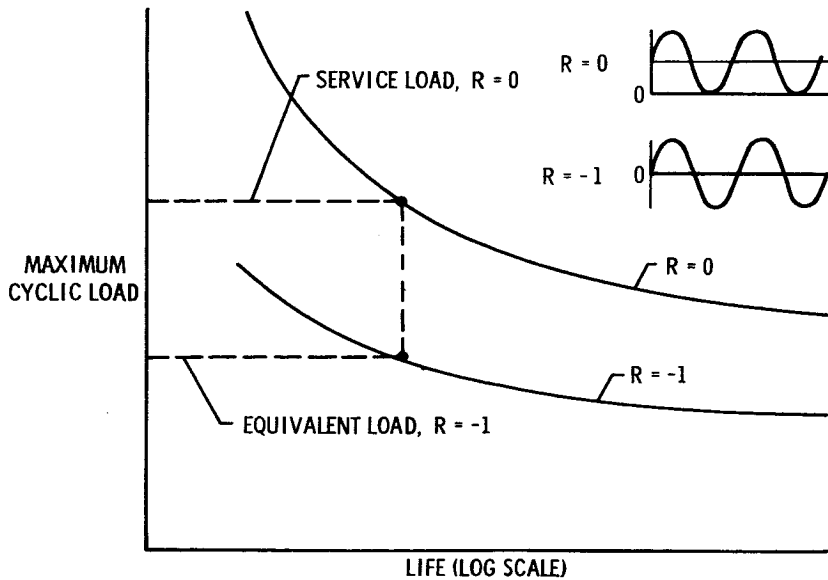
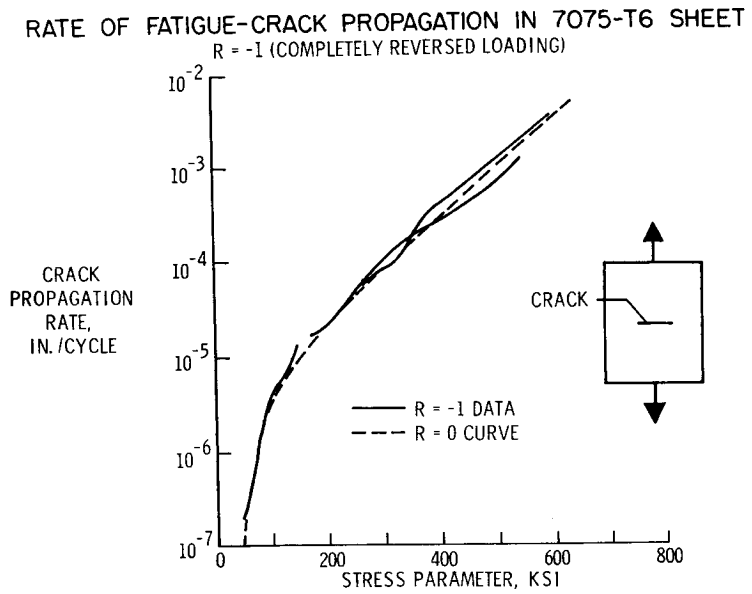
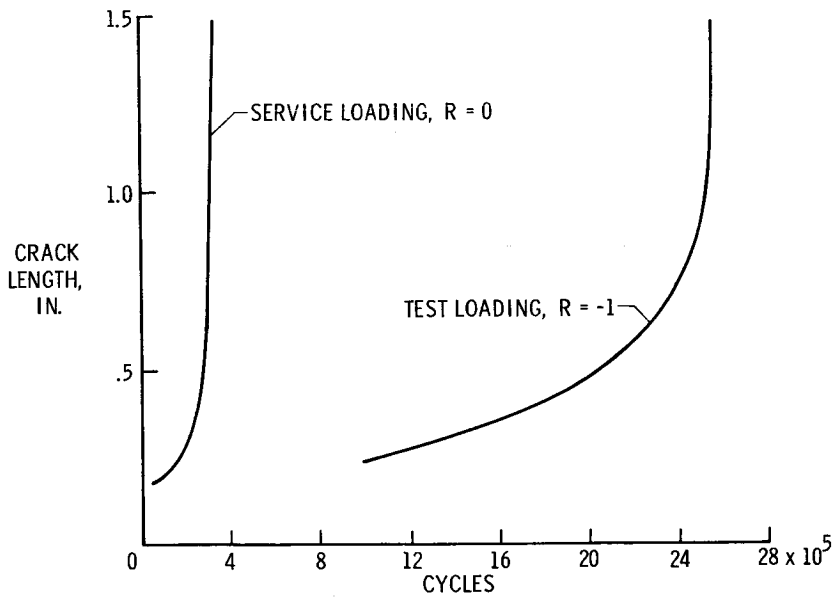


Figure 6



AXIAL-LOAD TESTS OF A PORTION OF A HELICOPTER BLADE



SUMMARY OF THE V/STOL STATE OF THE ART

By Charles H. Zimmerman

Langley Research Center

It is the purpose of this paper to summarize briefly the major points which have been presented in the preceding papers to aid the designer in forming an overall picture of the status of research on V/STOL aircraft and to present some of the needs for future research in this area.

The basic aerodynamic principles which govern aircraft design have been reviewed briefly and the mission capabilities of various V/STOL types have been presented in figures 1 and 2. It can be seen that the conventional helicopter, which was the only practicable aircraft capable of hovering when power plants were relatively heavy and bulky, remains the most desirable configuration when hovering is a major part of the mission. Because of considerations of rotor-blade stall, rotor-hub drag, and rotor instabilities, helicopters are not well suited to achievement of high speeds or large ranges. However, the power required in cruising can be greatly reduced by careful attention to drag reduction as compared with the power required when drag has been given little or no consideration. This decrease in drag will make possible both the achievement of a reasonably large ferry range for the helicopter and a substantial increase in its productivity in normal missions.

The speed limitation imposed by rotor-blade stall can be alleviated by transferring the propulsion function from the rotor to propellers and using a fixed wing to carry a large percentage of the weight in high-speed flight. The drag of the rotor and tendencies toward rotor instabilities remain serious problems and have caused many engineers to look for more suitable configurations where high speed and long range are the primary considerations and hovering is necessary only for the short time periods required to permit vertical take-offs and landings. Years of research, design, development, and experience have resulted in the conventional high-aspect-ratio, propeller-driven, subsonic airplane configuration as the one most suitable where range, efficiency, and operational flexibility is necessary and speeds greater than 400 knots are not required. It has been natural therefore to attempt to add to this configuration the capability of vertical take-off and landing.

Figure 3 shows a family of V/STOL aircraft which represent various approaches to this general solution. In this figure are four wing-propulsion systems which have been proposed. It has been assumed that a given load is to be carried in a given cargo-type fuselage. This

fuselage requires substantially the same stabilizing and control means regardless of the wing-propulsion system and will obviously require the same lifting and thrust forces for its sustentation and propulsion. With the exception of the tilt-rotor aircraft, the aircraft shown have roughly the same effective span in cruising flight and the same downwash velocity when hovering if the same gross weight is assumed. The tilt-rotor configuration has a lower effective span and a lower hovering downwash velocity.

Test-bed aircraft representing in a general way each of these concepts have been flown. An aircraft for operational evaluation can be built based on any one of these concepts. This does not mean that sufficient information is available to build the optimum aircraft of any one type or that the answers are known to all the problems that will be encountered. A great deal of research and development will be required before a completely satisfactory service aircraft of any of these types can be built.

The main problem now is to decide where research should be concentrated in order to proceed most efficiently and rapidly toward the final service aircraft. Unfortunately, a rational answer to this question can come only from operational experience which will provide answers to such questions as:

- (1) How much downwash velocity can be tolerated?
- (2) How much emphasis should be placed on speed?
- (3) How important is good hovering capability?
- (4) What is the acceptable pilot work load?

Operational experience will not, however, give all the answers. All of these machines have deficiencies which must be eliminated by careful design and development or at least reduced to tolerable levels. As pointed out in previous papers these machines all have, to a greater or lesser degree, special problems inherent in placing the fuselage in the upwash generated by pairs of lifting jets operating about a plane of symmetry. They all are subject, to a greater or lesser extent, to unpleasantness associated with wing stalling at some point in their flight envelopes. They each present a problem in connection with the requirement for adequate center-of-gravity travel. And, finally, they each present a problem of compromise between design requirements for static lift and high-speed propulsion.

As shown by figure 1, the requirement for high speed strongly indicates the use of a jet propulsion system. Here the problem is one

of finding a configuration suited to jet propulsion at high subsonic or supersonic speeds with a jet lifting system compatible with those high-speed requirements. Some of the aerodynamic problems associated with jet and fan lift arrangements have been presented. The major problems are thrust loss near the ground, pitching moments in transition, and high jet velocities.

These problems are not considered unsolvable except for the basic problem of high lifting jet velocities which will preclude use of such aircraft over many types of unprepared soils. It is expected that research directed toward solution of these problems will continue but it is believed that the future of jet V/STOL aircraft hinges largely on the availability of jet engines, or engine combinations, which can meet the requirement for extremely low weight and for both low drag and low specific fuel consumption at high speed.

The preceding discussion has concerned aerodynamics and, to a certain extent, propulsion problems; however, flying and handling qualities must also be considered. As pointed out and discussed previously, experience with conventional helicopters and airplanes plus that gained from the various test-bed vehicles and from studies with variable-stability helicopters and simulators has made possible specification of handling-qualities requirements which will be entirely adequate for V/STOL aircraft suitable for operational evaluation. On the other hand, sufficient information is not available to permit specification of detailed requirements for a service V/STOL aircraft and such specification should not be attempted until operational experience has been gained with suitable aircraft of this type.

It is relatively easy to specify the handling qualities desired in an aircraft; it is much harder to define the degree of departure from perfection that can be tolerated; and it is still harder, in general, to build an aircraft which fully complies with these requirements. The handling qualities of various test-bed aircraft, the reasons for their deficiencies, and, in most cases, the corrective measures which can be taken have been discussed. It should be clearly borne in mind that the test beds are undeveloped aircraft with novel features, and actually the surprising fact is not that they have deficiencies but rather that they fly as well as they do. No attempt will be made to review the deficiencies and their remedies but rather to point out general areas for attention. These problem areas are as follows:

- (1) Ground interference effects
- (2) Stalling or flow separation
- (3) Control power and damping
- (4) Pilot work load

In regard to the behavior near the ground, it is very clear that careful attention must be paid to fuselage shape, wing placement, control-surface or control-rotor location, and to the possible use of auxiliary shielding surfaces to minimize undesirable effects and maximize desirable characteristics. A program is underway which should provide better understanding of these phenomena but it is strongly indicated that model tests representing hovering near the ground will, in a development program for this type of aircraft, be as essential as conventional wind-tunnel tests.

It has been indicated that the stalling of lifting surfaces can be avoided or reduced to acceptable levels in certain cases but there is still a great deal to be done in the investigation of wing-rotor, wing-propeller, and wing-fan combinations in order that optimum configurations may be evolved. The National Aeronautics and Space Administration expects to continue to prosecute vigorously research in this area.

The provision of adequate control power and damping is largely an engineering problem. In this area efforts will be directed toward evolution of configurations which minimize those undesirable moment characteristics which impose unnecessary loads on the control system and toward the determination, through experience with variable-stability aircraft, simulators, existing test beds, and future experimental and service aircraft, of realistic control and damping requirements.

There is also the very real problem of pilot work load due to the necessity for changing the configuration during transition. Research, design, and development effort should be devoted to minimization of this problem by increasing the ranges of speed and power through which the aircraft can be safely operated without a configuration change. It is probable that automatic programming equipment can be used to alleviate the pilot's load in most instances but the designer must be fully aware of and respect the limitations inherent in his aircraft which automatic equipment cannot overcome. Also, it is true that, in general, automatic equipment increases costs and introduces maintenance and reliability problems, all of which are generally agreed to be undesirable.

In the area of loads and structures several papers have indicated that cyclic loadings present a major problem for the designer of V/STOL aircraft. This problem is one which requires better understanding and means of estimating the extent of the cyclic loadings so that the designer can minimize these loadings as much as possible in his design approach and can design rationally for the greatest structural efficiency to bear those loads which cannot be avoided. Some of the available information was presented. Efforts are being continued in this area, aided to a very important extent by support from the armed

L
1
4
3
5

services. Better analytical methods for estimation of dynamic loads have become available which also assist in making possible efficient rational design. However, it seems evident that despite all efforts to avoid or minimize them the cyclic loadings will continue to be a very important factor in the design of V/STOL aircraft and the problem of getting the greatest efficiency of design from a fatigue standpoint has been discussed.

V/STOL aircraft will bring with them serious operational problems, many of which have been encountered with helicopters. The problem of steep descents in connection with all-weather operation has been discussed and the very important point made that all-weather operation with any type of V/STOL aircraft will not be feasible until means can be developed to provide the pilot with reliable and adequate cues to enable him to find and maintain the proper position and orientation for landing at a selected spot while being plagued by wind shears and shifts and turbulence.

There are very serious problems associated with the operation of V/STOL aircraft from unprepared sites, a necessary requirement if certain military missions are to be accomplished with the desired high degree of mobility and flexibility. The maximum disk loading of the supporting rotors or propellers will almost certainly be dictated by the amount of dynamic pressure which can be tolerated without excessive troubles due to erosion of the types of terrain over which such operations must be conducted as indicated in figure 4. This may well dictate the type of aircraft required, and can be determined only by realistic field experience with suitable aircraft. Both the NASA and the armed services are continuing investigations in this area to extend to larger scale the small-scale results presented in figure 6. Another major problem in this area, that of the effect of the hurricane velocities in the vicinity is a function of aircraft weight, as shown by figures 5 and 6, and is actually worse in some respects for machines supported by lightly loaded rotors. In this area it is undoubtedly true that operational practices will have to be adapted to the velocities created in the vicinity of heavy V/STOL aircraft of any type.

The noise of airplanes and helicopters is one of the very objectionable features of their operation both in civilian and military service. The noise associated with the high powers necessary for large V/STOL aircraft can be alleviated somewhat by careful design and by engineering compromises but will remain a serious problem which will have to be taken into account in operational procedures, some of which have been discussed. Intensive research may indicate methods of reducing the noise output of high-powered turbine engines and lifting rotors but it is unlikely that any completely effective solution will be found in this area.

The most important problem in connection with the development of practical V/STOL aircraft which can support themselves financially in the civilian field and on the basis of usefulness in the military field is indicated in tables I and II. These tables show that, with the exception of the conventional helicopter which uses the same rotor for support in both hovering and forward flight and can hover with a relatively high power loading, all V/STOL aircraft suffer from the fact that the useful load which can be carried in vertical take-offs is a relatively small percentage of the gross weight. These tables also indicate the areas in which the weight penalties of V/STOL exist and hence the areas in which research, design, and development effort will provide the greatest returns in increasing the productivity of the aircraft. The weight of propulsion and lifting systems for all these aircraft, including the helicopter, is a very large item compared with that for the conventional airplane and is tied up in items such as propellers, rotors, and power transmission systems, the stress levels of which are dictated by fatigue considerations. Basic research in metallurgy tending to raise allowable fatigue stress levels in metals otherwise suitable for these components could result in substantially increased productivity of V/STOL aircraft of all types. The high installed power and refined mechanical components necessary in V/STOL aircraft make these aircraft relatively expensive. Research, design, development, and manufacturing techniques which will reduce the cost in money and manpower of producing and maintaining these items is urgently needed and will pay off to a far greater extent than would be true for the conventional airplane.

Tables I and II are based on weight breakdowns of existing aircraft and on manufacturer's estimates for the unconventional types. They are shown only to illustrate general points and are not suitable for close comparisons of competing types.

Conclusions which may be drawn in regard to the V/STOL state of the art are as follows:

1. With the information now available it is possible to build V/STOL aircraft suitable for operational testing and evaluation and, probably with some modification, useful as service aircraft.
2. A great deal of intensive research is still required to permit the construction of optimum V/STOL aircraft having the greatest utility and productivity.
3. In order that research may be properly guided and expended most productively toward the ultimate goal of practical, useful service aircraft, the type of information needed is that which can be obtained only from operational experience with V/STOL aircraft incorporating those features which on the basis of present knowledge and engineering judgment most nearly approach those which will finally be found most satisfactory.

4. There is no reason to expect a breakthrough which will materially alter this situation. Design and construction should proceed now of the best aircraft which the state of the art can produce.

TABLE I

**WEIGHT BREAKDOWN FOR ROTOR-POWERED
CONFIGURATIONS**

PAYLOAD = 4 TONS; RADIUS = 300 NAUTICAL MILES

	HELICOPTER	COMPOUND HELICOPTER	TILTING ROTOR
STRUCTURE AND EQUIPMENT	.30W	.37W	.38W
PROPULSION SYSTEM	.25	.29	.25
ROTOR	.11	.11	.11
ROTOR DRIVE	.10	.10	.08
PROPELLERS	-	.02	-
PROPELLER DRIVE	-	.02	-
ENGINES	.04	.04	.06
USEFUL LOAD	.45	.34	.37
FUEL	.19	.14	.14
PAYLOAD	.26	.20	.23

TABLE II

**WEIGHT BREAKDOWN FOR PROPELLER-POWERED
CONFIGURATIONS**

PAYLOAD = 4 TONS; RADIUS = 400 NAUTICAL MILES

	TILTING WING	TILTING DUCT	CONVENTIONAL AIRPLANE
STRUCTURE AND EQUIPMENT	.41W	.34W	.43W
PROPULSION SYSTEM	.22	.27	.07
PROPELLER	.09	.05	.02
DUCT	-	.07	-
GEARING	.06	.06	.02
ENGINE	.07	.09	.03
USEFUL LOAD	.37	.39	.50
FUEL	.17	.19	.20
PAYLOAD	.20	.20	.30

HOVERING AND CRUISE PERFORMANCE

$W_f = 0.03$ GROSS WEIGHT

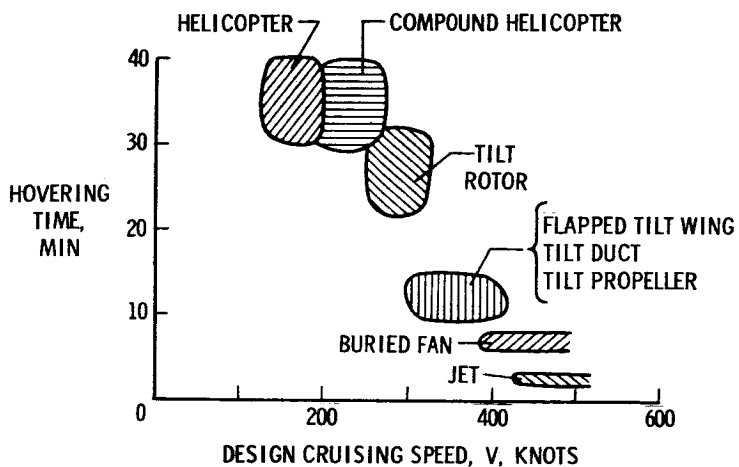


Figure 1

STOL PERFORMANCE

TAKE-OFF DISTANCE OVER 50-FOOT OBSTACLE;

$$\frac{W}{W_{VTOL}} = 1.2$$

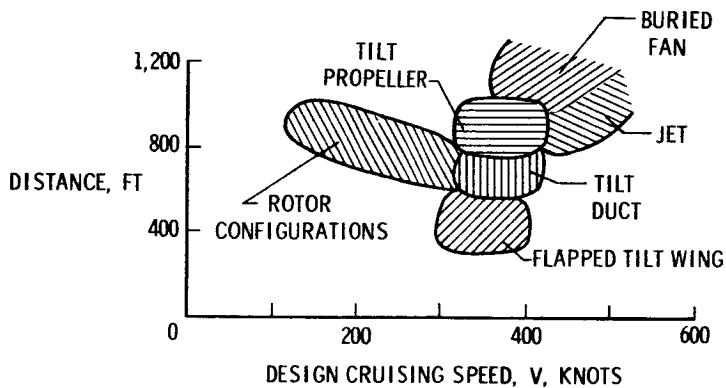


Figure 2

INTERMEDIATE - SPEED TYPES

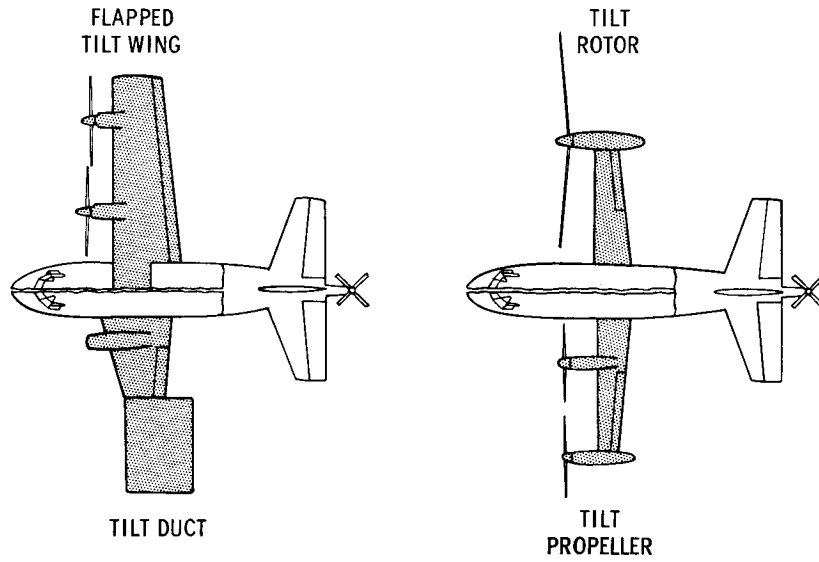


Figure 3

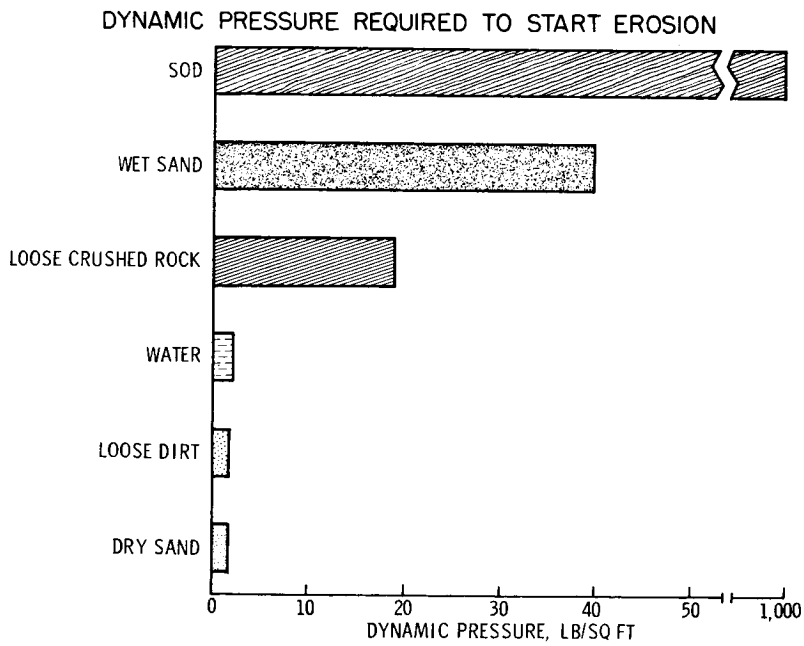


Figure 4

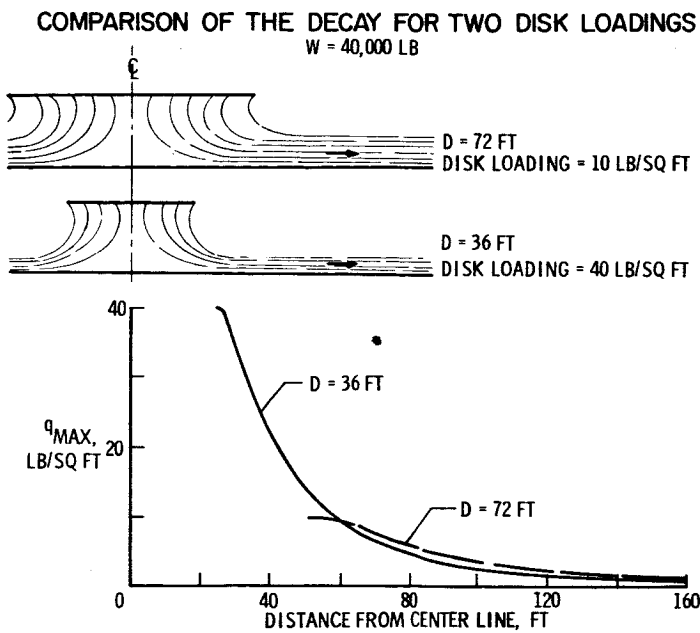


Figure 5

THICKNESS OF DYNAMIC PRESSURE PROFILES
 $W = 40,000 \text{ LB}; X = 72 \text{ FT}$

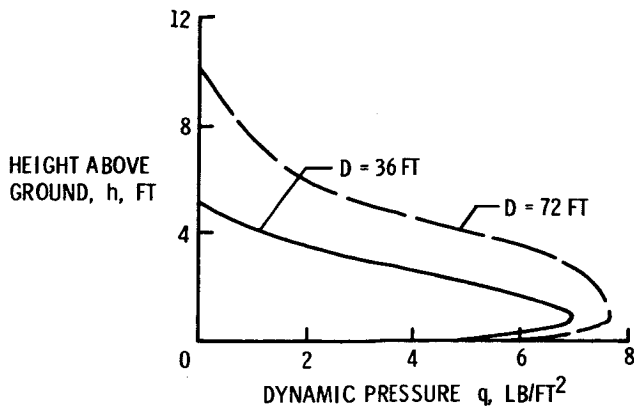


Figure 6